UNIVERSITÀ
DEGLI STUDI
DI TRIESTE

UNIVERSITÀ DEGLI STUDI DI TRIESTE
UNIVERSITÀ CA' FOSCARI VENEZIA

XXXV CICLO DEL DOTTORATO DI RICERCA IN CHIMICA

INTEGRATION OF CHEMISTRY AND BIOTECHNOLOGY FOR THE SUSTAINABLE VALORIZATION OF BIOMASS

Settore scientifico-disciplinare: **CHIM/06**

DOTTORANDO / A
MARIACHIARA SPENNATO

COORDINATORE
PROF. ENZO ALESSIO

SUPERVISORE DI TESI
PROF. LUCIA GARDOSSI

ANNO ACCADEMICO 2021/2022

TABLE OF CONTENTS

ABSTRACT

The present work was carried out in the Laboratory of Applied and Computational Biocatalysis (LACB) of the University of Trieste. The research is part of a national project (PRIN – MUR 2017) CARDIGAN (***CARDoon valorisation by InteGrAted biorefinery***), which was focused on the integration of chemical and biotechnological methods for the sustainable valorization of a typical biomass of marginal and semi-arid Italian territories: the cardoon, scientifically known as *Cynara cardunculus var. Altilis*.

The first part of the PhD work is focused on the extraction and valorization of bioactive molecules present in cardoon leaves (Chapter 2). The first activity undertaken was the optimization of experimental conditions for the supercritical CO_2 extraction ($scCO_2$) applied to the cardoon leaves. Secondly, the extracts were analysed by means of NMR and GC-MS with the objective of identifying the most important bioactive molecules and compar ing their abundance in extracts obtained with different extraction technologies, and from plants harvested in different seasons. A group headed by Professor Cinzia Pezzella at the University Federico II of Naples provided the extracts obtained using the Naviglio® technology and also by means of conventional batch extraction protocols with hot water. The analysis indicated that the $scCO_2$ method extracts preferentially hydrophobic components whereas the Naviglio® technology allows us to obtain extracts rich in sesquiterpene lactones (in particular cynaropicrin, a bioactive molecule with hepato-protectant activity). Based on these results, a first manuscript was published on the application of cardoon leaves extracts in the preparation of bio-based polymeric films formulated by the research group of Dr Gabriella Santagata at the IPCB-CNR Centre of Pozzuoli. It was demonstrated that the presence of cardoon leaves extracts increases the mechanical and barrier properties of the bio-based films, making these new materials potentially applicable for extending the shelf-life of food products or as mulching films (**Manuscript A: Mirpoor et al., 2021** https://doi.org/10.1016/j.foodhyd.2021.107099).

The study of the properties of the cardoon extracts continued in collaboration with a neurobiology research group at the University of Trieste. The different extracts, also including four selected pure molecules identified within them, were tested for their effect in rescuing neuronal development arrest in an in vitro model of Rett syndrome (RTT). The results show that only the $scCO_2$ cardoon leaves extract obtained from plants harvested in spring was able to induce a significant rescue of neuronal atrophy in RTT neurons, while the $scCO_2$ extract from an autumn harvest were active on wild type (WT) neurons. More importantly, the extracts rich in cynaropicrin demonstrated a toxic effect on both WT and RTT neurons.
(**Manuscript B: Spennato et. al. 2022,** https://doi.org/10.3390/molecules27248772).

The second part of the project is focused on the valorization of cardoon seed oil through enzymatic catalysis (Chapter 3). Epoxidized vegetable oils are important building blocks for the preparation of chemical intermediates for the synthesis of biolubricants and plasticizers.

The experimental activities included were initially the characterization of cardoon seed oil by means of ^{1}H NMR and ^{13}C NMR. Spectra show that linoleic acid is the main component, followed by oleic acid. The cardoon seed oil was hydrolyzed enzymatically by combining the action of two enzymes, Lipase B from *Candida antarctica* (CaLB) and Lipase from *Thermomyces lanuginosus* (TLL), either immobilized or native. This reaction was scaled up to 2L of cardoon seed oil. Finally, the chemo-enzymatic epoxidation of unsaturated fatty acids was performed using immobilized lipases. The advantages demonstrated by the chemoenzymatic method over the conventional chemical processes include a higher selectivity with low side products formation, mild reaction conditions, and no use of organic solvents. The experimental protocols were optimized using pure oleic, linoleic, and linolenic acids. To improve the environmental sustainability of the enzymatic process, a parallel study was carried out by addressing the covalent immobilization of lipases on a renewable carrier made by rice husk (Chapter 4). The study was intended to deliver some cost-effective, and sustainable, alternatives to the commercial fossil-based organic carriers for enzyme immobilization. The results of the study indicated that rice husk RH is a versatile natural composite material that can be used for the covalent immobilization of lipases (**Manuscript C: Spennato et al.,2021** https://doi.org/10.1016/j.bioeco.2021.100008). Compared with previous studies, the sustainability of the functionalization and immobilization protocols on rice husk were improved. The laccase-TEMPO functionalization (oxidation) of rice husk was performed with an optimized protocol that not only allows the reduction of the amount of enzyme employed but also enables its recycling. The oxidation method has the advantage of operating at pH values close to neutral, avoiding side reactions such as ß-eliminations in cellulose that cause the depolarization of the polysaccharidic chain. Future studies will aim to optimize the recycling of the laccase and will also aim to replace the TEMPO mediator with bio-based renewable mediators. More importantly, lipases were directly immobilized covalently on the oxidized rice husk without the use of spacers and toxic glutaraldehyde. Data demonstrated a good stability and recyclability of TLL and CaLB covalently immobilized on rice husk retaining >70% of activity after 10 cycles of hydrolysis. The results are comparable to those obtained using commercial epoxy methacrylic resins, which are expensive, fossil-based, and non-biodegradable. These biocatalysts immobilized on rice husk, because of their stability and robustness, are applicable in various reaction media, including aqueous systems and under mechanical stress. The CaLB immobilized on rice husk, both chemically and enzymatically oxidized, was tested in the chemo-enzymatic epoxidation of fatty acids and in the solvent-free polycondensation of bio-based monomers. Within the context of the present polycondensation study, a review manuscript has been written (**Manuscript D: Todea et al., 2021,** https://doi.org/10.3390/polym13234091).

The last part of this research is focused on the delignification of rice husk with the objective of improving its accessibility to oxidizing reagents and enzymes, while decreasing the hydrophobicity of this composite material. The results obtained so far indicate that the rice husk increases water retention capacity, and decreases its density, while maintaining its tri-dimensional structure and robustness. However, no significant improvement in terms of protein loading and biocatalyst performance has been observed in the enzymes immobilized on the delignified rice husk.

CHAPTER 1
OBJECTIVES AND BACKGROUND

1.1 OBJECTIVES

The Bioeconomy concept focuses on the sustainable production and conversion of renewable biomasses into a broad range of industrial products, materials, and energy. The development of technologies for an efficient processing of biomass into a spectrum of marketable bioproducts is essential for the setting-up of viable biorefineries. Biorefineries, defined as the sustainable counterpart of the petroleum refineries, are believed to leverage the turnabout from a linear to a circular “bio”-economy. The biorefinery is one of the main enabling strategies of the circular bioeconomy as it allows the closing of the cycles of biomass raw materials: reuse of forest, agricultural, and process and post-consumer residues.

Chemistry, integrated with biotechnologies, is able to contribute to the development of biorefineries, bio-based industry, and ultimately a sustainable and circular bioeconomy, (“Review of the 2012 European Bioeconomy Strategy”, 13.11.2017) without entering into conflict with the food supply chain (“Commission Notice — Guidelines for the feed use of food no longer intended for human consumption,” 2018). An example of this comes from the possibility of utilizing semi-arid or marginal land for the cultivation of oil plants that provide the raw materials for the production of polymers, lubricating oils, components for cosmetics, and herbicides. Several industrial applications have been already considered for cardoon biomass, namely for pulp and paper production (Piscioneri et al., 2000), (Raccuia and Melilli, 2007) power generation and domestic heating. In Italy, Novamont and Versalis have developed an important reindustrialization initiative, named MATRICA, which is focused on the use of cardoon oil principally for producing glycerol, azelaic acid, pelargonic acid, lubricants, and plasticizers.

This thesis is focused on the use and valorization of renewable raw materials and is part of the CARDIGAN national project (PRIN 2017), that gathers research group of the University of Naples, the University of Milan Bicocca and the CNR (Consiglio Nazionale delle Ricerche) of Pozzuoli.

The CARDIGAN project aims at investigating new technologies for the valorisation of cardoon feedstock by processing this biomass using chemical and biotechnological approaches, so as to achieve new high-value materials and products with low environmental impact. In the CARDIGAN project different parts of cardoon (seeds and leaves) are valorized to obtain biolubricants, bioplasticizers, bioactive molecules, and biobased polymers for the development of innovative packaging materials.

Two biomasses have been considered in the scope of this thesis research:

- cardoon (*Cynara cardunculus var. Altilis*) are herbaceous perennial plants, typical of the Mediterranean basin, that can also grow on marginal lands. Different parts of cardoon (seeds and leaves) were valorized in order to obtain bioactive molecules and biobased polymers for the development of innovative packaging materials (Chapter 2, manuscript A and B).
- rice husk, a lignocellulosic biomass that it is a waste available from rice processing, which has been functionalized to obtain bio-composite materials suitable for replacing fossil-based resins used for the immobilization of the enzymes applied in the processing of the cardoon seed oil (Chapter 4, manuscript C Spennato et.al 2021).

This thesis also intends to boost the integration between chemistry and biotechnologies for the benefit of a more sustainable modern chemical sector. Indeed, the percentage of chemical production based on biotechnology is estimated to increase from less than 2% in 2005 to approximately a quarter of all chemical production by 2025. By 2030, the market value of bio-based building blocks is expected to reach $ 3.2 billion (up from $700 million in 2013) and the production of bio-based polymers is expected to increase to $5.2 billion by 2030.

The project intends also to valorise bioactive ingredients (Chapter 2), including polyphenols and other natural antioxidant molecules, which are widely used as additives in industries. Notably, global demand for bioactive compounds in 2030 is expected to outstrip current EU production capacities. Estimates surrounding the biochemical products sector converge to indicate that chemicals produced using renewable resources are worth around €2.9 billion ("Agenzia per la coesione territoriale"). However, bio-based chemicals and materials suffer severe economic competition from fossil-based products that have been optimized over decades of industrial experience. Therefore, there is a strong need for research directed at optimizing the productivity and robustness of bioconversions to achieve cost-effective productions.

Overall, this thesis reports new and different approaches, in order to contribute to the achievement of the Green Deal objectives:

- ✓ ***Climate change mitigation.*** The synthetic processes using biotechnologies that have very low GGH emissions, as compared to conventional chemical synthetic routes. Moreover, the impact in terms of Natural Capital Impact is significantly reduced due to the use of renewable carbon feedstock.
- ✓ ***Climate change adaptation.*** *Cynara cardunculus* has proven to be a resilient and productive crop for the drylands of the Mediterranean area, and potentially transferable to other areas for promoting a similar platform of multi-products biorefineries.
- ✓ ***The sustainable use and protection of water and marine resources.*** The use of supercritical CO_2 for the extraction of bioactive molecules stops the need for the use of organic solvents, reduces waste and the occurrence of corresponding effluents. The use of a biomass typical of semiarid land allows us to minimize water usage.

- ✓ ***The circular economy, including waste prevention and recycling.*** The full, integrated valorization of cardoon biomass according to a cascade approach enables the closing of the circularity scheme and the economic viability of new value chains of bioeconomy, promoting new industrial and cross-sectoral synergies.
- ✓ ***Pollution prevention and control of air, water or land.*** Biocatalysts are highly selective catalysts, enabling the reduction of waste and auxiliaries. Moreover, they are very effective at mild conditions, enabling the saving of energy, GGH emission.
- ✓ ***The protection and restoration of biodiversity and ecosystems.*** The project also indirectly promotes the development of the most fragile areas, such as rural and coastal areas of the Mediterranean Basin, boosting the construction of new business models respectful of ecosystems and biodiversity, but attractive for young generations. The use of an autochthon plant, growth on marginal areas not suitable for food-crop cultivation remarkably reduces the impact in terms of land use, but rather prevents desertification and mitigates the current urgency due to soil degradation and nutrient depletion.

1.2 BACKGROUND

1.2.1 Valorization of biomass

Biomass represents an attractive source for the production of fuels and chemicals due to its versatility, renewable nature and low environmental impacts. Most biomass residues and waste is a complex and variable mixture of molecules, and separation becomes a key issue. Because the sources of biomass are so diverse, it is convenient to consider the chemistry in terms of four source-independent categories: polysaccharides, lignin, triglycerides (from fats and oils), and proteins (Tuck et al., 2012). Biomass represents an alternative source of carbon for the production of materials and plastics, as it allows for an evolution of current chemical industries, which use petroleum as a source of raw materials (Lola Domnina B. Pestaño and Wilfredo I. José, 2018). Chemicals and Materials from renewable resources is one of the prominent challenges for sustainable growth.

The development of technologies for an efficient processing of biomass into a spectrum of marketable bioproducts is essential for the setting-up of viable biorefineries. Biorefineries, defined as the sustainable counterpart of the petroleum refineries, are believed to leverage the turnabout from linear to circular (bio)economy.

The multidisciplinary approach, where different technological expertise is combined, will enable a more efficient use of natural resources, reducing the overall environmental impact, according to the circular economy paradigm. In this scenario the Bioeconomy concept focuses on the sustainable production and conversion of renewable biomasses into a broad range of industrial products, materials, energy. The reduction of our dependency on the limited fossil resources, of greenhouse gas emission and of waste generation are some of the benefits of the bio-based productions.

1.2.2 Cardoon as model biorefinery biomass

Fundamental for a right approach to sustainable growth is the proper choice of the renewable raw materials. In this project Cardoon has been chosen as case-study due the possibility to transform it into high-value materials and products with low environmental impact, inserting itself into a logic of total integration within the Mediterranean basin. Valorization of cardoon was carried out using catalysts, enzymes and bioprocesses following the criteria of Green Chemistry. Cardoon is a model biorefinery biomass, holding potential for the production of value-added products with a multidisciplinary approach: separation science, biotechnology, catalysis, science and technology of materials are used in this study. Diverse bio-based products are produced using different fractions of cardoon as described in the following chapters such as biopolymers, bioactive molecules, bioplastics, with final application in the field of packaging.

Cardoon biomass is also a rich source of valuable phytoconstituents, such as polyphenols and terpenoids, with well-known nutraceutical and pharmaceutical properties (Silva et al., 2022). Nutraceuticals or functional foods with antioxidant properties have recently been the object of intensive investigation due to their capacity to act on the triad of conserved core mechanisms underlying brain damage, which include oxidative stress, neurotrophic factors deficiency, and inflammation (Adelusi et al., 2021). Most plant extracts and pure bioactive ingredients typically show a polypharmacological profile, which today is considered more efficacious in preventing or attenuating neurological diseases than drugs responding to the “one drug-one target” concept which prevailed in the pharma industry in the last decades (Duran-Frigola et al., 2017). Despite that, the pharmacological mechanism of action of plant extracts was disclosed only in few cases, and the molecular mechanisms underlying their biological activity and the synergic action among the compounds of a phytochemical pool are mostly unknown.

In addition, the use of non-edible vegetable oils has been attracting more attention in recent years. Cardoon seed oil represents a non-edible alternative to soybean oil to obtain biolubricants and bioplasticizers through epoxidation reaction (Turco et al., 2019). Non-edible oils are not suitable for human food due to the presence of some toxic components in the oils and they are expected to employ lands that are semi-arid. (Almasi et al., 2021).

1.2.3 Lignocellulosic biomass

Lignocellulosic biomass represents the largest reserve of organic matter on earth. It constitutes the cell wall of plants and is composed of organic acids, salts, minerals and three biopolymers: cellulose, hemicellulose, and lignin.

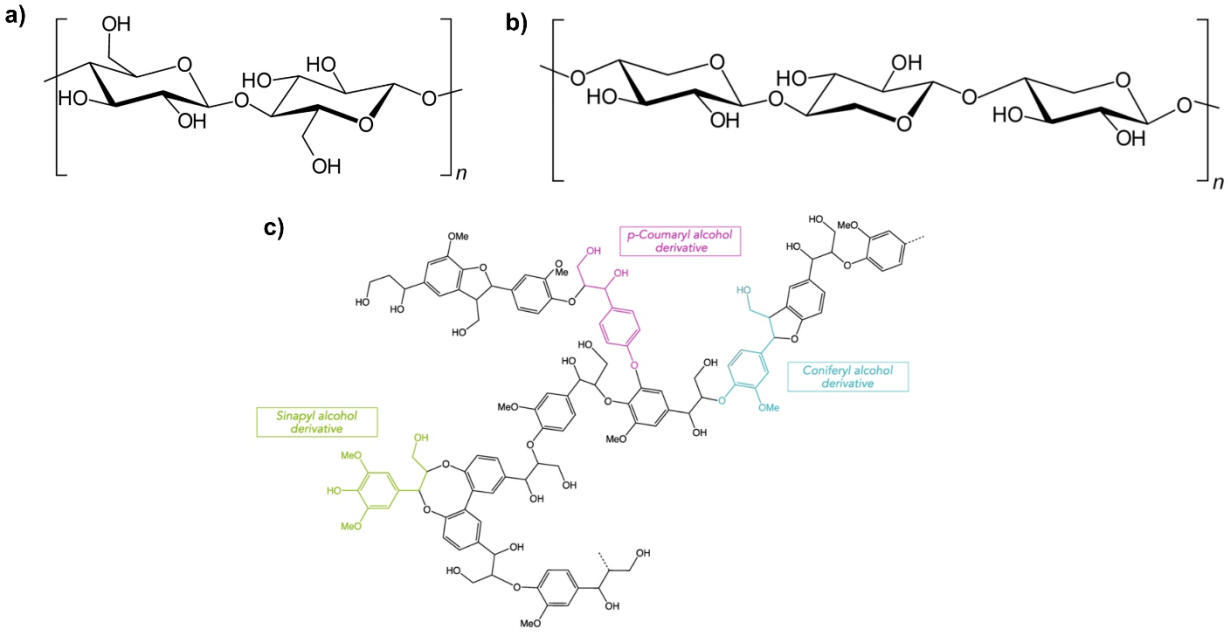

Figure 1.1 *Chemical structure of a) cellulose, b) hemicellulose, c) lignin.*

These three biopolymers are associated with each other forming a complex heterogeneous matrix whose composition can vary according to the biomass it constitutes and the area in which it is produced. Lignocellulosic materials are currently used for the production of bio-based chemicals, such as substrates for fermentation or as a source of biofuels in biorefineries (Tuck et al., 2012).

However, the concept of valorization of lignocellulosic biomass received an increasing attention especially for its potential conversion into products with value-added. The present project wants to respond to this challenge by converting a very inexpensive biomass, rice husk, into a functional material applicable in the biotechnology sector as carrier for enzyme immobilization as it is described in chapter 4 of this thesis.

In order to promote a wider uptake of immobilized enzymes for the production of high-volume and low-cost sustainable products, new carriers and immobilization strategies are needed and natural biopolymers from biomass represent attractive alternatives and on a global scale (Cantone et al., 2013).

1.2.4 Biocatalysis and immobilized enzymes

The term biocatalysis is used to indicate the catalysis of any reaction by natural catalysts, enzymes, or microorganisms, to perform chemical reactions. Biocatalysis is a multidisciplinary sector involving molecular biology, biochemistry, organic chemistry, and engineering, etc. (Narancic et al., 2015). The main advantages of biocatalysts are that: they are biodegradable and non-toxic for humans and for the environment; their usage enables working in a reasonable range of pressure and temperature conditions; and the use of

metals and organic solvents can be avoided. Another important feature of enzymes is their chemo-, regio-, and stereoselectivity; for this reason, they are often used for the synthesis of chiral molecules (i.e., steroids). Biocatalysis also has some drawbacks. If recombinant DNA technology paved the way to a broad availability of these catalysts, enzymes still remain not so available and the procedure of process optimization represents a major obstacle. Lastly, not every chemical reaction can be catalysed by known enzymes.

Immobilized enzymes are used in many sectors for the synthesis of pharmaceutical compounds, fine chemicals (Sheldon, 2007), and food and cosmetic products (Kirk et al., 2002). The use of immobilized enzymes, compared with using native enzymes, has several advantages: first, using insoluble enzymes allows its recycling and easier recovery separation from the reaction system, facilitating purification and avoiding product contamination. Secondly, immobilization often improves the stability of the biocatalyst. Immobilization, however, also has some limits relating to the cost of the immobilization procedure and the reduction of the catalytic activity of the enzyme due to conformational or covalent modifications. Finally, the use of immobilized enzymes often leads to variation of the reaction kinetics and to diffusion limitations (Cantone et al., 2013).

Nevertheless, immobilized enzymes are not widely used in industrial processes because the cost of the biocatalyst is not a critical factor in the planning of synthesis on an industrial scale. The design of an immobilization protocol is a complex procedure. It must consider not only the nature of the enzyme but also the chemical-physical characteristics of the solid support on which it is immobilized. Immobilization procedures are often a compromise between enzymatic activity recovered at the end of the process and the technological advantage that the new enzymatic preparation can offer. Various immobilization techniques are reported in literature. These can be classified according to the nature of the interaction between the enzymes and solid support.

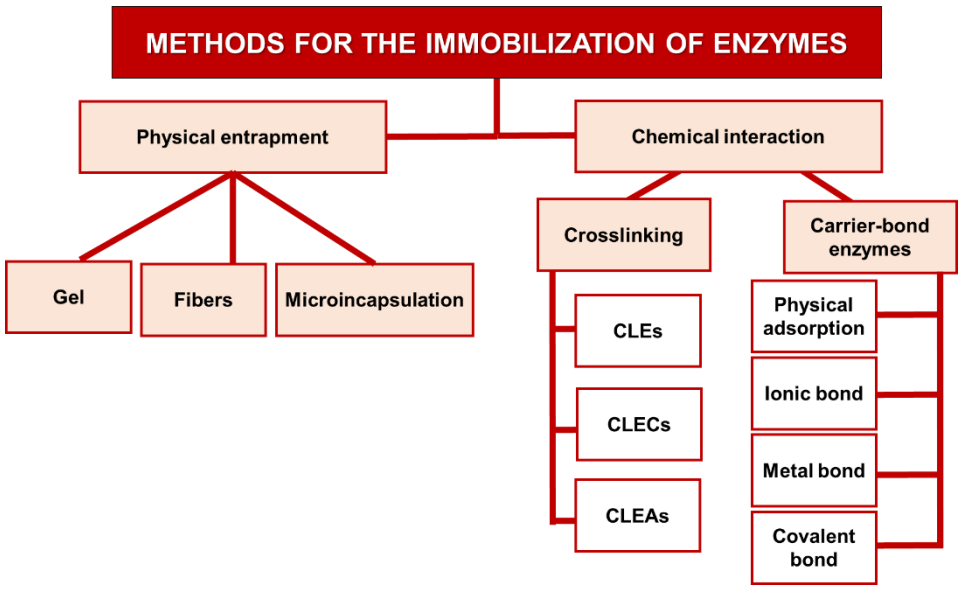

Figure 1.2 *Methods for the immobilization of enzymes. CLEs: cross-linked enzyme; CLECs: cross-linked enzymes crystal; CLEAs: cross-linked enzyme aggregates.*

Immobilization can occur by entrapment of the enzyme in a polymer fiber or in a gel or by encapsulation in a microcapsule formed by organic polymers (Betancor and Luckarift, 2008). With this method, no direct bond is established between the enzyme and the support. However, this method is limited to small molecules that can diffuse through the polymer matrix and for this reason it is applied only to the confinement of whole cells.

When using a solid support, immobilization can occur through adsorption of enzymes onto carriers via different types of interactions (Hanefeld et al., 2009). In most cases hydrophilic amino acids residues prevail on the surface of enzymes and the generally hydrophilic surface of enzymes can ensure adsorption via hydrogen bonds. In addition, enzymes may be glycosylated, further increasing the hydrophilicity of the protein.

Therefore, they can easily form hydrogen bonds with silicates or cellulose based carriers. Enzymes with a large lipophilic surface area will interact well with a hydrophobic organic resin via van der Waals forces. Enzymes can also be immobilized on ion exchange resins via ionic and strongly polar interactions, depending on the predominant charge on the enzyme.

Covalent immobilization occurs when a bond is created between the functional groups of the solid support and the side chains of amino acids exposed on the surface of enzymes. In this case the immobilization process involves a preliminary physical adsorption of the protein on the solid matrix followed by the formation of chemical bonds with the support. Generally, the protein undergoes a multiple anchoring which further stabilizes the structure of the protein. The formation of covalent bonds prevents the leaching of the protein during the process but leads to a greater conformational stress of the protein.

Enzymes can be immobilized also without the use of solid carriers, using techniques relying on crosslinking agents. The so-called CLEAs are crosslinked enzyme aggregates, and these techniques allow concentration of a high enzymatic activity in the enzyme, reducing the cost of using a carrier (Cao et al., 2003).

The choice of the support plays a key role in the immobilization process because their chemical-physical properties (such as particle size and shape, pore size, surface area and chemical nature of the matrix) influence the catalytic properties of the immobilized enzyme. A material that can be used as a carrier for enzymatic immobilization must be chemically inert, stable under operating conditions, and allow binding with the protein.

Different polymeric organic resins are available for immobilizations. They are produced in the form of spheres, or beads, the matrix of which can be made up of different materials: synthetic organic polymers obtained by polymerization of acrylic, methacrylic or styrene monomers, functionalized in diverse ways according to their use. The matrix can also be formed of natural water-insoluble polysaccharides such as cellulose, starch, agarose, and chitosan; or proteins such as albumin and gelatin. Furthermore, the matrix can also be formed by natural hydrogels or cryogels (Okano et al., 1990), inorganic solids including silicates, alumina, or zeolites (Wang and Caruso, 2005).

The resins that are currently most readily available are those made by acrylic and styrene polymers as they have been studied and optimized over the last twenty years. However, the

use of these supports has been shown to have a significant environmental impact. For example, it has been shown that in the production of immobilized enzymes the major source of pollution (in terms of CO_2 emissions, acidification, and eutrophication of water) is represented by the production of methacrylic epoxy supports and the entire immobilization process (DiCosimo et al., 2013).

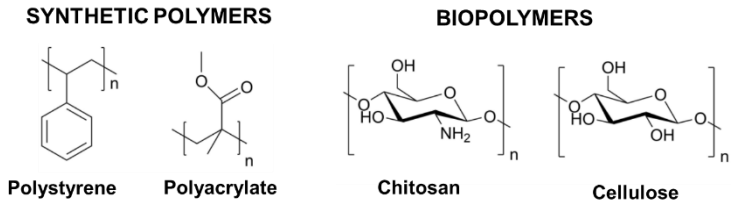

Figure 1.3 *Chemical structure of some organic polymers and biopolymers used as carriers for enzymes.*

Natural biopolymers from agricultural waste may represent attractive alternatives corresponding to the pressing challenges of introducing the use of sustainable and renewable carriers having low costs. In that respect, rice husk is investigated in this thesis as a potential replacer of fossil-based organic resins. Rice husk (RH) is an agricultural waste biomass and its production amounts to 120 million tons per year, mostly not valorised. In the context of the circular economy, it is a perfect example of how, starting from waste, it is possible to obtain a final resource with a very low environmental impact. It is a low density yet highly robust composite material used like adsorbents or additives for construction material (Corici et al., 2016). During the present research rice husk has been functionalized and transformed in a support for enzyme covalent immobilization applicable in the processing of non-edible vegetable oil (Cespugli et al., 2018).

1.2.5 Covalent immobilization of lipases

The biocatalysed reactions studied in this thesis were catalyzed by lipases, given the focus of the research is on the processing of the cardoon seed oil.

Lipases (triacylglycerol acyl hydrolases, EC 3.1.1.3) catalyse the hydrolysis and the synthesis of esters formed from glycerol and long-chain fatty acids. Lipases occur widely in nature, but only microbial lipases are commercially significant and have enormous applicative and industrial interest, both in the food and pharmaceutical, cosmetics and biofuel sectors (Schmid et al., 2001). Lipases are serine hydrolases. The catalytic triad is composed of serine, histidine and aspartic acid.

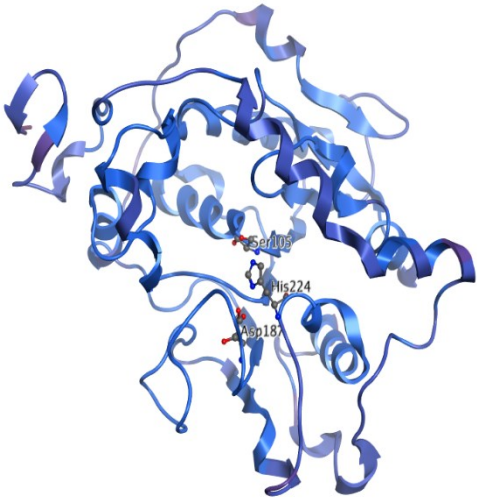

Figure 1.4 *The X-Ray crystallographic structure of lipase B from Candida antarctica (PDB: 1TCA) with catalytic triad: Asp187, His224, Ser105.*

The catalytic mechanism starts with the nucleophilic attack of oxygen on the sidechain of serine to carbonyl on the ester moiety of the substrate. The tetrahedral intermediate presents a negative charge stabilized by an H-bond interaction formed with the so-called oxyanion hole. Conversely, the charge on the protonated histidine is stabilized by an H-bond with the acid catalyst of the catalytic triad. Consequently, a proton transfer involving histidine and the alkoxy of the ester is carried out, leading to the release of the alcohol with the simultaneous formation of the acyl-enzyme intermediate. The acyl-enzyme intermediate is then deacylated thanks to the reaction with a new nucleophile (i.e., water, alcohols, amines). The histidine of the active site extracts a proton from the above-mentioned nucleophile and the hydroxyl anion reacts with the acyl-enzyme carbonyl. A second tetrahedral intermediate is formed and stabilized by the oxyanion hole. In the last step, the histidine loses a proton that is accepted by the serine with the simultaneous release of the product and active site environment regeneration (figure 1.5) (Jaeger et al., 1999).

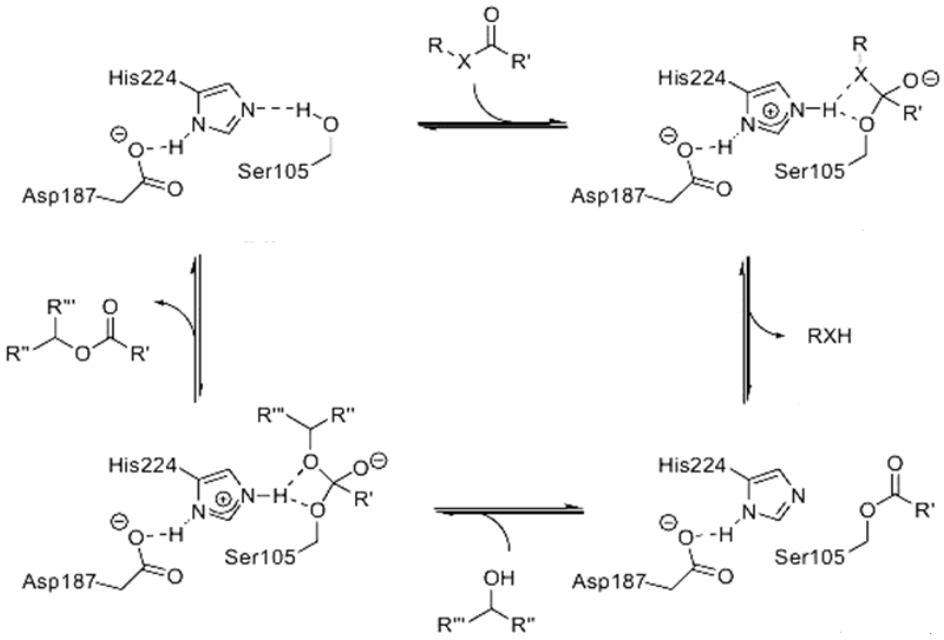

Figure 1.5 *Catalytic mechanism of lipases.*

They are known to be active even in anhydrous reaction media and their natural substrates are triglycerides, molecules that are insoluble in water and highly hydrophobic. Therefore, lipases by their nature do not operate in aqueous solutions but instead at the interface of hydrophobic phases. Indeed, most of the lipases, when placed in the aqueous system, take on an inactive "closed" conformation and need to be in contact with a hydrophobic phase to assume the "open" and active conformation. It was found that the immobilization of lipases carried out in an aqueous environment and hydrophobic supports leads to interactions between the opening of the active site of the enzyme, the most hydrophobic area of the enzyme, decreasing the accessibility of substrates to the catalytic site (Jaeger et al., 1999).

The difficulty of developing immobilization techniques for lipases is known. In literature and in patents, immobilization protocols are reported which provide for the adsorption of lipase on solid supports, and which normally lead to unsatisfactory immobilization yields. Instead, there are very few examples of covalent lipase immobilization techniques and in most cases the yields of immobilization are not reported as they are unsatisfactory.

Three different lipases are used in this work: lipase B from *Candida Antarctica* (CaLB), lipase from *Thermomyces lanuginosus* (TLL), and Lipase from *Rhizopus oryzae* (ROL). These lipases are widely employed in the food sector for the transesterification of oils and fats.

CaLB is a relatively thermostable lipase since it withstands up to 90°C in a non-aqueous environment. This enzyme is employed in numerous industrial fields, due to its high enantioselectivity, good thermal stability, wide range of substrates, and stability in various organic solvents and ionic liquids (Trodler and Pleiss, 2008). The high activity of TLL combined with its stability make it a good candidate for many applications in organic solvents and aqueous mixtures, but also in solvent-free reactions (Basso et al., 2007; Ferrario et al., 2011; Tangkam et al., 2008).

1.3 REFERENCES

Agenzia per la coesione territoriale, https://www.agenziacoesione.gov.it/ (accessed 11.20.22)

Basso, A., Braiuca, P., Cantone, S., Ebert, C., Linda, P., Spizzo, P., Caimi, P., Hanefeld, U., Degrassi, G., Gardossi, L., 2007. In Silico Analysis of Enzyme Surface and Glycosylation Effect as a Tool for Efficient Covalent Immobilisation of CalB and PGA on Sepabeads®. Adv. Synth. Catal. 349, 877–886. https://doi.org/10.1002/adsc.200600337

Betancor, L., Luckarift, H.R., 2008. Bioinspired enzyme encapsulation for biocatalysis. Trends Biotechnol. 26, 566–572. https://doi.org/10.1016/j.tibtech.2008.06.009

Cantone, S., Ferrario, V., Corici, L., Ebert, C., Fattor, D., Spizzo, P., Gardossi, L., 2013. Efficient immobilisation of industrial biocatalysts: criteria and constraints for the selection of organic polymeric carriers and immobilisation methods. Chem. Soc. Rev. 42, 6262–6276. https://doi.org/10.1039/C3CS35464D

Cao, L., Langen, L. van, Sheldon, R.A., 2003. Immobilised enzymes: carrier-bound or carrier-free? Curr. Opin. Biotechnol. 14, 387–394. https://doi.org/10.1016/s0958-1669(03)00096-x

Cespugli M., 2017. Integration of bioinformatics analysis and experimental biocatalysis for a comprehensive approach to the synthesis of renewable polyesters. Università degli studi di Trieste.

Cespugli, M., Lotteria, S., Navarini, L., Lonzarich, V., Del Terra, L., Vita, F., Zweyer, M., Baldini, G., Ferrario, V., Ebert, C., Gardossi, L., 2018. Rice Husk as an Inexpensive Renewable Immobilization Carrier for Biocatalysts Employed in the Food, Cosmetic and Polymer Sectors. Catalysts 8, 471. https://doi.org/10.3390/catal8100471

Commission Notice — Guidelines for the feed use of food no longer intended for human consumption https://circulareconomy.europa.eu/platform/sites/default/files/feed_guidelines. (accessed 11.20.22)

Corici, L., Ferrario, V., Pellis, A., Ebert, C., Lotteria, S., Cantone, S., Voinovich, D., Gardossi, L., 2016. Large scale applications of immobilized enzymes call for sustainable and inexpensive solutions: rice husks as renewable alternatives to fossil-based organic resins. RSC Adv. 6, 63256–63270. https://doi.org/10.1039/C6RA12065B

DiCosimo, R., McAuliffe, J., Poulose, A.J., Bohlmann, G., 2013. Industrial use of immobilized enzymes. Chem. Soc. Rev. 42, 6437–6474. https://doi.org/10.1039/C3CS35506C

Ferrario, V., Ebert, C., Knapic, L., Fattor, D., Basso, A., Spizzo, P., Gardossi, L., 2011. Conformational Changes of Lipases in Aqueous Media: A Comparative Computational Study and Experimental Implications. Adv. Synth. Catal. 353, 2466–2480. https://doi.org/10.1002/adsc.201100397

Hanefeld, U., Gardossi, L., Magner, E., 2009. Understanding enzyme immobilisation. Chem. Soc. Rev. 38, 453–468. https://doi.org/10.1039/B711564B

Jaeger, K.-E., Dijkstra, B.W., Reetz, M.T., 1999. Bacterial Biocatalysts: Molecular Biology, Three-Dimensional Structures, and Biotechnological Applications of Lipases. Annu. Rev. Microbiol. 53, 315–351. https://doi.org/10.1146/annurev.micro.53.1.315

Kirk, O., Borchert, T.V., Fuglsang, C.C., 2002. Industrial enzyme applications. Curr. Opin. Biotechnol. 13, 345–351. https://doi.org/10.1016/S0958-1669(02)00328-2

Narancic, T., Davis, R., Nikodinovic-Runic, J., O' Connor, K.E., 2015. Recent developments in biocatalysis beyond the laboratory. Biotechnol. Lett. 37, 943–954. https://doi.org/10.1007/s10529-014-1762-4

Naviglio, D., Scarano, P., Ciaravolo, M., Gallo, M., 2019. Rapid Solid-Liquid Dynamic Extraction (RSLDE): A Powerful and Greener Alternative to the Latest Solid-Liquid Extraction Techniques. Foods 8, 245. https://doi.org/10.3390/foods8070245

Okano, T., Bae, Y.H., Jacobs, H., Kim, S.W., 1990. Thermally on-off switching polymers for drug permeation and release. J. Controlled Release 11, 255–265. https://doi.org/10.1016/0168-3659(90)90138-J

Piscioneri, I., Sharma, N., Baviello, G., Orlandini, S., 2000. Promising industrial energy crop, Cynara cardunculus: a potential source for biomass production and alternative energy. Energy Convers. Manag. 41, 1091–1105. https://doi.org/10.1016/S0196-8904(99)00135-1

Raccuia, S.A., Melilli, M.G., 2007. Biomass and grain oil yields in Cynara cardunculus L. genotypes grown in a Mediterranean environment. Field Crops Res. 101, 187–197. https://doi.org/10.1016/j.fcr.2006.11.006

Schmid, A., Dordick, J.S., Hauer, B., Kiener, A., Wubbolts, M., Witholt, B., 2001. Industrial biocatalysis today and tomorrow. Nature 409, 258–268. https://doi.org/10.1038/35051736

Sheldon, R.A., 2007. Enzyme Immobilization: The Quest for Optimum Performance. Adv. Synth. Catal. 349, 1289–1307. https://doi.org/10.1002/adsc.200700082

SWD(2017)374, Review of the 2012 European Bioeconomy Strategy, 13.11.2017, n.d.

Tangkam, K., Weber, N., Wiege, B., 2008. Solvent-free lipase-catalyzed preparation of diglycerides from co-products of vegetable oil refining. Grasas Aceites 59, 245–253. https://doi.org/10.3989/gya.2008.v59.i3.515

Trodler, P., Pleiss, J., 2008. Modeling structure and flexibility of Candida antarctica lipase B in organic solvents. BMC Struct. Biol. 8, 9. https://doi.org/10.1186/1472-6807-8-9

Wang, Y., Caruso, F., 2005. Mesoporous Silica Spheres as Supports for Enzyme Immobilization and Encapsulation. Chem. Mater. 17, 953–961. https://doi.org/10.1021/cm0483137

CHAPTER 2
VALORIZATION OF CARDOON LEAVES EXTRACTS

2.1 SUMMARY

The first part of this PhD project was focused on the valorization of cardoon leaves. This study uses *Cynara cardunculus* var. *Altilis*., a cultivated cardoon from *the Asteraceae* family, a dicotyledonous herb abundant in the Mediterranean basin. Cardoon from the Asteraceae family is a wild robust perennial plant, growing naturally in harsh habitats characterized by high temperatures, salinity, and drought (Gironés-Vilaplana et al., 2012). It is well known that leaves of the *Cynara cardunculus* contain different bioactive molecules with antioxidant (Kukić et al., 2008), anti-microbial (Scavo et al., 2019), and biological activity (Silva et al., 2022). The first objective of the research was to compare different extraction methods of bioactive molecules from the leaves and their valorization as antioxidant additives in plastic formulations. Cardoons were collected in different harvest periods, from November 2019 to November 2020, at Novamont S.p.A. plantation in Terni (Italy). The leaves were lyophilized and used for supercritical CO_2 extractions ($scCO_2$) (De Zordi et al., 2017). Several experimental extraction protocols were evaluated: by changing pressure (130-225 bar), temperature (35°C – 45°C), and the time of extraction (2 – 5 hours). The composition of the extracts was compared with results obtained by the group at the University of Napoli Federico II using the Naviglio® extractor, based on a solid-liquid dynamic extraction (Naviglio et al., 2019), and also with data obtained using conventional batch extraction protocols (with hot water). These extracts were characterized by ^{1}H NMR and GC-MS analysis. Using $scCO_2$ it was possible to extract highly hydrophobic compounds like squalene and waxes. Higher amounts of cynaropicrin, a sesquiterpene lactone, was identified in the extracts obtained using Naviglio® technology. Based on this first set of experimental data obtained by the team at Napoli University and our group, a first manuscript was published describing the application of cardoon leaves extracts in the formulation and functional bio-based polymeric films potentially applicable in extending the shelf-life of food products or as mulching films. It was demonstrated that the presence of cardoon leaves extracts increases the mechanical and barrier properties of the obtained materials (Manuscript A: Mirpoor et al., 2022).

The investigation into the properties of extracts from cardoon leaves continued by collaborating with a neurobiology research group based at the Department of Life Science of the University of Trieste. The activity of the cardoon bioactive molecules in rescuing neuronal development arrest was tested in an *in vitro* model of Rett syndrome (RTT) (Nerli et al., 2020). In this case the same extraction methodologies ($scCO_2$ and Naviglio®) were compared using cardoon leaves from plants harvested at different maturity stages (spring and autumn). The $scCO_2$ hydrophobic extracts resulted in the richest in squalene, 3ß-taraxerol, and lupeol. On the other hand, the Naviglio® extract showed the highest content

of cynaropicrin, a molecule known for its hepato-protectant activity. Only the $scCO_2$ cardoon leaves extract obtained from plants harvested in spring was able to induce a significant rescue of neuronal atrophy in RTT neurons, while the $scCO_2$ extract from the autumn harvest was shown to be active on wild type (WT) neurons. More importantly, the extracts rich in cynaropicrin had a toxic effect on both WT and RTT neurons, thus indicating the importance of an accurate dosage of bioactive compounds in natural extracts before their use (Manuscript B: Spennato et al.,2022).

2.2 INTRODUCTION

2.2.1 Botanical characteristics and distribution of cardoons

Cynara cardunculus L. is a Mediterranean plant belonging to the Asteraceae family. The plants belonging to this species are commonly labelled with the generic name of 'cardoon' and are used for numerous food and phytopharmaceutical purposes, and to perform combustion and pyrolysis (Gominho et al., 2018). They are characterized by the presence of a group of thorny plants with showy flowers that belong to the Asteraceae family, the same as the gerberas and lettuce (Curt et al., 2014).

The taxonomy of the species belonging to genus *Cynara* is not so simple, due to the morphological similarities within *Cynareae* plants, which requires the use of distinctive, not always evident, characteristics. The *Cynara* genus comprises the botanical varieties of *C. cardunculus L.* that are diploid. The Asteraceae family includes the globe artichoke, the most widespread species (*Cynara cardunculus var. scolymus L.*), the cultivated cardoon (*Cynara cardunculus L. var. altilis*), and their ancestor the wild cardoon (*var. sylvestris*) (Portis et al., 2005).

Cynara species are robust, herbaceous plants with a size ranging between 0.5 and 3 meters. Figure 2.1 shows the cultivation of *Cynara cardunculus* var. *Altilis* used in the present study.

Figure 2.1 *Plantation of cultivated cardoon in Terni (Novamont Spa site).*

Of the entire Italian production of artichoke and cardoon it has been estimated that about 89% of this is destined for fresh consumption; the percentage destined for export is very low, while the remaining 11% of production is used in the processing industry (Fratianni et al., 2007).

In Italy, the cultivation of the *Cynara* species is concentrated in the central and southern regions given the *C. cardunculus* is well adapted to the Mediterranean climatic conditions characterized by low precipitation (Fernández et al., 2006). The plant grows at temperatures in the range of 7–38°C and during dormancy periods it can survive at temperatures above 40°C and below 7°C (Curt et al., 2014). Regarding soil characteristics, it can survive at the ranges of pH 5.0–8.6, and 4-10 $dScm^{-1}$ soil salinity. It has been reported that cardoons can grow at soil depths of 50–150 cm but deep soils are recommended due to the root characteristics (Lag-Brotons et al., 2014). Cardoon shows great adaptability (Benlloch-González et al., 2005) in the presence of a water deficit and high salinity levels (Pagnotta et al., 2017), these being characteristic of the Mediterranean sub-arid climate, where cardoon realises its full production potential. The cycle of this plant is autumn–winter–spring, with a vegetative stasis phase between spring and autumn. Given these characteristics, the cardoon can withstand severe drought and high soil salinity (Benlloch-González et al., 2005), representing a potential alternative crop with beneficial effects regarding soil properties, erodibility, biological and landscape diversity (Fernando et al., 2018).

The main cardoon crop by-products are leaves, stalks, seeds, and root, which are then reused for biomass, oil (Encinar et al., 1999), biodiesel (Fernández et al., 2006) and feed production (Ierna and Mauromicale, 2010). A recent study demonstrated the possibility of using bioprocesses in the production of polyhydroxy butyrate (PHB) and medium-chain length polyhydroxyalkanoates (mcl-PHA), starting, respectively, from root inulin and seed oil (Turco et al., 2022). Leaves represent about 48% of the total biomass from cardoon

cultivation, with an annual average of 10-20 t dm ha^{-1} $year^{-1}$ in Europe. (Fernández et al., 2006). A schematic representation of *Cynara cardunculus* is presented in figure 2.2.

Figure 2.2 *Cynara cardunculus var. altilis.*

2.2.2 Extraction methods applied to cardoon plants

Various literature reports different extraction techniques applied to cardoon leaves with the objective of identifying their molecular content. Traditional methods used on plant materials are distillation, solvent extraction, maceration, pressing, reflux extraction, and Soxhlet extraction, using different organic and inorganic solvents, as well as water. Each technique and solvent has advantages and disadvantages, such as long extraction times, high temperatures required, solvent quantity required, and solvent toxicity. Most commonly, phytochemical compounds are extracted with solvents such as ethanol or methanol in batch systems (Zhang et al., 2018). Dichloromethane was used as the solvent in Soxhlet extraction to obtain more lipophilic leaves extract from *C. cardunculus L. var. altilis* in which fatty acids and sesquiterpene lactones were identified (Ramos et al., 2013). Nevertheless, classical extraction procedures require long working times, use of toxic solvents, and high energy consumption (Azmir et al., 2013). For this reason, non-conventional techniques were introduced. Techniques such as ultrasound-assisted extraction (UAE), enzyme-assisted

extraction (EAE), microwave-assisted extraction (MAE), and supercritical fluid extraction (SFE) allow us to reduce the extraction time and the amount of solvent required, so as to increase selectivity and decrease decomposition of thermolabile compounds (Azmir et al., 2013).

In particular, SFE using carbon dioxide ($scCO_2$) as solvent was widely used for extraction from leaves. This technique was applied to *Myrtus communis* leaves, olive leaves, and *Salvia officinalis L.* leaves in order to extract lipophilic compounds such as essential oils, tocopherol, carnosic acid and carnosol (Ghasemi et al., 2011),(Pavić et al., 2019). When ethanol or methanol were added as cosolvents, polar molecules were additionally extracted. Recently, $scCO_2$ was used to increase the extraction yield of oil and pentacyclic triterpenes from globe artichoke leaves (Dai et al., 2019). To the best of our knowledge, $scCO_2$ had never been evaluated on *C. cardunculus var. altilis* leaves.

A valuable alternative to conventional and non-conventional extraction methods is the Naviglio® technology, based on a rapid solid-liquid dynamic extraction (RSLDE) (Naviglio et al., 2019). Using a suitable solvent at room temperature, a negative gradient pressure is generated between the outlet and the inlet of a solid matrix. Initial equilibrium conditions are then suddenly restored, inducing a “forced extraction” of the substances not chemically bonded to the principal structure of the plant material. This technology results in a shorter extraction time and preservation of molecule integrity. Naviglio® extractor was employed on *Stevia rebaudina* leaves, to extract stevial glycosides. Using water as solvent, 1197.8 mg/L rebaudioside A and 413.6 mg/L stevioside were recovered after only 20 minutes of extraction, compared to the 90 minutes required with conventional maceration. Moreover, using water and ethanol 60:40 v/v, extracts with strong antioxidant potential were obtained from *Cagnulari grape marc*, with high polyphenol and anthocyanins contents (Posadino et al., 2018).

2.2.3 Main organic compounds identified in cardoon and their biological effects

Traditionally C. cardunculus has been used for human consumption (Barbosa et al., 2020) given its high nutritional value. Cardoons are also considered a source of bioactive molecules due to nutraceutical and pharmaceutical properties (Silva et al., 2022).

Literature discusses the potential uses of the leaves of *Cynara cardunculus L. var.altilis*, due to the presence of a wide range of organic compounds. They are known for their therapeutic potential as a diuretic, hypocholesterolaemia (Ramos et al., 2017), cardiotonic, antidiabetic, anti-hemorrhoidal agent (Barracosa et al., 2019), anti-inflammatory, anticancer, antioxidant, hepatoprotective, hypolipidemic, and antidiabetic activity (Silva et al., 2022).

C. cardunculus L. var. altilis extracts from leaves are antioxidant and have antimicrobial properties against bacteria and fungi (Ramos et al., 2013). Many studies focus on the antioxidant properties of leaf extracts, showing that it is strictly related to the polyphenol fraction. Polyphenols play an important role in growth, reproduction, and protection for the cardoon plants (Beckman, 2000), and show that the conditions of cultivation may affect the phenolic composition of cardoon extracts (Moglia et al., 2008). Studies also explore the

effect of cardoon polyphenols in lipid metabolism, through the reduction of cholesterol and endogenous triglyceride production (Barracosa et al., 2019).

Mainly polyphenols are hydroxycinnamic derivatives, such as mono- and di-caffeoylquinic acids, and flavonoids (Barbosa et al., 2020), such as apigenin, luteolin (Pandino et al., 2011) and silymarin, a complex of organic molecules, mostly present in the seeds of *Carduus marianus L., Asteraceae* (Pandino et al., 2011). High content of these compounds confers antibacterial properties (Barracosa et al., 2019).

From traditional medicine, the biologically polyphenolic components that are extracted from the leaves of *Cynara scolymus* have been scientifically proven to be effective on pathologies involving the biliary tract, on scurvy, and on anaemia. They facilitate digestion and have an anti-atherosclerotic effect (Gebhardt, 1997). For these reasons they are used in the complementary treatment to a high-calorie high-fat diet, with the aim of reducing the undesirable effects of drugs taken by patients to control metabolic disorders (Ben Salem et al., 2019).

The main lipophilic components are represented by pentacyclic triterpenes and sesquiterpenes, known for their antioxidant activity (Ramos et al., 2017, 2013; Scavo et al., 2019).

Pentacyclic triterpenes have also been identified as the main lipophilic constituents of *C. cardunculus L. var. altilis*, although less present in these leaves, where they represent only 8% of total extracted compounds. On the other hand, fatty acids are reported to be mainly concentrated in the leaves, especially the saturated ones obtained by using the Soxhlet extraction method with dichloromethane (Ramos et al., 2013). Using this extraction method squalene was also detected in *C. cardunculus L. var*. *altilis*, an intermediate terpene in the biosynthesis of cholesterol and steroid hormones. Squalene is widely distributed in nature (Huang et al., 2009). Experimental studies have shown that squalene can effectively inhibit chemically induced skin, colon, and lung tumorigenesis in rodents (Auffray, 2007).

The phytotoxicity, cytotoxicity, antiviral activity, fungicidal activity and antimicrobial activity are all attributable to the presence of sesquiterpene lactones (Barbosa et al., 2020; Fernández et al., 2006). In particular, cynaropicrin and grosheimin have previously been identified in high amount in the globe artichoke (*Cynara cardunculus var. scolymus*) (Eljounaidi et al., 2015;Rouphael et al., 2016). Cardoon leaf extracts are rich in cynaropicrin, a sesquiterpene lactone (Ramos et al., 2017). Cynaropicrin was isolated from artichoke (*Cynara scolymus L.)* in 1960 for the first time and was later also found in *Cynara cardunculus L*. Cynaropicrin has important pharmacological uses Cynaropicrin: can indirectly inhibit the hepatitis C virus, as evidenced by various scientific studies; it is effective as an anti-inflammatory can control the activity of pro-inflammatory cytokines TNF-α; and has high antioxidant power. Therefore, cynaropicrin, used as an adjunct to cancer treatment therapy, could prevent the progression of liver cancer (Moujir et al., 2020).

2.3 OBJECTIVES OF THE CHAPTER: EXPLOITATION OF THE BIOACTIVE MOLECULES OF CARDOON

The valorization of biomolecules component in cardoon leaves extract was possible after the set-up of suitable protocols for supercritical CO_2 extraction ($scCO_2$) and the characterization of the chemical components of the extracts, which was carried out also for the extracts obtained at the University of Napoli Federico II using different extraction methods (Naviglio® and batch method).

The exploitation of the biological activity of the biomolecules contained in the cardoon leaves extracts has been investigated in the present thesis according to two lines of research:

1) use as additives in the formulation of bio-plastics obtained from proteins extracted from cardoon seeds, with the objective of improving mechanical and barrier features, as well as antioxidant properties for food and agricultural applications. It was demonstrated that the presence of cardoon leaves extracts increases the mechanical and barrier properties of the obtained materials. These results are encouraged to pursue in the study of potential application of these functional bio-plastics for the food sector with the aim of prolonging food fresh and maintaining the water vapor permeability value as low as possible confirming the potential of *Cynara cardunculus* as a biomass to be exploited within a circular biorefinery scheme for the production of high value products (Manuscript A: Mirpoor et al., 2021);

2) tested for their neuroprotectant properties against neurodegenerative diseases in vitro models of Rett syndrome (RTT). The rational of this approach stays on the observation that many plant-derived medications typically have a polypharmacological profile with antioxidant, anti-inflammatory and neurotrophic properties. The different extracts, but also four selected pure molecules identified in them, were tested for their effect of in rescuing neuronal development arrest in an in vitro model of Rett syndrome (RTT). Samples were obtained from plants harvested at different maturity stages and extracted with two different methodologies, Naviglio® and supercritical carbon dioxide ($scCO_2$). While $scCO_2$ extracts more hydrophobic fractions, the Naviglio® method extracts phenolic compounds and less hydrophobic components. Only the $scCO_2$ cardoon leaves extract obtained from plants harvested in spring induced a significant rescue of neuronal atrophy in RTT neurons, while the $scCO_2$ extract from autumn harvest resulted to be active on wild type (WT) neurons. More importantly, the extracts rich in cynaropicrin demonstrated a toxic effect on both WT and RTT neurons. This study indicates that it is crucial to design optimal extraction procedures, both in terms of selection of harvesting period and extractive technologies, to maximize the pharmacological potential of bioactive extracts. natural extracts consist of complex mixtures whose composition depends upon the extraction methods employed (Manuscript B, Spennato et al., 2022).

2.4 MATERIALS AND METHODS

2.4.1 Extraction by means of supercritical CO_2 of cardoon leaves and stalks

The cardoon plants (*C. cardunculus var. altilis) used in these studies* were kindly provided by Novamont Spa (Novara, Italy) and were taken from plants cultivated in Terni in Spring and Autumn 2020 and from an experiment of Sant'Angelo dei Lombardi (Avellino, Italy) in Aprile 2019. Details regarding other chemicals are reported in the "Materials and methods" sections of Manuscript A and Manuscript B.

The first set of $scCO_2$ extractions was performed on the plants collected in Autumn 2019 at Terni plantation (Novamont Spa site).

Cardoons were pre-treated by separating leaves and stalks, which resulted in 9 kg of fresh material. The material was cut by means of garden scissors in pieces of about 1 cm (leaves) or 2 cm (stalks), which were temporarily stored under vacuum in plastic bags (about 200g each) at -20°C. The material was dried by means of a first step of lyophilization for 48 h. The treatment allowed to remove about 82-85% of water, calculated by weigh difference. A second treatment in oven at 40°C for other 48 h was carried out that led to the removal of further 0.5% of water, respect to the lyophilized samples. The dried samples were temporarily stored under vacuum in plastic bags at +3°C.

Figure 2.3 *Lyophilisation of cardoons.*

6-8 g of dried leaves were loaded in a 100 mL extractor. The scO_2 extraction system was composed by a Separex SFE 20 unit (figure 2.4) (heated stainless-steel extractor 100-200 mL, laminating valve Tescom 304 26-1000, heated collecting chamber) connected to a liquid CO_2 cylinder, a high-pressure pump Lewa EKM210V1 and an EL-FLOW Bronkhorst flowmeter. Conditioning was performed for 30 min and then the extraction was started turning on the pump with a carbon dioxide flowrate of 120 L h^{-1} for 2 h at 45°C and 225 bar. The extracts were collected by dissolving the oily mixture in diethyl ether (< 1 mL). The extraction yields were 3.7 and 2.0 % (w w^{-1}) in the case of Autumn and Spring harvested plants respectively.

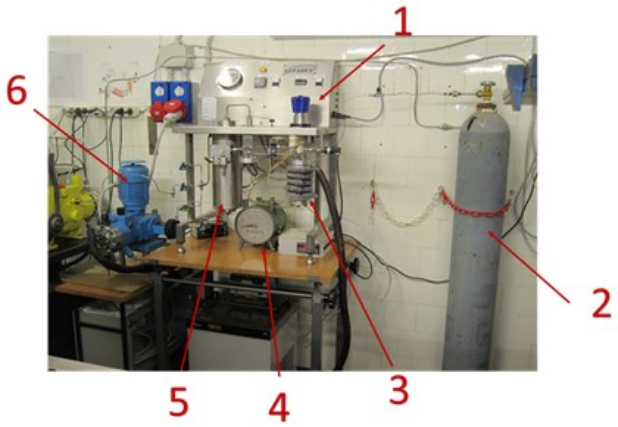

Figure 2.4 *scCO₂ instrument used for the extraction.*

The scCO₂ extraction instrument is composed by:

1. Laminating valve Tescom 26-1000
2. Liquid CO_2 cylinder
3. Heated separator. Flowmeter
5. Stainless-steel extractor (100-200 mL) with electric heating band
6. Pump Lewa EKM210V1 for liquid CO_2

2.4.2 Naviglio® extraction method (performed by a research group of University Federico II of Naples)

Filter bag (porosity of 100 μm) was filled with 40 g of cut cardoon leaves and then it was inserted into extraction chamber of Naviglio® extractor Lab. Model 500 cm3 capacity. Extractions were conducted using 625 mL of anhydrous ethanol at room temperature at pressure value of 9 bar, static phase 2 min: dynamic phase 2 min, with 12 s stop piston. Liquid samples (10 mL) were collected at 2, 4, 8 and 24 h (Naviglio, 2003). The leaf extracts (CLE) were kept at 4 ◦C until analysis. Ethanol was chosen as solvent for phenols extraction as described in literature (Kukic et al., 2008; Pinelli et al., 2007; Scavo, Pandino, et al.,2019).

2.4.3 Batch method (performed by a research group of University Federico II of Naples)

40 g of cardoon leaves were placed in a batch at room temperature with constant shaking while taking samples at the same times as extraction using Naviglio® extractor. Extracts were filtered through a Whatman filter paper and supernatants were kept at 4°C until analysis.

2.4.4 Characterization of extracts by ^{1}H-NMR

The NMR analysis was performed by dissolving 10 mg of CLE in 0.7 mL of deuterated chloroform. The ^{1}H NMR spectra were acquired at 25 °C by a Varian VNMRS 500 NMR spectrometer (11.74 T) operating at 500 MHz for proton, using 256 scans, interleaved by 7.7 s, with 45° pulses, employing a spectral width of 8012.8 Hz over 32 K complex points.

2.4.5 Characterization of extracts by GC-MS

The sample was prepared by dissolving 1 mg of CLE in 1 mL of diethyl ether and GC-MS analysis was carried out by a Shimazu GC-MS-QP2020 gas chromatograph. The gas chromatograph was equipped with a 30 m × 0.25 mm fused-silica capillary column (SLB5ms) coated with 0.25 µm film of poly (5% phenyl, 95% dimethyl siloxane). The temperature was monitored from 50 °C to 280 °C. The mass spectrometer was set to scan 33–700 m/ z. Samples were injected (1 µL) with a splitting ratio 1:20 and the injector temperature was set to 280 °C. The column oven was initially at 50 °C and was held for 2 min after the injection, followed by temperature ramping at 8 °C/min up to 250 °C, and 250–280 °C at 3 °C/min. The total run time was 63.33 min. Peaks were identified by comparing their mass spectra with the NIST14s database.

2.4.6 Quantification of bioactive molecules

The bioactive molecules were quantified by GC-MS (Shimadzu GC-MS-QP2020). Calibration curves were constructed by using commercial standards of cynaropicrin squalene, taraxerol, lupeol and dodecane as internal standard. In following figures (2.5÷2.8) are reported the calibration curve of each bioactive molecules. The analysis was performed on samples prepared by dissolving 0.7 mg of each CLE in 1 mL of diethyl ether. The separation was obtained on a 30 m- 0.25 mm fused-silica capillary column (SLB5ms) coated with a 0.25m film of poly(5% phenyl, 95% dimethyl siloxane). The mass spectrometer was set to scan the m/z range 33–700. Samples were injected (1 µL) with a splitting ratio 1:20 and the injector temperature was set to 280 °C. The column oven was initially set at 50 °C and maintained for 2 min after the injection, followed by a temperature ramp (8°C/min) up to 250 °C followed by a second ramp (3°C/min) up to 280°C. The total analysis time was 63.33 min.

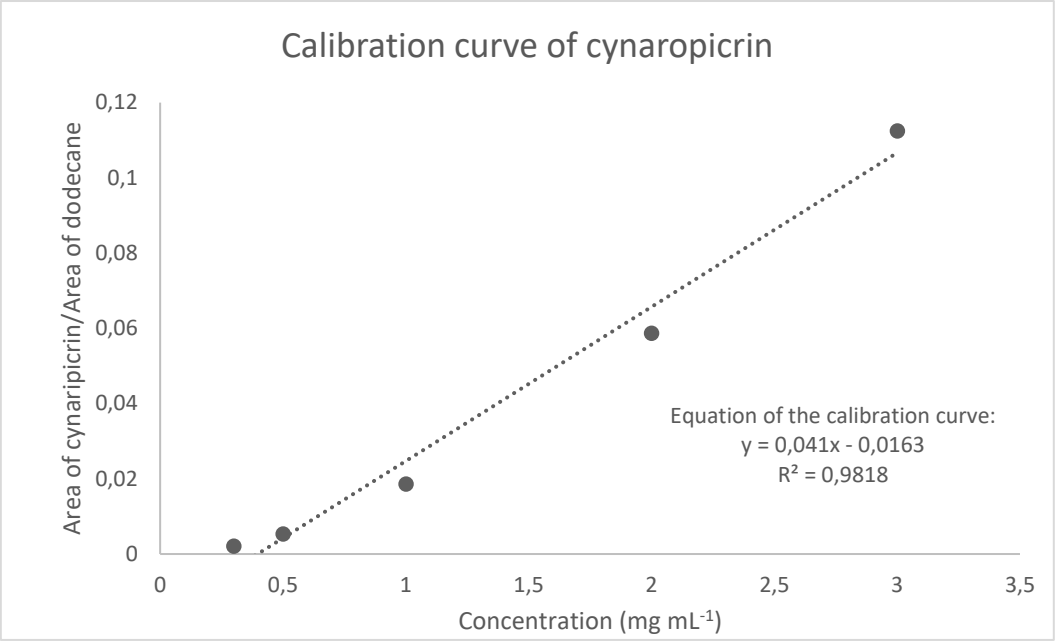

Figure 2.5 *Calibration curve of cynaropicrin obtained with GC-MS.*

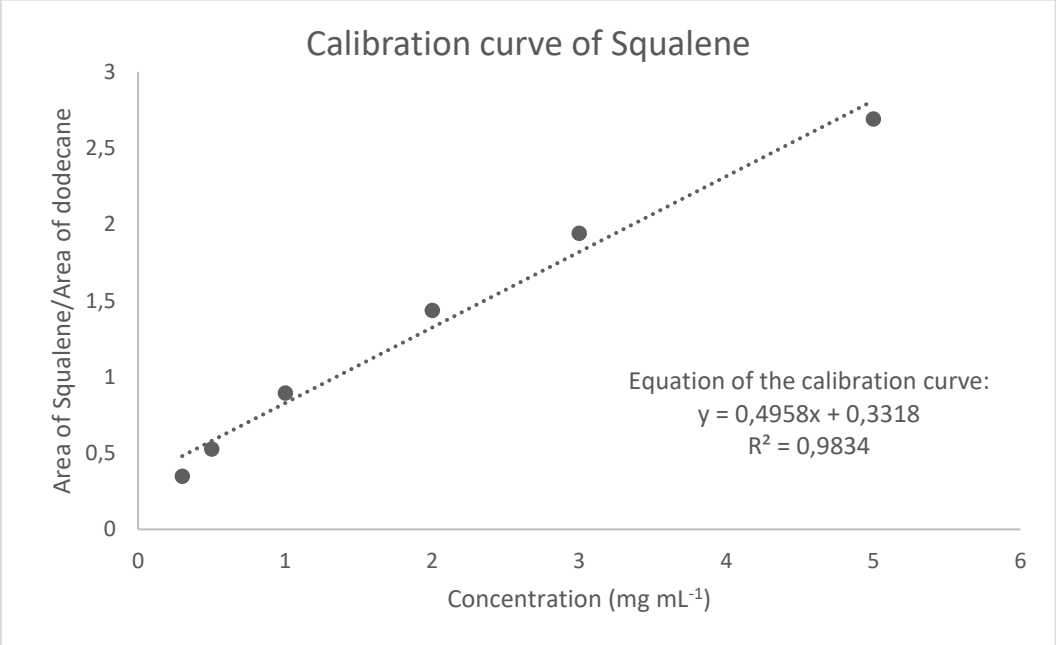

Figure 2.6 *Calibration curve of squalene obtained with GC-MS.*

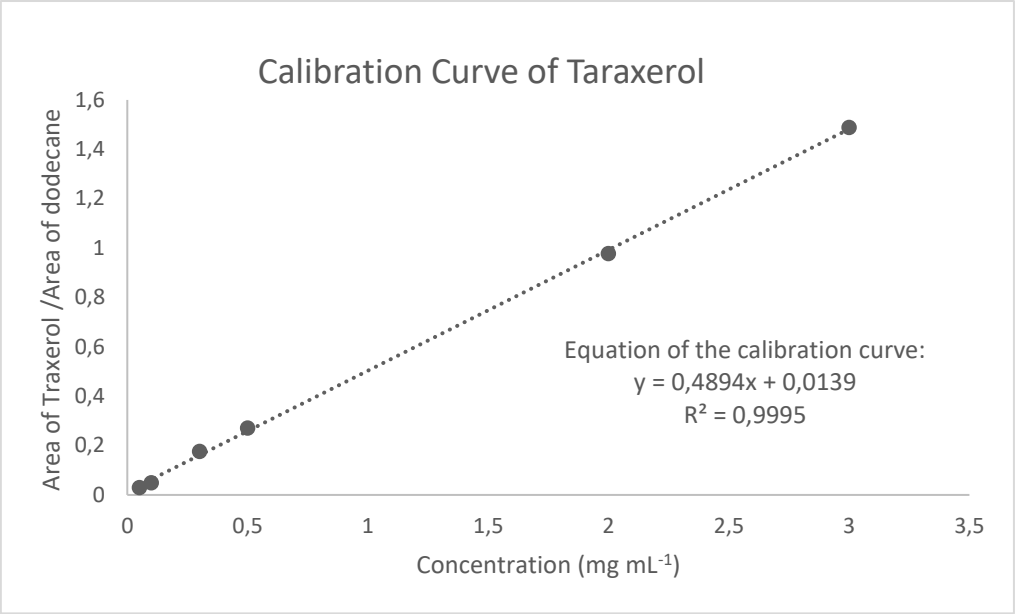

Figure 2.7 *Calibration curve of taraxerol obtained with GC-MS.*

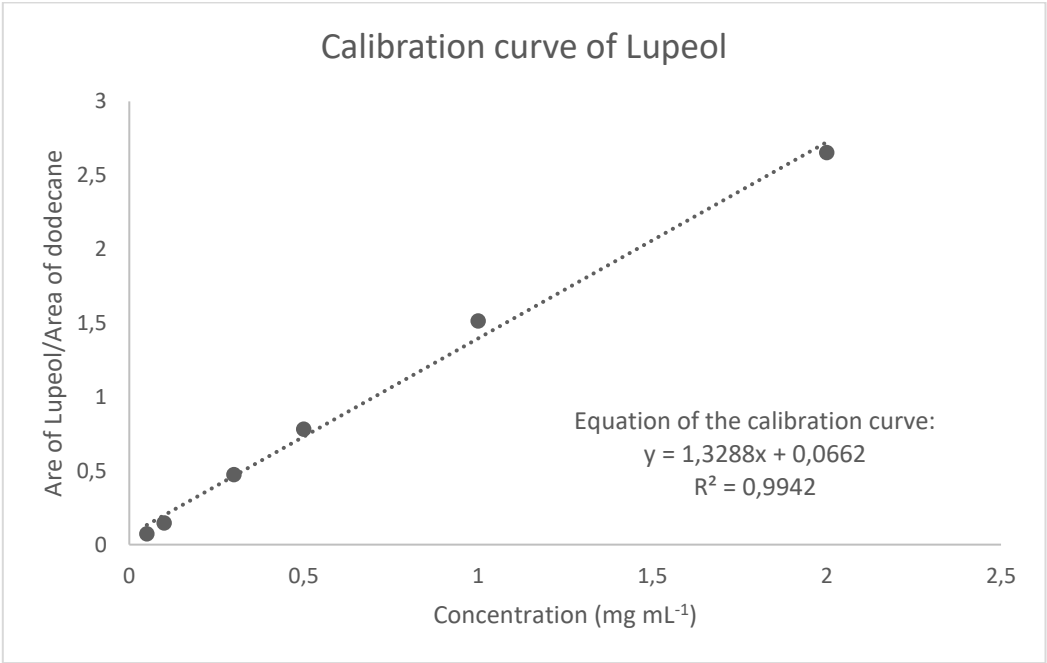

Figure 2.8 *Calibration curve of lupeol obtained with GC-MS.*

2.5 RESULTS AND DISCUSSIONS

2.5.1 Supercritical CO_2 extraction on leaves and stalks collected at Terni plantation in different harvest periods

Table 2.1 explicates the experimental conditions, which were adapted from protocols reported in a previous experimental study on cardoon (Alexandre et al., 2012) and the yields obtained from the extractions of the dried vegetable samples, both stalks and leaves.

Table 2.1 Extraction using $scCO_2$ from leaves and stalks collected in Autumn 2019.

#	Sample	Quantity loaded into the extractor (g)	Pressure (bar)	Temperature (°C)	Time of extraction (h)	Yield (% w w^{-1})
1	Stalks	10.45	130	35	2	<0.1
2	Stalks	9.83	225	45	2	<0.1
3	Leaves	6.78	225	45	2	<0.5
4	Leaves	7.49	130	35	2	1.0
5	Leaves	6.85	130	35	5	<0.5

The results indicate that the extraction yield values were very low. No extract was obtained from the stalks, whereas 1% w w^{-1} was extracted from the leaves using experimental conditions p=130 bar, T=35°C and time= 2 hours (entry #4 in table 2.1). In addition, the extraction time does not appear to affect the extraction yield, since an extraction time of 5 hours did not increase the yield. On the basis of these preliminary results, the experimental work was continued only on leaves and by processing cardoons collected in spring and autumn 2020 from the same plantation.

Several $scCO_2$ extraction conditions were tested starting from those of experiment #4. Cardoon leaves extracts (CLEs) were obtained in different yield percentages as reported in table 2.2.

Table 2.2 Experimental conditions and yields of $scCO_2$ extractions from leaves collected in spring and autumn 2020.

#	Harvest	Quantity loaded into the extractor (g)	Pressure (bar)	Temperature (°C)	Time of extraction (h)	Yield (% w w^{-1})
6	Spring (May2020)	9.77	130	35	2	0.47
7		9.86	225	45	2	0.63
8		10.08	225	45	2	1.02
9		10.15	225	45	2	0.67
10		10.08	300	50	2	0,79
11		10.15	300	50	2	2
12	Autumn (November 2020)	10.06	225	45	2	4.5
13		9.09	225	45	2	3.7

For spring leaves, the highest extraction yield was obtained with the experimental conditions described in entry 11 of table 2.2 (300 bar, 50°C). In the case of leaves collected in autumn 2020 higher yields were obtained working at 225 bar, 45 °C for 2 hours (#12-13 in table 2.2).

Figure 2.9 shows the extracts from the spring harvest (a) and the autumn harvest (b).

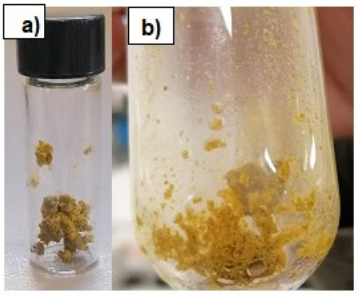

Figure 2.9 *$scCO_2$ extracts obtained from leaves collected in spring and autumn of 2020 using a) spring extract obtained using as experimental conditions 300 bar and 50 °C; b) autumn extracts obtained using 225 bar and 45°C.*

2.5.2 Characterization of extracts obtained by $scCO_2$

The different $scCO_2$ extracts were characterized using ^{1}H NMR spectroscopy and GC-MS and the main results are reported here below.

Autumn 2019 harvest at Novamont S.p.A. site

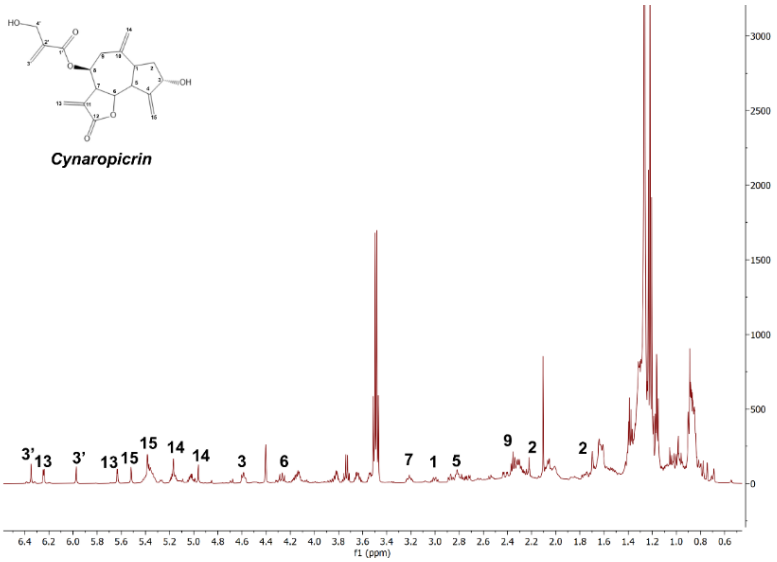

Figure 2.10 *^{1}H-NMR (500 MHz, $CDCl_3$) spectrum of extracts leaves collected in* ***autumn*** *2019 (table 2.1, entry #4).*

Figure 2.10 shows the ^{1}H-NMR spectrum of extracts from the leaves collected in autumn 2019. It was possible to identify sterols (δ: 0.55 m, -CH_3), triterpenes (δ: 0.69 s, -CH_2), fatty acids (δ: 0.85-0.93, m, -CH_3; δ:1.20-1.42 m; -CH_2 of alkyl chains; δ: 1.6, m -CH_2CH_2COOH; δ: 2.06, m -CH_2-CH-CH-; δ: 2.23 m -CH_2COO). Moreover, the typical signals of cynaropicrin were identified (signals assignment in the figure 2.10 by the comparison with the signals of the pure cynaropicrin reported in figure 2.11 taken from the work of Ha et al., 2003 (Ha et al., 2003).

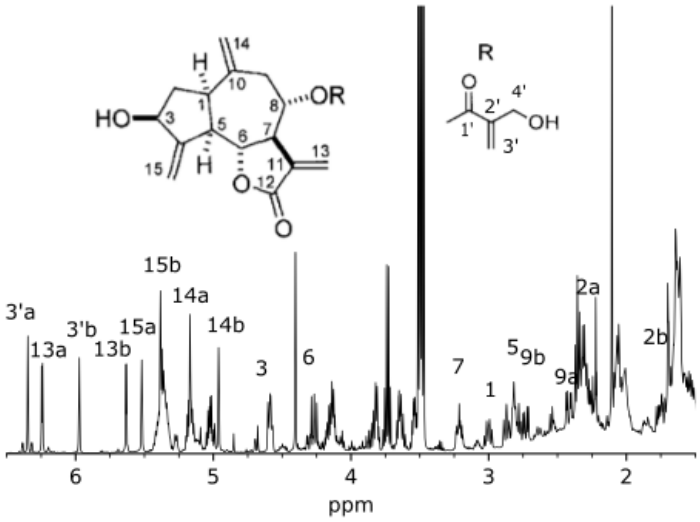

Figure 2.11 *Characteristic ^{1}H NMR signals of cynaropicrin assigned on the basis of literature data Ha et al., 2003 (Ha et al., 2003).*

Spring 2020 harvest at Novamont S.p.A. site

Figure 2.12 shows the ^{1}H NMR spectrum of the extraction from leaves collected in spring 2020 (#11 table 2.2).

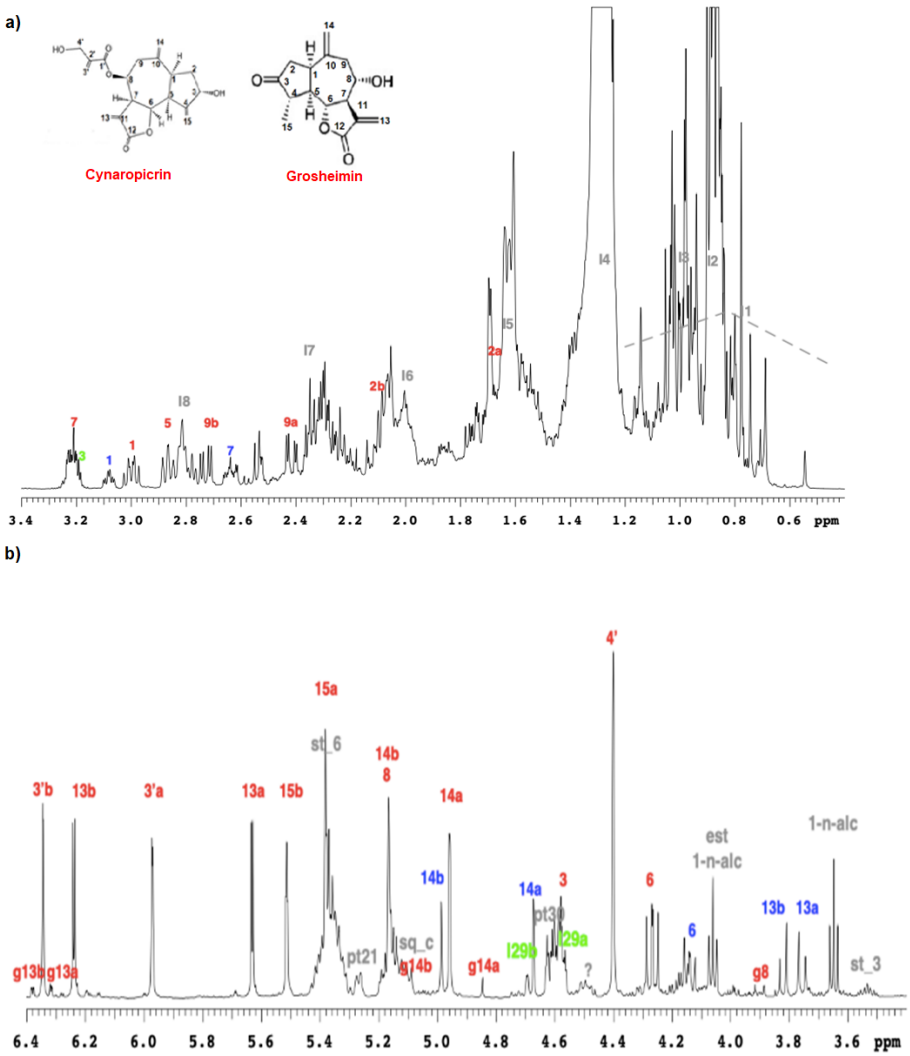

Figure 2.12 *^{1}H-NMR (500 MHz, CDCl3) spectrum of extracts leaves collected in* ***spring*** *2020 signals attributed to cynaropicrin (red) and signals to groshemin (blue), triterpenes (green), fatty acid (grey): a) region 0.6-3.4ppm . δ: 0.54 m, -CH_3 of sterols; δ: 0.69 s, -CH_2 of triterpenes; δ: 0.85-0.93, m, -CH_3 of fatty acids δ:1.20-1.42 m; -CH_2 of alkyl chains; δ: 1.6, m -CH_2CH_2COOH of fatty acids; δ: 2.06, m -CH_2-CH-CH-; δ: 2.23 m -CH_2COO and b) region 3.6-6.4 ppm.*

The spectrum in figure 2.12 is dominated by the presence of alkyl chain signals. In the spectrum it is possible to see the signals of sterols (Forgo and Kövér, 2004), phytosterols (Suttiarporn et al., 2015) and triterpenes (green signals in figure 2.12) as taraxerol and lupeol (Reynolds et al., 1986). Grey signals are attributed to: I2 as the region of -CH_3 of fatty acids chains, I3 as the region of -CH_3 of the linoleic and linolenic acids chains, I4 as the region of

-CH_2 related to alchilic chains, I5 as the region of -CH_2CH_2COOH of fatty acids, I6 as the region of -CH_2CH=CH, and I7 representing the -CH_2COO (Ramos et al., 2013; Sobolev et al., 2005).

<u>Autumn 2020 harvest at Novamont S.p.A. site</u>

Figure 2.13 shows the ^{1}H NMR spectrum of the extraction from leaves collected in autumn 2020 (#12 table 2.2).

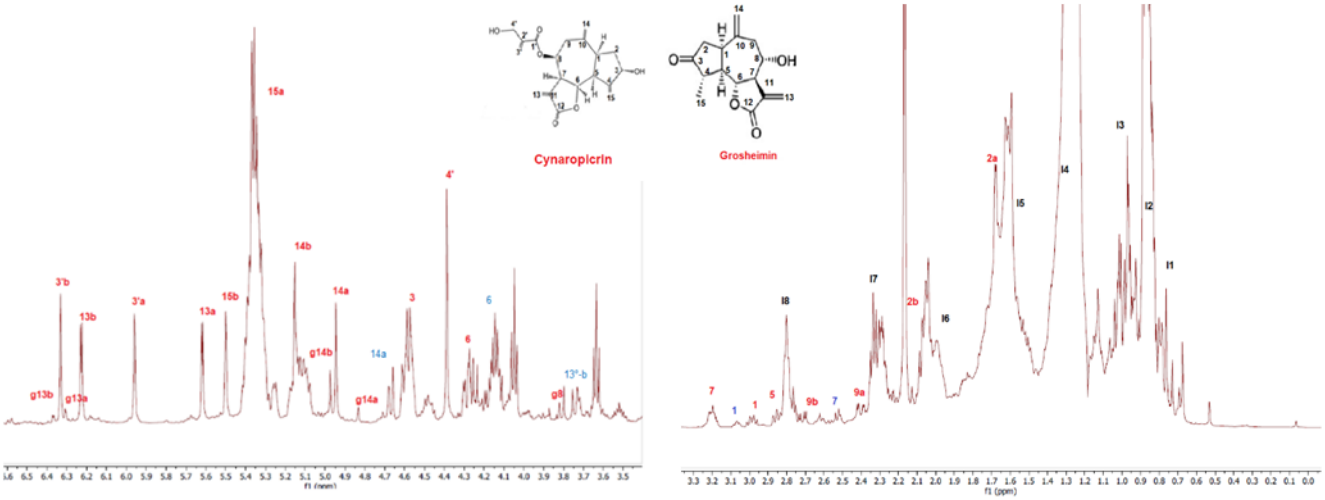

Figure 2.13 *^{1}H-NMR (500 MHz, CDCl3) spectrum of extracts leaves collected in autumn 2020: δ: 0.53 -CH_3 of sterols; δ: 0.71 -CH_2 of triterpenes; δ: 0.85-0.96 -CH3 of fatty acids; δ:1.30-1.22 -CH_2 of alkyl chains; δ: 1.59 -CH_2CH_2COOH of fatty acids; δ: 2.16 -CH_2-CH-CH- of fatty acids; δ: 2.21 -CH2COO; δ:4.61-4.54 signals of lupeol; δ:4.65-4.67 signal of taraxerol, δ:4.27, 4.48,4.94,5.14,6.33,6.22,5.95,5.61,5,49 typical signals of cynaropicrin.*

In this extract, similarly to the extract from leaves collected in spring 2020 (figure 2.12), it was possible to identify the presence of cynaropicrin, this is represented by the signals in red. In this spectrum it was also possible to identify another interesting molecule: grosheimin (red signals named “g”) (Adekenova et al., 2016). The signals marked in blue were attributed to a further molecule present in the sample: the 11,13-dihydroxy-8-desoxigrosheimin, a sesquiterpene lactone with a single double exocyclic bond. This was unexpected because the compound had only been found in small quantities in cardoon extracts (Shimizu et al., 1988). In figure 2.14 the structures of these three sesquiterpene lactones can be seen.

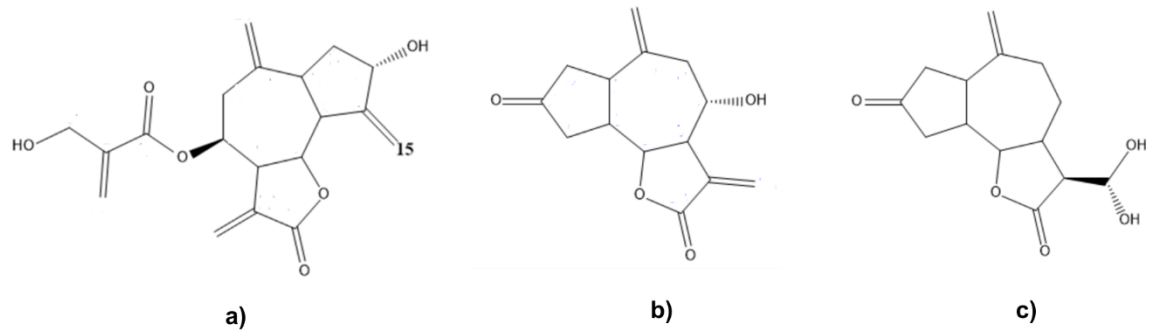

Figure 2.14 *Structures of a) cynaropicrin; b) grosheimin; c) 11,13-dihydroxy-8-desoxigrosheimin.*

The best extracts of the leaves collected in spring and autumn 2020 (entry #11 and 12 of table 2.2) were then characterized by means of GC-MS (figure 2.15).

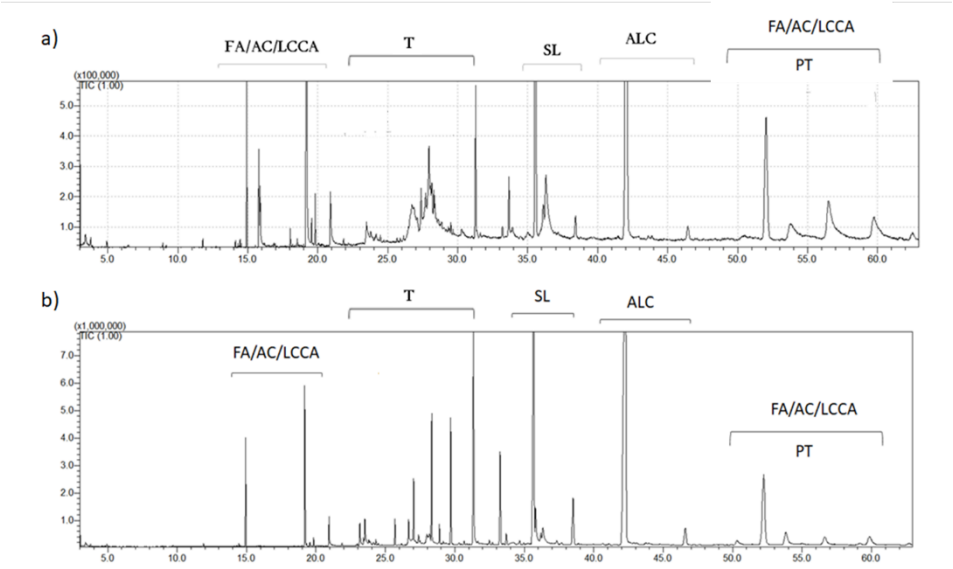

Figure 2.15 *GC-MS chromatogram of extracts: a) harvest spring 2020), b) harvest autumn 2020: FA= fatty acids, AC= aromatic compounds, LCCA= long chain aliphatic alcohols, T= triterpenes, SL= sesquiterpene lactones, ALC= alkanes with long chains, PT= pentacyclic triterpenes.*

The chromatograms are very complex but in the first part of the chromatogram it was possible to identify fatty acids (FA), aromatic compounds (AC), and long chain aliphatic alcohols (LCCA).

The GC-MS chromatogram indicates the presence of triterpenes (T), in particular squalene that was difficult to identify only by ^{1}H NMR, because its characteristic signals were covered by other molecules.

At RT (retention time) 35 minutes was identified the sesquiterpene lactones as cynaropicrin and grosheimin (SL).

The last part of the chromatogram is characterised by the signals of alkanes with long chains (ALC) and stearyl esters (STE) (Mathe et al.,2004;Ramos et al., 2013). There are also peaks related to pentacyclic triterpenes (PT), and they are in agreement with the ^{1}H NMR spectra of figures 2.12 and 2.13 where it was possible to identify the signals related to lupeol and taraxasterol, pentacyclic triterpenes molecules.

Spring 2019 harvest at Sant'Angelo field

The $scCO_2$ extraction was applied also to the leaves collected in spring 2019 from a different plantation, namely an experimental field in Sant'Angelo (Avellino). The extraction was performed at 225 bar, 45 °C for 2 hours of extraction. The yield of this extraction was 2% w w^{-1}. Characterization of these extracts was performed by using ^{1}H NMR spectroscopy (figure 2.16) and GC-MS (figure 2.17).

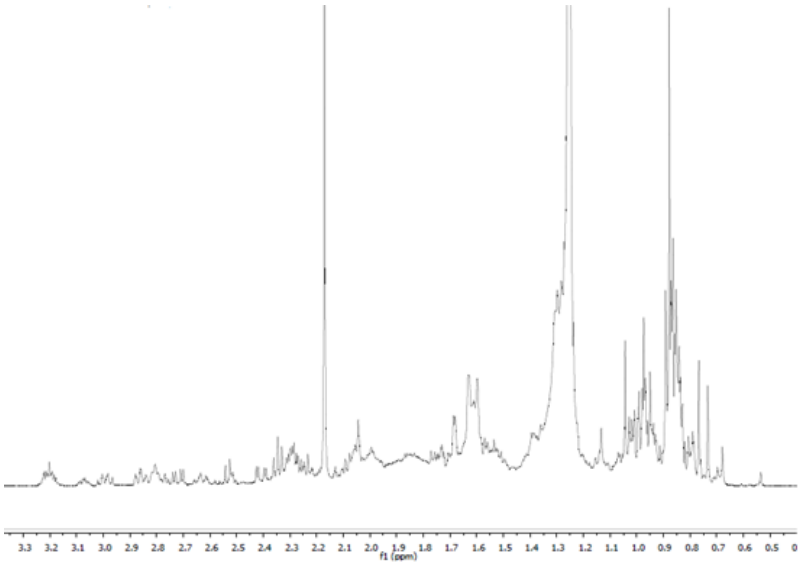

Figure 2.16 *^{1}H NMR spectrum of extract from leaves collected from the Sant'Angelo field in spring 2019.*

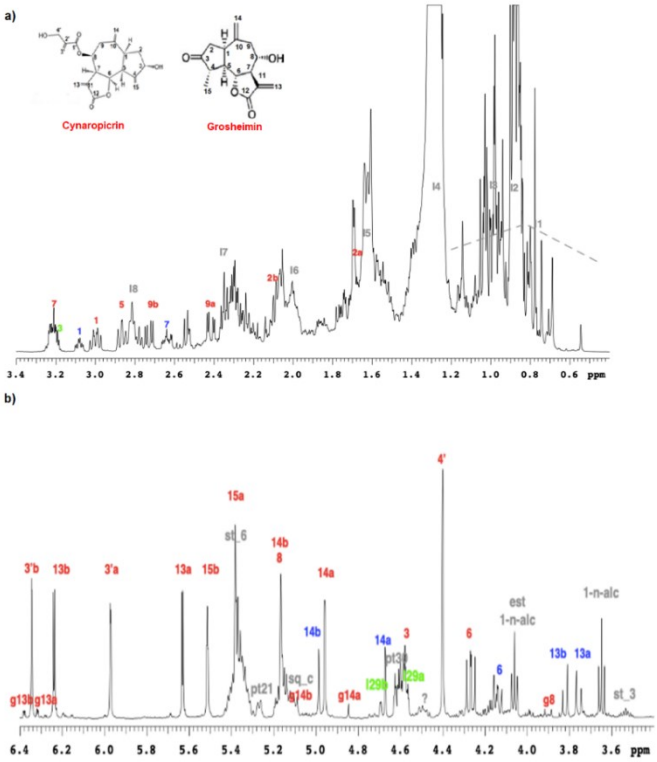

Figure 2.17 *(reported above) [1]H-NMR (500 MHz, CDCl3) spectrum of extracts of leaves collected in spring 2020 signals attributed to cynaropicrin (red) and signals to groshemin (blue), triterpenes (green), fatty acid (grey): a) region 0.6-3.4ppm . δ: 0.54 m, -CH_3 of sterols; δ: 0.69 s, -CH_2 of triterpenes; δ: 0.85-0.93, m, -CH_3 of fatty acids δ:1.20-1.42 m; -CH_2 of alkyl chains; δ: 1.6, m -CH_2CH_2COOH of fatty acids; δ: 2.06, m -CH_2-CH-CH-; δ: 2.23 m -CH_2COO and b) region 3.6-6.4 ppm.*

The [1]H NMR spectrum (figure 2.16) was comparable to the [1]H NMR spectrum of the extracts from the leaves taken from the Terni field in spring 2020 at the Novamont S.p.A. site (figure 2.12). The spectrum shows the presence of the -CH_3 of sterols and triterpenes, the -CH_3 of the chains of *fatty acids*, and the -CH_3 of the chains of linoleic and linolenic acids (Sobolev et al., 2005). It was possible to identify cynaropicrin, grosheimin and 11,13-dihydroxy-8-desoxigrosheimin, like the samples analysed before (Adekenova et al., 2016). The presence of these molecules was confirmed by the GC-MS chromatogram reported in figure 2.18.

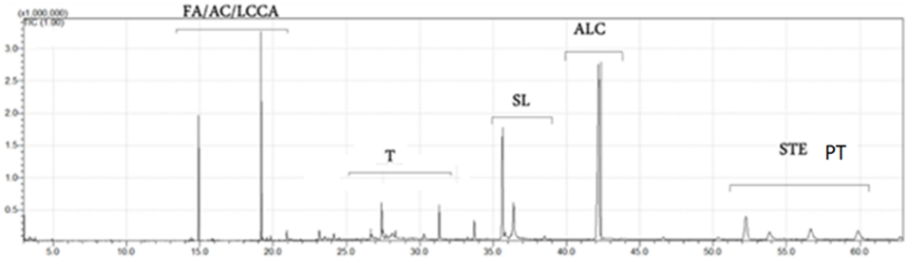

Figure 2.18 *GC-MS chromatogram of CLE from Sant'Angelo plantation from spring leaves 2019: FA= fatty acids, AC= aromatic compounds, LCCA= long chain aliphatic alcohols, T= triterpenes, SL= sesquiterpene lactones, ALC= alkanes with long chains, STE= stearyl esters; PT= pentacyclic triterpenes.*

The chromatogram indicates the presence of fatty acids (FA), aromatic compound (AC), and long chain aliphatic alcohols (LCCA). Moreover, the chromatogram also indicates the presence of triterpenes (T). At RT = 35 minutes the chromatogram shows the presence of sesquiterpene lactones, cynaropicrin and grosheimin. The last part of chromatogram is characterised by signals of alkanes with long chains (ALC), stearyl esters (STE) (Mathe et al., 2004; ,Ramos et al., 2013) and pentacyclic triterpenes (lupeol and taraxerol), the presence of which is also confirmed by ^{1}H NMR analysis.

2.5.3 Characterization of extracts obtained using Naviglio® and batch methods

The results of $scCO_2$ extractions were compared with results obtained for the extracts from the University of Naples, partner in the CARDIGAN project, using Naviglio® technology or batch extraction methods. The details of the extraction procedures are reported in section "Materials and Methods" in subsections 2.4.2 and 2.4.3. These two extraction methods were applied to cardoon leaves collected in two different fields: the Novamont S.p.A. site and the experimental field of Sant'Angelo. The raw material was collected in spring 2019 and spring 2020. The samples are summarized in the table 2.3.

Table 2.3 Characterized samples received from University of Naples.

Plantation	Harvest period	Extraction method	Extraction time (h)
Sant'Angelo	Spring 2019	Naviglio®	24
Sant'Angelo	Spring 2019	Batch	24
Novamont Spa	Spring 2020	Naviglio®	24
Novamont Spa	Spring 2020	Batch	24

These extracts were characterized using ^{1}H NMR and GC-MS. The analysis shows a clear presence of cynaropicrin and fatty acids, in particular linoleic acid. We can see this in Figure 2.19 (a,b) which shows the ^{1}H NMR spectrum of cardoon extract obtained from leaves collected in spring 2019 in the Sant'Angelo field using Naviglio®.

In these extracts the signals of ethanol are also evident, due to the utilization of ethanol as solvent for both Naviglio® and batch extraction methods. Another compound identified in these extracts are pheophytins that are responsible of the extracts' green colour (Sobolev et al., 2005) (figure 2.20, a,c).

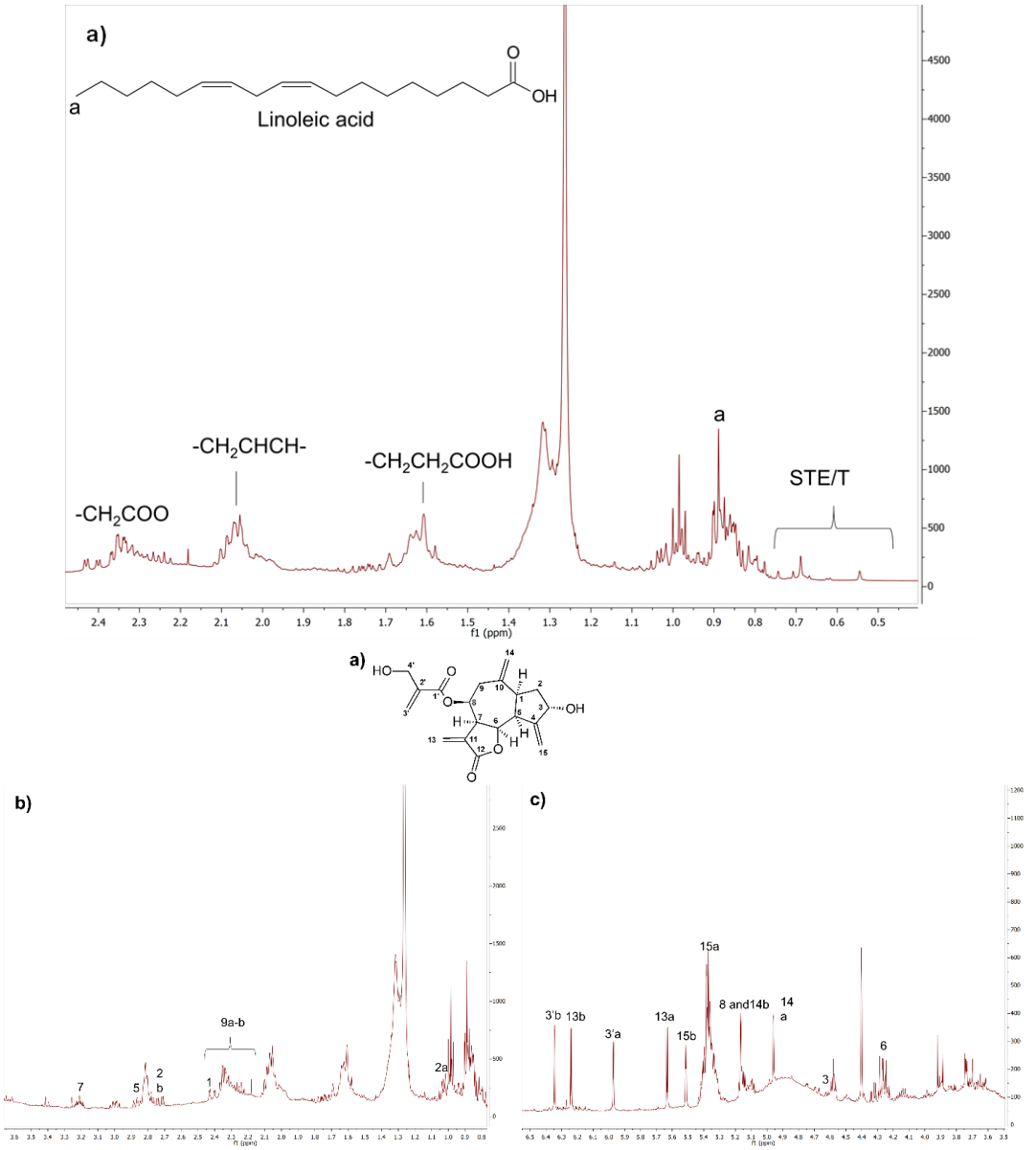

Figure 2.19 *^{1}H NMR spectrum (500 MHz, $CDCl_3$) of spring 2019 extracts from Sant'Angelo field obtained by using Naviglio®. a) in the range of 0.4–2.4 ppm. Further experimental details are given in the text. b) Signals of cynaropicrin in the range of 0.9–3.6 ppm; c) signals of cynaropicrin in the range of 3.5–6.5 ppm δ: 2.43, dt; 2a δ: 1.09, ddd; 2b δ:2.07, dt; 3 δ:4.62, tt; 5 δ:2.84,dd; 6, δ:4.27,dd; 7 3.27, tt; 8 and 14b δ:5.17,ttt; 9a-b δ:2.25–2.45, dd; 13a δ:5.62,d; 13b, δ:6.25,d; 14a δ:4.96,d; 15a δ: 5.43,t; 15b δ:5.52,t; 3' a δ:5.9,m; 3' b δ:6.35, m.*

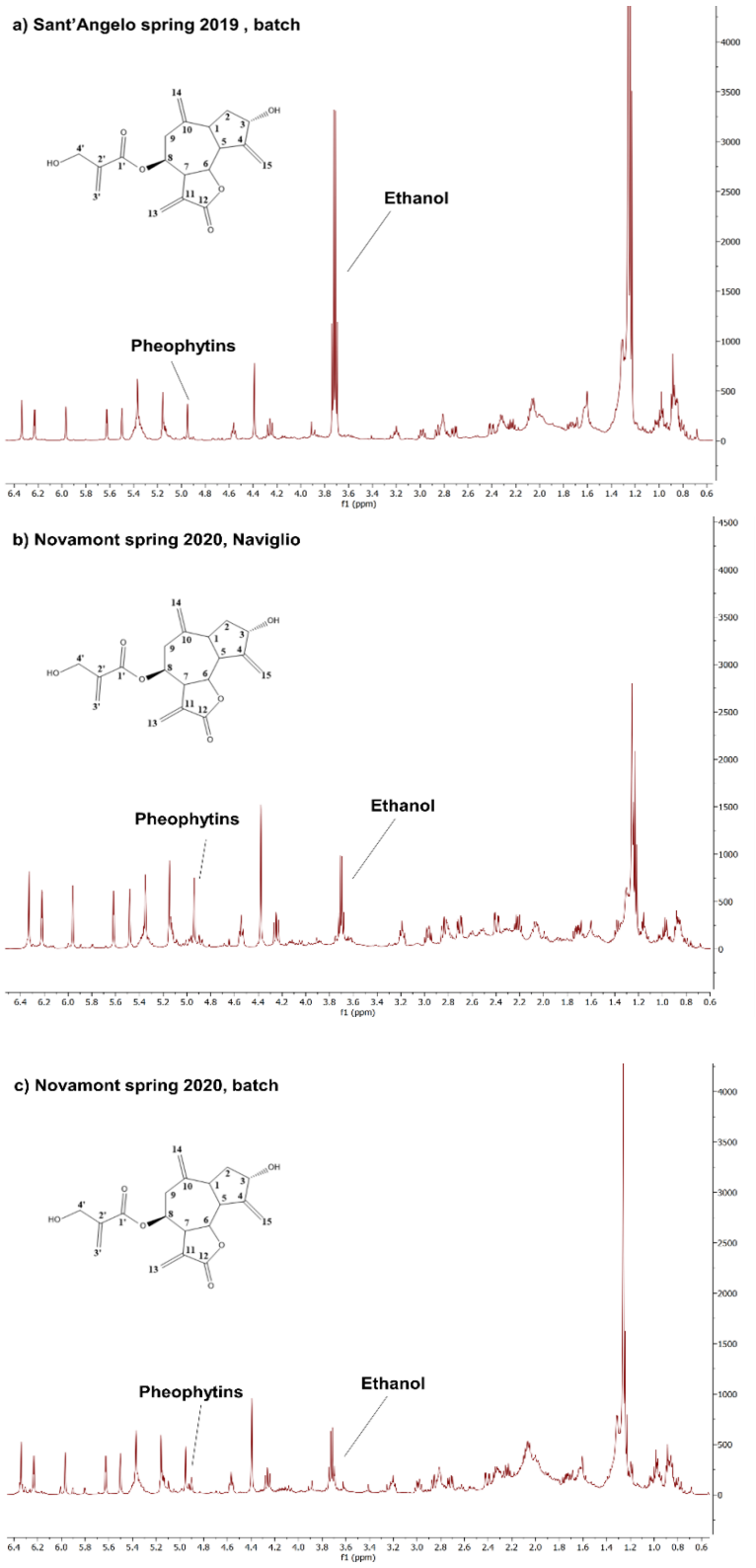

Figure 2.20. *^{1}H NMR spectrum (500 MHz, $CDCl_3$) of a) Sant'Angelo spring 2019, batch; b) Novamont spring 2020, Naviglio; c) Novamont spring 2020, batch. Signals of cynaropicrin: δ: 2.43ppm, dt; 2a δ:1.09ppm, ddd; 2b δ:2.07ppm, dt; 3 δ:4.62ppm , tt; 5 δ:2.84ppm,dd; 6, δ:4.27ppm,dd; 7 3.27ppm, tt; 8 and 14b δ:5.17ppm,ttt; 9a-b δ:2.25–2.45ppm, dd; 13a δ:5.62ppm,d; 13b, δ:6.25ppm,d; 14a δ:4.96ppm,d; 15a δ: 5.43ppm,t; 15b δ:5.52ppm,t; 3' a δ:5.9ppm,m; 3' b δ:6.35ppm, m; δ:4.49 ppm signal of pheophytins; δ: 3.7ppm signal of ethanol.*

The GC-MS chromatograms corresponding to the four extracts are presented in figure 2.21 a-d.

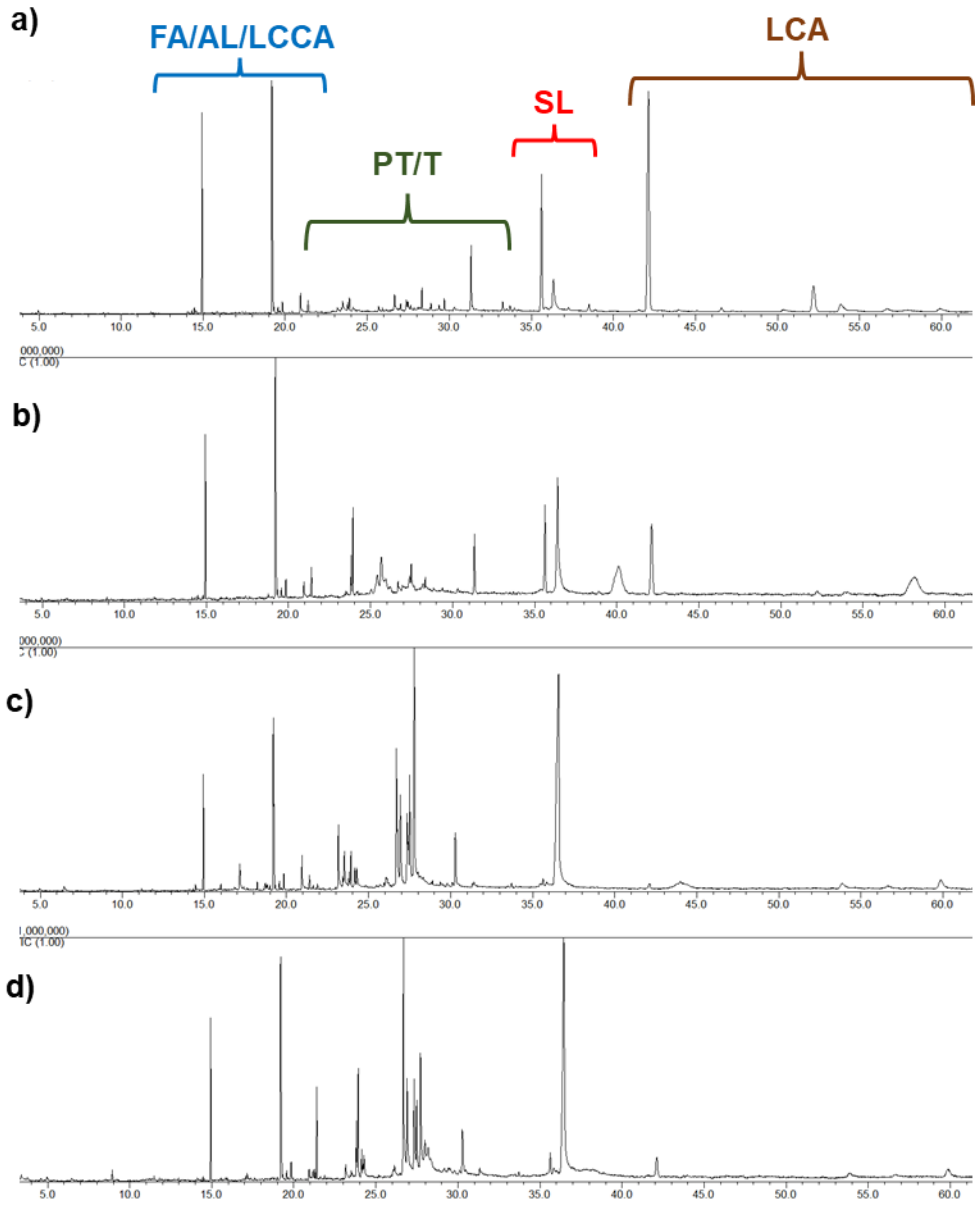

Figure 2.21 *GC-MS chromatogram of the four extracts obtained at the University of Naples using the Naviglio technology (a,c) and the batch method (b,d). Each colour zone corresponds to a specific group of compounds: Blue=fatty acids, aromatic compounds, and long chain aliphatic alcohols; green= triterpenes and pentacyclic triterpenes, red=sesquiterpene lactones; brown=alkanes with long chains.*

More details of the signals corresponding to the molecules present in the extracts can be found in the GC-MS chromatogram (figure 2.22) of the extracts obtained by means of the Naviglio® and using the leaves collected at the Sant'Angelo plantation in spring 2019. This sample was analyses in detail because it was used for the project related to the formulation of functional bio-based films described in Manuscript A hereinafter (section 2.5.6.1).

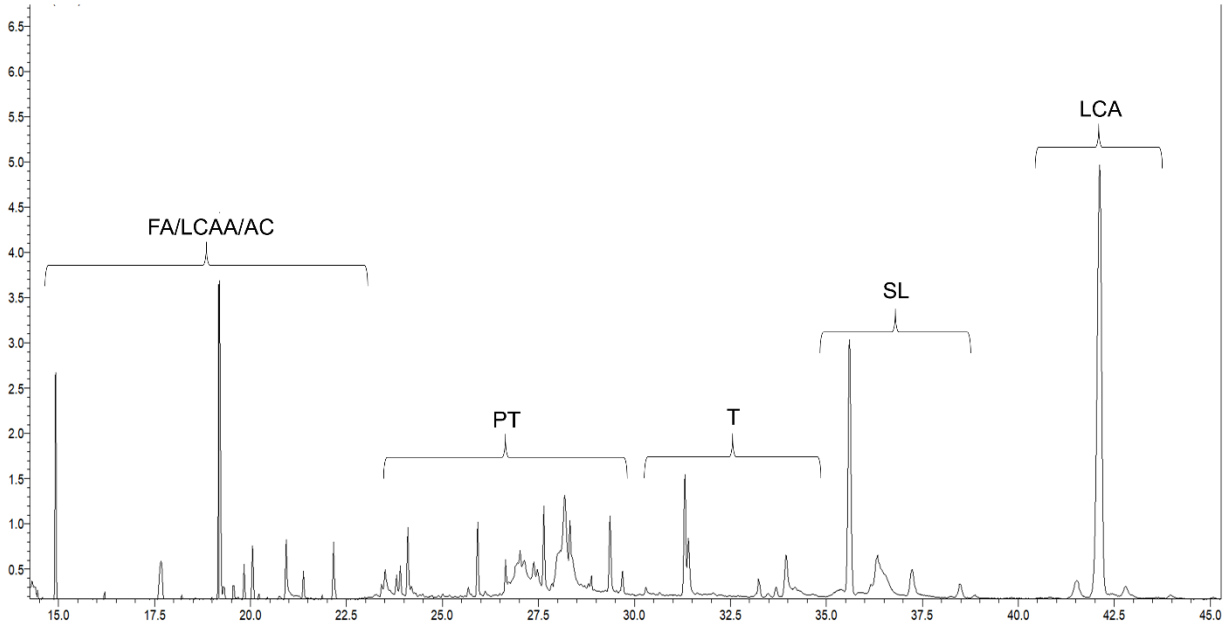

Figure 2.22 *GC-MS chromatogram: FA= fatty acids, AC= aromatic compounds, LCCA= long chain aliphatic alcohols, PT= pentacyclic triterpenes, T= triterpenes, SL= sesquiterpene lactones, ALC= alkanes with long chains, STE= stearyl esters.*

The GC-MS chromatogram provides qualitative information about the chemical composition of the extract (Mathe et al., 2004). The sesquiterpene lactones, cynaropicrin and grosheimin, can be identified at RT ranging from 35.61 to 37.25 minutes. The molecular formula of cynaropicrin is $C_{19}H_{22}O_6$, while that of grosheimin is $C_{15}H_{18}O_4$. It is not possible to discriminate between the peaks related to each of the two molecules due to the similarities in the molecular fragmentation for each of the two molecules with qualitative GC-MS analysis.

Fatty acids (RT = 19.17 minutes), long-chain aliphatic alcohols (RT = from 19.50 to 22 minutes) and some aromatic compounds were also detected in traces. The signal at 31.26 minutes is ascribable to squalene, whereas the signals in the range 23.45–29.73 minutes correspond to pentacyclic triterpenes. Finally, the signals of hydrophobic long chain alkanes are visible at the range 40–42.5 minutes.

2.5.4 Characterization of extracts obtained after two subsequent extraction methods (Novamont plantation, autumn 2019 and spring 2020)

The leaves collected at Novamont plantation in autumn 2019 and spring 2020 were also extracted by combining a first $scCO_2$ extraction step and a subsequent step using Naviglio® technology. The objective was to explore the possibility of extracting specific fractions of bioactive molecules by using different extraction methods. In fact, the $scCO_2$ method extracts more hydrophobic molecules and in principle the residue is expected to contain mainly the

less hydrophobic polyphenolic fraction, which can be efficiently extracted in the presence of a polar organic solvent.

The extracts obtained after the two subsequent treatments were analysed by ^{1}H NMR. Figures 23a and 23b show the ^{1}H NMR spectra of the extracts obtained from the autumn and spring harvest, respectively. They are very similar, with the predominant signals of cynaropicrin (numbers in red in the figures); there are also traces of signals of grosheimin (blue in figures). Other signals are related to fatty acid chains as reported in spectra in section 2.5.2.

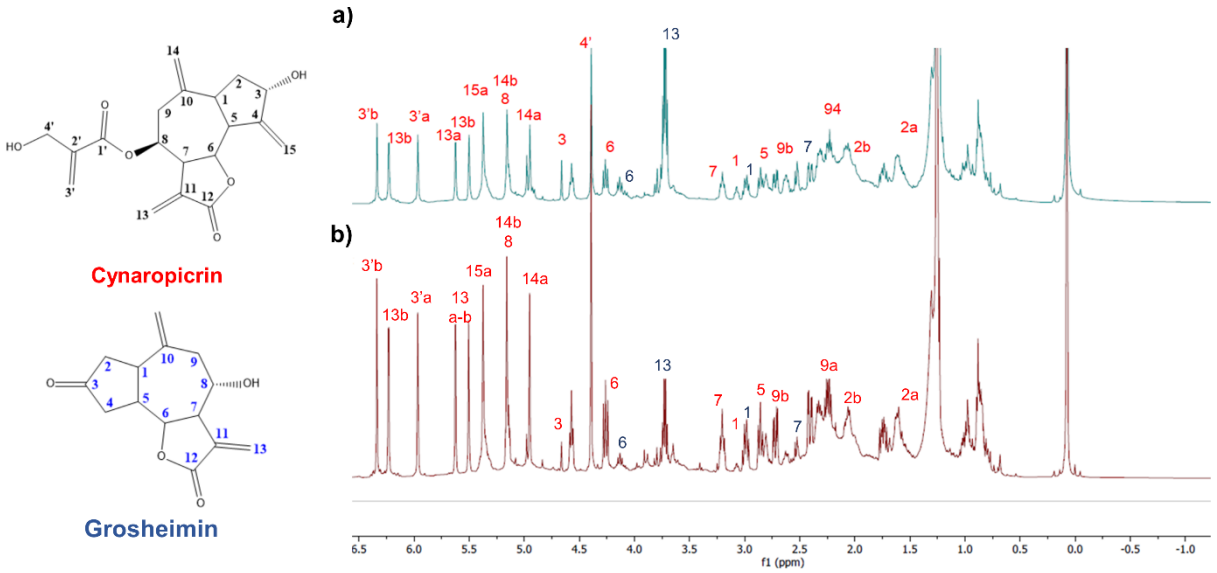

Figure 2.23 *^{1}H NMR (500 MHz, $CDCl_3$) spectra of extracts obtained after the $scOO_2$ + Naviglio® methods in sequence : a) autumn 2019 harvest, b) 2020 harvest (Terni plantation).*

The application of the two complementary extraction methods allowed us to obtain a fraction of bioactive molecules containing mainly sesquiterpene lactones, cynaropicrin in particular.

2.5.5 Semi-quantitative analysis of cynaropicrin in all extracts by ^{1}H NMR analysis

Due to the complexity of the chemical composition of the extracts obtained in this study, the NMR signals are widely overlapped, making integration difficult and the quantification of each molecule not feasible. Therefore, a first quantification was focused only on cynaropicrin, a bioactive molecule with relevant pharmacological activities as reported in section 2.2.3 (Moujir et al., 2020). The cynaropicrin was clearly identified in the extract by means of ^{1}H NMR.

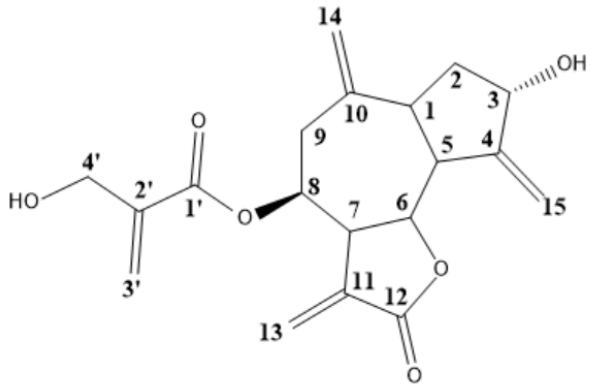

Figure 2.24 *Structure of cynaropicrin.*

The quantification of cynaropicrin was accomplished by taking as a reference the ^{1}H NMR signal of -CH_2 protons at 4' position (figure 2.24), having a theoretical integral value of 2. Considering the integral value of all protons present in the spectrum in the range 0.5-6.5 ppm, the proton of cynaropicrin corresponds to the % of the protons present in the mixture by applying the following equations:

$$\%\ cynaropicrin = \frac{22}{I_t}\ x\ 100$$

Where 22 is the total number of protons of cynaropicrin and I_t is the theoretical integral value of all protons in the range 6.5-0.5 ppm calculated as follows:

$$Theoretical\ integral\ value\ (range\ 0.6 - 6.5\ ppm) = \frac{84.12\ x\ 2}{Iexp} = 197.98$$

Where *IexpTOT*: experimental integral value of all protons in the range 0.5-6.5ppm

Iexp: experimental integral value of the -CH_2 protons at 4' position.

Figure 2.25 reports the histogram that represents the percentage of cynaropicrin in all extracts considered in this study.

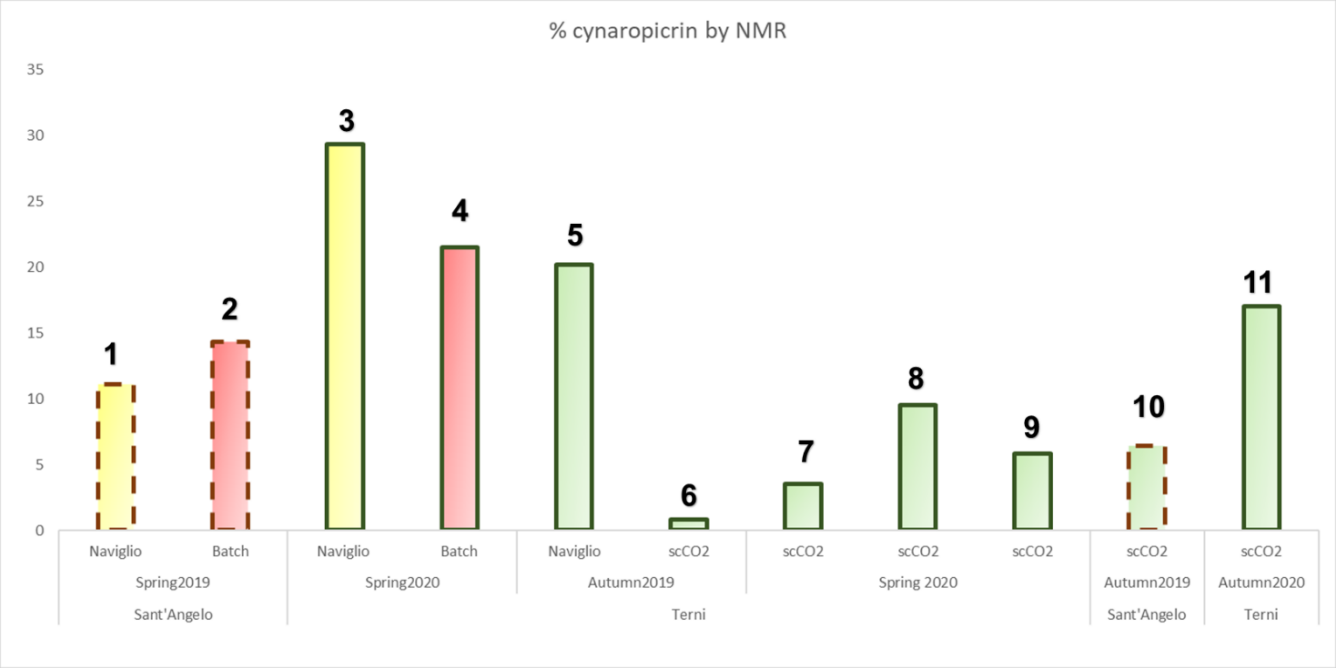

Figure 2.25 *Percentage of cynaropicrin in all cardoon leaves extracts. Samples 6-11 were obtained in different $scCO_2$ extraction conditions: 6-7: 130 bar, 35°C; 8: 225 bar, 45°C; 9: 300 bar, 50°C; 10-11 225 bar, 45°C.*

As can be seen from the histogram, sample 3 contains the largest amount of cynaropicrin (29%). This sample was obtained with Naviglio® technology from leaves collected in spring 2020 from the plantation in Terni.

Among the $scCO_2$ extracts from the spring 2020 harvest, the higher extraction yield was obtained using 225 bar and 45°C for two hours (column 8 in figure 2.24) with 9.5% of cynaropicrin extracted. The extraction yield with $scCO_2$ increased using the leaves of autumn 2020, reaching 17% (column 11 in figure 2.24) under the same experimental conditions (225 bar and 45°C).

When combining $scCO_2$ extraction with subsequent Naviglio® technology a higher cynaropicrin yield was obtained for the leaves collected in spring 2020 (respectively, 14% and 5.75% in Figure 2.26).

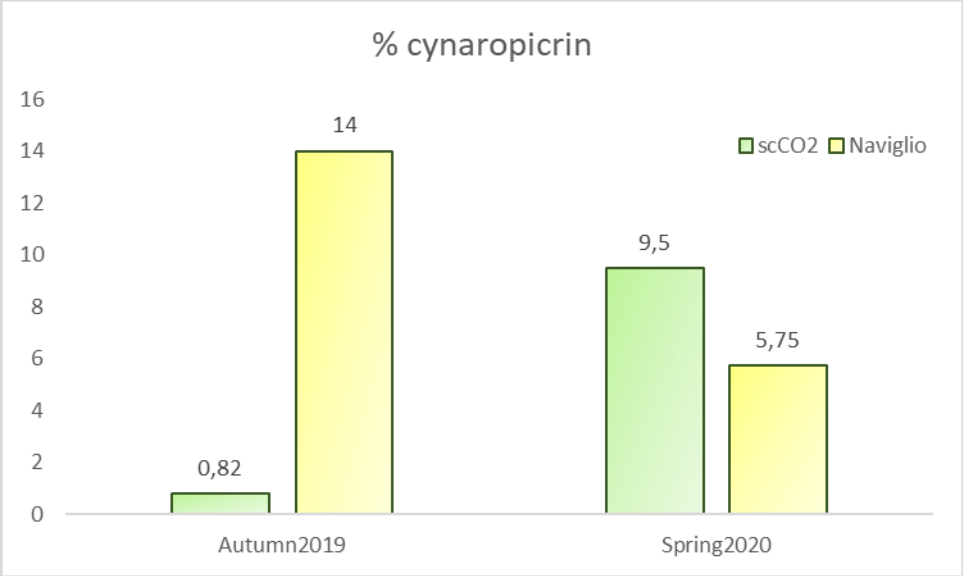

Figure 2.26 *Percentage of cynaropicrin obtained by a combination of $scCO_2$ extraction step and a subsequent Naviglio® technology in autumn 2019 and spring 2020. Green parts of histogram are columns 6 and 9, respectively, of figure 2.24*

2.5.6 Application of cardoon leaves extracts (CLEs) for the formulation and functionalization of bio-based polymeric films

On the basis of the data obtained in the study of characterization of the cardoon leaves extracts, two research projects were accomplished, having as objective the exploitation of the biological properties of the bio-active molecules. A first project, in collaboration with two research groups of the University Federico II of Naples, addressed the application of cardoon leaf extracts for the formulation and functionalization of bio-based polymeric films. It was demonstrated that the presence of cardoon leaves extracts increases the mechanical and barrier properties of the obtained materials as described in the publication reported hereinafter (Manuscript A). The study employed the extract obtained using Naviglio® technology from leaves collected from the Sant'Angelo plantation in spring 2019. The ^1H NMR characterization is reported in figure 2.18 and GC-MS characterization is reported in Figure 2.20a in section 2.5.3 above.

The functional bio-based films of "Manuscript A" were formulated at the University of Naples starting from proteins extracted from cardoon oil seed cakes. The extracts obtained by the Naviglio® method were dried and resuspended in ethanol. This extract was added to the cardoon-seed protein solution at different concentrations and the mixture was stirred for 1 hour. Glycerol was then added to obtain a final concentration of 50% (w/w protein) and the solution was cast on plastic petri dishes and finally dried in an environmental chamber at 25°C and 45% relative humidity for 24 hours. The dried films were peeled off and conditioned at 25 °C and 50% relative humidity, by saturated magnesium nitrate solution, for 24 hours before the analyses.

The bio-based films were characterized in terms of zeta potential, particle size, contact angle, along for their morphological and mechanical properties and antioxidant activity.

It is notable that particle size of CPs (Cardoon Proteins) FFS (Film Forming Solution) increased by the incorporation of higher concentrations of antioxidants in the FFS compared to the control sample. These results could be attributed to the interactions between the CP functional groups and the phenolic hydroxyl groups of antioxidants that formed larger CPs polymers that increase the polydispersity index (PDI), that is an indicator of relative variance in the particle size distribution.

- The protein surface charges were also affected by the addition of antioxidants and all the FFSs were stable, with negative zeta potential higher than 28 mV showing the high stability of solution. Zeta potential of CPs FFS decreased as a function of increasing the concentration of antioxidants due to the participation of negative functional groups of CPs in protein-polyphenols interaction and/or interactions between the CPs surface and CLE (cardoon leaves extract) that can modify the surface charge of the proteins.
- The ***contact angle*** of the different FFSs was measured and the results show that the addition of increasing amounts of CLE significantly decreased the contact angle value of the CP FFS in comparison to the control sample, thus indicating that the hydrophobicity of CP FFS significantly increased in the presence of increasing CLE concentrations.
- Thinner films were obtained by reducing the content of CPs until 70% and with a concurrent increase in the CLE amount to 30%. Results indicated that the film thickness slightly increased as a function of the CLE amount present in the film matrix, probably due to the interaction of CLE component(s) with the CP polymeric chains, via hydrogen bonding and hydrophobic forces. Polyphenols may lead to protein crosslinking, thus, increasing the film thickness.
- The films functionalized with 15% CLE were slightly less flexible than the ones prepared in the absence of the phenolic components showing a lower elongation at break, however a significant increase in tensile strength and Young's modulus was observed as a result of CLE incorporation. The presence of CLE in the CP-based films increased their opacity. The density of CP-based films significantly increased by increasing CLE concentration, suggesting that the formation of hydrogen and hydrophobic bonds between proteins and CLE components increased by increasing CLE concentrations and led to a more compact film microstructure. The structural morphology of the films prepared with CLE appeared more homogeneous, continuous and smooth. On the other hand, the film prepared in the presence of 15% CLE seems smoother and more compact than that cast with 30%.
- ***Film barrier properties.*** CP-based films containing 15% CLE exhibited water vapor (WV) permeability values lower than those observed by testing CP films prepared in CLE absence, while WV water vapor permeability was found to be significantly increased with respect to control samples in the films obtained in the presence of CLE double concentration (30%).
- ***Antioxidant activity.*** Data show that the films freshly manufactured in the absence of CLE exhibited a marked antioxidant activity and that the addition of 30% CLE improved this property since the observed scavenging activity against DPPH radical

of the films increased from 30% to 60%. The antioxidant activity of all films remained quite stable after 30 days at room temperature, suggesting their potential exploitation as active packaging for shelf-life extension of foodstuffs. The materials functionalized with the highest amount of CLE seem to be still endowed with the highest antioxidant activity (45%) even after a period of 70 days, suggesting their possible application in protecting some foods from the oxidation.

In conclusion, these results are encouraging for those interested in pursuing the study of potential applications of these functional bio-plastics for the food sector with the aim of prolonging food freshness and keeping the water vapor permeability value as low as possible. Furthermore, a higher O_2 barrier property is also important since oxygen causes, for example, the rancidity of fatty acids. Therefore, the study confirmed the potential of *Cynara cardunculus* as a biomass to be exploited within a circular biorefinery scheme for the production of high value products.

2.5.6.1. **Manuscript A** *"A biorefinery approach for the conversion of Cynara cardunculus biomass to active films"*

Food Hydrocolloids 122 (2022) 107099

Contents lists available at ScienceDirect

Food Hydrocolloids

journal homepage: www.elsevier.com/locate/foodhyd

A biorefinery approach for the conversion of Cynara cardunculus biomass to active films

Seyedeh Fatemeh Mirpoor [a,1], Simona Varriale [a,1], Raffaele Porta [a,d], Daniele Naviglio [a], Mariachiara Spennato [b], Lucia Gardossi [b], C. Valeria L. Giosafatto [a,d,*], Cinzia Pezzella [c]

[a] Department of Chemical Sciences, University of Naples "Federico II", Complesso Universitario di Monte Sant'Angelo, Naples, 80126, Italy
[b] Dipartimento di Scienze Chimiche e Farmaceutiche, Università Degli Studi di Trieste, Via Licio Giorgieri 1, 34127, Trieste, Italy
[c] Department of Agricultural Sciences, University Federico II, Via Università 100, 8055, Portici, Italy
[d] Center for Studies on Bioinspired Agro-Environmental Technology (BAT), University of Naples "Federico II", Naples, Italy

ARTICLE INFO

Keywords:
Cynara cardunculus
Biorefinery
Bio-plastics
Cardoon seed proteins
Phenolic compounds

ABSTRACT

Cardoon *(Cynara cardunculus)*, an herbaceous perennial plant able to grow with high productivity in dry and hot regions, as well as in unproductive soils, was used as a biomass source for the production of both bioactive compounds derived from leaves and proteins extracted from seeds. Naviglio® technology was found as an efficient method to obtain a cardoon leaf extract (CLE) characterized by high phenol content and oxygen scavenging activity. On the other hand, cardoon proteins (CPs) were demonstrated to give rise to handleable greenish films endowed with promising mechanical and barrier properties in the presence of glycerol used as plasticizer. Hence, the CLE was used to functionalize the films that were further characterized. Film microstructure observed by SEM revealed a good compatibility among CPs and CLE, showing a uniform distribution of the leaf extract components throughout the film network that reflected, in turn, an improvement in the mechanical and barrier properties of the obtained material. In addition, the CLE containing films exhibited higher hydrophobicity, as indicated by the contact angle measurement and by the evaluation of water solubility and swelling degree experiments. Finally, CLE-containing films showed a marked antioxidant activity, highlighting the potential of *Cynara cardunculus* to be exploited as a biorefinery where different low-value renewable biomass materials are turned in several higher value bio-based products.

1. Introduction

Cynara cardunculus L., commonly named cardoon, is a perennial dicotyledonous plant widely distributed in the Mediterranean area that grows naturally in harsh habitat conditions with high temperature, elevated salinity and arid summer (Benlloch-González, Fournier, Ramos, & Benlloch, 2005). This plant is part of the Asteraceae (or Compositae) family, including the globe artichoke [var. *scolymus* (L.) Fiori], the cultivated cardoon (var. *altilis*), and the wild cardoon [var. *sylvestris* (Lamk) Fiori], considered to be their common ancestor (Pesce, Negri, Bacenetti, & Mauromicale, 2017). Although native from the Mediterranean area, cardoon has been spread to several other countries like the United States of America, Mexico, Australia, and New Zealand (https://www.cabi.org/isc/datasheet/17584). Due to its natural habitat, cardoon can grow in ash and poor conditions, with high temperatures, severe drought, and in infertile stony soils (Fernández, Curt, & Aguado, 2006), and, therefore, it is a very cheap and accessible crop. Besides, cardoon is a pollinator-supporting industrial crop, so that it is beneficial for the biodiversity. The high biomass productivity of cardoon has been exploited for multiple purposes, ranging from traditional uses to industrial applications. Mauromicale, Sortino, Pesce, Agnello, and Mauro (2014) studied the potential ability of cultivated and wild cardoons to produce energy in terms of biomass, achenes, and energy yield. The authors concluded that both cultivated and wild cardoon are potential energy crops and improved the soil fertility characteristics by increasing organic matter, total nitrogen, available phosphorus, and exchangeable potassium content. The annual average outcome of cultivated cardoon is 14.6 t/ha of dry biomass, 550 kg/ha of achenes, and 275 Gj/ha yields, while for wild cardoon, the outcome is 7.4 t/ha of dry biomass, 240 kg/ha of achenes, and 138 Gj/ha of energy yield. Cardoon has been popularly used by Greeks and Romans as food

* Corresponding author. Department of Chemical Sciences, University of Naples "Federico II", Complesso Universitario di Monte Sant'Angelo, Naples, 80126, Italy.
E-mail address: giosafat@unina.it (C.V.L. Giosafatto).
[1] Equally contributing authors.

https://doi.org/10.1016/j.foodhyd.2021.107099
Received 10 May 2021; Received in revised form 14 July 2021; Accepted 8 August 2021
Available online 9 August 2021
0268-005X/

Abbreviations

DPPH	2,2-diphenyl-1-picrylhydrazyl
ABTS	2,2′-azino-bis(3-ethylbenzothiazoline-6-sulfonic acid)
TPC	total phenolic content
GAE	gallic acid equivalent
CLE	cardoon leaf extract
FFS	film forming solution
CP	cardoon protein
COC	cardoon oilseed cake
DW	dry weight
FW	fresh weight
TE	Trolox equivalent
TS	tensile strength
YM	Young's modulus
EB	elongation at break
WV	water vapor

and medicine and is part of the Mediterranean diet for the preparation of several dishes. In fact, cardoon flowers are used in soups, stews and salads (Fratianni, Tucci, Palma, Pepe, & Nazzaro, 2007), while the leaves are known for their therapeutic potential as a diuretic, choleretic, cardiotonic, antidiabetic and anti-hemorrhoidal agent (Ramos et al., 2017; Velez et al., 2012). Beside its application as functional food, cardoon biomass has been used as lignocellulosic feedstock for biodiesel and biomethane production (Pesce et al., 2017; Toscano, Sollima, Genovese, Melilli, & Raccuia, 2016, pp. 429–442). Nevertheless, cardoon has been reported as a source of bioactive compounds such as flavonoids, chlorogenic acids and anthocyanins, which have been used for medicinal and cosmetic purposes (Ierna, Sortino, & Mauromicale, 2020; Lattanzio et al., 2009; Mandim et al., 2020; Petropoulos et al., 2019). The environmental sustainability of this plant, together with its bioactive components have made cardoon a recognised key multipurpose crop in biorefinery by processing all the non-edible parts to produce a variety of interesting compounds for potential application in green chemistry (Gominho, Dolores, Lourenço, Fernández, & Pereira, 2018; Pappalardo, Toscano, Puglia, Genovese, & Raccuia, 2020; Turco et al., 2019). Thanks to its adaptability to dry regions, cardoon can be considered a good candidate as a perennial field crop able to grow on marginal lands, thus, it does not compete with food crops (Fagnano, Impagliazzo, Mori, & Fiorentino, 2015). From cardoon seeds it is possible to extract an oil characterized by a very nutritious profile, rich in unsaturated fatty acids, adapted for the production of alternative vegetable oils and herbal formulations for human consumption (Mirpoor, Giosafatto, & Porta, 2021). The remaining by-product after oil extraction is a valuable source of fibers, proteins as well as of bioactive compounds (Genovese et al., 2016). As far as the leaves, many studies have focused on the antioxidant potential of their extracts, strictly related to the polyphenol fraction, mainly composed of hydroxycinnamic derivatives, such as mono- and dicaffeoylquinic acids, and flavonoids, such as apigenin and luteolin (Dias et al., 2018; Falleh et al., 2008; Pandino, Lombardo, Mauromicale, & Williamson, 2011; Scavo, Pandino, et al., 2019). Recent studies (Barbosa et al., 2020) have indicated that cardoon leaves are rich in several polyphenol compounds, with several health benefits. As matter of fact, cardoon leaves contain antimicrobial and antioxidant compounds that have been suggested for use as natural additives for extending the shelf life of food products. Moreover, as leaves are considered cardoon by-products, they can have economic benefits if their natural antioxidants, with benefits to human health, are extracted and applied in food packaging to increase shelf life. Nevertheless, cardoon by-products and their potential for application in food packaging is still not entirely known and it would be worthy to investigate.

Several protocols for the extraction of bioactive molecules from cardoon leaves have been previously described; dried or fresh leaves are mixed with a solvent (ethanol, methanol, acetone or alcoholic solutions) and incubated with shaking (Falleh et al., 2008; Fratianni et al., 2007; Kukić et al., 2008; Pandino et al., 2011). An alternative to these traditional extraction methods could be the use of the Naviglio® extractor, based on a solid-liquid dynamic extraction. By using a suitable solvent, the generation of a negative gradient pressure between the outlet and the inlet of a solid matrix containing some extractable material, followed by a sudden restoration of the initial equilibrium conditions, induces the forced extraction of substances not chemically bonded to the principal structure of which the solid is formed (Naviglio, 2003). This would result in a shorter extraction time, higher extraction yields and preservation of integrity of the components. Naviglio® extraction has already been reported as an innovative technology for the recovery of phenolic compounds from different types of solid matrixes, emerging as a greener alternative to the latest solid-liquid extraction techniques (Naviglio, Scarano, Ciaravolo, & Gallo, 2019; Panzella et al., 2020; Scarano et al., 2020). The Naviglio® extractor is scalable up to 400 L capacity, and is economically feasible due to the following reasons: *i)* the total consumption of this equipment, mainly related to the compressed air, is very negligible, being about 50 W/h; *ii)* it does not require any increase in temperature; *iii)* the extraction method alternates static phase, where the consumption of energy is quite zero, to dynamic one in which consumption reaches the maximum (about 100 W/h). Furthermore, many studies have been done in recent years on binding and conjugating flavonoids and polyphenols with proteins in order to improve the functionality of proteins as well as for developing active protein-based films (Mirpoor, Hosseini, & Nekoei, 2017; Mirpoor, Hosseini, & Yousefi, 2017; Quan, Benjakul, Sae-leaw, Balange, & Maqsood, 2019; Taghavi Kevij, Salami, Mohammadian, & Khodadadi, 2020). Generally, biopolymers from agricultural sources are an interesting option for biodegradable/edible plastics production since agricultural industry generates a high quantity of different by-products containing biomacromolecules, such as proteins and polysaccharides, considered good candidates for the production of hydrocolloid bio-plastics. In fact, proteins from soy and different legumes as well as several carbohydrates, such as pectins, chitosan and starch are extensively used in this sector (Giosafatto, Fusco, Al-Asmar, & Mariniello, 2020). However, despite the huge worldwide production of these agricultural biomasses, they are basically used for animal feeding and on a small amount for bio-plastic production. In this respect, seed oilcakes might be considered valuable by-products for biobased materials development as they are endowed with high amount of fiber, polysaccharides and proteins that can be further utilized. In this paper the phenols were extracted from *Cynara cardunculus* leaves, comparing Naviglio® extractor and maceration methods, using ethanol as solvent. The leaf extracts from both methods were analysed in terms of phenolic content and antioxidant activity. Further towards a development of a cardoon-based biorefinery, in the present work for the first time the seed proteins obtained following the oil removal were exploited for the production of novel bio-plastics potentially able to become candidates for replacing a portion of the petroleum-derived plastics highly pollutant for the environment. In this scenario, it is worth to say that actually Novamont company (https://agro.novamont.com/en/the-innovative-agricultural-system) is trying to exploit cardoon biomass for the development of a biorefinery for the production of low environmental impact bioproducts, even though the company is not exploiting the proteins from cardoon seeds for the manufacturing of bio-plastics. The bio-plastics obtained in this study were then functionalized with cardoon leaf-derived extracts and the obtained materials were finally characterized according to their physico-chemical characteristics, such as mechanical, barrier, morphological and hydrophobicity features, as well as antioxidant properties by evaluating film radical scavenging activity.

2. Materials and methods

2.1. Materials

Ethanol (100%) was supplied by VWR International (Fontenay-sous-Bois, France), 2,2′-azino-bis(3-ethylbenzothiazoline-6-sulfonic acid) (ABTS) was purchased from AppliChem GmbH (Darmstadt, Germany). Trolox was purchased from Sigma-Aldrich, Inc. (St. Louis, MO). *N*-Hexane (99%) and Folin-Ciocalteau reagent were supplied by Carlo Erba Reagents (Val de Reuil, France). Glycerol (GLY) (~99%) and 2,2-diphenyl-1-picrylhydrazyl (DPPH) were purchased from Sigma Chemical Co. (USA). All other chemicals and reagents used were of analytical grade.

Cardoon was recovered in April from a field experiment made in Sant'Angelo dei Lombardi (Avellino, Italy), a hilly area about 700 m above sea level, characterized by cold and rainy winters and low-fertility soil. The soil was composed by 38.5% clay, 25% silt and 36.5% sand, with a pH 8.1 and a content of 0.1% N and 1.3% organic matter (Ottaiano et al., 2017). The leaves were separated from the fresh plants and stored in vacuum sealed plastic bags at −20 °C. For extract preparation, cardoon leaves were thawed at room temperature and cut into 1 cm^2 pieces. Cardoon seeds were obtained from the same field.

2.2. Cardoon leaf extract preparation

A cardoon leaf extract (CLE) was obtained by filling a filter bag (porosity 100 μm) with 40 g of cut cardoon leaves and then, by inserting it into the Naviglio® extractor chamber (Lab. model 500 cm3 capacity). Extraction was performed using 625 mL of 100% ethanol (96% v/v) at room temperature and at pressure value of 9 bar (static phase 2 min; dynamic phase 2 min, with 12 s stop piston). Liquid samples (10 mL) were collected at 2, 4, 8 and 24 h. The CLE was kept at 4 °C until it was analysed. Moreover, further 40 g of cut cardoon leaves were placed in a bottle kept under dark conditions and subjected to maceration at room temperature with constant shaking for the same times of extraction carried out with Naviglio® extractor. The CLEs were filtered through a Whatman filter paper and supernatants were kept at 4 °C until they were analysed.

2.2.1. Naviglio® method

Filter bag (porosity of 100 μm) was filled with 40 g of cut cardoon leaves and then it was inserted into extraction chamber of Naviglio® extractor Lab. model 500 cm^3 capacity. Extractions were conducted using 625 mL of anhydrous ethanol at room temperature at pressure value of 9 bar, static phase 2 min; dynamic phase 2 min, with 12 s stop piston. Liquid samples (10 mL) were collected at 2, 4, 8 and 24 h (Naviglio, 2003). The leaf extracts (CLE) were kept at 4 °C until analysis. Ethanol was chosen as solvent for phenols extraction as described in literature (Kukić et al., 2008; Pinelli et al., 2007; Scavo, Pandino, et al., 2019).

2.2.2. Maceration method

40 g of cut cardoon leaves were used for the comparative analysis with maceration, which was placed in a bottle kept under dark conditions at room temperature with constant shaking. Samples were taken at the same times as extraction using Naviglio® extractor. The CLE were filtered through a Whatman filter paper and supernatants were kept at 4 °C until analysis.

2.3. Total phenolic content analysis

The total phenolic content (TPC) was determined using the Folin-Ciocalteau reagent as previously described (Siddiqui, Rauf, Latif, & Mahmood, 2017) with small changes. The calibration curve was plotted by mixing 100 μL of 10–250 μg/mL gallic acid solutions in ethanol with 500 μL of Folin-Ciocalteu reagent (diluted 10-fold with water) and allowed to stand at room temperature for 5 min. Then, 400 μL of 7.5% w/v Na_2CO_3 solution were added to the mixture and the absorbance was measured after 30 min at 765 nm using UV-1600PC Spectrophotometer (VWR, Leuven, Belgium). For CLEs, 100 μL of each sample were mixed with the same reagent, as performed for constructing the calibration curve and, after 3 h, the absorbance was measured to determine the total CLE phenolic contents. The results were expressed as gallic acid equivalents (GAE). All determinations were carried out in triplicate.

2.4. Antioxidant activity determination

2.4.1. ABTS radical cation decolourisation assay

ABTS activity was quantified in terms of percentage inhibition of the $ABTS^{\bullet+}$ radical cation by antioxidants in each sample. ABTS radical cation ($ABTS^{\bullet1}$) was produced by reacting 7 mM ABTS stock solution (dissolved in water) with 2.45 mM potassium persulfate and allowing the mixture to stand in the dark at room temperature for 12–16 h before use (Re et al., 1999). For the study of CLE phenolic compounds, the $ABTS^{\bullet1}$ solution was diluted with water to an absorbance of 0.70 at 734 nm. After addition of 1 mL of diluted $ABTS^{\bullet1}$ solution to 10 μL of CLE, the absorbance reading was taken exactly 1 min after the initial mixing and up to 10 min using a UV-1600PC Spectrophotometer (VWR, Leuven, Belgium). CLEs were diluted two-times prior the analysis and 10 μL of ethanol in 1 mL of diluted $ABTS^{\bullet1}$ solution was used as control. Inhibition of the $ABTS^{\bullet+}$ radical cation was expressed as Scavenging effect (S) and calculated using the equation:

$$S\ (\%) = 100 \times (A_0 - A_s)/A_0 \quad (1)$$

where A_0 is the absorbance of the control (containing all reagents except the sample to be tested), and A_s is the absorbance of the tested sample. All determinations were carried out in triplicate.

2.4.2. In vitro antioxidant and free radical scavenging activity

$DPPH^{\bullet}$ radical scavenging activity was quantified in terms of percentage inhibition of a pre-formed free radical by antioxidants in each sample. 0.005% (w/v) DPPH radical was prepared in methanol as previously described (Kukić et al., 2008) with some modifications. For the study of phenolic compounds, DPPH solution was diluted with methanol to an absorbance of 0.70 at 517 nm 100 μL of CLE were mixed with 900 μL of diluted DPPH solution, shaken and left for 30 min in the dark. CLEs and film forming solutions (FFSs) were diluted two-times and 20-times, respectively, prior the analysis. Absorbance was measured at 517 nm using UV-1600PC Spectrophotometer (VWR, Leuven, Belgium); 1 mL methanol was used as blank, while 100 μL of ethanol in 900 μL of DPPH solution were used as control. Neutralisation of DPPH radical was calculated using the equation:

$$S\ (\%) = 100 \times (A_0 - A_s)/A_0 \quad (2)$$

where S is the Scavenging effect, A_0 is the absorbance of the control (containing all reagents except the sample to be tested), and A_s is the absorbance of the tested sample. Results were compared with the activity of 6-hydroxy-2,5,7,8-tetramethylchroman-2-carboxylic acid (Trolox). All determinations were carried out in triplicate.

For the evaluation of scavenging activity of film containing CLE, 0.005% (w/v) DPPH radical was prepared in methanol. 10 mg of film were incubated in 5 mL of DPPH solution, shaken and left for 30 min in the dark. 5 mL of DPPH solution were used as control. Absorbance was measured in a 6-wells plate at 517 nm using Benchmark Plus Microplate Spectrophotometer (Bio-Rad Laboratories, Hercules, CA).

2.5. Characterization of cardoon leaf extract

The volatile triterpenes and sesquiterpenes, known for their antioxidant activity, were identified by GC-MS. The sample was prepared by dissolving 1 mg of CLE obtained by Naviglio® method in 1 mL of diethyl

ether and GC-MS analysis was carried out by a Shimazu gas chromatograph. The gas chromatograph was equipped with a 30 m × 0.25 mm fused-silica capillary column (SLB5ms) coated with 0.25 μm film of poly (5% phenyl, 95% dimethyl siloxane). The temperature was monitored from 50 °C to 280 °C. The mass spectrometer was set to scan 33–700 m/z. Samples were injected (1 μL) with a splitting ratio 1:20 and the injector temperature was set to 280 °C. The column oven was initially at 50 °C and was held for 2 min after the injection, followed by temperature ramping at 8 °C/min up to 250 °C, and 250–280 °C at 3 °C/min. The total run time was 63.33 min (Mathe, Culioli, Archier, & Vieillescazes, 2004).

The NMR analysis was performed in order to confirm the presence of the bioactive molecules observed by GC-MS analysis (see section 3.2) and for carrying out a semi-quantitative evaluation of the content of cynaropicrin respect to the other components of the CLE (see section 3.2). The NMR analysis was performed by dissolving 10 mg of CLE in 0.7 mL of deuterated chloroform. Samples were analysed on a Varian VNMRS 500 MHz NMR spectrometer at 500 MHz.

Finally, an aliquot of CLE was diluted in 70% ethanol and loaded on Vivaspin® (3 kDa and 10 kDa cut-off) ultrafiltration devices in order to determine the presence of high molecular weight molecules. The eluate fraction was recovered and dried at 60 °C overnight and the dry weight (DW) determined.

2.6. Extraction of cardoon seed proteins

Cardoon seeds were grinded at a speed of 1000 rpm for 3 min in a Knife Mill Grindomix GM 200 (Grindomix GM200, Retsch GmbH, Haan, Germany) and then defatted for 6 h by using a soxhlet apparatus (3:1, v/w hexane:grinded seeds) and, finally, the obtained cardoon oilseed cake (COC) was dried at 50 °C in an oven for 2 h. Isoelectric-precipitation technique was used for extracting cardoon proteins (CPs) from COC, according to Dapčević-Hadnađev, Hadnađev, Lazaridou, Moschakis, and Biliaderis (2018) with minor modifications. COC was suspended in water at 1:10 ratio (w/v) and 1.0 N NaOH was added under constant stirring to adjust the pH to 11. After 1 h of stirring, the suspension was centrifuged for 15 min at 5000 rpm and the pH of the collected supernatant was adjusted to 5.4 using 1.0 N HCl. Then, the precipitate was separated by another centrifugation at 5000*g* for 15 min and the obtained pellet collected and dried in an environmental chamber at 25 °C and 45% relative humidity. The protein content of the obtained CP powder was determined by the Kjeldahl's method (AACC, 2003) using a nitrogen conversion factor of 6.25.

2.7. Preparation of cardoon protein-based films

CP was dispersed in distilled water (2% w/v), the pH was adjusted to 12.0 by 1 N NaOH and the dispersion was stirred for 2 h at room temperature for complete CP dissolution. The preliminary attempts to produce CP-based films have been carried out by using 200, 300 and 400 mg of CPs added with different concentrations of GLY (10–50%, w/w protein) as plasticizer, in order to find the optimum conditions for developing handleable films.

CLE obtained as described above by Naviglio® method was dried and resuspended in ethanol up to get a final concentration of 16 mg/mL. This extract was added to the CP solution at different concentrations and the mixture was stirred for 1 h. GLY was then added to obtain a final concentration of 50% (w/w protein) and the solution was stirred for further 30 min. The prepared FFSs were cast on plastic petri dishes (8 cm diameter) and finally dried in an environmental chamber at 25 °C and 45% relative humidity (RH) for 24 h. The dried films were peeled off and conditioned at 25 °C and 50% RH, by saturated magnesium nitrate solution, for 24 h before the analyses.

2.8. Zeta potential, particle size and contact angle measurements

The effect of different concentrations of CPs, GLY and CLE on the mean hydrodynamic diameter (particle size) and the electric charge (zeta potential) values of the FFSs, as well as of CPs diluted in alkaline water (0.1 mg/mL, pH 12) by using 0.1 N NaOH, was measured by a zetasizer (Nano-ZSP, Malvern, Worcestershire, UK) at 25 °C. The effect of pH on both zeta potential and particle size of CP dissolved in water at pH 12.0 was studied by transferring 1 mL solution into the autotitrator and adjusting the pH to different values starting from pH 12.0 to pH 2.0 by adding 1.0, 0.1, and 0.01 N HCL. All measurements were performed in triplicate.

Contact angle values of the FFSs prepared in the presence or absence of CLE were determined using a homemade goniometer and parafilm (Bemis Co., Inc., Neenah, WI, USA) stripes as hydrophobic surfaces. 10 μL of each FFS were deposited on the surface of parafilm strip fixed on the horizontal stage, and the images of each FFS drop were captured using a fixed digital microscopic camera (PS Pro, China) at the moment of contact of the drop with the surface (0 time) and after 30 s. Contact angles between baseline of the FFS drops and the surfaces were then measured using Image J software. Five measurements for each FFS was reported as the average of its contact angle value.

2.9. Cardoon seed protein-based film characterization

2.9.1. Colour, opacity and density measurements

The colour parameters of CP-based films prepared in the absence or presence of different concentrations of CLEs were measured using a Mightex® HRS series compact CCD spectrometer HRS-VIS-025 (Mightex, Toronto, ON). All measurements were made at 5 random positions of each film. The colour parameters, including L as well as "a" and "b" values, indicate lightness/darkness (0–100), greenness/redness (−60 to +60) and blueness/yellowness (−60 to +60), respectively, of the materials tested. Total colour difference (ΔE) was determined by the following equation:

$$\Delta E \cdot = \cdot \sqrt{(L^{*} - \ L)^{2} + (a^{*} - \ a)^{2} + (b^{*} - \ b)^{2}} \quad (3)$$

where L* (99.94), a* (−1.07) and b* (3.74) were the colour parameter values of the standard white tile (Bai et al., 2019).

Film opacity was evaluated by a spectrophotometer according to the method described by Taghavi Kevij et al. (2020). The film specimens (4 cm × 1 cm) were attached to the cell and inserted into a spectrophotometer. The empty cell was used as a blank and the absorbance of each film specimen was read at 600 nm. The opacity of the films was calculated as a ratio between the obtained absorbance value and the film thickness (mm).

Density was determined according to the procedure described by Cruz-Díaz, Cobos, Fernández-Valle, Díaz, and Cambero (2019) with some modifications. The film samples (2 cm × 2 cm) were weighed, their thickness measured at three random places and, finally, the dry matter density was calculated as the ratio between the weight and volume of each film (thickness × film surface area). All the analyses were carried out in triplicate.

2.9.2. Fourier transform infrared (FTIR) spectroscopy

The interactions between CLE and CP in the film matrix were investigated by recording the FT-IR spectra using FTIR Nicolet 5700 spectrophotometer (Thermo Fisher Scientific, Waltham, MA, USA). Infrared spectra analysis was performed using the Omnic software in the range of 4000–500 cm^{-1} with a spectral resolution of 2 cm^{-1}.

2.9.3. Scanning electron microscopy analyses

Film microstructure was examined by both surface and cross section analysis using a field emission scanning electron microscope (FE-SEM, FEI Nova NanoSEM450, Thermo Fisher, Scientific, MA, USA). In order to

prepare the films for cross-sectional analysis, each sample was cryo-fractured in liquid nitrogen, then coated with a thin layer of gold and platinum using a vacuum sputter coater and, finally, observed at an accelerating voltage of 5 kV.

2.9.4. Mechanical properties and thickness

Film thickness was measured from the average of the thickness determined at five different locations of each film using an electronic digital micrometer (IP65 Alpa Metrology Co., Pontoglio, Italy, sensitivity 0.001 mm). Film tensile strength (TS), Young's modulus (YM) and elongation at break (EB) were determined according to ASTM D882 - 18 (1997) method using an Instron universal testing instrument (Model 5543 A, Instron Engineering Corp., Norwood, MA, USA), with a 1000 N load cell. The film strips (8 cm × 1 cm) were fixed between two grips of the instrument with an initial grip distance and crosshead speed of 40 mm and 5 mm/min, respectively.

2.9.5. Hydrophilicity properties

Film moisture content was evaluated by the method of Roy and Rhim (2020) by weighing each film sample (2 cm × 2 cm) before and after drying in an oven at 105 °C for 24 h. Moisture content was calculated as the percentage of the film weight loss with respect to the initial weight of the film.

Water solubility of the films was measured according to the procedure of Adilah, Jamilah, Noranizan, and Hanani (2018) with some slight modifications. The initial weight (W_i) of each film sample (2 cm × 2 cm) was obtained by oven drying at 105 °C for 24 h. The dried films were then immersed in 30 mL of distilled water and stirred in a shaker incubator at 25 °C for 24 h. After that, the final weight (W_f) of the samples were obtained by separating the non-soluble parts of the films and drying in oven at 105 °C for another 24 h. Finally, water solubility was calculated using the following equation:

$$\text{Water solubility } (\%) = [(W_i - W_f)/W_i] \times 100 \quad (4)$$

Film swelling ratio was measured according to the method of Roy, Rhim, and Jaiswal (2019). The initial weight (Wi) of each film sample (2 cm × 2 cm) was measured and, then, the films were immersed in 30 mL distilled water at 25 °C for 1 h. After that, the excess water was drained with filter paper, the surface water of films was dried with an absorbent paper and, finally, the films were weighed again (W_s). Film swelling ratio was calculated using the following equation:

$$\text{Swelling ratio } (\%) = (W_s - W_i) \times 100/Wi \quad (5)$$

The surface wettability of film samples was studied using a home-made water contact analyser. Each film strip was placed on the horizontal stage and then made in contact with 10 μL of distilled water. The image of the water drop was immediately captured using a fixed digital microscopic camera (PS Pro, China). The contact angle between water drop and the film surface was measured by an Image J software and five measurements were performed to calculate the average of the contact angle value of each film sample.

2.9.6. Gas and water vapor permeability

Film permeability to WV water vapor, O_2 and CO_2 was measured in duplicate for each film, according to the modified method ASTM D3985 - 05 (2010), ASTM F 2476-05 (2005), ASTM F1249-13, 2013 using a MultiPerm instrument (ExtraSolutions s.r.l., Pisa, Italy). After conditioning the film samples for 24 h at 50% RH, they were placed into the aluminium masks and their exposed surface area was reduced to 5 cm^2.

2.9.7. Statistical analysis

The experiments were always performed in triplicate and in a completely randomized design. In order to determine the significant difference between treatments, one-way analysis of variance (ANOVA) and Duncan's multiple range tests ($p < 0.05$) were done using the Statistical Package for the Social Sciences (SPSS19, SPSS Inc., Chicago, IL, USA) software. Pearson correlation (r) to measure the strength of the linear relationship between TPC and antioxidant activity were calculated using the same software.

3. Results and discussion

3.1. Cardoon leaf extract preparation and evaluation of phenol content and antioxidant activity

CLE was obtained by two different methods: conventional maceration and Naviglio® extraction. Both processes were carried out using 100% ethanol as solvent, collecting samples after 2, 4, 8 and 24 h. The extracts were analysed and compared in terms of total phenol content (TPC) using Folin-Ciocalteau assay. Naviglio® extracts were characterised by a higher TPC than maceration extracts regardless the extraction time (Fig. 1, A). In particular, Naviglio® CLE showed an increase in the TPC over the time, from 86.8 ± 3.5 mg GAE/L (corresponding to 140 mg GAE/100 g (fresh weight FW) of leaves at 2 h to 147.2 ± 4.4 mg GAE/L (corresponding to 230 mg GAE/100 g (FW fresh weight) of leaves at 24 h.

These results are in agreement with TPC of leaves of several artichoke cultivars, ranging from 141.7 ± 20.5 to 264.5 ± 44.7 mg GAE/100 g (FW fresh weight) of leaves extracted using hydro methanolic solution (Rouphael et al., 2016). On the contrary, TPC did not change significantly in leaf samples obtained by the maceration method at the different extraction times. In particular, the highest value of TPC obtained by maceration after 24 h was lower than that detected after 2 h by Naviglio® extraction. Furthermore, no further increase in TPC was observed over 24 h extraction by both methods.

It is worth noting that, by using Naviglio® extractor, the values of mg GAE/L and mg/mL of extract showed a positive correlation with time increase ($r = 0.915$), since an increase in TPC content was achieved by prolonging the extraction time. In fact, the amount of GAE/g (dry weight DW) in the extracts did not significantly change with the time (Fig. 1, B). On the contrary, in the case of CLE obtained by maceration, no linear correlation was determined between mg GAE/L and mg/mL ($r = 0.067$): the highest amount of GAE/g (DW dry weight) was achieved after 2 h and significantly decreased thereafter, indicating an increase of components in the extracts other than phenols. Naviglio® extraction has been recently applied reported as a green technology for the to the recovery of phenolic compounds from different sources types of solid matrix (Naviglio et al., 2019; Panzella et al., 2020). Up to 69.9 ± 7.3 mg GAE/g of extract have been obtained from the flowering aerial parts of *Schizogyne sericea* using both water and ethanol as solvents (Caprioli et al., 2017), whereas Posadino et al. (2018) have reported the extraction of phenols from wine waste (*Cagnulari* Grape Marc) using water: ethanol (60:40 v/v) as solvent with a recovering of 4000 mg/L ± 0.05 TPC containing specific anthocyanins. Moreover, the extraction of 9210.4 ± 45.8 mg GAE/L has been reported from crushed, dried and shredded grapes using water as solvent (Gallo et al., 2019) and aqueous vine shoot extracts, resulting into high phenolic content, have been obtained by Naviglio® method (Sánchez-Gómez, Zalacain, Alonso, & Salinas, 2014). Djeridane et al. (2006) reported that TPC in plants of Asteraceae family was higher than that detected in several other plants reported in literature, probably due to the ability to grow in harsh habitat conditions. Polyphenols extraction from cardoon leaves has been carried out by using different solvents such as ethanol, methanol or hydroalcoholic mixtures (Barbosa et al., 2020). According to Ramos et al. (2014), 22.6 GAE/g (DW dry weight) of extract were obtained from *C. cardunculus* L. var. altilis using methanol/water/acetic acid (49.5:49.5:1) after removing the lipophilic fraction. Similarly, 14.79 mg GAE/g (DW dry weight) of extract were obtained by using methanol (Falleh et al., 2008), and 50 mg GAE/g (DW dry weight) of extract were obtained by subsequent extraction with ethanol (Kukić et al., 2008). These differences in TPC reported in literature may be related to

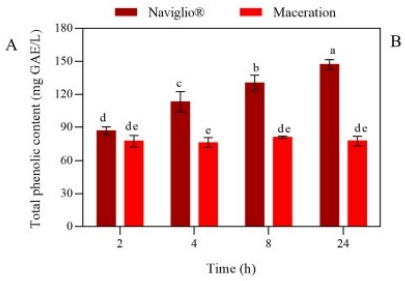

B

Sample	Naviglio® Extraction		Maceration Extraction	
	mg/mL extract	mg GAE/ g DW extract	mg/mL extract	mg GAE/ g DW extract
2 h	1.6	58.0	1.0	80.8
4 h	1.9	61.1	1.2	64.2
8 h	2.0	68.2	1.3	64.9
24 h	2.9	53.8	1.6	51.9

Fig. 1. A) Total phenolic content in cardoon leaves extracted by Naviglio® and maceration methods. CLE were analysed by using the Folin-Ciocalteau reagent. Values with different small letters (a–e) are significantly different (Duncan's multiple range tests, $p < 0.05$). B) Comparison of extraction efficiency of the two methods. Gallic acid equivalent (GAE), dry weight (DW). Further experimental details are given in the text.

intrinsic factors, such as genetics, as well as extrinsic ones, including geographical location, handling methodologies, storage, and extraction procedures (Fratianni et al., 2007). In addition, the distribution of secondary metabolites, such as polyphenols, may be dependent on the life cycle stage of the plant (Del Baño et al., 2003). The values of GAE/g (DW dry weight) detected in this work by using Naviglio® extractor fall within the range reported in literature, demonstrating the applicability of this method to the cardoon leaves.

Antioxidant activity of samples collected at different extraction times with both methods was evaluated using ABTS radical cation decolourisation and DPPH radical scavenging activity assays. Both methodologies are based on the reaction of the radicals ($DPPH^{\bullet}$ and $ABTS^{\bullet 1}$) with the antioxidant molecules which can be determined by spectrophotometric analysis (Dawidowicz, Wianowska, & Olszowy, 2012; Re et al., 1999). ABTS assay is commonly used for both hydrophilic and hydrophobic antioxidants, whereas DPPH is more efficient for hydrophobic systems as it is dissolved in organic solution (Bitencourt, Fávaro-Trindade, Sobral, & Carvalho, 2014; Floegel, Kim, Chung, Koo, & Chun, 2011). Regardless the assay method applied, Naviglio® extracts showed higher scavenging activity than the samples obtained by maceration (Fig. 2).

In particular, all the samples obtained by Naviglio® extractor displayed up to two and three fold the antioxidant activity with respect to the samples obtained by maceration, measured with either DPPH or ABTS assays, respectively. Furthermore, Naviglio® extract showed an increasing antioxidant activity as the extraction time increased, ranging from 41.2% ± 3.4 at 2 h of extraction to 64.5% ± 0.4 at 24 h of extraction using DPPH assay. These results reflect the same trend observed for the TPC determination, since the antioxidant activity of Naviglio® extract evaluated over the extraction time correlates with the TPC measured in the extract, showing highly significant correlation coefficients (r) (0.994 and 0.71) in both DPPH and ABTS assays. The observed correlation between TPC and antioxidant activity supports the hypothesis that this class of compounds directly contributes to the free

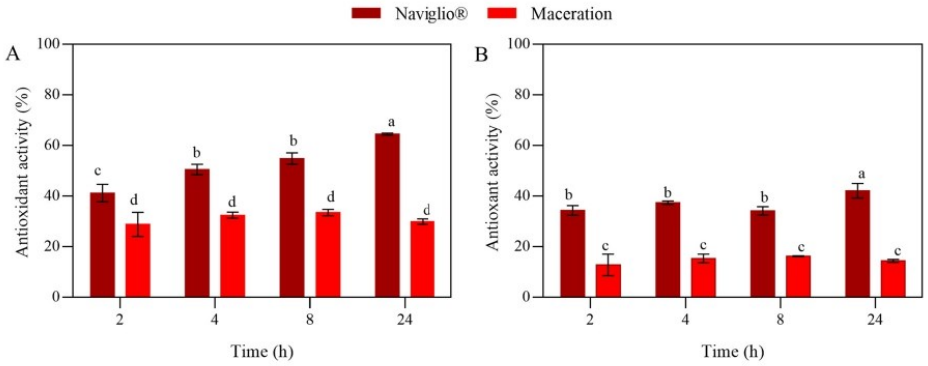

C

Sample	Naviglio® Extraction		Maceration Extraction	
	µg TE/g FW	µmol TE/ 100g FW	µg TE/g FW	µmol TE/ 100g FW
2 h	912.4	364.5	652.9	306.7
4 h	1107.8	442.6	728.3	333.0
8 h	1199.4	479.2	750.5	305.5
24 h	1401.9	560.1	676.0	372.3

Fig. 2. Antioxidant activity of cardoon leaf extracts obtained by Naviglio® and maceration methods detected following DPPH (A) and ABTS (B) assays. Values with different small letters (a–d) are significantly different (Duncan's multiple range tests, $p < 0.05$)). Comparison of antioxidant activity of the extracts are expressed as ratio of Trolox equivalents (TE) and fresh weight (FW) of extracts (C).

radical scavenging activity of the extracts.

It is worthy to note that the extract obtained by maceration does not follow the trend exhibited by the Naviglio® extract, showing an almost constant scavenging activity over the time (Fig. 2), in agreement with the TPC data. The antioxidant activity values measured in Naviglio CLEs are consistent with those reported in literature for the extracts of leaves of other species of *Cynara* genus. A radical scavenging activity in the range of 28.7%–94% has been reported for Green Globe and Violet artichoke (*Cynara scolymus* L.) varieties (Ben Salem et al., 2017; Biel, Witkowicz, Piątkowska, & Podsiadło, 2020). When referred to the Trolox standard, the antioxidant activities of the samples obtained with Naviglio® extractor were higher than those reported for methanolic extracts of leaves from *Cynara cardunculus* var. *ferocissima* (Madeira cardoon), expressed in the same way (176 μmol eq. Trolox/100 g) (Gouveia & Castilho, 2012).

3.2. Characterization of cardoon leaf extract

The characterization of the components of the Naviglio® extracts at 24 h was carried out by GC-MS and ^{1}H NMR spectroscopy. The panel a) of Fig. 3 shows a typical chromatogram of the extract, where the peaks were identified by comparing their mass spectra with the NIST14s database and with literature data (Mathe et al., 2004; Ramos et al., 2013). The GC-MS chromatogram provides qualitative information on the chemical composition of the CLE. The volatile pentacyclic triterpenes and sesquiterpenes, known for their antioxidant activity, are the main families of lipophilic components previously identified in the CLE (Ramos et al., 2013; Scavo, Rial, et al., 2019). In particular, cynaropicrin ($C_{19}H_{22}O_6$) and grosheimin ($C_{15}H_{18}O_4$) (RT = 35.61–37.25 min) have been identified in higher amount in the leaves than in other parts of cardoon and globe artichoke (Eljounaidi et al., 2015; Ramos et al., 2013; Rouphael et al., 2016). Grosheimin has also been previously reported in globe artichoke (Bernhard, 1982). Since the structures of the two sesquiterpene lactones are similar, it was not possible to identify their specific molecular fragmentation. Fatty acids (RT = 19.17 min), long-chain aliphatic alcohols (RT = from 19.50 to 22 min) and some aromatic compounds were also detected in traces. In particular, linoleic acid was identified, as also confirmed by ^{1}H NMR characterization (Fig. 3, panel b) (Ramos et al., 2013; Sobolev, Brosio, Gianferri, & Segre, 2005). The signal at 31.26 min is ascribable to squalene, whereas the signals corresponding to pentacyclic triterpenes fall in the range 23.45–29.73 min. Finally, the signals of hydrophobic long chain alkanes is visible at the range 40–42.5 min. Pentacyclic triterpenes have been identified as the main liphophilic constituents of *C. cardunculus* L. var. *altilis*, although less present in the leaves, where they represent only 8% of total detected compounds. On the other hand, fatty acids are reported to be mainly concentrated in the leaves, especially the saturated ones (Ramos et al., 2013). Furthermore, Rouphael et al. (2016) reported a wide range of phenolic compounds, including flavonoids, hydroxycinnamic acids, tyrosols, and lignans, in the extracts of leaves of different cultivars of artichoke. The characterization by ^{1}H NMR spectroscopy confirmed the presence of lupeol (Reynolds et al., 1986), and pheophytins (Sobolev et al., 2005) (Fig. 3, panel b). The cynaropicrin, a well known bioactive molecule endowed with antioxidant activity, was clearly identified by means of ^{1}H NMR in the extract, because of its typical signals. A semi-quantitative evaluation of its content respect to all other components was carried out because it was possible to integrate the signals of cynaropicrin by taking as a reference the signal of -CH2 protons at 4′ position, having a theoretical integral value of 2 and an observed experimental integral value of 0.85. When considering that the integral value of all protons present in the spectrum (range 0.5–6.5 ppm) is 84.14, it results that the proton of cynaropicrin correspond to the 11% of the protons present in the mixture (Fig. 3, panel c).

Finally, CLE was further analysed by ultrafiltration to determine the average molecular weight of its components. No retention of high molecular weight molecules was determined after ultrafiltration with neither 10 kDa nor 3 kDa cut-off membranes, indicating that CLE contained molecules smaller than 3 kDa.

3.3. Cardoon protein-based films

3.3.1. Zeta potential and particle size of film forming solutions

The data reported in Fig. 4 show that CPs were positively charged in the acidic pH range, since the detected zeta potential was found to increase from a value of about −40.00 mV at pH 12 to that of about −30 mV at pH 7.0 and 0 mV just under pH 4.0, indicating that the electrostatic repulsion pattern was gradually modified as a result of the gradual deprotonation of carboxyl groups and protonation of the amino groups of each CPs present in the sample. As far as the CP particle size, it also varied, like zeta potential, as a function of pH. In fact, at pH $\leq$ 5 high molecular mass protein species were present in the solution, likely because the isoelectric point of CPs was between pH 4 and 5 where the zeta potential value was around 0 mV. CP zeta potential and particle size were measured also in FFSs prepared at pH 12 by varying the concentrations of both proteins and GLY, used as plasticizer. All the FFSs tested were quite stable, regardless of protein and GLY concentration, zeta potential value fluctuating between −28 mV and −33 mV (Table 1).

As far as the particle size, it did not change by varying the GLY content, but it significantly increased by enhancing CP concentration, likely as a consequence of protein aggregation. However, the observed size distribution in the range of 300–400 nm is in agreement with previous results obtained with protein-based FFSs prepared by using other oilcakes (Mirpoor et al., 2020, 2021).

3.3.2. Thickness and mechanical properties of cardoon protein-based films

FFSs previously analysed for the particle size and zeta potential have been used for the preparation of bio-plastics by the casting method. It is worthy to note that the minimum GLY concentration to obtain handleable films under the described experimental conditions was 30% (w/w of CP), since the films cast in the absence or lower amount (10 and 20%) of plasticizer were brittle and not able to be peeled off from the plates. The handleable films were thus characterized for their thickness and mechanical properties (e.g. tensile strength, elongation at break and YMYoung's modulus) (Fig. 5).

As expected, the film thickness was found to increase by enhancing CP concentration independently on GLY amount present in the FFSs. Conversely, all the parameters characterising the mechanical properties of the films changed by varying both CP and plasticizer concentrations. In fact, TS tensile strength and YM Young's modulus decreased whereas EB elongation at break increased by enhancing GLY amounts at all the CP concentrations used. On the other hand, the investigated mechanical properties increased as function of CP amount. This effect was the result of the well known capacity of the plasticizer to increase the free volume and the polymer mobility by decreasing the attractive intermolecular forces into the protein matrix. Porta, Di Pierro, Roviello, and Sabbah (2017) also observed a similar effect for bitter vetch protein-based films prepared with two different plasticizers, such as GLY and spermidine. Sun et al. (2019) demonstrated that such phenomenon occurs also with carbohydrate-based materials, since they reported that chitosan/starch blended films had a greater extensibility when plasticizing components were added. In conclusion, among the different films produced, the one obtained from 400 mg of CP and 50% GLY was selected for the further investigations, possessing the highest EB elongation at break (154.19 ± 8.25) and acceptable TS tensile strength (1.69 ± 0.33) and YM Young's modulus (53.59 ± 6.89) (Fig. 5).

3.3.3. Zeta potential, particle size, contact angle and antioxidant activity of cardoon protein-based film forming solutions containing cardoon leaf extract

FFSs, prepared with 400 mg CPs and 50% GLY, were added with different amounts of CLE in order to test their zeta potential, particle size, contact angle and antioxidant activity as well as the properties of the derived films. Regarding the particles, it should be mentioned that

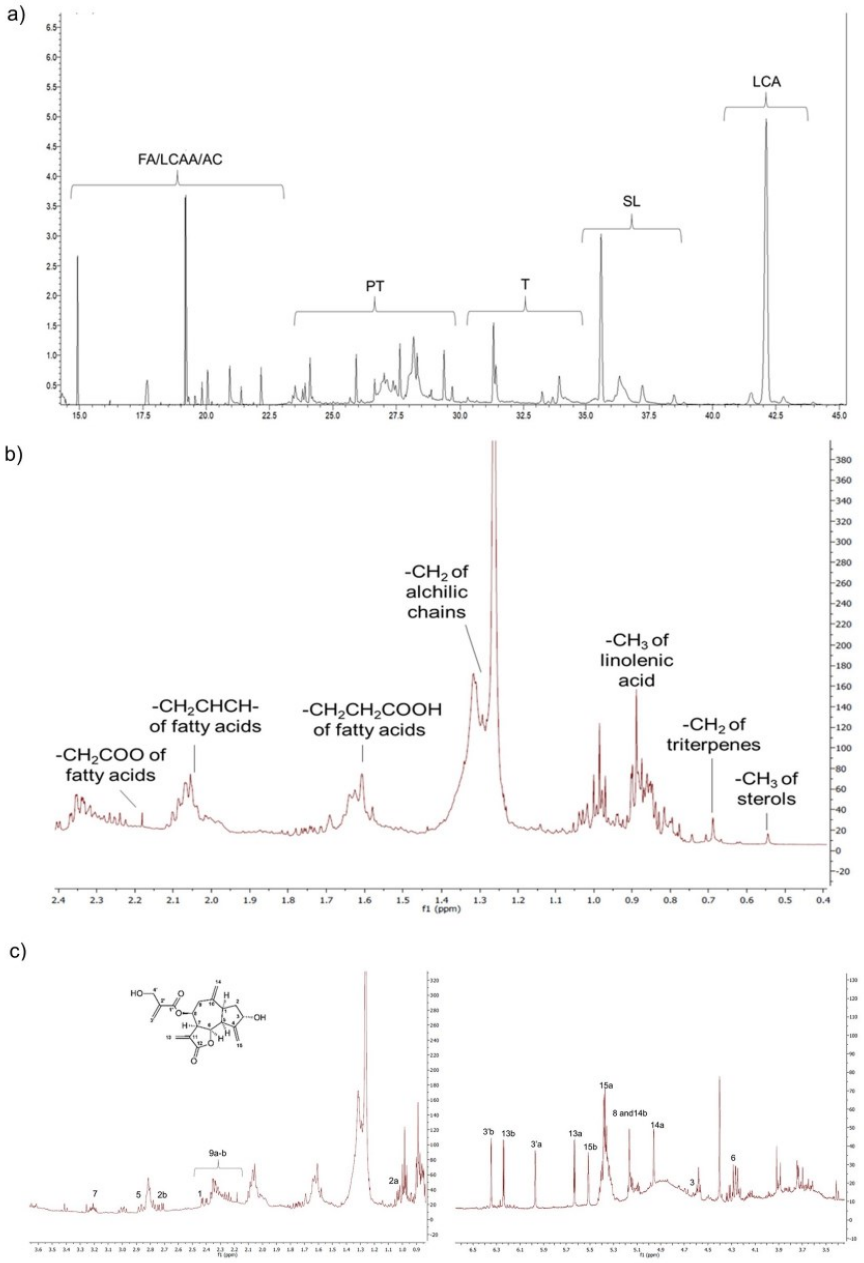

Fig. 3. a) GC-MS chromatogram; b) ^{1}H NMR spectrum of a cardoon leaf extract obtained by Naviglio® method. The GC-MS peaks represent the total ion current (TIC) of the compounds: FA = fatty acids; LCAA = long chains aliphatic alcohols, AC = aromatic compounds; PT = pentacyclic triterpenes; T = triterpene; SL = sesquiterpene lactones; LCA = long chain alkanes. ^{1}H NMR spectrum was detected in the range of 0.4–2.4 ppm. Further experimental details are given in the text. c) Signals of cynaropicrin in the range of 0.9–3.6 ppm (on the left) and signals of cynaropicrin in the range of 3.5–6.5 ppm (on the right). ^{1}H NMR (500 MHz, CD3OD): 1 δ: 2.43, dt; 2a δ: 1.09, ddd; 2b δ:2.07, dt; 3 δ:4.62, tt; 5 δ:2.84,dd; 6, δ:4.27,dd; 7 3.27, tt; 8 and 14b δ:5.17,ttt; 9a-b δ:2.25–2.45, dd; 13a δ:5.62,d; 13b, δ:6.25,d; 14a δ:4.96,d; 15a δ: 5.43,t; 15b δ:5.52,t; 3′a δ:5.9,m; 3′b δ:6.35, m.

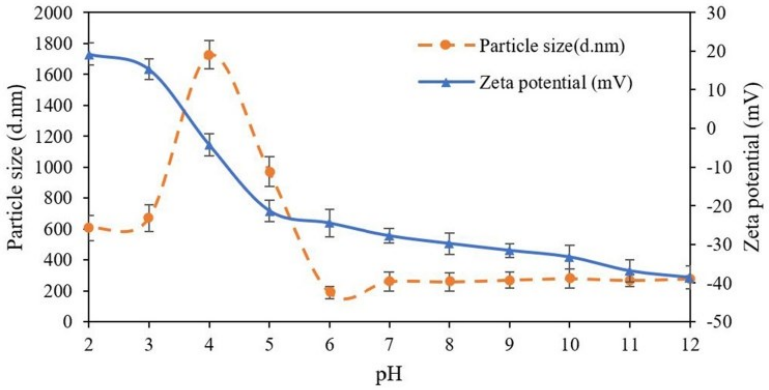

Fig. 4. Cardoon protein zeta potential and particle size measurements vs different pH values.

Table 1
Effect of different concentrations of cardoon proteins (CPs) and glycerol (GLY) on particle size and zeta potential on CP film forming solutions prepared at pH 12[a].

CPs *(mg)*	GLY *(% w/w)*	Particle size *(d.nm)*	Zeta Potential *(mV)*	PDI
200	30	312.7 ± 3.7^{c}	−31.50 ± 1.49 ^{cd}	0.44 ± 0.03^{c}
	40	309.2 ± 3.5^{c}	−31.63 ± 0.58 ^{cd}	0.43 ± 0.02^{c}
	50	310.6 ± 2.7^{c}	−32.56 ± 1.42^{d}	0.42 ± 0.02^{c}
300	30	379.3 ± 7.1^{b}	−29.63 ± 1.61 ^{bc}	0.52 ± 0.04^{b}
	40	379.0 ± 10.2^{b}	−29.70 ± 0.85 ^{bc}	0.51 ± 0.02^{b}
	50	381.8 ± 16.5^{b}	−29.45 ± 1.52 ^{ab}	0.53 ± 0.03^{b}
400	30	436.2 ± 4.8^{a}	−28.51 ± 0.40^{a}	0.60 ± 0.02^{a}
	40	435.0 ± 6.3^{a}	−28.78 ± 0.86^{a}	0.61 ± 0.04^{a}
	50	433.3 ± 5.9^{a}	−29.17 ± 0.46^{a}	0.60 ± 0.02^{a}

[a] Different small letters (a–d) indicate significant differences among the values reported in each column (Duncan's multiple range tests, $p < 0.05$). Polydispersion index (PDI). Further experimental details are given in text.

they consist of different kinds of proteins, some fibres and phenols (coming from the seed oilcakes), glycerol used as plasticizer and finally, as far as the activated FFSs, the CLE. From the performed experiments, it is possible to note that particle size of CPs FFS increased by incorporation of higher concentration of antioxidant in the FFS compared to the control sample, as reported in Table 2. These results could be attributed to the interactions between the CP functional groups and the phenolic hydroxyl groups of antioxidants that formed larger CPs polymers that increase the polydispersity index (PDI), that is an indicator of relative variance in the particle size distribution. These results are in agreement with a linear increase in polydispersity index. The protein surface charges were also affected by the addition of antioxidants and all the FFSs were stable with negative zeta potential higher than −28 mV shows the high stability of solution (Bhattacharjee, 2016). As shown in Table 2, zeta potential of CPs FFS decreased as a function of increasing the concentration of antioxidants due to the participation of negative functional groups of CPs in protein-polyphenols interaction and/or interactions between the CPs surface and CLE that can modify the surface charge of the proteins. The same results were reported for changing the surface charge of soy protein isolate and whey protein isolate based films loaded by curcumin by Chen, Li, and Tang (2015) and Taghavi Kevij et al. (2020), respectively.

The contact angle of the different FFSs was measured on parafilm, the semi-transparent, flexible film composed of a proprietary blend of waxes and polyolefins currently used in research laboratories. The results reported in Fig. 6 clearly show that the addition of increasing amounts of CLE significantly decreased the contact angle value of the CP FFS in comparison to the control sample, thus indicating that the hydrophobicity of CP FFS significantly increased in the presence of increasing CLE concentrations (Fig. 6).

The higher hydrophobicity of the FFS prepared in the presence of CLE might be dependent on the decrease in the number of free hydrophilic groups of CPs involved in the interactions between protein and CLE components (Fathi, Almasi, & Pirouzifard, 2019).

Furthermore, FFS antioxidant activity was preliminarily evaluated using the DPPH radical scavenging activity assay with the aim of choosing the right amount of CLE to graft in the CP-based films. CP containing FFS had a marked antioxidant activity also in the absence of CLE and, whereas the antioxidant activity of the samples added with an amount of CLE up to 3% were at the same level of the control, it progressively increased in the presence of 5, 10, 15 and 30% (w/w) CLE (Fig. 7). For this reason, CP-based films were manufactured by preparing FFSs containing 15% and 30% CLE.

3.3.4. FT-IR spectra of CP-based films incorporated wit CLE

The FT-IR spectra of CP-based films incorporated or not with CLE are shown in Fig. 8. The sharp peaks in the spectrum of neat CP-based film in the range of 1649 cm^{-1} are attributed to the amide I (C=O stretching vibrations) and in the range of 1544 cm^{-1} to the amide II (N–H bending with C–N groups stretching vibrations) are the regions that employed to study the secondary structure properties of proteins (Mohammadian et al., 2019). The FT-IR results of the films incorporated with different amounts of CLE showed a significant shift in the position of these peaks to the lower wavenumbers. These alterations in the peak positions could be attributed to new molecular arrangement in the film matrix due to the interactions between the polypeptide chain of the protein and CLE molecules (Moghadam, Salami, Mohammadian, Khodadadi, & Emam-Djomeh, 2020). Moreover, there are the characteristic peaks around 2878 cm^{-1} and 3270 cm^{-1} in the CP-based films, that correspond to the aliphatic C–H stretching vibrations of CH_2 functional groups and O–H stretching overlapping N–H stretching vibrations, respectively. The incorporation of CLE in the CP-based films matrix caused a considerable shift in the position of these peaks (Chentir et al., 2019; Taghavi Kevij et al., 2020). A common peak observed in the spectra of all the

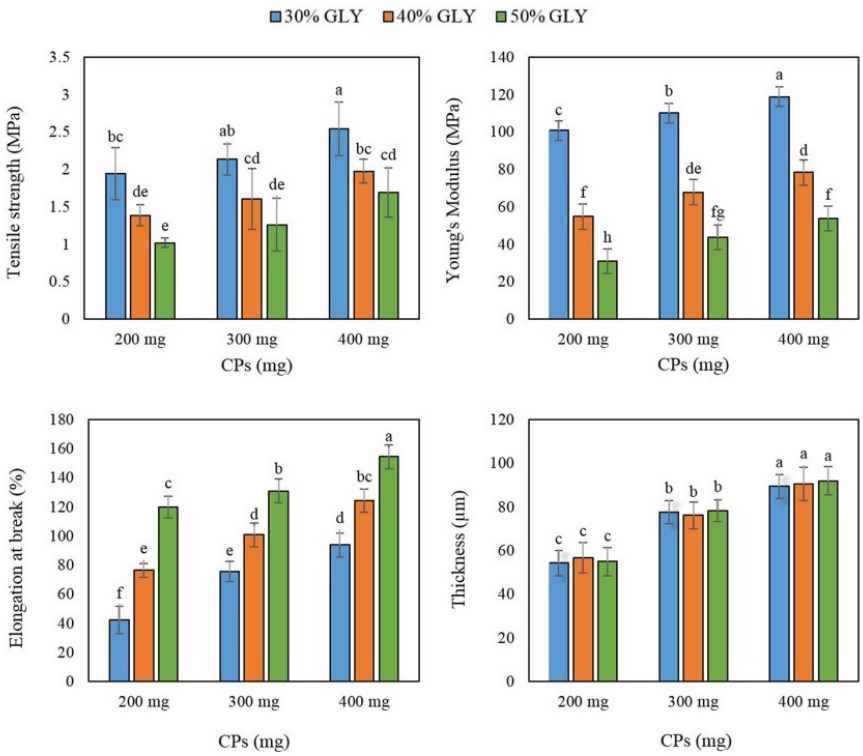

Fig. 5. Effect of different amounts of cardoon proteins (CPs) on the thickness and mechanical properties of films prepared at pH 12 and containing different glycerol (GLY) concentrations. Different small letters (a–g) indicate significant differences among the values reported in each bar (Duncan's multiple range tests, $p < 0.05$). Further experimental details are given in the text.

Table 2
Effect of different concentrations of cardoon leaf extract (CLE) on Z-average and zeta potential of cardoon proteins (400 mg) film forming solutions prepared at pH 12 in the presence of 50% glycerol (GLY)[a].

CLE (% w/w)	Mean particle size (d.nm)	Zeta potential (mV)	PDI (%)
0	411.00 ± 8.20^{c}	−34.35 ± 1.41^{c}	0.47 ± 0.01^{c}
15	441.4 ± 10.08^{b}	−31.69 ± 0.95^{b}	0.52 ± 0.03^{b}
30	512.10 ± 12.22^{a}	−28.84 ± 1.12^{a}	0.58 ± 0.02^{a}

[a] Different small letters (a–d) indicate significant differences among the values reported in each column (Duncan's multiple range tests, $p < 0.05$). Polydispersion index (PDI). Further experimental details are given in text.

investigated samples at around 1040 cm^{-1} is related to OH group of glycerol, indicating the incorporation of glycerol into the film matrix (Moghadam et al., 2020).

3.3.5. *Physicochemical, morphological and mechanical properties of cardoon protein-based films containing cardoon leaf extract*

Films containing different ratios of CP/CLE amounts were manufactured to investigate the effects of CLE on the formation of CP-based materials. To this aim FFSs containing a constant presence of 400 mg of total mass were prepared by increasing the percentage of CLE and parallely decreasing the CP amount. The data reported in Table 3 indicate that thinner films were obtained by reducing the content of CPs until 70% and a concurrent increase in the CLE amount to 30%.

At the same time the mechanical performance of the obtained materials was found to get worse having been observed a progressive decrease of all the parameters (TS, tensile strength, elongation at break EB and YM Young's modulus). Therefore, these findings suggested to test the influence of increasing CLE concentrations on the films manufactured with a constant CP amount (400 mg). Fig. 9 shows that the film thickness slightly increased as a function of CLE amount present in the film matrix, probably due to the interaction of CLE component(s) with the CP polymeric chains, via

Hydrogen bonding and hydrophobic forces (Arciello et al., 2021). In fact, polyphenols may lead to protein crosslinking, thus, increasing the film thickness. These findings were consistent with the results of Hanani, Yee, and Nor-Khaizura (2019) and Moghadam et al. (2020) who observed the effects of pomegranate peel powder on fish gelatin and mung bean protein films, respectively. In addition, both TS tensile strength and YM Young's modulus of films containing 15% CLE were found markedly increased, whereas only a lower, but significant, reduction of the elongation at break EB value was detected in the films prepared in the presence of the same amount of CLE compared to the control samples. However, it should be noted that, by enhancing CLE concentration to 30%, both ~~TS~~ tensile strength and ~~YM~~ Young's modulus values decreased, whereas elongation at break EB slightly increased, with respect to the values detected with films containing 15% CLE. These findings suggest that hydrogen bonding and/or hydrophobic interactions between some CLE components, possibly polyphenols, and CP reactive groups might be responsible for the observed reinforcement of the film network at lower CLE concentrations (Moghadam et al., 2020). Conversely, higher amounts of CLE active molecules could reduce TS tensile strength and increase the flexibility of the CP-based films due to

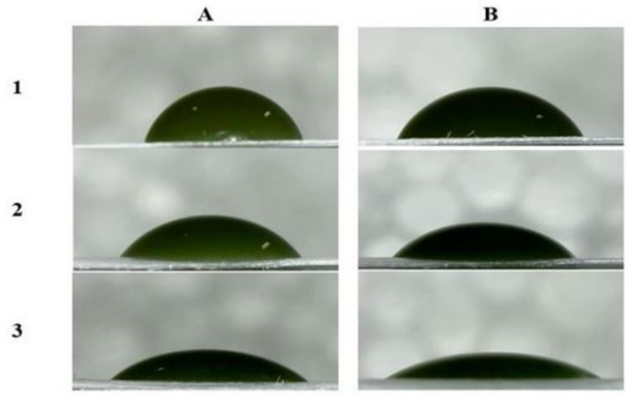

Fig. 6. Images of drops on parafilm surface, captured immediately (A) and after 30 s (B), and contact angle (ɵ) values of film forming solution (FFS), containing cardoon protein (CP) and 50% glycerol, prepared at pH 12 in the absence (1) or presence of 15% (2) and 30% (3) of cardoon leaf extract (CLE). Different small letters (a–c) indicate significant differences among the values reported in each column (Duncan's multiple range tests, $p < 0.05$). Further experimental details are given in the text.

FFS	0 *(sec)*	30 *(sec)*
CP	66.20 ± 0.12 [a]	58.60 ± 0.31 [a]
CP + 15% CLE	50.33 ± 1.15 [b]	41.53 ± 0.63 [b]
CP+ 30% CLE	40.70 ± 1.65 [c]	28.50 ± 1.27 [c]

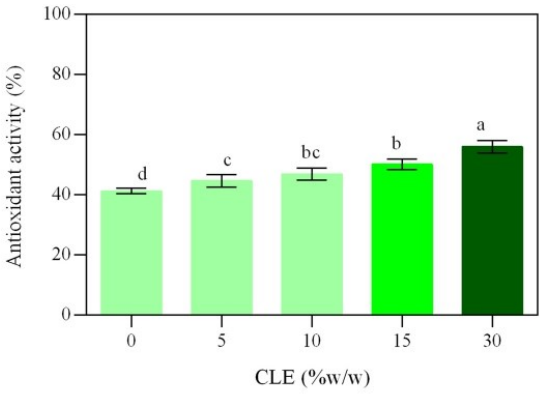

Fig. 7. Antioxidant activity of cardoon protein-based film forming solutions containing different concentrations of cardoon leaf extract (CLE) determined by DPPH assay. Values with different small letters (a–d) are significantly different (Duncan's multiple range tests, $p < 0.05$). Further experimental details are given in the text.

their possible plasticizing effects, as previously reported for bitter vetch protein-based films added with different polyphenol containing extracts (Arabestani, Kadivar, Shahedi, Goli, & Porta, 2016) or for whey protein- and fish gelatin-based films in which curcumin and mango peel extracts were, respectively, incorporated (Adilah et al., 2018; Taghavi Kevij et al., 2020). The films functionalized with 15% CLE were slightly less flexible than the ones prepared in the absence of the phenolic components showing a lower elongation at break, however a significant increase in tensile strength and Young's modulus was observed as a result of CLE incorporation. The same observations were reported by Arciello et al. (2021) who studied whey protein-based bio-plastics prepared with the addition of phenolic extracts from Pecan nuts.

Furthermore, it is well known that color parameters and opacity of the films play a key role in consumers' willingness to choose packed food products, and, in addition, these parametes can affect food quality, specially for the foods that are sensitive to the light (Baek, Kim, & Song, 2018). As shown in Fig. 10 and inferred from the data reported in Table 4, all the CP-based films had low L*, b* and a* values determining a dark greenish-yellow color of the films. The presence of CLE in the CP-based films increased their opacity and the a* and b* values by increasing its concentrations. The higher a* and b* values of films obtained in the presence of higher amount of CLE indicate that the films were more close to green and yellow colors, compared to the control film, probably due to the natural pigments present in CLE. Moreover, also the lightness (L* value) of the film samples was reduced by increasing CLE concentrations. The density of CP-based films significantly increased by increasing CLE concentration, suggesting that the formation of hydrogen and hydrophobic bonds between proteins and CLE components increased by increasing CLE concentrations and led to a more compact film microstructure. Similar behaviour has been previously reported by Riaz et al. (2018) who observed an increasing trend in the density of chitosan-based films by increasing its polyphenols content.

As ar fas as the structural morphology, the films prepared in the absence of CLE exhibited some irregularities and large pores in both surface and matrix (Fig. 10, B1 and C1), whereas the microstructural images of the CLE containing films appeared more homogeneous, continuous and smooth. On the other hand, the film prepared in the presence of 15% CLE seems smoother and more compact than that cast with 30% CLE especially in the cross-section where several holes, voids and discontinuities are quite visible (Fig. 10, B2 and C2 and B3 and C3).

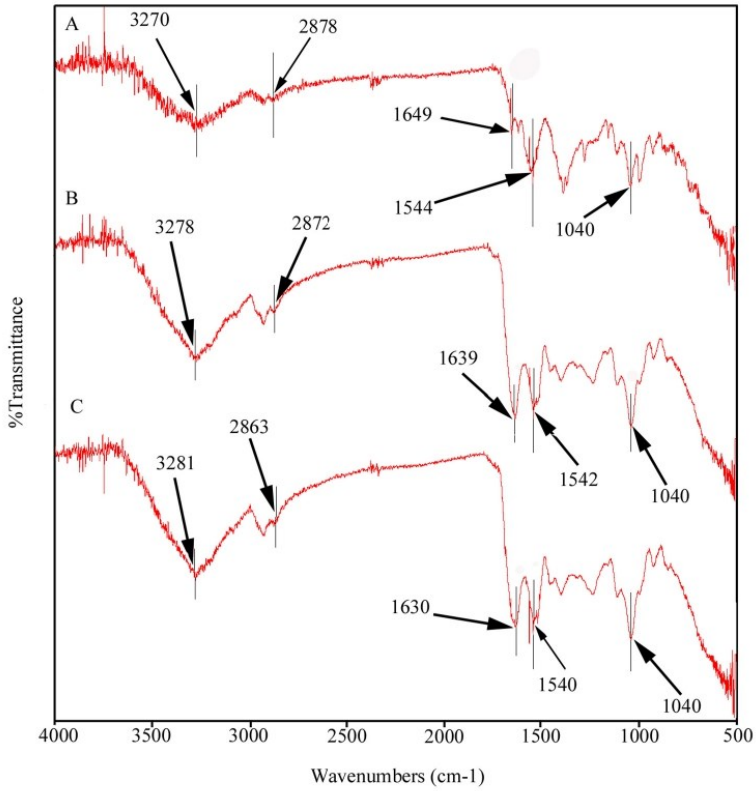

Fig. 8. FT-IR spectra of films prepared in the absence (A) and the presence of 15% (B) and 30% (C) of cardoon leaf extract (CLE).

Table 3
Effect of different cardoon protein (CP)/cardoon leaf extract (CLE) ratios on the thickness and mechanical properties of films prepared at pH 12[a].

CP/CLE *(% w/w)*	TS *(MPa)*	EB *(%)*	YM *(MPa)*	Thickness *(μm)*
100	1.86 ± 0.23^{a}	141.21 ± 6.14^{a}	62.39 ± 7.74^{a}	86.84 ± 5.92^{a}
90/10	1.64 ± 0.31^{a}	132.83 ± 5.27^{a}	56.47 ± 6.31^{ab}	77.31 ± 5.47^{a}
80/20	1.29 ± 0.17^{ab}	107.62 ± 7.41^{b}	49.93 ± 4.71^{bc}	65.72 ± 6.28^{ab}
70/30	1.17 ± 0.06^{b}	92.43 ± 6.08^{b}	34.15 ± 5.73^{c}	49.32 ± 4.88^{c}

[a] Tensile strength (TS), elongation at break (EB), Young's module (YM). Different small letters (a–c) indicate significant differences among the values reported in each column (Duncan's multiple range tests, $p < 0.05$). Further experimental details are given in text.

3.3.6. Water resistance of cardoon protein-based films containing cardoon leaf extract

The moisture content, solubility, swelling ratio and contact angle values of CP-based films containing different amount of CLE are reported in Fig. 11. It is well known that the moisture content of the protein-based films is related to the free volume occupied by water molecules that is in turn influenced by the conformation of the protein and the number of exposed polar groups, and the consequent surface polarity of the polymeric matrix (Sarıcaoglu & Turhan, 2020). The CP-based films revealed a declining tendency for moisture content after incorporation of CLE components, probably due to their hydrophobic properties that limited the water retention in the film matrix (Emam-Djomeh, Moghaddam, & Yasini Ardakani, 2015; Sarıcaoglu & Turhan, 2020). Similar results were obtained by Shams, Ebrahimi, & Khodaiyan (2019) who studied the effects of the orange peel extract added to nanocomposite films made with whey protein and gelatin. Also the reduced tendency for water content of chitosan films observed after incorporation of apple peel polyphenols (Riaz et al., 2018) seems in agreement with the present results.

Furthermore, since both water solubility and swelling of the protein-based films are considered as important factors for their possible applications, mainly in the humid enviroment (Batista, Araújo, Peixoto Joele, Silva, & Lourenço, 2019; Haghighi et al., 2019), also the effect of CLE on these film features was analysed. The data reported in Fig. 11 clearly indicate that both water solubility and swelling ratio of the CLE containing films significantly decreased in comparison with the control CP films. In fact, the hydrophobic nature of several molecules present in CLE might be responsible for the formation of a more compact protein matrix able to maintain the integrity of the films upon their immersion in water, as well as for the reduced interactions among protein and water molecules.

In agreement with these results, Nur Hanani, Aelma Husna, Nurul Syahida, Nor Khaizura, and Jamilah (2018) showed that the water solubility of gelatin/polyethylene bilayer films markedly improved after their enrichment with different fruit peels.

Finally, it is well known that the contact angle is a valid indicator of hydrophobicity of the film surface and that this parameter is affected by different factors such as heterogeneity, surface roughness, particle and

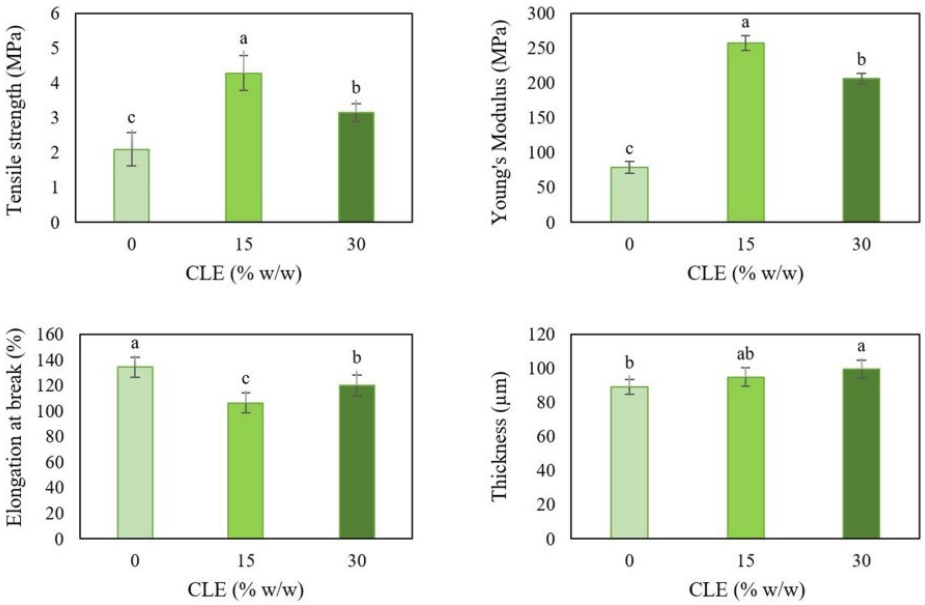

Fig. 9. Thickness and mechanical properties of cardoon protein-based films containing different concentrations of cardoon leaf extract (CLE). Values with different small letters (a–c) are significantly different (Duncan's multiple range tests, $p < 0.05$). Further experimental details are given in the text.

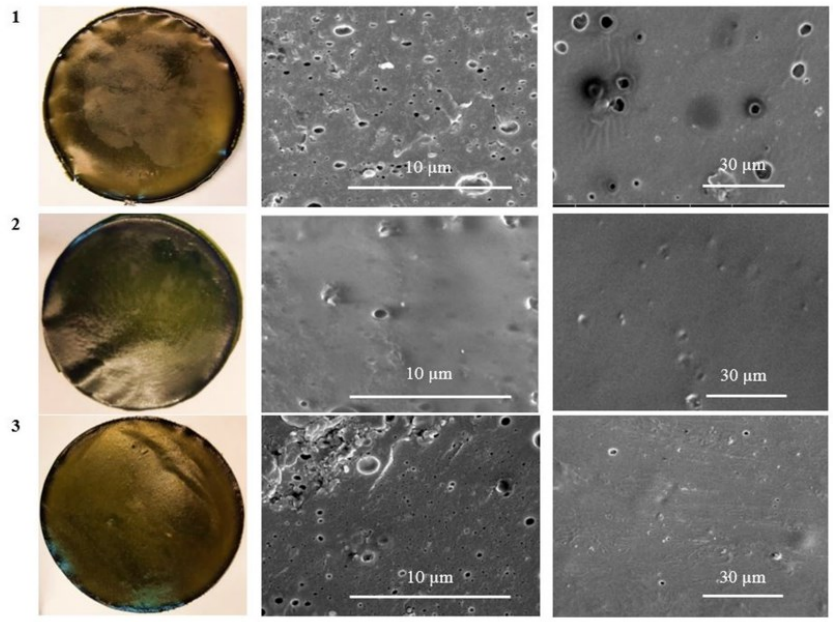

Fig. 10. Images of films (A), prepared in the absence (1) and presence of either 15% (2) or 30% (3) of cardoon leaf extract, and of their SEM cross sections (B, magnification 8000 ×) and surfaces (C, magnification 4000 ×). Further experimental details are given in the text.

pore size of the film matrix (Abdelhedi et al., 2018; Hebbar, Isloor, & Ismail, 2017). As shown in Fig. 11, the incorporation of CLE into CP-based films significantly increased their contact angle values compared to those of control films. These findings suggest that the presence of CLE components in the CP film matrix might increase the smothness of the film surface leading to an increase in the

Table 4
Colour parameters, opacity and density of cardoon proteins-based films containing different concentrations of cardoon leaf extracts (CLE).

CLE %, w/w)	L	a	b	ΔE	Opacity (mm^{-1})	Density (g/cm^3)
0	28.42 ± 0.87[a]	−2.25 ± 0.10[a]	13.82 ± 0.69[c]	72.22 ± 1.54[c]	14.89 ± 0.17[c]	1.19 ± 0.01[c]
15	23.64 ± 1.03[b]	−2.81 ± 0.07[b]	15.51 ± 0.84[b]	77.20 ± 1.08[b]	16.14 ± 0.35[b]	1.28 ± 0.02[b]
30	20.44 ± 0.57[c]	−3.29 ± 0.15[c]	20.04 ± 0.56[a]	81.16 ± 1.12[a]	17.61 ± 0.28[a]	1.34 ± 0.01[a]

[a]L, a and b values indicate lightness/darkness (0–100), greenness/redness (−60 to +60) and blueness/yellowness (−60 to +60), respectively; ΔE, total color difference. Values with different small letters (a-c) are significantly different (Duncan's multiple range tests, $p < 0.05$). Further experimental details are given in the text.

hydrophobicity of their surface, as a consequence of the interactions between CPs and CLE components able to decrease the number of protein hydrophilic groups. Increasing of the surface hydrophobicity of mung bean protein-based films enriched with pomegranate peel powder was previously reported by Moghadam et al. (2020).

3.3.7. Film barrier properties of cardoon protein-based films containing cardoon leaf extract

The resistance to water vapor (WV) permeation of CP-based films prepared in the presence or absence of two different CLE concentrations is reported in Table 5. CP-based films containing 15% CLE exhibited WV water vapor permeability values lower than those observed by testing CP films prepared in CLE absence, while WV water vapor permeability was found significantly increased with respect to control samples in the films obtained in the presence of CLE double concentration (30%). The enhancement of WV water vapor barrier properties of films containing a lower CLE amount could be attributed to the decrease of the free space among the CP chains due to the formation of hydrogen bonds and/or hydrophobic interactions among protein and CLE components that could probably decrease the penetration and diffusion of WV water vapor through the film matrix.

Conversely, the addition of higher amounts of CLE to the CP-based FFS probably prevented an homogeneous distribution of the same components in the film matrix, thus determining an opposite effect on the WV water vapor permeability of the resulting films. In this regard, Moghadam et al. (2020) reported that WV water vapor barrier properties of mung bean protein-based films increased in the presence of pomegranate peel powder, whereas Adilah et al. (2018) did not observe any significant change in WV water vapor permeability of the fish gelatin films by adding increasing amounts of mango peel.

Furthermore, as shown in Table 5, even the permeabilities to both O_2 and CO_2 of the CP films containing CLE were observed to significantly decrease with respect to those of control films, probably as a consequence of the lower number of pores observed by SEM in the film surface and cross-section images (Fig. 10). More in particular, the interactions between CP and CLE components might be responsible for the reduced diffusion paths of the gas molecules through the film networks (Laufer, Kirkland, Cain, & Grunlan, 2013). However, also the O_2 and CO_2

Table 5
Water vapor (WV) and gas permeability of cardoon protein (CP)-based films containing different concentrations of cardoon leaf extract (CLE)[a].

CLE (% w/w of CP)	WV	O_2	CO_2
	(cm^3 mm m^{-2} d^{-1} kPa^{-1})		
0	0.05 ± 0.01[a]	2.24 ± 0.01[a]	6.53 ± 0.42[a]
15	0.02 ± 0.01[b]	1.19 ± 0.06[b]	1.89 ± 0.37[b]
30	0.08 ± 0.01[c]	1.64 ± 0.08[c]	3.47 ± 0.82[c]

[a] Different small letters (a–c) indicate significant differences among the values reported in each column (Duncan's multiple range tests, $p < 0.05$). Further experimental details are given in text.

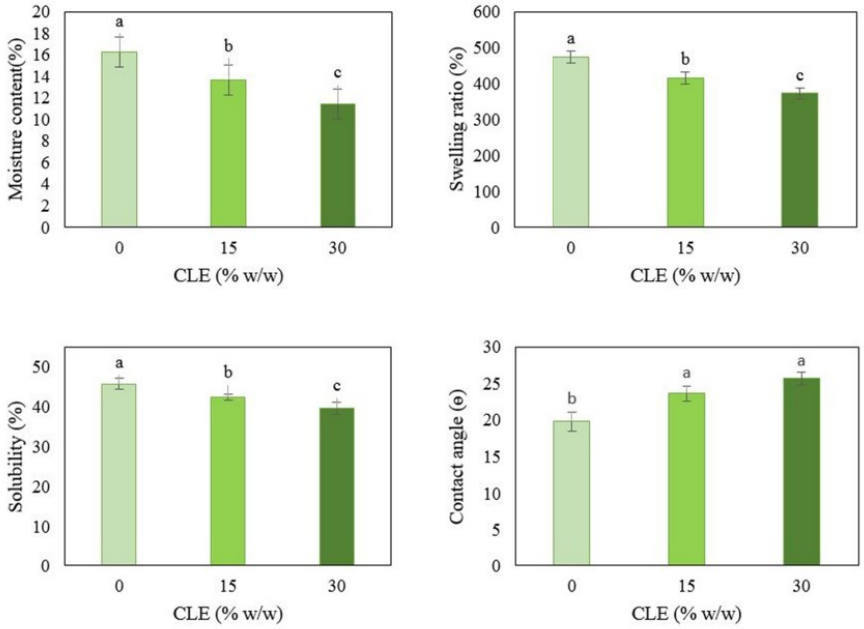

Fig. 11. Moisture content, water solubility, swelling and contact angle of cardoon protein-based films containing different concentrations of cardoon leaf extract (CLE). Values with different small letters (a–c) are significantly different (Duncan's multiple range tests, $p < 0.05$). Further experimental details are given in the text.

permeability values of CP films containing higher aumounts of CLE were found to be higher than those containing 15% CLE. Similar findings were obtained by Galus and Kadzińska (2016) who reported an increase in gas permeabilities by increasing almond and walnut oil concentrations in the whey protein films. Therefore, also these data seem to reflect the microstructure of the prepared films, since an increase in pores and voids in the film network was observed in the films prepared with the highest (30%) CLE concentration (Fig. 10, B3). Similar results were reported by Bai et al. (2019) who studied the effects of different amounts of quercetin on carboxymethyl chitosan based films. Nevertheless, it is worthy to note that the behaviour in terms of barrier properties of the films containing CLE is not far from that observed for another protein-based bio-plastic, such as the one produced by using whey proteins functionalized with a phenolic extract (30% w/w of proteins) obtained from Pecan nutshell (Arciello et al., 2021). In fact, the authors found out that the permeabilities towards water vapor and the two types of gases performed by the whey protein film prepared with the extract were found to be significantly lower compared to those of the unfunctionalized one. The authors concluded that these results are useful for a potential application of such bio-plastics in the food sector, since, to keep food fresh, the water vapor permeability value should be maintained as low as possible. Furthermore, a higher O_2 barrier property is also important since oxygen causes, for example, the rancidity of fatty acids (Arciello et al., 2021).

3.3.8. *Antioxidant activity of cardoon protein-based films containing cardoon leaf extract*

CP-based films containing CLE were tested for DPPH radical scavenging activity over time. Fig. 12 shows that the films freshly manufactured in the absence of CLE exhibited a marked antioxidant activity and that the addition of 30% CLE improved this property since the observed scavenging activity against DPPH radical of the films increased form 30% up to 60%. The antioxidant activity of all films remained quite stable after 30 days at room temperature, suggesting their potential exploitation as active packaging for shelf life extension of foodstuffs. Similar results were obtained by Moghadam et al. (2020) who described a range of scavenging activity from 14% to 65% for mung bean protein-based films enriched with different amounts of pomegranate peel powder, whilst Adilah et al. (2018) and Hanani et al. (2019) reported an enhancement of the scavenging activity up to 89% and up to 72% for fish gelatin films added with mango kernel extract and pomegranate peel powder, respectively. From Fig. 12 it also possible to note that over a period of 70 days the antioxidant activity decreased roughly of 25% for all the bio-plastics tested, likely because of the oxidation of the phenolic compounds responsible of conferring the films with this biological activity. Nevertheless, the materials functionalized with the highest amount of CLE seem to be still endowed with the highest antioxidant activity (45%) even after a period of 70 days, suggesting their possible application in protecting some foods from the oxidation.

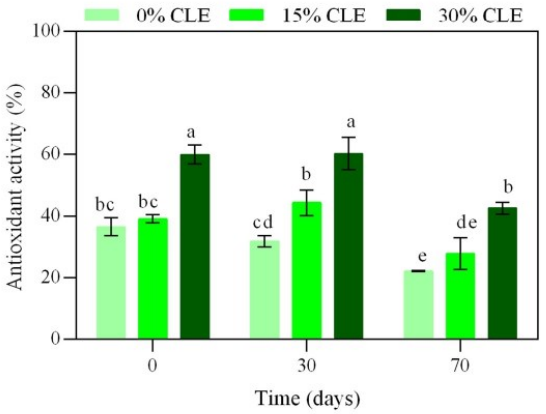

Fig. 12. Effect of different concentrations of cardoon leaf extract (CLE) on the antioxidant activity of cardoon protein-based films measured by DPPH assay at different times of storage. Values with different small letters (a–e) are significantly different (Duncan's multiple range tests, $p < 0.05$). Further experimental details are given in the text.

4. Conclusions

The objective of this paper was to valorise different *Cynara cardunculus* segments by extracting bio-based products useful for an integrated application. A method for recovery of a functional cardoon leaf extract (CLE) was set up and its composition analysis revealed the presence of several low molecular weight molecules (such as two sesquiterpene lactone, cynaropicrin and grosheimin) of potential attractiveness as bioactive compounds. In addition, proteins extracted from cardoon seeds were tested as raw material for producing, in the presence of glycerol, manipulable bio-plastics endowed with promising mechanical and barrier features, as well as antioxidant properties. Towards the development of a *Cynara cardunculus* biorefinery, the obtained CLE was added to the protein-based film forming solutions and the characterization of the derived films showed a significant improvement of all the properties of the manufactured material. The CLE-containing films appeared smoother and more homogenous, and showed also a higher and lasting antioxidant activity that conferred a higher value to the obtained bio-plastics. Therefore, all the presented data envisage *Cynara cardunculus* as a potential biomass resource for the development of a plant biorefinery devoted to the production of innovative bio-based products according to the principles of the circular bio-economy. In particular, the produced bio-plastics may be exploited for extending the shelf-life of different kinds of foodstuffs due to the fact that, besides showing good mechanical and barrier properties, they are endowed with antioxidant features that are of a paramount importance for food protection. Nevertheless, a potential use of such biomaterials as mulching sheets is also advisable.

Author contributions

Seyedeh Fatemeh Mirpoor: Investigation; Methodology; Formal analysis; Writing-original draft. Simona Varriale: Investigation; Methodology; Formal analysis; Writing-original draft. Raffaele Porta: Supervision; Funding acquisition; Conceptualization; Writing review and editing. Daniele Naviglio: Methodology; Investigation. Mariachiara Spennato: Methodology; Investigation. Lucia Gardossi: Methodology; Investigation. C. Valeria L. Giosafatto: Supervision; Conceptualization; Writing review and editing. Cinzia Pezzella: Supervision; Conceptualization; Writing review and editing.

Declaration of competing interest

None.

Acknowledgments

We thank Prof. Rocco Di Girolamo for performing microscopy analyses and Prof. Massimo Fagnano for providing Cardoon in April 2019. This research was funded by the grant PRIN: Progetti di Ricerca di Interesse Nazionale –Bando 2017– "CARDoon valorisation by InteGrAted biorefiNery (CARDIGAN)" of Italian Ministero dell'Università e della Ricerca (COD. 2017KBTK93).

References

AACC. (2003). *Approved methods of AACC*. St. Paul, MN, USA: The Association. Available at: https://methods.aaccnet.org/default.aspx. (Accessed 5 May 2021).

Abdelhedi, O., Nasri, R., Jridi, M., Kchaou, H., Nasreddine, B., Karbowiak, T., et al. (2018). Composite bioactive films based on smooth-hound viscera proteins and gelatin: Physicochemical characterization and antioxidant properties. *Food Hydrocolloids, 74*, 176–186. https://doi.org/10.1016/j.foodhyd.2017.08.006

Adilah, A. N., Jamilah, B., Noranizan, M. A., & Hanani, Z. A. N. (2018). Utilization of mango peel extracts on the biodegradable films for active packaging. *Food Packaging and Shelf Life, 16*, 1–7. https://doi.org/10.1016/j.fpsl.2018.01.006

Arabestani, A., Kadivar, M., Shahedi, M., Goli, S. A. H., & Porta, R. (2016). Characterization and antioxidant activity of bitter vetch protein-based films containing pomegranate juice. *Lebensmittel-Wissenschaft und -Technologie- Food Science and Technology, 74*(74), 77–83. https://doi.org/10.1016/j.lwt.2016.07.025

Arciello, A., Panzella, L., Dell'Olmo, E., Abdalrazeq, M., Moccia, F., Saglione, R., et al. (2021). Development and characterization of antimicrobial and antioxidant whey protein-based films functionalized with Pecan (*Carya illinoinensis*) nut shell extract. *Food Packaging and Shelf Life, 29*, Article 100710. https://doi.org/10.1016/J.FPSL.2021.100710

ASTM F1249 - 13: Standard test method for water vapor transmission rate through plastic film and sheeting using a modulated infrared sensor. Retrieved from https://www.astm.org/DATABASE.CART/HISTORICAL/F1249-13.htm, (2013).

ASTM D3985 - 05. (2010). Standard test method for oxygen gas transmission rate through plastic film and sheeting using a coulometric sensor. Retrieved from https://www.astm.org/DATABASE.CART/HISTORICAL/D3985-05.htm.

ASTM D882 - 18. (1997). Standard test method for tensile properties of thin plastic sheeting - ANSI blog. Retrieved from https://www.astm.org/Standards/D882.

ASTM F 2476-05. (2005). Standard test method for the determination of carbon dioxide gas transmission rate (CO2 TR) through barrier materials using an infrared detector. Retrieved from https://www.astm.org/DATABASE.CART/HISTORICAL/F2476-05.htm.

Baek, S.-K., Kim, S., & Song, K. (2018). Characterization of *Ecklonia cava* alginate films containing cinnamon essential oils. *International Journal of Molecular Sciences, 19*(11), 3545. https://doi.org/10.3390/ijms19113545

Bai, R., Zhang, X., Yong, H., Wang, X., Liu, Y., & Liu, J. (2019). Development and characterization of antioxidant active packaging and intelligent Al 3+ -sensing films based on carboxymethyl chitosan and quercetin. *International Journal of Biological Macromolecules, 126*, 1074–1084. https://doi.org/10.1016/j.ijbiomac.2018.12.264

Barbosa, C. H., Andrade, M. A., Vilarinho, F., Castanheira, I., Fernando, A. L., Loizzo, M. R., et al. (2020). A new insight on cardoon: Exploring new uses besides cheese making with a view to zero waste. *Foods, 9*(5), 1–22. https://doi.org/10.3390/foods9050564

Batista, J. T. S., Araújo, C. S., Peixoto Joele, M. R. S., Silva, J. O. C., & Lourenço, L. F. H. (2019). Study of the effect of the chitosan use on the properties of biodegradable films of myofibrillar proteins of fish residues using response surface methodology. *Food Packaging and Shelf Life, 20*, Article 100306. https://doi.org/10.1016/j.fpsl.2019.100306

Ben Salem, M., Affes, H., Athmouni, K., Ksouda, K., Dhouibi, R., Sahnoun, Z., et al. (2017). Chemicals compositions, antioxidant and anti-inflammatory activity of *Cynara scolymus* leaves extracts, and analysis of major bioactive polyphenols by HPLC. *Evidence-based Complementary and Alternative Medicine, 2017*, 4951937. https://doi.org/10.1155/2017/4951937, 2017.

Benlloch-González, M., Fournier, J. M., Ramos, J., & Benlloch, M. (2005). Strategies underlying salt tolerance in halophytes are present in *Cynara cardunculus*. *Plant Science, 168*(3), 653–659. https://doi.org/10.1016/j.plantsci.2004.09.035

Bernhard, H. (1982). Quantitative determination of bitter sesquiterpenes from *Cynara scolymus* L. (artichoke) and *Cynara cardunculus* L. (Kardone) (Compositae). *Section Title: Plant Biochemistry, 57*(7), 179–180.

Bhattacharjee, S. (2016, August 10). DLS and zeta potential - what they are and what they are not? *Journal of Controlled Release, 235*, 337–351. https://doi.org/10.1016/j.jconrel.2016.06.017

Biel, W., Witkowicz, R., Piątkowska, E., & Podsiadło, C. (2020). Proximate composition, minerals and antioxidant activity of artichoke leaf extracts. *Biological Trace Element Research, 194*(2), 589–595. https://doi.org/10.1007/s12011-019-01806-3

Bitencourt, C. M., Fávaro-Trindade, C. S., Sobral, P. J. A., & Carvalho, R. A. (2014). Gelatin-based films additivated with curcuma ethanol extract: Antioxidant activity and physical properties of films. *Food Hydrocolloids, 40*, 145–152. https://doi.org/10.1016/j.foodhyd.2014.02.014

Caprioli, G., Iannarelli, R., Sagratini, G., Vittori, S., Zorzetto, C., Sánchez-Mateo, C. C., et al. (2017). Phenolic acids, antioxidant and antiproliferative activities of Naviglio® extracts from *Schizogyne sericea* (Asteraceae). *Natural Product Research, 31*(5), 515–522. https://doi.org/10.1080/14786419.2016.1195383

Chen, F. P., Li, B. S., & Tang, C. H. (2015). Nanocomplexation between curcumin and soy protein isolate: Influence on curcumin stability/bioaccessibility and in vitro protein digestibility. *Journal of Agricultural and Food Chemistry, 63*(13), 3559–3569. https://doi.org/10.1021/acs.jafc.5b00448

Chentir, I., Kchaou, H., Hamdi, M., Jridi, M., Li, S., Doumandji, A., et al. (2019). Biofunctional gelatin-based films incorporated with food grade phycocyanin extracted from the Saharian cyanobacterium *Arthrospira sp*. *Food Hydrocolloids, 89*, 715–725. https://doi.org/10.1016/J.FOODHYD.2018.11.034

Cruz-Díaz, K., Cobos, Á., Fernández-Valle, M. E., Díaz, O., & Cambero, M. I. (2019). Characterization of edible films from whey proteins treated with heat, ultrasounds and/or transglutaminase. Application in cheese slices packaging. *Food Packaging and Shelf Life, 22*, Article 100397. https://doi.org/10.1016/j.fpsl.2019.100397

Dapčević-Hadnađev, T., Hadnađev, M., Lazaridou, A., Moschakis, T., & Biliaderis, C. G. (2018). Hempseed meal protein isolates prepared by different isolation techniques. Part II. gelation properties at different ionic strengths. *Food Hydrocolloids, 81*, 481–489. https://doi.org/10.1016/j.foodhyd.2018.03.022

Dawidowicz, A. L., Wianowska, D., & Olszowy, M. (2012). On practical problems in estimation of antioxidant activity of compounds by DPPH method (Problems in estimation of antioxidant activity). *Food Chemistry, 131*(3), 1037–1043. https://doi.org/10.1016/j.foodchem.2011.09.067

Del Baño, M. J., Lorente, J., Castillo, J., Benavente-García, O., Del Río, J. A., Ortuño, A., et al. (2003). Phenolic diterpenes, flavones, and rosmarinic acid distribution during the development of leaves, flowers, stems, and roots of *Rosmarinus officinalis*. Antioxidant activity. *Journal of Agricultural and Food Chemistry, 51*(15), 4247–4253. https://doi.org/10.1021/jf0300745

Dias, M. I., Barros, L., Barreira, J. C. M., Alves, M. J., Barracosa, P., & Ferreira, I. C. F. R. (2018). Phenolic profile and bioactivity of cardoon (*Cynara cardunculus* L.) inflorescence parts: Selecting the best genotype for food applications. March *Food Chemistry, 268*, 196–202. https://doi.org/10.1016/j.foodchem.2018.06.081.

Djeridane, A., Yousfi, M., Nadjemi, B., Boutassouna, D., Stocker, P., & Vidal, N. (2006). Antioxidant activity of some algerian medicinal plants extracts containing phenolic compounds. *Food Chemistry, 97*(4), 654–660. https://doi.org/10.1016/j.foodchem.2005.04.028

Eljounaidi, K., Comino, C., Moglia, A., Cankar, K., Genre, A., Hehn, A., et al. (2015). Accumulation of cynaropicrin in globe artichoke and localization of enzymes involved in its biosynthesis. *Plant Science, 239*, 128–136. https://doi.org/10.1016/j.plantsci.2015.07.020

Emam-Djomeh, Z., Moghaddam, A., & Yasini Ardakani, S. A. (2015). Antimicrobial activity of pomegranate (*Punica granatum* L.) peel extract, physical, mechanical, barrier and antimicrobial properties of pomegranate peel extract-incorporated sodium caseinate film and application in packaging for ground beef. *Packaging Technology and Science, 28*(10), 869–881. https://doi.org/10.1002/pts.2145

Fagnano, M., Impagliazzo, A., Mori, M., & Fiorentino, N. (2015). Agronomic and environmental impacts of giant reed (*Arundo donax* L.): Results from a long-term field experiment in hilly areas subject to soil erosion. *Bioenergy Research, 8*(1), 415–422. https://doi.org/10.1007/s12155-014-9532-7

Falleh, H., Ksouri, R., Chaieb, K., Karray-Bouraoui, N., Trabelsi, N., Boulaaba, M., et al. (2008). Phenolic composition of *Cynara cardunculus* L. organs, and their biological activities. *Comptes Rendus Biologies, 331*(5), 372–379. https://doi.org/10.1016/j.crvi.2008.02.008

Fathi, N., Almasi, H., & Pirouzifard, M. K. (2019). Sesame protein isolate based bionanocomposite films incorporated with TiO2 nanoparticles: Study on morphological, physical and photocatalytic properties. *Polymer Testing, 77*, Article 105919. https://doi.org/10.1016/j.polymertesting.2019.105919

Fernández, J., Curt, M. D., & Aguado, P. L. (2006). Industrial applications of *Cynara cardunculus* L. for energy and other uses. *Industrial Crops and Products, 24*(3), 222–229. https://doi.org/10.1016/J.INDCROP.2006.06.010

Floegel, A., Kim, D. O., Chung, S.-J., Koo, S. I., & Chun, O. K. (2011). Comparison of ABTS DPPH assays to measure antioxidant capacity in popular antioxidant-rich US foods. *Journal of Food Composition and Analysis, 24*, 1043–1048. https://doi.org/10.1016/j.jfca.2011.01.008

Fratianni, F., Tucci, M., Palma, M. De, Pepe, R., & Nazzaro, F. (2007). Polyphenolic composition in different parts of some cultivars of globe artichoke (*Cynara cardunculus* L. var. *scolymus* (L.) Fiori). *Food Chemistry, 104*(3), 1282–1286. https://doi.org/10.1016/j.foodchem.2007.01.044

Gallo, M., Formato, A., Giacco, R., Riccardi, G., Lungo, D., Formato, G., et al. (2019). Mathematical optimization of the green extraction of polyphenols from grape peels through a cyclic pressurization process. *Heliyon, 5*(4), Article e01526. https://doi.org/10.1016/j.heliyon.2019.e01526

Galus, S., & Kadzińska, J. (2016). Whey protein edible films modified with almond and walnut oils. *Food Hydrocolloids, 52*, 78–86. https://doi.org/10.1016/j.foodhyd.2015.06.013

Genovese, C., Platania, C., Venticinque, M., Calderaro, P., Argento, S., Scandurra, S., et al. (2016). Evaluation of cardoon seeds presscake for animal feeding. *Acta Horticulturae, 1147*, 323–328. https://doi.org/10.17660/ActaHortic.2016.1147.45

Giosafatto, C. V. L., Fusco, A., Al-Asmar, A., & Mariniello, L. (2020). Microbial transglutaminase as a tool to improve the features of hydrocolloid-based bioplastics, 2020, Vol. 21, Page 3656 *International Journal of Molecular Sciences, 21*(10), 3656. https://doi.org/10.3390/IJMS21103656.

Gominho, J., Dolores, M., Lourenço, A., Fernández, J., & Pereira, H. (2018). Biomass and bioenergy *Cynara cardunculus* L . as a biomass and multi-purpose crop : A review of 30 years of research. December 2017 *Biomass and Bioenergy, 109*, 257–275. https://doi.org/10.1016/j.biombioe.2018.01.001.

Gouveia, S. C., & Castilho, P. C. (2012). Phenolic composition and antioxidant capacity of cultivated artichoke, Madeira cardoon and artichoke-based dietary supplements. *Food Research International, 48*(2), 712–724. https://doi.org/10.1016/j.foodres.2012.05.029

Haghighi, H., Biard, S., Bigi, F., De Leo, R., Bedin, E., Pfeifer, F., et al. (2019). Comprehensive characterization of active chitosan-gelatin blend films enriched with different essential oils. *Food Hydrocolloids, 95*, 33–42. https://doi.org/10.1016/j.foodhyd.2019.04.019

Hanani, Z. A. N., Yee, F. C., & Nor-Khaizura, M. A. R. (2019). Effect of pomegranate (*Punica granatum* L.) peel powder on the antioxidant and antimicrobial properties of fish gelatin films as active packaging. *Food Hydrocolloids, 89*, 253–259. https://doi.org/10.1016/j.foodhyd.2018.10.007

Hebbar, R. S., Isloor, A. M., & Ismail, A. F. (2017). Contact angle measurements. In *Membrane characterization* (pp. 219–255). https://doi.org/10.1016/B978-0-444-63776-5.00012-7

Ierna, A., Sortino, O., & Mauromicale, G. (2020). Biomass, seed and energy yield of *Cynara cardunculus* L. As affected by environment and season, 2020, Vol. 10, Page 1548 *Agronomy*, *10*(10), 1548. https://doi.org/10.3390/AGRONOMY10101548.

Kukić, J., Popović, V., Petrović, S., Mucaji, P., Ćirić, A., Stojković, D., et al. (2008). Antioxidant and antimicrobial activity of *Cynara cardunculus* extracts. *Food Chemistry*, *107*(2), 861–868. https://doi.org/10.1016/j.foodchem.2007.09.005

Lattanzio, V., Kroon, P. A., Linsalata, V., Cardinali, A., Agro-ambientali, D. S., & Vegetale, D. (2009). Globe artichoke : A functional food and source of nutraceutical ingredients. *Journal of Functional Foods*, *1*(2), 131–144. https://doi.org/10.1016/j.jff.2009.01.002

Laufer, G., Kirkland, C., Cain, A. A., & Grunlan, J. C. (2013). Oxygen barrier of multilayer thin films comprised of polysaccharides and clay. *Carbohydrate Polymers*, *95*(1), 299–302. https://doi.org/10.1016/j.carbpol.2013.02.048

Mandim, F., Inês, M., Pinela, J., Barracosa, P., Ivanov, M., & Ferreira, I. C. F. R. (2020). Chemical composition and in vitro biological activities of cardoon (*Cynara cardunculus* L . var . *altilis* DC .) seeds as influenced by viability. November 2019 *Food Chemistry*, *323*, Article 126838. https://doi.org/10.1016/j.foodchem.2020.126838.

Mathe, C., Culioli, G., Archier, P., & Vieillescazes, C. (2004). Characterization of archaeological frankincense by gas chromatography-mass spectrometry. *Journal of Chromatography A*, *1023*(2), 277–285. https://doi.org/10.1016/j.chroma.2003.10.016

Mauromicale, G., Sortino, O., Pesce, G. R., Agnello, M., & Mauro, R. P. (2014). Suitability of cultivated and wild cardoon as a sustainable bioenergy crop for low input cultivation in low quality Mediterranean soils. *Industrial Crops and Products*, *57*, 82–89. https://doi.org/10.1016/J.INDCROP.2014.03.013

Mirpoor, S. F., Giosafatto, C. V. L., Di Pierro, P., Di Girolamo, R., Regalado-González, C., & Porta, R. (2020). Valorisation of *Posidonia oceanica* sea balls (egagropili) as a potential source of reinforcement agents in protein-based biocomposites. *Polymers*, *12*(12), 2788. https://doi.org/10.3390/polym12122788

Mirpoor, S. F., Giosafatto, C. V. L., & Porta, R. (2021). Biorefining of seed oil cakes as industrial co-streams for production of innovative bioplastics. A review. *Trends in Food Science & Technology*, *109*, 259–270. Retrieved from https://www.sciencedirect.com/science/article/pii/S0924224421000194.

Mirpoor, S. F., Hosseini, S. M. H., & Nekoei, A. R. (2017a). Efficient delivery of quercetin after binding to beta-lactoglobulin followed by formation soft-condensed core-shell nanostructures. *Food Chemistry*, *233*, 282–289. https://doi.org/10.1016/j.foodchem.2017.04.126

Mirpoor, S. F., Hosseini, S. M. H., & Yousefi, G. H. (2017b). Mixed biopolymer nanocomplexes conferred physicochemical stability and sustained release behavior to introduced curcumin. *Food Hydrocolloids*, *71*, 216–224. https://doi.org/10.1016/j.foodhyd.2017.05.021

Moghadam, M., Salami, M., Mohammadian, M., Khodadadi, M., & Emam-Djomeh, Z. (2020). Development of antioxidant edible films based on mung bean protein enriched with pomegranate peel. *Food Hydrocolloids*, *104*, Article 105735. https://doi.org/10.1016/j.foodhyd.2020.105735

Mohammadian, M., Salami, M., Momen, S., Alavi, F., Emam-Djomeh, Z., & Moosavi-Movahedi, A. A. (2019). Enhancing the aqueous solubility of curcumin at acidic condition through the complexation with whey protein nanofibrils. *Food Hydrocolloids*, *87*, 902–914. https://doi.org/10.1016/J.FOODHYD.2018.09.001

Naviglio, D. (2003). Naviglio's principle and presentation of an innovative solid-liquid extraction technology: Extractor Naviglio®. *Analytical Letters*, *36*(8), 1647–1659. https://doi.org/10.1081/AL-120021555

Naviglio, D., Scarano, P., Ciaravolo, M., & Gallo, M. (2019). Rapid solid-liquid dynamic extraction (rslde): A powerful and greener alternative to the latest solid-liquid extraction techniques. *Foods*, *8*(7), 245. https://doi.org/10.3390/FOODS8070245, 2019, Vol. 8, Page 245.

Nur Hanani, Z. A., Aelma Husna, A. B., Nurul Syahida, S., Nor Khaizura, M. A. B., & Jamilah, B. (2018). Effect of different fruit peels on the functional properties of gelatin/polyethylene bilayer films for active packaging. *Food Packaging and Shelf Life*, *18*, 201–211. https://doi.org/10.1016/j.fpsl.2018.11.004

Ottaiano, L., Di Mola, I., Impagliazzo, A., Cozzolino, E., Masucci, F., Mori, M., et al. (2017). Yields and quality of biomasses and grain in *Cynara cardunculus* L. grown in southern Italy, as affected by genotype and environmental conditions. *Italian Journal of Agronomy*, *12*(4), 375–382. https://doi.org/10.4081/ija.2017.954

Pandino, G., Lombardo, S., Mauromicale, G., & Williamson, G. (2011). Phenolic acids and flavonoids in leaf and floral stem of cultivated and wild *Cynara cardunculus* L. genotypes. *Food Chemistry*, *126*(2), 417–422. https://doi.org/10.1016/j.foodchem.2010.11.001

Panzella, L., Moccia, F., Nasti, R., Marzorati, S., Verotta, L., & Napolitano, A. (2020). Bioactive phenolic compounds from agri-food wastes: An update on green and sustainable extraction methodologies. May *Frontiers in Nutrition*, *7*, 1–27. https://doi.org/10.3389/fnut.2020.00060.

Pappalardo, H. D., Toscano, V., Puglia, G. D., Genovese, C., & Raccuia, S. A. (2020). March. *Cynara cardunculus L . As a multipurpose crop for plant secondary metabolites production in marginal stressed lands*, *11* pp. 1–14). https://doi.org/10.3389/fpls.2020.00240.

Pesce, G. R., Negri, M., Bacenetti, J., & Mauromicale, G. (2017). The biomethane, silage and biomass yield obtainable from three accessions of *Cynara cardunculus*. September 2016 *Industrial Crops and Products*, *103*, 233–239. https://doi.org/10.1016/j.indcrop.2017.04.003.

Petropoulos, S. A., Fernandes, Â., Tzortzakis, N., Sokovic, M., Ciric, A., Barros, L., et al. (2019). Bioactive compounds content and antimicrobial activities of wild edible Asteraceae species of the Mediterranean fl ora under commercial cultivation conditions. October 2018 *Food Research International*, *119*, 859–868. https://doi.org/10.1016/j.foodres.2018.10.069.

Pinelli, P., Agostini, F., Comino, C., Lanteri, S., Portis, E., & Romani, A. (2007). Simultaneous quantification of caffeoyl esters and flavonoids in wild and cultivated cardoon leaves. *Food Chemistry*, *105*(4), 1695–1701. https://doi.org/10.1016/j.foodchem.2007.05.014

Porta, R., Di Pierro, P., Roviello, V., & Sabbah, M. (2017). Tuning the functional properties of bitter vetch (*Vicia ervilia*) protein films grafted with spermidine. *International Journal of Molecular Sciences*, *18*(12). https://doi.org/10.3390/ijms18122658

Posadino, A. M., Biosa, G., Zayed, H., Abou-Saleh, H., Cossu, A., Nasrallah, G. K., et al. (2018). Protective effect of cyclically pressurized solid–liquid extraction polyphenols from cagnulari grape pomace on oxidative endothelial cell death. *Molecules*, *23*(9), 1–12. https://doi.org/10.3390/molecules23092105

Quan, T. H., Benjakul, S., Sae-leaw, T., Balange, A. K., & Maqsood, S. (2019). September 1). Protein–polyphenol conjugates: Antioxidant property, functionalities and their applications. *Trends in Food Science & Technology*, *91*, 507–517. https://doi.org/10.1016/j.tifs.2019.07.049

Ramos, P. A. B., Guerra, A. R., Guerreiro, O., Freire, C. S. R., Silva, A. M. S., Duarte, M. F., et al. (2013). Lipophilic extracts of *Cynara cardunculus* L. var. *altilis* (dc): A source of valuable bioactive terpenic compounds. *Journal of Agricultural and Food Chemistry*, *61*(35), 8420–8429. https://doi.org/10.1021/jf402253a

Ramos, P. A. B., Guerra, Â. R., Guerreiro, O., Santos, S. A. O., Oliveira, H., Freire, C. S. R., et al. (2017). Antiproliferative effects of *Cynara cardunculus* L. Var. *altilis* (DC) lipophilic extracts. *International Journal of Molecular Sciences*, *18*(1). https://doi.org/10.3390/ijms18010063

Ramos, P. A. B., Santos, S. A. O., Guerra, Â. R., Guerreiro, O., Freire, C. S. R., Rocha, S. M., et al. (2014). Phenolic composition and antioxidant activity of different morphological parts of *Cynara cardunculus* L. var. *altilis* (DC). *Industrial Crops and Products*, *61*, 460–471. https://doi.org/10.1016/j.indcrop.2014.07.042

Re, R., Pellegrini, N., Proteggente, A., Pannala, A., Yang, M., & Rice-Evans, C. (1999). Antioxidant activity applying an improved ABTS radical cation decolorization assay, 2007 *Free Radical Biology & Medicine*, *26*, 51.

Reynolds, W. F., McLean, S., Poplawski, J., Enriquez, R. G., Escobar, L. I., & Leon, I. (1986). Total assignment of 13C and 1H spectra of three isomeric triterpenol derivatives by 2D NMR: An investigation of the potential utility of 1H chemical shifts in structural investigations of complex natural products. *Tetrahedron*, *42*(13), 3419–3428. https://doi.org/10.1016/S0040-4020(01)87309-9

Riaz, A., Lei, S., Akhtar, H. M. S., Wan, P., Chen, D., Jabbar, S., et al. (2018). Preparation and characterization of chitosan-based antimicrobial active food packaging film incorporated with apple peel polyphenols. *International Journal of Biological Macromolecules*, *114*, 547–555. https://doi.org/10.1016/j.ijbiomac.2018.03.126

Rouphael, Y., Bernardi, J., Cardarelli, M., Bernardo, L., Kane, D., Colla, G., et al. (2016). Phenolic compounds and sesquiterpene lactones profile in leaves of nineteen artichoke cultivars. *Journal of Agricultural and Food Chemistry*, *64*(45), 8540–8548. https://doi.org/10.1021/acs.jafc.6b03856

Roy, S., & Rhim, J. W. (2020). Preparation of carbohydrate-based functional composite films incorporated with curcumin. *Food Hydrocolloids*, *98*, Article 105302. https://doi.org/10.1016/j.foodhyd.2019.105302

Roy, S., Rhim, J. W., & Jaiswal, L. (2019). Bioactive agar-based functional composite film incorporated with copper sulfide nanoparticles. *Food Hydrocolloids*, *93*, 156–166. https://doi.org/10.1016/j.foodhyd.2019.02.034

Sánchez-Gómez, R., Zalacain, A., Alonso, G. L., & Salinas, M. R. (2014). Vine-shoot waste aqueous extracts for re-use in agriculture obtained by different extraction techniques: Phenolic, volatile, and mineral compounds. *Journal of Agricultural and Food Chemistry*, *62*(45), 10861–10872. https://doi.org/10.1021/jf503929v

Sarıcaoglu, F. T., & Turhan, S. (2020). Physicochemical, antioxidant and antimicrobial properties of mechanically deboned chicken meat protein films enriched with various essential oils. *Food Packaging and Shelf Life*, *25*, Article 100527. https://doi.org/10.1016/j.fpsl.2020.100527

Scarano, P., Naviglio, D., Prigioniero, A., Tartaglia, M., Postiglione, A., Sciarrillo, R., et al. (2020). Sustainability: Obtaining natural dyes from waste matrices using the prickly pear peels of *Opuntia ficus-indica* (L.) miller, 2020, Vol. 10, Page 528 *Agronomy*, *10*(4), 528. https://doi.org/10.3390/AGRONOMY10040528.

Scavo, A., Pandino, G., Restuccia, C., Parafati, L., Cirvilleri, G., & Mauromicale, G. (2019). Antimicrobial activity of cultivated cardoon (*Cynara cardunculus* L. var. *altilis* DC.) leaf extracts against bacterial species of agricultural and food interest. December 2018 *Industrial Crops and Products*, *129*, 206–211. https://doi.org/10.1016/j.indcrop.2018.12.005.

Scavo, A., Rial, C., Varela, R. M., Molinillo, J. M. G., Mauromicale, G., & Macias, F. A. (2019). Influence of genotype and harvest time on the *Cynara cardunculus* L. Sesquiterpene lactone profile. *Journal of Agricultural and Food Chemistry*, *67*(23), 6487–6496. https://doi.org/10.1021/acs.jafc.9b02313

Shams, B., Ebrahimi, N. G., & Khodaiyan, F. (2019). Development of antibacterial nanocomposite: Whey protein-gelatin-nanoclay films with orange peel extract and tripolyphosphate as potential food packaging. *Advances in Polymer Technology*, *2019*. https://doi.org/10.1155/2019/1973184

Siddiqui, N., Rauf, A., Latif, A., & Mahmood, Z. (2017). Spectrophotometric determination of the total phenolic content, spectral and fluorescence study of the herbal Unani drug Gul-e-Zoofa (*Nepeta bracteata* Benth). *Journal of Taibah University Medical Sciences*, *12*(4), 360–363. https://doi.org/10.1016/j.jtumed.2016.11.006

Sobolev, A. P., Brosio, E., Gianferri, R., & Segre, A. L. (2005). Metabolic profile of lettuce leaves by high-field NMR spectra. *Magnetic Resonance in Chemistry*, *43*(8), 625–638. https://doi.org/10.1002/mrc.1618

Sun, K. Q., Li, F. Y., Li, J. Y., Li, J. F., Zhang, C. W., Chen, S., et al. (2019). Optimisation of compatibility for improving elongation at break of chitosan/starch films. *RSC Advances*, *9*(42), 24451–24459. https://doi.org/10.1039/c9ra04053f

Taghavi Kevij, H., Salami, M., Mohammadian, M., & Khodadadi, M. (2020). Fabrication and investigation of physicochemical, food simulant release, and antioxidant properties of whey protein isolate-based films activated by loading with curcumin through the pH-driven method. *Food Hydrocolloids, 108*, Article 106026. https://doi.org/10.1016/j.foodhyd.2020.106026

Toscano, V., Sollima, L., Genovese, C., Melilli, M. G., & Raccuia, S. A. (2016). *Pilot plant system for biodiesel and pellet production from cardoon : Technical and economic feasibility*. https://doi.org/10.17660/ActaHortic.2016.1147.60

Turco, R., Tesser, R., Cucciolito, M. E., Fagnano, M., Ottaiano, L., Mallardo, S., et al. (2019). Cynara cardunculus biomass recovery: An eco-sustainable, nonedible resource of vegetable oil for the production of poly(lactic acid) bioplasticizers. *ACS Sustainable Chemistry & Engineering, 7*(4), 4069–4077. https://doi.org/10.1021/acssuschemeng.8b05519

Velez, Z., Campinho, M. A., Guerra, Â. R., García, L., Ramos, P., Guerreiro, O., et al. (2012). Biological characterization of *Cynara cardunculus* l. Methanolic extracts: Antioxidant, anti-proliferative, anti-migratory and anti-angiogenic activities. *Agriculture, 2*(4), 472–492. https://doi.org/10.3390/agriculture2040472

2.5.7 Evaluation of the neuroprotective effects of cardoon bioactive molecules

Nutraceuticals or functional foods with antioxidant properties have recently been the subject of intensive investigation due to their capacity to act on the triad of conserved core mechanisms underlying brain damage, which include: oxidative stress, neurotrophic factors deficiency, and inflammation (Adelusi et al., 2021; Khadka et al., 2020).

Most plant extracts and pure bioactive ingredients typically have a polypharmacological profile, which today is considered more efficacious in preventing or attenuating neurological diseases than drugs responding to the “one drug-one target” concept which prevailed in the pharma industry in previous decades (Duran-Frigola et al., 2017; Youdim and Buccafusco, 2005).

Despite this, the pharmacological mechanism of the action of plant extracts was disclosed only in few cases, and the molecular mechanisms underlying their biological activity and the synergic action among the compounds of a phytochemical pool are mostly unknown.

The potential of polyphenols as neuroprotective agents against neurodegenerative diseases (especially Alzheimer and Parkinson) and cerebral ischemia has been recently investigated, demonstrating their beneficial effects thanks to their antioxidant properties and tissue regenerative properties (Haddadi et al., 2020).

Other molecules contained in cardoon plants demonstrated neuroprotective properties, in particular silymarin, an extract of *Silybum marianum* cardoon, containing a mixture of 3 main substances (silibinin, silycristin and silydianin) and various minor components (Saller et al., 2001). It is a flavonoid with a 1,4-dioxane ring containing a double bond between carbon 2 and carbon 3 in the benzopyran ring.

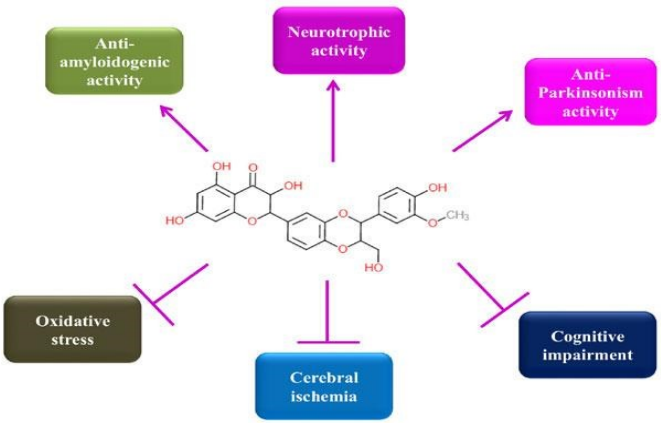

Figure 2.27 *Neuroprotective effects of silymarin.*

The mechanism of silymarin is linked to its ability to reduce oxidative stress, to its anti-inflammatory activity, to the ability to alter both the cellular apoptosis mechanism by activating estrogenic receptors that have a neuroprotective effect when they are activated. However, it has low solubility in water and, conversely, low bioavailability, making its pharmacological use impracticable since only quantities between 23% and 47% of silymarin reaches the systemic circulation after oral administration (Ullah and Khan, 2018).

In light of the recent studies on the neuroprotective properties of various plant extracts and cardoons in particular, this thesis has investigated the bioactive properties of different extracts of cardoon leaves in rescuing neuronal development arrest in an in vitro model of Rett syndrome (RTT). The rationale of this approach stems from the observation that many plant-derived medications typically have a polypharmacological profile with antioxidant, anti-inflammatory, and neurotrophic properties. Polypharmacological property, i.e., the ability of a single drug to act on multiple targets, is considered potentially a more successful strategy than drugs with a single target, especially in disorders with syndromic, polysymptomatic characteristics. RTT is the second leading genetic cause of mental retardation in females and is mainly caused by mutations in the X-linked MECP2 gene (Amir et al., 1999). RTT is considered a paradigmatic brain disease as it presents the classical triad of core mechanisms, comprising oxidative stress, neurotrophic factors deficiency, and inflammation common in most neurodevelopmental and neurodegenerative diseases (Leoncini et al., 2015). A major hallmark of RTT is brain atrophy with smaller and more closely packed neurons having decreased dendritic complexity causing general neural network malfunctioning (Bauman et al., 1995; Weng et al., 2011).

Clinically, RTT patients show developmental arrest, loss of speech and motor abilities, seizures, breathing abnormalities, and behavioural problems including autism (Belichenko et al., 1994; Fukuda et al., 2005; Kaufmann et al., 2000). Rett syndrome has been shown to be reversible in transgenic mice (Guy et al., 2007) but clinical trials have had so far limited success in reverting RTT (Clarke and Abdala Sheikh, 2018).

Neuronal atrophy can be reproduced in vitro, and figure 2.27 shows several examples of neurons corresponding to specific neuronal diseases: autism spectrum disorder (ASD), schizophrenia, Alzheimer's disease, Fragile X syndrome, and Down syndrome.

Focusing on the Rett syndrome neuron, it is evident that it has fewer and shorter dendrites (Kulkarni and Firestein, 2012).

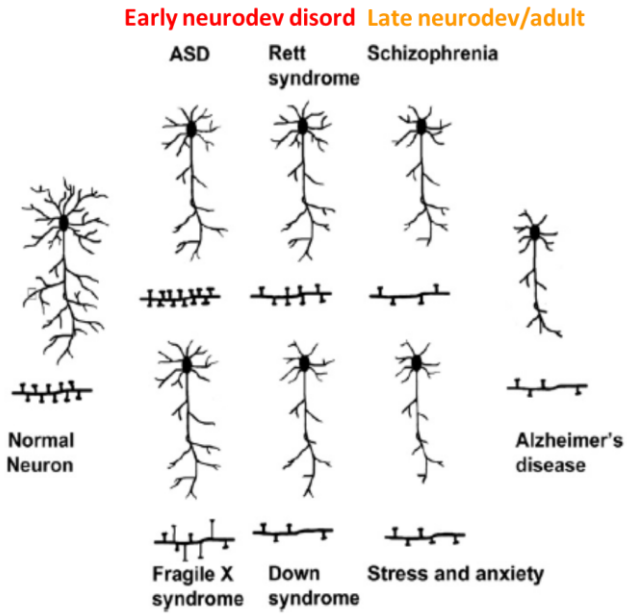

Figure 2.28 *Neuronal atrophy is a common feature of several neuronal diseases.*

Development of neurons occurs in six stages as is shown in figure 2.29. At day 0.25 neurons present lamellipodia. In the second stage at DIV 0.5 we can see minor processes that became primary dendrites at the 3° stage (from DIV 1 to DIV 3). The primary dendrites stabilize between DIV 4 and DIV 6, at the 4° stage of the development. Then there is a characteristic dynamic phase with branch instability, so that dendrites grow and retract dynamically until DIV 10-DIV15 that correspond to the last phase number 6, during which there is the final maturation of WT neurons. This is the physiological outgrowth of WT neurons.

In this scenario, RTT neurons show a delay in development starting from DIV 3 ending up with an incomplete synaptic coupling at DIV 10-15, when neurons should reach the mature morphology. Toward the 7 stages, from DIV 1 to DIV 21, we can see that at the level of the DIV 6, DIV 11-12, and DIV 14 to DIV 16 there is a significant reduction in the RTT TDL in respect to the WT. These DIV represent 3 different potential therapeutic windows in our in vitro model for Rett syndrome.

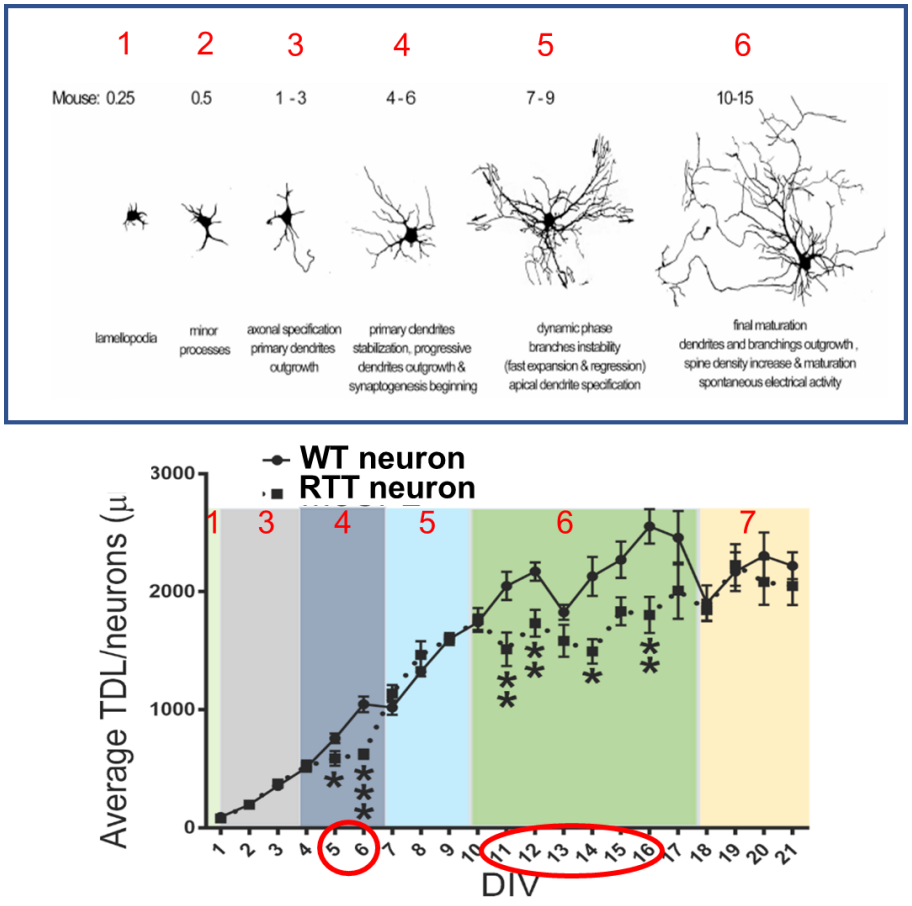

Figure 2.29 *Stages of development of neurons.*

On the basis of the literature evidence, the evaluation of the effect of cardoon leaves extract on wild mouse neurons was studied in collaboration with the neurobiology group of the Department of Life Sciences at the University of Trieste.

The extracts investigated in this study were obtained from plants harvested in spring and autumn 2020 in Terni plantation and leaves were extracted either with $scCO_2$ or with the Naviglio® methods: scCO2Au, scCO2Sp (Table 2.2 section 2.5.1) and NaviglioSp (Table 2.3, section 2.5.3).

This shows that the harvest period and maturity stages have a relevant effect on the chemical composition of extracts obtained from plant tissues. As already reported in the literature for various plant species, early maturity coincides with the highest content of phenolic compounds (Mandim et al., 2021).

This work was focused particularly on triterpenes and sesquiterpene lactones because of their known biological activities. Attention was paid also to squalene, a triterpene that is an intermediate in the cholesterol biosynthesis pathways, widely distributed in nature (Huang et al., 2009). Several studies show that squalene can effectively inhibit chemically induced skin, colon, and lung tumorigenesis in rodents (Auffray, 2007).

Taraxerol, a triterpene that has been isolated from several plant species, was considered because of its various pharmacological properties already demonstrated, such as the acetylcholinesterase (AChE) inhibition activity in vitro. Taraxerol also has anti-amnesic activity that may hold significant therapeutic value in alleviating certain memory impairments observed in Alzheimer disease (Berté et al., 2018).

Lupeol is a significant lupine-type triterpene isolated in plants, fungi, and animals. This bioactive molecule has several biological effects: anticancer, antiprotozoal, chemo-preventive, and anti-inflammatory properties (Gallo and Sarachine, 2009). The biological relevance of cynaropicrin has been previously described and commented on (section 2.2.3).

A comparison of the three extracts is presented in figure 2.30 that reports the GC-MS chromatograms of the three mixtures.

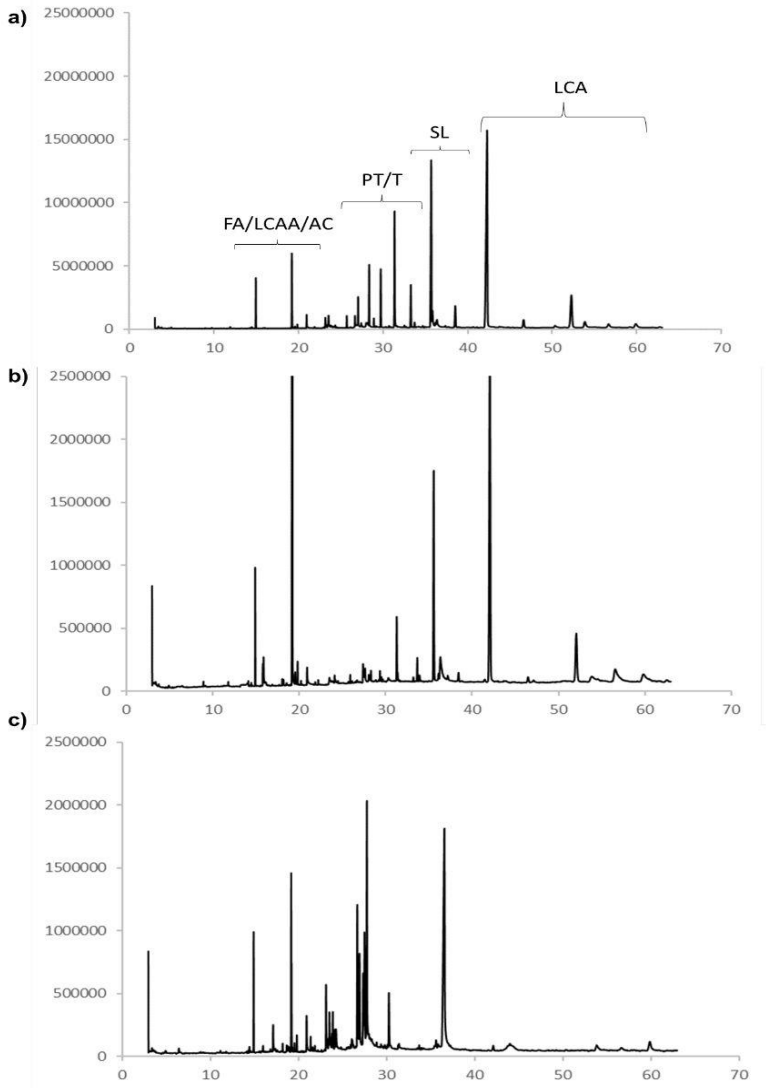

Figure 2.30 *GC-MS chromatograms of the three extracts from cardoon leaves obtained using different extractive technologies: a) Autumn harvest with scCO2 (scCO2Au); b) Spring harvest with sc CO2 (scCO2Sp); c) spring harvest using Naviglio® technology (NaviglioSp). FA=fatty acids; LCAA= long-chain aliphatic alcohols; AC=aromatic compounds; PT= pentacyclic triterpenes; T=triterpenes; SL= sesquiterpene lactone; LCA= long chain alkanes.*

The GC-MS analysis provides information on the chemical components, which were identified by comparing the corresponding mass values with data available from the NIST14s database and in the literature. Details about the characterization are available in sections 2.5.2 and 2.5.3 (figure 2.12, 2.13 and 2.19b).

Table 2.4 reports the concentration of the bioactive molecules calculated using calibration curves performed with GC-MS analysis.

Table 2.4 Composition of the principal bioactive molecules in the three solutions of cardoon leaf extracts.

	Composition* in $scCO_2Au$ (w w^{-1})	Composition* in $scCO_2Sp$ (w w^{-1})	Composition* in NaviglioSp (w w^{-1})
Cynaropicrin	0.040	0.020	0.230
Squalene	0.480	0.390	0.110
3ß-Taraxerol	0.070	0.030	<0.001
Lupeol	0.090	0.050	0.010

***** Composition expressed as w w^{-1} of each bioactive molecule /1 mg of extract.

The extracts obtained using $scCO_2$, specific for very hydrophobic molecules, are very rich in squalene. The rest of the hydrophobic extracts are mainly composed of waxes and fatty acids. There is an increased amount of squalene in the autumn extract compared to leaves collected in spring. The spring extract obtained with the Naviglio® method, employing ethanol as solvent, is the richest in cynaropicrin.

Notably, the $scCO_2$ extract obtained from plants harvested in spring 2020 at the Terni plantation was able to induce a significant rescue of neuronal atrophy in RTT neurons, while the $scCO_2$ extract from the autumn 2022 harvest was only active on WT neurons.

The study also employed single pure bioactive molecules for specific biological tests: cynaropicrin, squalene, 3ß-taraxerol and lupeol. Interestingly, when bioactive molecules were tested individually, no positive effect was observed on the neurons. A significant neurotoxic effect of cynaropicrin was evident at different concentrations, both when using the complex extracts (Naviglio® spring) and when using the pure molecule.

The results here reported pave the way for further studies to explore the application of cardoon extracts but, even more importantly, the present study demonstrates that the effective exploitation of the pharmacological potential of cardoon extracts requires a careful determination of their composition.

2.5.7.1 **Manuscript B** *"Neuroprotective properties of cardoon leaves extracts against neurodevelopmental deficits in an in vitro model of Rett syndrome 3 depend on the extraction method and harvest time"*

molecules

MDPI

Article

Neuroprotective Properties of Cardoon Leaves Extracts against Neurodevelopmental Deficits in an In Vitro Model of Rett Syndrome Depend on the Extraction Method and Harvest Time

Mariachiara Spennato [1], Ottavia Maria Roggero [2], Simona Varriale [3], Fioretta Asaro [1], Angelo Cortesi [4], Jan Kašpar [1], Enrico Tongiorgi [2], Cinzia Pezzella [3] and Lucia Gardossi [1,*]

[1] Department of Chemical and Pharmaceutical Sciences, University of Trieste, Via L. Giorgieri 1, 34127 Trieste, Italy
[2] Department of Life Sciences, University of Trieste, Via L. Giorgieri 5, 34127 Trieste, Italy
[3] Department of Chemical Sciences, University Federico II of Naples, Via Cinthia, 4, 80126 Napoli, Italy
[4] Department of Engineering and Architecture, University of Trieste, Via Alfonso Valerio 6/A, 34127 Trieste, Italy
* Correspondence: gardossi@units.it

Abstract: This study investigates the bioactive properties of different extracts of cardoon leaves in rescuing neuronal development arrest in an in vitro model of Rett syndrome (RTT). Samples were obtained from plants harvested at different maturity stages and extracted with two different methodologies, namely Naviglio® and supercritical carbon dioxide ($scCO_2$). While $scCO_2$ extracts more hydrophobic fractions, the Naviglio® method extracts phenolic compounds and less hydrophobic components. Only the $scCO_2$ cardoon leaves extract obtained from plants harvested in spring induced a significant rescue of neuronal atrophy in RTT neurons, while the $scCO_2$ extract from the autumn harvest stimulated dendrite outgrowth in Wild-Type (WT) neurons. The $scCO_2$ extracts were the richest in squalene, 3ß-taraxerol and lupeol, with concentrations in autumn harvest doubling those in spring harvest. The Naviglio® extract was rich in cynaropicrin and exerted a toxic effect at 20 µM on both WT and RTT neurons. When cynaropicrin, squalene, lupeol and 3ß-taraxerol were tested individually, no positive effect was observed, whereas a significant neurotoxicity of cynaropicrin and lupeol was evident. In conclusion, cardoon leaves extracts with high content of hydrophobic bioactive molecules and low cynaropicrin and lupeol concentrations have pharmacological potential to stimulate neuronal development in RTT and WT neurons in vitro.

Keywords: cardoon leaves; plant extracts; bioactive molecules; Rett syndrome; bioeconomy; supercritical carbon dioxide; Naviglio®

Citation: Spennato, M.; Roggero, O.M.; Varriale, S.; Asaro, F.; Cortesi, A.; Kašpar, J.; Tongiorgi, E.; Pezzella, C.; Gardossi, L. Neuroprotective Properties of Cardoon Leaves Extracts against Neurodevelopmental Deficits in an In Vitro Model of Rett Syndrome Depend on the Extraction Method and Harvest Time. *Molecules* **2022**, 27, 8772. https://doi.org/10.3390/molecules27248772

Academic Editor: Arjun H. Banskota

Received: 25 October 2022
Accepted: 7 December 2022
Published: 10 December 2022

1. Introduction

Nutraceuticals or functional foods with antioxidant properties have recently been the object of intensive investigation due to their capacity to act on the triad of conserved core mechanisms underlying brain damage, which include oxidative stress, neurotrophic factors deficiency and inflammation [1,2]. Most plant extracts and pure bioactive ingredients typically show a polypharmacological profile [3,4] but the molecular mechanisms underlying their biological activity and the synergic action among the compounds of a phytochemical pool are mostly unknown. More importantly, natural extracts consist of complex mixtures whose composition depends upon the extraction methods employed [5]. Green tea polyphenols, resveratrol (a non-flavonoid polyphenol of red grapes), and curcumin (a polyphenol present in turmeric, *Curcuma longa*) are examples of such natural products. More recently, Omega 3 supplements have also been considered for neurodevelopmental brain diseases [6]. Interestingly, Silymarin, which is a mixture of polyphenolic flavonolignan, isolated from the seeds of *Silybum marianum*, has recently been introduced as supportive treatment for Alzheimer's and Parkinson's neurodegenerative diseases [7].

Cardoon (*Cynara cardunculus* L.), from the Asteraceae family, is a wild robust perennial species native to the Mediterranean basin [8] and has been cultivated in this region since ancient times with high productivity. It is naturally present in harsh habitat conditions characterized by high temperature, salinity [9] and drought [10,11]; therefore, it represents a valuable model of biomass for biorefinery development not competing for land dedicated to food crops. Cardoon biomass already finds applications in pulp and paper production and power generation, but it can also be valorized for the production of bioplastics, biolubricants [12], biopesticides, and ingredients for the cosmetic sector. More recently, cardoon biomass was used as sustainable feedstock for the production of polyhydroxyalkanoates (PHAs) [13]. Finally, cardoon biomass is also a rich source of valuable phytoconstituents, such as polyphenols and terpenoids, with well-known nutraceutical and pharmaceutical properties [14]. The leaves are known for their therapeutic potential as a diuretic, choleretic, cardiotonic, antidiabetic and anti-hemorrhoidal agent [5] as well as anti-inflammatory, anticancer, antioxidant, hepatoprotective, hypolipidemic, and antidiabetic activity [14].

Recent studies have shown the antioxidant activity of leaves extracts is strictly related to the polyphenol fraction [15,16]. In this respect, several extraction methods of bioactive molecules from cardoon leaves were previously described. Generally, leaves (dry or fresh) are mixed with different polar solvents, such as ethanol, methanol, acetone, or alcoholic solutions, and incubated with shaking [17–19]. An alternative to these traditional extraction methods was the use of the Naviglio® extractor, based on a solid-liquid dynamic extraction, which allows the recovery of phenolic compounds from different types of solid matrixes, at short extraction times, with high yields and easiness of scalability [20].

This study explores cardoon biomass as a source of bioactive ingredients for application in the treatment of Rett syndrome (RTT), a paradigmatic neurodevelopmental disorder that presents the classical triad of brain disease core mechanisms [21]. Even if RTT is a rare genetic disease affecting 1:10.000 girls worldwide, it represents the second leading genetic cause of mental retardation in females [21]. RTT is mainly caused by mutations in the X-linked MeCP2 gene [21] and is characterized by delayed neuronal development, leading to brain atrophy with smaller neurons having decreased complexity of neuronal dendritic processes [22]. Clinically, RTT patients show developmental arrest, loss of speech and motor abilities, seizures, breathing abnormalities, and behavioral problems including autism [23–25]. More specifically, using an in vitro model of RTT based on primary neuronal hippocampal cultures from MeCP2 gene-deleted mice (MeCP2$^{-/y}$ mice) [26,27], we have analyzed the effect of different extracts of cardoon leaves obtained from plants harvested at different maturity stages and extracted with two different methodologies, namely the Naviglio® and the supercritical carbon dioxide ($scCO_2$) extraction methods. The characterization of the main components of the different extracts allowed for the correlation of the observed beneficial or toxic biological responses to different composition profiles of the extracts.

2. Results and Discussions

2.1. Characterization of Cardoon Leaves Extracts

While $scCO_2$ is specific for the extraction of very hydrophobic fractions, the Naviglio® method is effective in extracting phenolic compounds and less hydrophobic components thanks to the action of polar solvents. More generally, supercritical fluids extraction (SFE) has the main advantage of process flexibility and allows for the elimination of polluting organic solvents, thereby avoiding expensive post-processing of the extracts for solvent elimination [28].

The obtained samples of cardoon leaves extracts (CLEs) are labelled in the following text as $scCO_2$Au, $scCO_2$Sp and NaviglioSp, where Au and Sp refer to leaves collected in autumn and spring, respectively, and $scCO_2$ and Naviglio indicate the supercritical CO_2 extraction and Naviglio® extraction technologies, respectively. The different CLEs were characterized by Gas Chromatography-Mass Spectrometry (GC-MS) and Nuclear Magnetic Resonance (^{1}H NMR) spectroscopy. Figure 1 reports a comparison of the GC-

MS chromatograms of the extracts obtained using supercritical CO_2 from cardoon leaves collected in spring ($scCO_2Sp$) and autumn ($scCO_2Au$) (Figure 1a,b). Moreover, the leaves collected in spring were also extracted by means of Naviglio® methods (NaviglioSp).

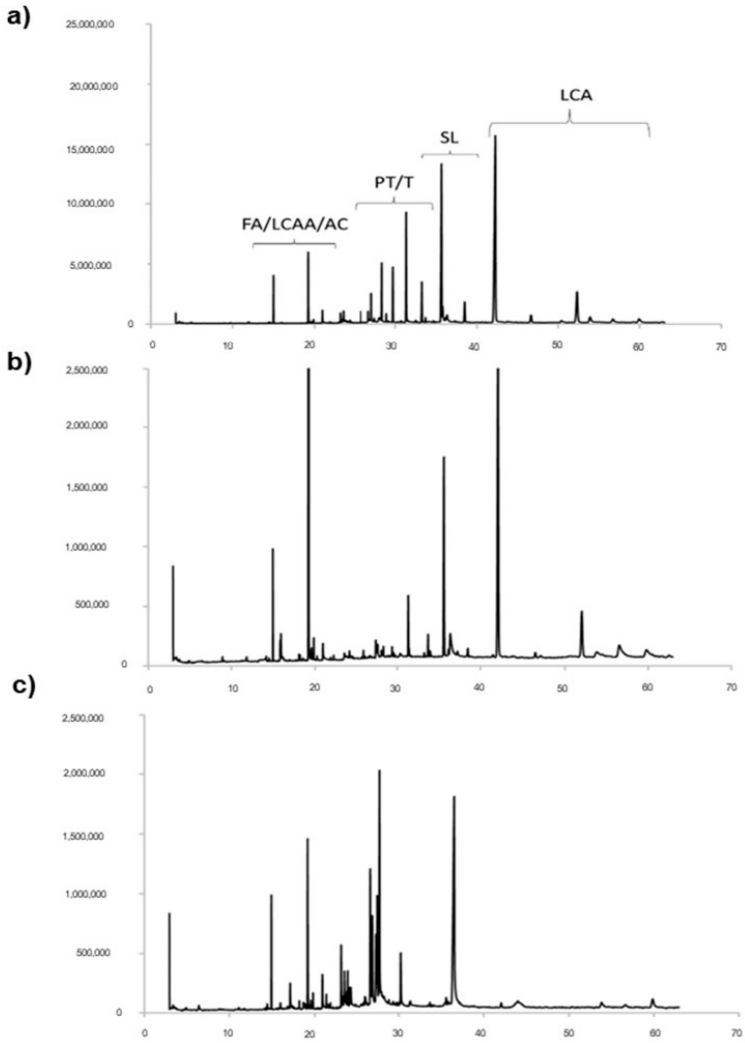

Figure 1. GC-MS chromatograms of the three extracts from cardoon leaves obtained using different extractive technologies: (**a**) autumn harvest with supercritical CO_2 ($scCO_2Au$); (**b**) spring harvest with supercritical CO_2 ($scCO_2Sp$); (**c**) spring harvest using Naviglio® technology (NaviglioSp). FA = fatty acids; LCAA = long-chain aliphatic alcohols; AC = aromatic compounds; PT = pentacyclic triterpenes; T = triterpenes; SL= sesquiterpene lactone; LCA = long-chain alkanes.

The GC-MS analysis provides qualitative and quantitative information on the chemical components, which were identified by comparing the corresponding mass values with data available from the NIST14s database and the literature [29]. The predominant chemical species are pentacyclic triterpenes and sesquiterpenes, volatile lipophilic molecules known for their antioxidant activity [5,30]. Cynaropicrin and grosheimin (RT = 35.61–37.25 min) are sesquiterpene lactones known for being present in the highest amount in cardoon

leaves as compared to other parts of the plant [5,31,32]. The GC-MS chromatograms (Figure 1) also indicate the presence of fatty acids (RT = 19.18 min), in particular linolenic acid [33], long-chain aliphatic alcohols (RT = from 19.50 to 22 min) and traces of aromatic compounds. Previous studies already indicated that fatty acids, especially saturated ones, are mainly concentrated in the leaves [5]. The signal at RT = 31.26 min is ascribable to squalene, whereas the signals corresponding to pentacyclic triterpenes fall in the range 23.45–29.73 min. Finally, the signals of hydrophobic long-chain alkanes are visible in the range 40–42.5 min.

We then focused our attention on the four bioactive molecules reported in Table 1, which are abundant in the extracts, although with quantitative differences that are ascribable to the extractive methods (Figure 2). They are three triterpenes (squalene, taraxerol and lupeol) and a sesquiterpene (cynaropicrin) known for their bioactivities, which are relevant for the purpose of this investigation. The leaves extracts were analyzed by GC-MS to evaluate the concentration of the four biomolecules (Table 1).

Table 1. Composition of the principal bioactive molecules in the three solutions of cardoon leaves extracts.

	Composition * in $scCO_2$Au ($w\ w^{-1}$)	**Composition * in $scCO_2$Sp ($w\ w^{-1}$)**	**Composition * in NaviglioSp ($w\ w^{-1}$)**
Cynaropicrin	0.040	0.020	0.230
Squalene	0.480	0.390	0.110
3ß-Taraxerol	0.070	0.030	<0.001
Lupeol	0.090	0.050	0.010

* Composition expressed as $w\ w^{-1}$ of each bioactive molecule/1 mg of extract.

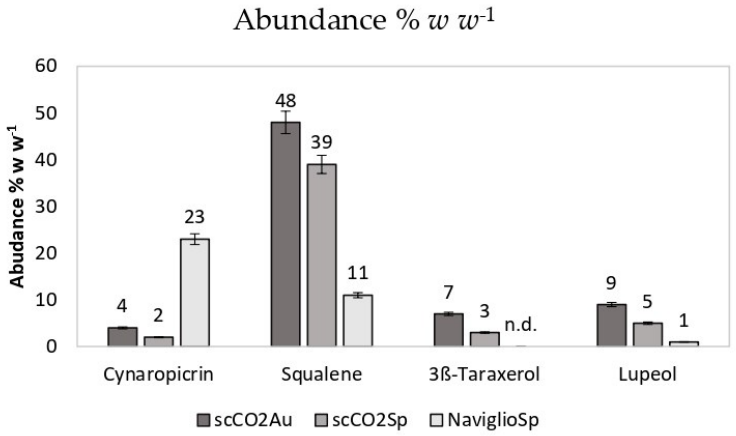

Figure 2. Abundance % $w\ w^{-1}$ of each bioactive molecule measured by GC-MS. Data are the results of triplicated analysis and standard deviations are reported.

Squalene is a triterpene that is an intermediate in cholesterol biosynthesis pathways, widely distributed in nature [34]. Experimental studies have shown that squalene can effectively inhibit chemically induced skin, colon, and lung tumorigenesis in rodents [35]. Taraxerol is a triterpene that has been isolated from several plant species, and its various pharmacological properties have already been identified, such as the acetylcholinesterase (AChE) inhibition activity in vitro. Taraxerol has anti-amnesic activity that may hold significant therapeutic value in alleviating certain memory impairments observed in Alzheimer

disease [36]. Lupeol is a significant lupene-type triterpene isolated in plants, fungi, and the whole animal kingdom. This bioactive molecule has several biological effects: anticancer, antiprotozoal, chemo-preventive, and anti-inflammatory properties [37]. Cynaropicrin is a sesquiterpene lactone that was isolated from artichoke (*Cynara scolymus* L.) in 1960 for the first time and was also found later in *Cynara cardunculus* L. Cynaropicrin has important pharmacological activities, such as antitumoral, anti-inflammatory, anti-trypanosome and anti-hepatitis C virus properties, among many others [38].

Figure 2 shows the abundance in % $w\ w^{-1}$ of each bioactive molecule (% $w\ w^{-1}$ i.e., the weight of the molecule of interest with respect to the total extract weight used for GC-MS analysis).

The extracts obtained using supercritical CO_2, specific for very hydrophobic molecules, are very rich in squalene. The rest of the hydrophobic extracts is mainly composed by waxes and fatty acids. Notably, there is an increased amount of squalene in the autumn extract as compared to leaves collected in spring. The spring extract obtained with the Naviglio method, employing ethanol as solvent, is the richest in cynaropicrin. The harvesting and maturity stages are crucial in determining the chemical composition of natural products obtained from plant tissues, with early maturity coinciding with the highest content of phenolic compounds, as already reported for various plant species [39].

2.2. Characterization of Cardoon Leaves Extracts Using NMR Spectroscopy

Figure 3 reports, as an example, the ^{1}H NMR spectrum of the extract obtained using supercritical CO_2 extraction of the spring harvest ($scCO_2Sp$). The spectrum is dominated by the strong signal of the CH_2 of alkyl chains. On the basis of the literature data, the following signals can be recognized: -CH_3 of sterols (δ: 0.54 ppm), –CH_2 of triterpenes (δ: 0.69 ppm). The signals of the fatty acids are visible in the range δ: 0.85–0.93 ppm (–CH_3) and at δ: 1.6 ppm –CH_2CH_2COOH, at δ: 2.06, m –CH_2-CH=CH-, and at δ: 2.23 m –CH_2COOH, besides weaker signals of sesquiterpene lactones and triterpenes can be observed [5].

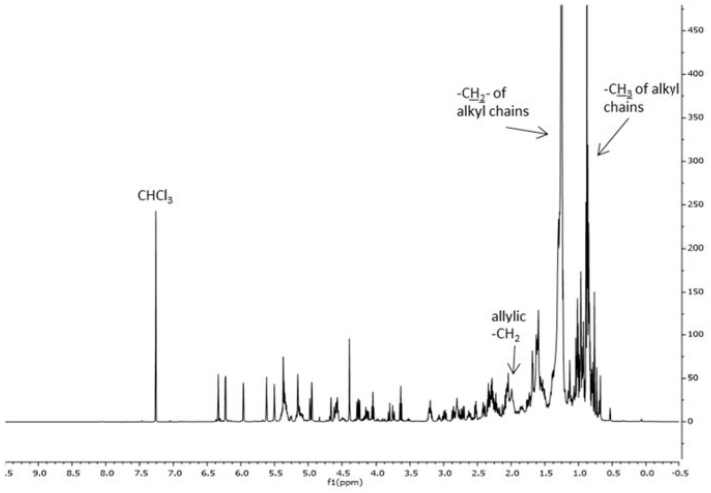

Figure 3. ^{1}H NMR spectrum of the CLE $scCO_2Sp$. ^{1}H NMR (500 MHz, $CDCl_3$): δ: 0.54, –CH_3 of sterols; δ: 0.69, –CH_2 of triterpenes; δ: 0.85–0.93, –CH_3 of alkyl chains; δ: 1.20–1.42, –CH_2 of alkyl chains; δ: 1.6, –CH_2CH_2COOH of fatty acids; δ: 2.06, –CH_2-CH=CH-; δ: 2.23 –CH_2COO; δ: 3.5–6.5 alkene signals–compare also Figure 4.

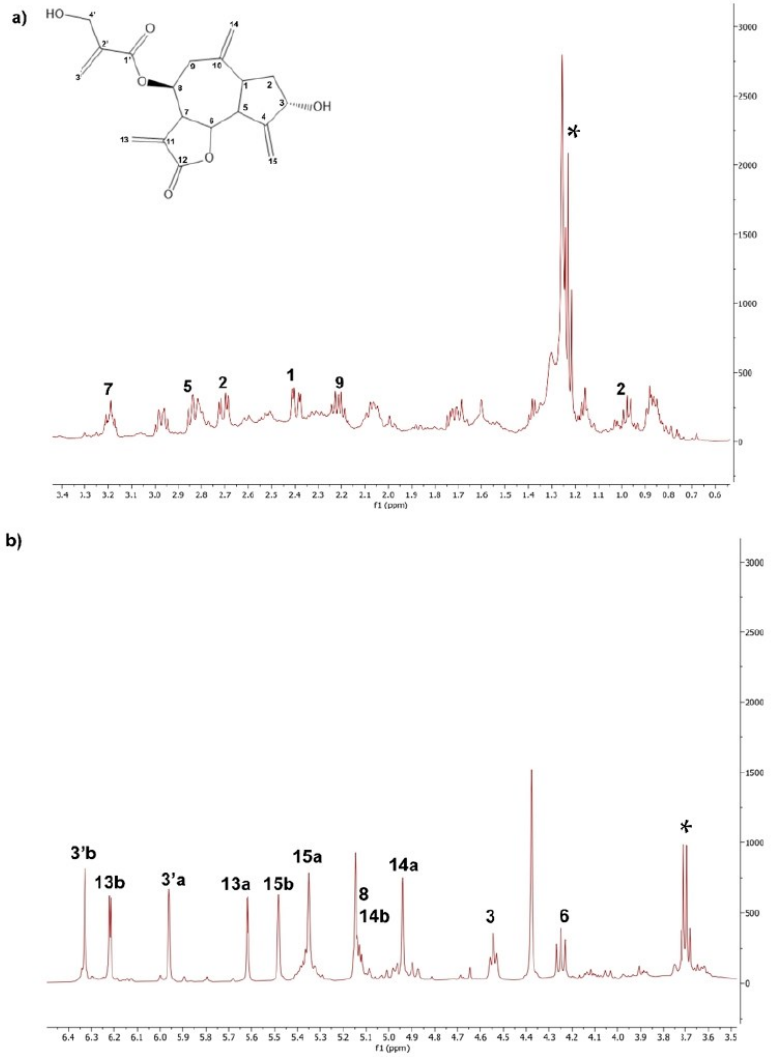

Figure 4. Details of the ^{1}H-NMR spectrum of the CLE NaviglioSp. (**a**) Signals of cynaropicrin in the range of 0–3.4 ppm; (**b**) Signals of cynaropicrin in the range of 3.5–6.5 ppm. ^{1}H-NMR (500 MHz, $CDCl_3$): **1** δ: 2.43, dt; **2a** δ: 1.09, ddd; **2b** δ: 2.07, dt; **3** δ: 4.62, tt; **5** δ: 2.84, dd; **6**, δ: 4.27, dd; **7** 3.27, tt; **8** and **14b** δ: 5.17, ttt; **9a–b** δ: 2.25–2.45, dd; **13a** δ: 5.62, d; **13b**, δ: 6.25, d; **14a** δ: 4.96, d; **15a** δ: 5.43, t; **15b** δ: 5.52, t; **3′a** δ: 5.9, m; **3′b** δ: 6.35, m. * marks residual ethanol signals.

The ^{1}H NMR spectrum of extracts obtained using supercritical CO_2 from leaves collected in autumn ($scCO_2Au$) is available in SI (Figure S1 in SI).

The ^{1}H NMR spectrum of the CLEs obtained using the Naviglio® technology (NaviglioSp) shows a significant presence of linolenic acid (δ: 0.9 ppm) and cynaropicrin. In addition, there are weak signals assignable to pheophytins, which give the characteristic green color to these extracts (δ: 4.49, –CH of pheophytins) [35]. Many signals of cynaropicrin, the most abundant sesquiterpene lactone, appear in the 6.5–3.5 ppm spectral region shown in Figure 4. For sake of completeness, both the ^{1}H and ^{13}C NMR whole scale spectra of all the extracts are reported in SI (Figures S1 and S2 in SI, respectively).

2.3. Evaluation of Cardoon Leaves Extracts on Rett Syndrome In Vitro Model

We previously established an in vitro model of Rett syndrome (RTT) [27] based on primary neuronal hippocampal cultures prepared using brains extracted from mice in which the MeCP2 gene was deleted (MeCP2$^{-/y}$ mice) [26]. Starting from days-in-vitro 6 (DIV 6), cultured MeCP2$^{-/y}$ neurons show atrophic morphology due to an arrest in neuronal growth [27]. Here, we tested the efficacy of CLEs in rescuing RTT neuronal development arrest using a miniaturized version of this assay optimized for reproducible and robust drug screening in 96-well plate format [40].

In a first set of experiments, Wild-Type (WT) and MeCP2$^{-/y}$ (KO) neurons were incubated for 3 days, from DIV 3 to DIV 6, with the three different cardoon extracts ($scCO_2$Sp, $scCO_2$Au and NaviglioSp) at two concentrations (5 µM and 20 µM) expressed as a total mole concentration of the four considered bioactive molecules by considering a weight-averaged molecular weight. High content imaging microscopy analysis based on the NeuriteQuant software [31,40] (Figure 5A) was used to measure two morphological parameters, i.e., the total dendritic length (TDL; sum of the extension of all dendrites of a neuron in µm) and the number of dendritic endpoints (EP, a measure of the number of terminal branches of the dendrites of a neuron).

In WT neurons, the $scCO_2$Au extract at 20 µM induced a significant increase of both TDL (133% ± 42.4 S.E.M; $p = 0.0339$) and EP (162% ± 53 S.E.M.; $p = 0.0137$) with respect to WT DMSO control (TDL = 100% ± 10.3 S.E.M.; EP = 100% ± 9.4 S.E.M) (Figure 5B,D). No significant effect was seen with the other extracts either at 5 or 20 µM concentrations (Figure 5B–D) while the NaviglioSp extract at 20 µM induced a significant neuronal toxicity, as indicated by the dramatic reduction in the morphological parameters and the number of neurons remaining in culture after the treatment (Figure 5B–D; $p = 0.0005$ for TDL, $p = 0.0004$ for EP, and $p = 0.0154$ for the number of neurons with respect to DMSO). In KO neurons, only the $scCO_2$Sp extract at 5 µM showed a significant increase in TDL (321% ± 76 S.E.M; $p = 0.0003$) with respect to KO DMSO (TDL = 100% ± 9.8 S.E.M) (Figure 5E,F), while the other extracts were ineffective (Figure 5E,F) and the NaviglioSp extract at 20 µM induced a significant neurotoxicity (Figure 5E–G; $p = 0.0028$ for TDL, $p = 0.0021$ for EP, and $p = 0.0094$ for the number of neurons with respect to DMSO). In conclusion, only the cardoon $scCO_2$Sp extract was able to induce a significant rescue of neuronal atrophy in RTT neurons, while the $scCO_2$Au extract resulted to be active on WT neurons and the NaviglioSp was toxic on both WT and KO neurons.

In a second set of experiments, we tested the efficacy of individual pharmacologically active ingredients present in the different cardoon extracts, namely cynaropicrin, squalene, lupeol and taraxerol (Table 1). Each bioactive ingredient was incubated on WT and KO hippocampal neurons for 3 days from DIV 6, at the concentration of 5 or 20 µM, and TDL and EP were measured as experimental read-out (Figure 6A). No individual bioactive compound was able to replicate the positive effect on TDL and EP observed with the whole extracts of $scCO_2$Sp and $scCO_2$Au in KO or WT neurons (Figure 5B,C,E,F). However, we observed a significant neurotoxic effect of cynaropicrin at both 5 and 20 µM, and of lupeol at the higher concentration of 20 µM (Figure 6B–G). In particular, cynaropicrin 5 µM ($p = 0.0039$), and 20 µM ($p = 0.0039$) for WT TDL; cynaropicrin 5 µM ($p = 0.0019$), 20 µM ($p = 0.0019$) for WT EP; cynaropicrin 5 µM ($p = 0.0263$) for the number of WT neurons; cynaropicrin 20 µM ($p = 0.0263$) for the number of WT neurons; Squalene 5 µM ($p = 0.0081$), 20 µM ($p = 0.0107$) for WT EP; lupeol 20 µM ($p = 0.0197$) for WT TDL, ($p = 0.0019$) for WT EP, ($p = 0.0097$) for the number of WT neurons; cynaropicrin 5 µM ($p = 0.0044$), 20 µM ($p = 0.0044$) for KO TDL; cynaropicrin 5 µM ($p = 0.0019$), and 20 µM ($p = 0.0019$) for KO EP; cynaropicrin 5 µM ($p = 0.0148$) for the number of KO neurons; cynaropicrin 20 µM ($p = 0.0148$) for the number of KO neurons. Squalene 5 µM ($p = 0.0001$) for KO EP; lupeol 20 µM ($p = 0.0044$) for KO TDL, and $p = 0.0019$ for KO EP, $p = 0.0148$ for the number of KO neurons. These results support the conclusion that single bioactive ingredients are not sufficient to induce the positive effects of the whole extracts but are able to fully exert the toxic effects.

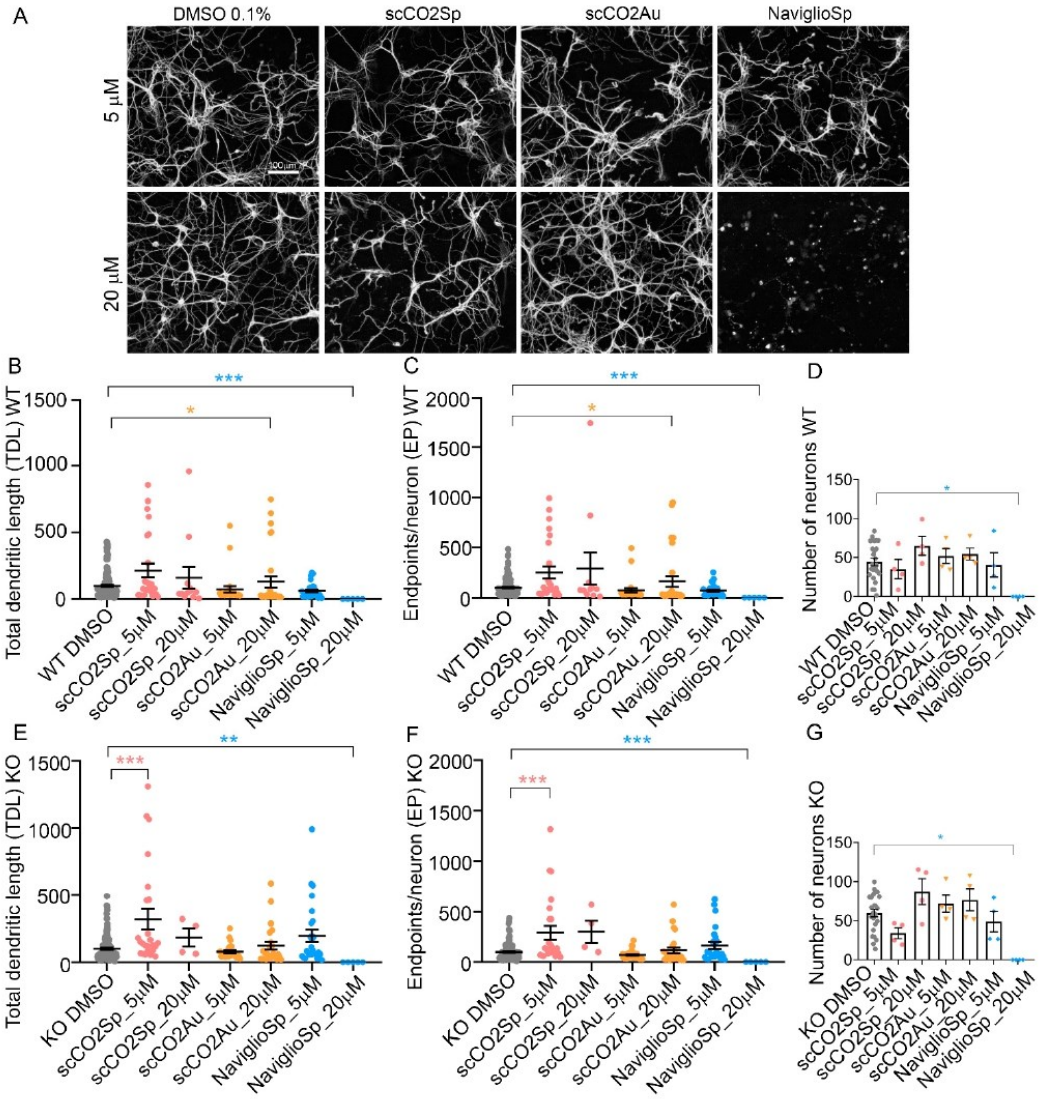

Figure 5. Treatments of neuronal cultures with cardoon extracts. (**A**) NeuriteQuant morphological analysis of TDL and Endpoints of DIV 6 hippocampal WT neurons, plated at the density of 160 cells mm^{-2} ($n = 2$). From left, WT neurons treated with DMSO 0.1% (control condition), $scCO_2Sp$ extract, $scCO_2Au$ extract, NaviglioSp extract. First line represents neurons treated at the concentration of 5 µM (in DMSO 0.1%), second line at 20 µM (in DMSO 0.1%). Scale bar: 100 µm. (**B**,**C**) Quantitative data of WT neurons, reporting the average TDL per neuron (µm) and the average number of endpoints per neuron. n = 22 images for a total of 2 independent biological replicates (cell cultures). (**D**) Number of WT neurons per each condition. (**E**,**F**) Quantitative data of MeCP2 KO neurons, reporting the average TDL per neuron (µm) and the average number of endpoints per neuron. n = 22 images for a total of 2 independent biological replicates (cell cultures). (**G**) Number of MeCP2 KO neurons per each condition. Kruskal–Wallis with Dunnett's multiple comparisons test vs. DMSO conditions. *** $p < 0.001$, ** $p < 0.01$, * $p < 0.05$.

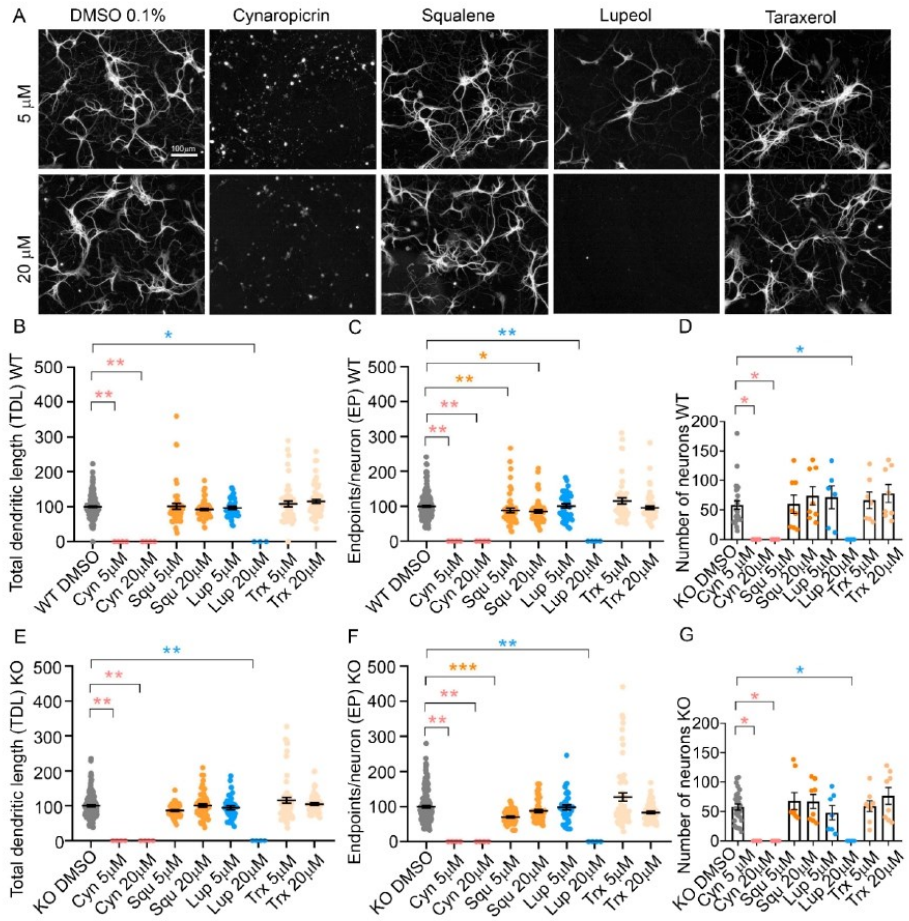

Figure 6. Treatments of neuronal cultures with bioactive molecules. (**A**) NeuriteQuant morphological analysis of TDL and Endpoints of WT hippocampal neurons at DIV 6 (n = 4). From left, WT neurons treated with DMSO 0.1% (control condition), cynaropicrin, squalene, lupeol, taraxerol. First line represents neurons treated at the concentration of 5 µM (in DMSO 0.1%), second line at 20 µM (in DMSO 0.1%). Scale bar: 100 µm. (**B**,**C**) Quantitative data of WT neurons, reporting the average TDL per neuron (µm) and the average number of endpoints per WT neuron n = 44 images for a total of 4 independent biological replicates (cell cultures). (**D**) Number of WT neurons per each condition. (**E**,**F**) Quantitative data of MeCP2 KO neurons, reporting the average TDL per neuron (µm) and the average number of endpoints per neuron. n = 44 images for a total of 4 independent biological replicates (cell cultures). (**G**) Number of MeCP2 KO neurons per each condition. Kruskal–Wallis with Dunnett's multiple comparisons test vs. DMSO conditions. *** $p < 0.001$, ** $p < 0.01$, * $p < 0.05$.

The use of primary neuronal cultures for screening large libraries of small molecules is a standard in the pharmaceutical industry and has been widely described in the literature for in vitro models of neurodegenerative disorders such as Alzheimer's, Parkinson's, Huntington's diseases, and Amiotrophic Lateral Sclerosis [41–43]. More recently, similar approaches have also been undertaken for neurodevelopmental diseases such as Rett and Fragile-X syndromes [44]. Major limitations with these in vitro models concern, first of all, the mutation present in the mouse model used for neuronal cultures, which not necessarily corresponds to the actual mutation present in the majority of patients. This is the case for

instance of Rett syndrome in which multiple mutations exist (more than 100, with 8 being the most frequent ones) leading to a variety of symptoms and disease severity [45]. In addition, there is a wide debate concerning the developmental stage at which the drugs screening should be carried out to obtain valuable results. Reasons of convenience have suggested that we should carry out the majority of drug screenings at an early stage of development, in order to obtain highly reproducible cultures within the shortest possible time, leading to obvious economies in terms of time and people employed. However, the necessity of an appropriate matching between drug screening and the onset of the most important cellular defects and aberrant processes has to be taken into consideration. In our case, we previously described in detail the various stages of development in vitro of a neuron from mice deleted of the MecP2, mimicking Rett syndrome [27]. More specifically, we showed that significant growth arrest in terms of reduced total dendritic length and number of secondary dendrites can already be quantified at DIV 6, while synaptogenesis is apparently normal at this stage, becoming clearly reduced at later stages, in particular from DIV 9 onward [27]. Collectively, these previous studies indicate the suitability of the use of primary in vitro cultures for drug screening. As regard to the effective bioavailability of plant extracts in the brain, some information is available but some in vivo studies have found rapid targeting into the brain upon oral or systemic delivery for flavonoids [46] and other polyphenol metabolites [47].

Taraxerol, squalene and lupeol found in cardoon leaves extracts are synthesized in plants through a common biosynthetic pathway called the mevalonate pathway, starting from Acetyl-CoA as a primary source. Specifically, squalene is the primary precursor for the synthesis of triterpenoids including taraxerol, and lupeol by taraxerol synthase [48]. Most interestingly, in mammalian cells squalene is also the precursor of cholesterol through the squalene epoxidase pathway, which is defective in Rett syndrome, leading to a significant reduction in cholesterol availability in the brain [49]. Lupeol has shown neuroprotective properties in animal models of neurodegenerative disorders [50], traumatic brain injury or ischemia [51,52] and, similar to taraxerol, also to have anti-inflammatory and pro-neurotrophic actions in vitro [53,54]. Comparatively less information is available for squalene, which was shown to counteract neuronal cell death in an in vitro model of Alzheimer's-like injury [55]. Although in our experiments we used concentrations of taraxerol, squalene and lupeol within a range comparable to the one used in the in vitro studies cited above [53–55], we did not detect significant neuroprotective activity against neurodevelopmental deficits in our in vitro Rett syndrome model. Differences in cellular models adopted, i.e., mouse hippocampal neurons in our study versus rat hypothalamic or cortical neurons, or an immortalized cell line in the other studies, may provide a first explanation for the different results obtained. On the other hand, our results suggest that the coexistence of deficits in multiple metabolic pathways, which is typical of syndromic disorders such as Rett syndrome, may require a coordinated polypharmacological approach against multiple targets, which may be achieved only with a complex mixture of bioactive components.

3. Materials and Methods

Solvents, reagents, and standard solutions of bioactive molecules were purchased from Merck KGaA, Darmstadt (Germany) and used as received if not otherwise specified.

Cardoon leaves were kindly provided by Novamont (Novara, Italy) and were taken from the cultivation of *Cynara cardunculus* var. *altilis* in Terni in spring and autumn 2020.

3.1. Preparation of Leaves Samples

The cardoons were pre-treated by separating leaves from the stalks. Cardoon samples were obtained from a biorefinery crop, which was harvested in large quantities in a precise period of the year. Therefore, in this study we did not consider individual plants. It must be underlined that in our previous study we demonstrated that the yield of extractions

conducted on different samples and aliquots of the same batch of plants has an error of less than 5% [16].

The material was cut by means of garden scissors in square pieces of about 1 cm, which were temporarily stored under vacuum in plastic bags (about 200 g each) at −20 °C. The material used for $scCO_2$ extraction was dried by means of a first step of lyophilization for 48 h. The treatment allowed us to remove about 82–85% of water, calculated by weight difference. A second treatment in an oven at 40 °C for 48 h led to the removal of a further 0.5% of water, with respect to the lyophilized samples. The dried samples were temporarily stored under vacuum in plastic bags at +3 °C before analysis.

Cardoon leaves addressed to the Naviglio® extractor were separated from the fresh plants and stored in vacuum-sealed plastic bags (about 200 g each) at −20 °C. For extract preparation, cardoon leaves were thawed at room temperature and cut into 1 cm pieces.

3.2. Extraction Methods

1. Supercritical CO_2 extraction: 6–8 g of dried leaves was loaded in a 100 mL extractor. The $scCO_2$ extraction system [56] was composed by a Separex SFE 20 unit (heated stainless-steel extractor 100–200 mL, laminating valve Tescom 26-1000, heated collecting chamber) connected to a liquid CO_2 cylinder, a high-pressure pump Lewa EKM210V1 and an EL-FLOW Bronkhorst flowmeter. Conditioning was performed for 30 min and then the extraction was started by turning on the pump with a carbon dioxide flowrate of 120 L h^{-1} for 2 h at 45 °C and 225 bar. The extracts were collected by dissolving the oily mixture in diethyl ether (<1 mL). The extraction yields were 3.7 and 2.0 % ($w\ w^{-1}$) in the case of autumn- and spring-harvested plants, respectively.
2. Naviglio® method: Filter bags (porosity of 100 µm) were filled with 40 g of cut cardoon leaves and then inserted into the extraction chamber of the Naviglio® extractor (500 cm^3 capacity). Extractions were conducted using 625 mL of anhydrous ethanol at 25 °C (9 bar, static phase 2 min; dynamic phase 2 min, with 12 s stop piston). Liquid samples were collected at 24 h. The extraction yield was 4.8 % ($w\ w^{-1}$). The cardoon leaf extracts (CLE) were stored at 4 °C until analysis. Ethanol was chosen as a solvent for phenols extraction, as described in the literature [16].

3.3. Characterization of Extracts by Means of NMR

The ^1H and ^{13}C NMR analysis was performed by dissolving 10 mg of CLE in 0.7 mL of deuterated chloroform. The NMR spectra were acquired at 25 °C by a Varian VNMRS 500 NMR spectrometer (11.74 T) operating at 500 MHz for proton and 125 MHz for carbon, using 256 scans for proton and 16000 scans for carbon, interleaved by 7.7 s for proton and 2.05 s for carbon, with 45° pulses, employing a spectral width of 8012.8 Hz for proton and 31250 Hz for carbon over 32 K complex points. The signals were assigned according to the literature [5,57].

3.4. Quantification of Cynaropicrin, Squalene, Taraxerol and Lupeol

The bioactive molecules were quantified by GC-MS (Shimadzu GC-MS-QP2020). Calibration curves were constructed by using commercial standards of cynaropicrin (SI, Figure S4), squalene (SI, Figure S5), taraxerol (SI, Figure S6) and lupeol (SI, Figure S7) and dodecane as internal standard. The analysis was performed on samples prepared by dissolving 0.7 mg of each CLE in 1 mL of diethyl ether. The separation was obtained on a 30 m × 0.25 mm fused-silica capillary column (SLB5ms) coated with a 0.25 µm film of poly(5% phenyl, 95% dimethyl siloxane). The mass spectrometer was set to scan the m/z range 33–700. Samples were injected (1 µL) with a splitting ratio 1:20 and the injector temperature was set to 280 °C. The column oven was initially set at 50 °C and maintained for 2 min after the injection, followed by a temperature ramp (8 °C min^{-1}) up to 250 °C followed by a second ramp (3 °C min^{-1}) up to 280 °C. The total analysis time was 63.33 min [29].

3.5. Mice Strain and Genotyping

The animal use was approved by the Italian Ministry of Health (authorization n. 693/2021-PR issued on Sept. 6th, 2019), in conformity with the Italian legislation D.Lgs 116/92. Animals were housed under standard conditions, in ventilated cages, in a 12/12 h light/dark cycle with food and water ad libitum. Wild-Type (WT) C57BL/6 male mice (Charles River Laboratories, Calco, LC, Italy) were crossed with C57BL/6 female heterozygous for the deletion of exon 3 and 4 in MeCP2 gene1 [26]; MeCP2$^{-/+}$, B6.129P2(C)-Mecp2tm1.1Bird/J, stock: 003890, Jackson Laboratories, Bar Harbor, Maine) to obtain Wild-Type (MeCP2$^{+/y}$, WT) and Knock-Out (MeCP2$^{-/y}$, KO) male mice.

The mice genotype was determined using DNA extracted from tails using KAPA Express kit (EXPEXTKB; Roche). Polymerase Chain Reaction (PCR) was performed using KAPA2G Fast DNA polymerase with the following primers: 5′- AAATTGGGTTACACCGCTGA-3′ (Common Forward 9875, Jackson Laboratory), 5′-CTGTATCCTTGGGTCAAGCTG-3′ (Wild-Type Reverse oIMR7172, Jackson Laboratory), 5′- CCACCTAGCCTGCCTGTACT-3′ (Mutant Reverse 9877, Jackson Laboratory). PCR reaction was performed in a final volume of 25 µL set as follows: initial denaturation at 95 °C for 3 min then, 95 °C for 20 s, 58 °C for 20 s, 72 °C for 20 s (35 cycles) and final elongation at 72 °C for 2 min.

3.6. Culture of Hippocampal Primary Neurons (HPN)

Primary hippocampal neuronal cultures were prepared from P0 and P1 male mice, both Wild-Type (MeCP2$^{+/y}$, WT) and Knock-Out (MeCP2$^{-/y}$, KO), according to Baj et al., 2014 [27]. In brief, mice were sacrificed by decapitation, hippocampi were extracted (under bright field microscope) and collected in cold Hank's balanced salt solution HBSS (sodium bicarbonate ($NaHCO_3$) 4.2 mM, Hank's salt powder 0.952%, HEPES 12 mM, D-Glucose, 200 µM kynurenic acid, BSA, magnesium sulphate ($MgSO_4$), Sigma, St. Louis, MO, USA). The tissue digestion was performed by adding 0.25% Trypsin (Euroclone, Milan, Italy) for 8 min at 37 °C. The enzymatic digestion was blocked with 1.5 mL of Dulbecco's Modified Eagle Medium high glucose (DMEM, Euroclone, Milan, Italy), supplemented with 10% Fetal Bovine Serum (FBS, Euroclone, Milan, Italy) and penicillin-streptomycin (P/S, Euroclone, Milan, Italy). The tissue was centrifugated at 800 rpm for 5 min at room temperature (25 °C) and then resuspended with 1 mL of DMEM + 10% FBS and mechanically triturated. Cells were counted with the dye exclusion method using Trypan Blue (Sigma) in the Burker chamber (Eppendorf), obtaining 800,000–900,000 cells from each mouse. Cells were plated in 96 MW plates (Sarstedt, Nümbrecht, Germany), previously treated with 0.2% Poly-L-Ornithine (PORN, Sigma) to allow the attachment of cells. Cells were seeded at the density of 160 cell mm^2 and were grown at 37 °C and 5% CO_2 in Neurobasal (Invitrogen, Waltham, MA, USA) supplemented with 2% B-27 (Invitrogen), 1 mM L-glutamine and 1% penicillin-streptomycin. Cell medium was changed at DIV 3 including Cytosine β-D-arabinofuranoside (Ara-C, Sigma) at the final concentration of 2.5 µM to inhibit proliferation of non-neuronal cells. Cells were maintained in culture until DIV 6 (Figure 7).

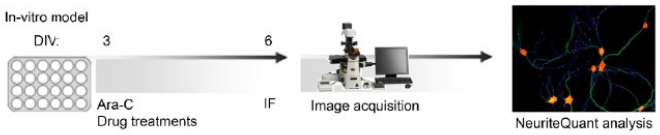

Figure 7. Workflow for phenotypic screening. Primary hippocampal neurons were plated at DIV 0 in 96 multi-well, and at DIV 3 were added D-Arabinofuranoside (ARA-C, Sigma) and treatments with extracts or bioactive molecules. Neurons were fixed in PFA 4% at DIV 6 and immunofluorescence (IF) was performed with anti-MAP2 (red), and anti-NeuN (green). Images were acquired using Nikon Eclipse Ti-E epifluorescence live imaging microscope equipped with Nikon DS-Qi2 camera, using 10× objective. Eleven random fields (3.0 × 3.0) per well were acquired and analyzed individually. Total Dendritic Length (TDL) and the number of Endpoints per neuron (EP) were measured with NeuriteQuant software, implemented as a plugin of ImageJ [58].

3.7. Treatments

Treatments with extracts or bioactive molecules were performed for 3 days, from DIV 3 to DIV 6 (Figure 7). The extracts $scCO_2Au$, $scCO_2Sp$ and NaviglioSp were tested at concentrations 5 µM and 20 µM obtained as follows: a 5 mM solution in 100% DMSO was firstly diluted 1:100 and then 1:10 to reach a 5 µM solution of extract in culture medium containing ultimately, upon dilution, 0.1% of DMSO. The same dilution steps were applied to the 20 mM solution to reach a final 20 µM concentration (n = 22 images for a total of 2 independent biological replicates).

The same concentrations were used to test the single bioactive molecules: cynaropicrin (Cyn), squalene (Squ), lupeol (Lup) and taraxerol (Trx) (n = 22 images for a total of 4 independent biological replicates). In a previous study, we provided evidence that the number of neurons per mm^2 and the average TDL in cultures treated with DMSO 0.1% are not significantly different with respect to the untreated condition [40]. Thus, DMSO 0.1% represents the control condition of each treatment.

3.8. Immunofluorescence

Hippocampal primary cultures were fixed at DIV 6 using 4% Paraformaldehyde (PFA, Sigma) in PBS 1x for 15 minutes at room temperature, then washed with PBS 1x and permeabilized using PBS-Triton 0.1% for 15 minutes. In order to avoid unspecific bindings, the blocking solution was added with PBS-Triton 0,1% and 2% Bovine Serum Albumin (BSA, Sigma) for 15 min. Primary antibodies (Table 2) were specific to detect the Microtubule-associated protein 2 (MAP2), an abundant microtubule-associated protein implicated in the formation and outgrowth of neuronal processes (dendrites and axons), and to detect Neuronal nuclei (NeuN), present specifically in the nuclei of mature neurons [50,59]. Primary antibodies were diluted in blocking solution and cells were incubated for 1:30 h at room temperature in a dark humified chamber and oscillated in a rocker. Cells were washed with PBS1x (5 min/wash) and then incubated with the secondary antibodies anti-rabbit IgG Alexa Fluor568 (Invitrogen, A10042) and anti-mouse IgG Alexa Fluor488 (Invitrogen, A11001) for 1:30 h at room temperature, in a dark humified chamber and on a rocker. Both secondary antibodies were diluted 1:1000. Cells were washed with PBS-Triton 0.1% and then with PBS 1x (5 min/wash) and incubated with Hoechst 33342 (10 mg ml^{-1}, Sigma) at the dilution 1:1000 (final concentration 10 µg ml^{-1}) in PBS1x for 7 min. Then, Hoechst was washed with PBS1x.

Table 2. Primary antibodies used.

Primary Antibody	Species	Dilution	Company	Code
Anti-MAP2	Rabbit	1:500	Genetex	GTX50810
Anti-NeuN	Mouse	1:500	LS-Bio	LS-C312122-100

3.9. Image Acquisition

Images were acquired at the Nikon Eclipse Ti-E epifluorescence live imaging microscope equipped with a motorized stage and a Nikon DS-Qi2 camera (CMOS sensor, 16.25-megapixel, 14 bit gray levels). Acquisitions were performed using the software Nis-Elements 4.60 with the module "JOBS" for automated imaging. Per single well, 11 random images (3.0 × 3.0 fields) were acquired using the 10x objective. Image size was 14 bit-1636 × 1088 pixels, which corresponds to 1.440 mm × 0.957 mm. The number of seeded neuronal and non-neuronal cells were respectively obtained by automatic counting of NeuN-positive neurons and Hoechst-positive cells with the "Objective-analyser" plugin for Nis-Element 4.60. Image acquisition parameters: 900 ms of exposure time for MAP2, 2 s of exposure time for NeuN, 20 ms of exposure time for Hoechst, filters at 1.

3.10. NeuriteQuant Morphological Analysis

Each image was analyzed individually with the NeuriteQuant open-source software, which is able to perform the fast and accurate analysis of a large set of images [44]. For each image, the following parameters were measured:

1. Total Dendritic Length: sum of the length of all the dendrites present in one image;
2. Number of Endpoints per neuron: number of terminal points counted at the end of visible dendritic staining (MAP2).

The analysis is highly sensitive and independent from signal intensity, allowing the detection of both neurites characterized by a strong signal or by a weaker signal intensity. In order to perform the analysis, four parameters have to be set:

1. Neurite detection width: 12;
2. Neurite detection threshold: 8;
3. Neurite clean-up threshold: 170;
4. Neuronal cell body detection: 300.

Before starting the morphological analysis with NeuriteQuant, we used the Enhance Local Contrast (CLAHE) plugin of ImageJ to enhance the immunofluorescence signal to obtain a better contrast of the image.

3.11. Statistical Analysis

All the statistical data analysis and data representation were performed on Prism 8.0 software (Graphpad), while data organization was performed using Microsoft Excel 2018 (build 14326.20508) (Office). All data were checked using the Shapiro–Wilk normality test. One-way ANOVA for multiple comparisons to compare more than two groups was performed when data were normally distributed. When data were not normally distributed, the statistical difference was calculated using the Kruskal–Wallis test comparing more than two groups. Outlier detection was performed using Grubb's test with GraphPad software.

4. Conclusions

The demonstration that the reactivation of the MECP2 gene in a mouse model can rescue large part of the Rett syndrome-like phenotypes has revealed that the disease is reversible, paving the way towards the search for new treatments [58,60]. Recent studies have discovered that lipid metabolism is perturbed in the brain and in the liver of mouse models of Rett syndrome, and this deficit, and other general symptoms of the disease, were rescued by regulating the cholesterol synthesis pathway either genetically or pharmacologically [45,49]. Hence, it is very intriguing that the $scCO_2$ hydrophobic extracts are rich in squalene, one of the intermediates of cholesterol synthesis, even though in our experiments pure squalene was not sufficient to revert dendritic atrophy in vitro, suggesting that the whole extract provides a better neuroprotective effect than single molecules. In conclusion, the significant rescue of the aberrant phenotype of RTT neurons obtained with the hydrophobic $scCO_2$ extract of leaves from *Cynara cardunculus* var *altilis* harvested in spring warrants further studies to characterize in detail the composition of the extracts and further investigate the mechanism of action in Rett syndrome. Overall, this study indicates that it is crucial to design optimal extraction procedures, both in terms of selection of harvesting period and extractive technologies, to maximize the pharmacological potential of bioactive extracts.

Supplementary Materials: The following supporting information can be downloaded at: https://www.mdpi.com/article/10.3390/molecules27248772/s1, Figure S1: ^{1}H-NMR (500 MHz, $CDCl_3$) spectrum of the CLE (a) $scCO_2Au$; (b) NaviglioSp 1; Figure S2: ^{13}C NMR spectra from samples: (a) $scCO_2Au$, (b) $scCO_2Sp$, (c) NaviglioSp; Figure S3. GC-MS chromatogram and fragmentation of bioactive molecules. (a) cynaropicrin; (b) squalene, (c) 3ß-taraxerol and (d) lupeol; Figure S4. GC-MS calibration curve of cynaropicrin; Figure S5. GC-MS calibration curve of Squalene; Figure S6. GC-MS calibration curve of Taraxerol; Figure S7. GC-MS calibration curve of Lupeol. References [5,61] are cited in the supplementary materials.

Author Contributions: Conceptualization, L.G., C.P., E.T. and F.A.; methodology, M.S., O.M.R., S.V., A.C. and J.K.; software, O.M.R.; formal analysis, M.S.; O.M.R. and S.V.; investigation, M.S., O.M.R., S.V., F.A., A.C., C.P., L.G. and E.T.; data curation, L.G., F.A., C.P., J.K. and E.T.; writing—original draft preparation, L.G., E.T., C.P., M.S., O.M.R. and S.V.; writing—review and editing, all authors; visualization, M.S. and O.M.R.; supervision, L.G., E.T., C.P., A.C. and F.A.; funding acquisition, L.G., C.P. and E.T. All authors have read and agreed to the published version of the manuscript.

Funding: This research was funded by Italian Ministero dell'Istruzione dell'Università, CARDIGAN project (CARDoon valorization by InteGrAted biorefinery, Progetti di Ricerca di Interesse Nazionale-Bando 2017). Ottavia Roggero is recipient of a PhD fellowship of the University of Trieste co-funded by ProRett research ONLUS (Italy).

Institutional Review Board Statement: The animal use was approved by the Italian Ministry of Health (authorization n. 693/2021-PR issued on Sept. 6th, 2019), in conformity to the Italian legislation D.Lgs 116/92.

Informed Consent Statement: Not applicable.

Data Availability Statement: The data presented in this study are available on request from the corresponding author.

Acknowledgments: We are grateful to Novamont S.p.A. for the kind donation of the cardoon plants. The authors wish to remember with gratitude Dario Solinas, who has always provided fundamental help and training to all researchers involved in the extraction with supercritical fluids. We want to dedicate this work to his memory, remembering his work and his talent.

Conflicts of Interest: The authors declare no conflict of interest.

Sample Availability: Samples of the compounds are available from the authors.

References

1. Adelusi, T.I.; Akinbolaji, G.R.; Yin, X.; Ayinde, K.S.; Olaoba, O.T. Neurotrophic, anti-neuroinflammatory, and redox balance mechanisms of chalcones. *Eur. J. Pharmacol.* **2021**, *891*, 173695. [CrossRef] [PubMed]
2. Khadka, B.; Lee, J.-Y.; Park, D.H.; Kim, K.-T.; Bae, J.-S. The Role of Natural Compounds and their Nanocarriers in the Treatment of CNS Inflammation. *Biomolecules* **2020**, *10*, 1401. [CrossRef]
3. Duran-Frigola, M.; Siragusa, L.; Ruppin, E.; Barril, X.; Cruciani, G.; Aloy, P. Detecting similar binding pockets to enable systems polypharmacology. *PLoS Comput. Biol.* **2017**, *13*, 1005522. [CrossRef] [PubMed]
4. Youdim, M.B.H.; Buccafusco, J.J. Multi-functional drugs for various CNS targets in the treatment of neurodegenerative disorders. *Trends Pharmacol. Sci.* **2005**, *26*, 27–35. [CrossRef] [PubMed]
5. Ramos, P.A.B.; Guerra, Â.R.; Guerreiro, O.; Freire, C.S.R.; Silva, A.M.S.; Duarte, M.F.; Silvestre, A.J.D. Lipophilic Extracts of *Cynara cardunculus* L. var. altilis (DC): A Source of Valuable Bioactive Terpenic Compounds. *J. Agric. Food Chem.* **2013**, *61*, 8420–8429. [CrossRef]
6. De Felice, C.; Cortelazzo, A.; Signorini, C.; Guerranti, R.; Leoncini, S.; Pecorelli, A.; Durand, T.; Galano, J.-M.; Oger, C.; Zollo, G.; et al. Effects of ω-3 polyunsaturated fatty acids on plasma proteome in Rett syndrome. *Mediat. Inflamm.* **2013**, *2013*, 723269. [CrossRef] [PubMed]
7. Haddadi, R.; Shahidi, Z.; Eyvari-Brooshghalan, S. Silymarin and neurodegenerative diseases: Therapeutic potential and basic molecular mechanisms. *Phytomedicine* **2020**, *79*, 153320. [CrossRef]
8. Fernández, J.; Curt, M.D.; Aguado, P.L. Industrial applications of *Cynara cardunculus* L. for energy and other uses. *Ind. Crops and Prod.* **2006**, *24*, 222–229. [CrossRef]
9. Benlloch-González, M.; Fournier, J.M.; Ramos, J.; Benlloch, M. Strategies underlying salt tolerance in halophytes are present in Cynara cardunculus. *Plant Sci. J.* **2005**, *168*, 653–659. [CrossRef]

10. Gironés-Vilaplana, A.; Valentão, P.; Andrade, P.B.; Ferreres, F.; Moreno, D.A.; García-Viguera, C. Phytochemical profile of a blend of black chokeberry and lemon juice with cholinesterase inhibitory effect and antioxidant potential. *Food Chem.* **2012**, *134*, 2090–2096. [CrossRef]
11. Torres, C.M.; Ríos, S.D.; Torras, C.; Salvadó, J.; Mateo-Sanz, J.M.; Jiménez, L. Sustainability analysis of biodiesel production from Cynara Cardunculus crop. *Fuel* **2013**, *111*, 535–542. [CrossRef]
12. Todea, A.; Deganutti, C.; Spennato, M.; Asaro, F.; Zingone, G.; Milizia, T.; Gardossi, L. Azelaic Acid: A Bio-Based Building Block for Biodegradable Polymers. *Polym. J.* **2021**, *13*, 4091. [CrossRef] [PubMed]
13. Turco, R.; Corrado, I.; Zannini, D.; Gargiulo, L.; Di Serio, M.; Pezzella, C.; Santagata, G. Upgrading cardoon biomass into Polyhydroxybutyrate based blends: A holistic approach for the synthesis of biopolymers and additives. *Bioresour. Technol.* **2022**, *363*, 127954. [CrossRef] [PubMed]
14. Silva, L.R.; Jacinto, T.A.; Coutinho, P. Bioactive Compounds from Cardoon as Health Promoters in Metabolic Disorders. *Foods* **2022**, *11*, 336. [CrossRef] [PubMed]
15. Pandino, G.; Lombardo, S.; Mauromicale, G.; Williamson, G. Phenolic acids and flavonoids in leaf and floral stem of cultivated and wild Cynara cardunculus L. genotypes. *Food Chem.* **2011**, *126*, 417–422. [CrossRef]
16. Mirpoor, S.F.; Varriale, S.; Porta, R.; Naviglio, D.; Spennato, M.; Gardossi, L.; Giosafatto, C.V.L.; Pezzella, C. A biorefinery approach for the conversion of Cynara cardunculus biomass to active films. *Food Hydrocoll.* **2022**, *122*, 107099. [CrossRef]
17. Falleh, H.; Ksouri, R.; Chaieb, K.; Karray-Bouraoui, N.; Trabelsi, N.; Boulaaba, M.; Abdelly, C. Phenolic composition of Cynara cardunculus L. organs, and their biological activities. *Comptes Rendus Biol.* **2008**, *331*, 372–379. [CrossRef] [PubMed]
18. Fratianni, F.; Tucci, M.; Palma, M.D.; Pepe, R.; Nazzaro, F. Polyphenolic composition in different parts of some cultivars of globe artichoke (*Cynara cardunculus* L. var. scolymus (L.) Fiori). *Food Chem.* **2007**, *104*, 1282–1286. [CrossRef]
19. Kukić, J.; Popović, V.; Petrović, S.; Mucaji, P.; Ćirić, A.; Stojković, D.; Soković, M. Antioxidant and antimicrobial activity of Cynara cardunculus extracts. *Food Chem.* **2008**, *107*, 861–868. [CrossRef]
20. Naviglio, D.; Scarano, P.; Ciaravolo, M.; Gallo, M. Rapid Solid-Liquid Dynamic Extraction (RSLDE): A Powerful and Greener Alternative to the Latest Solid-Liquid Extraction Techniques. *Foods* **2019**, *8*, 245. [CrossRef]
21. Amir, R.E.; Van den Veyver, I.B.; Wan, M.; Tran, C.Q.; Francke, U.; Zoghbi, H.Y. Rett syndrome is caused by mutations in X-linked MECP2, encoding methyl-CpG-binding protein 2. *Nat. Genet.* **1999**, *23*, 185–188. [CrossRef] [PubMed]
22. Bauman, M.L.; Kemper, T.L.; Arin, D.M. Microscopic observations of the brain in Rett syndrome. *Neuropediatrics* **1995**, *26*, 105–108. [CrossRef] [PubMed]
23. Belichenko, P.V.; Oldfors, A.; Hagberg, B.; Dahlström, A. Rett syndrome: 3-D confocal microscopy of cortical pyramidal dendrites and afferents. *Neuroreport* **1994**, *5*, 1509–1513. [CrossRef]
24. Fukuda, T.; Itoh, M.; Ichikawa, T.; Washiyama, K.; Goto, Y. Delayed maturation of neuronal architecture and synaptogenesis in cerebral cortex of Mecp2-deficient mice. *J. Neuropathol. Exp. Neurol.* **2005**, *64*, 537–544. [CrossRef]
25. Kaufmann, W.E.; MacDonald, S.M.; Altamura, C.R. Dendritic cytoskeletal protein expression in mental retardation: An immuno-histochemical study of the neocortex in Rett syndrome. *Cereb. Cortex* **2000**, *10*, 992–1004. [CrossRef] [PubMed]
26. Guy, J.; Hendrich, B.; Holmes, M.; Martin, J.E.; Bird, A. A mouse Mecp2-null mutation causes neurological symptoms that mimic Rett syndrome. *Nat. Genet.* **2001**, *27*, 322–326. [CrossRef]
27. Baj, G.; Patrizio, A.; Montalbano, A.; Sciancalepore, M.; Tongiorgi, E. Developmental and maintenance defects in Rett syndrome neurons identified by a new mouse staging system in vitro. *Front. Cell Neurosci.* **2014**, *8*, 18. [CrossRef] [PubMed]
28. Reverchon, E.; De Marco, I. Supercritical fluid extraction and fractionation of natural matter. *J. Supercrit. Fluids* **2006**, *38*, 146–166. [CrossRef]
29. Mathe, C.; Culioli, G.; Archier, P.; Vieillescazes, C. Characterization of archaeological frankincense by gas chromatography–mass spectrometry. *J. Chromatogr. A* **2004**, *1023*, 277–285. [CrossRef] [PubMed]
30. Scavo, A.; Pandino, G.; Restuccia, C.; Parafati, L.; Cirvilleri, G.; Mauromicale, G. Antimicrobial activity of cultivated cardoon (*Cynara cardunculus* L. var. altilis DC.) leaf extracts against bacterial species of agricultural and food interest. *Ind. Crops Prod.* **2019**, *129*, 206–211. [CrossRef]
31. Eljounaidi, K.; Comino, C.; Moglia, A.; Cankar, K.; Genre, A.; Hehn, A.; Bourgaud, F.; Beekwilder, J.; Lanteri, S. Accumulation of cynaropicrin in globe artichoke and localization of enzymes involved in its biosynthesis. *Plant. Sci. J.* **2015**, *239*, 128–136. [CrossRef] [PubMed]
32. Rouphael, Y.; Bernardi, J.; Cardarelli, M.; Bernardo, L.; Kane, D.; Colla, G.; Lucini, L. Phenolic Compounds and Sesquiterpene Lactones Profile in Leaves of Nineteen Artichoke Cultivars. *J. Agric. Food Chem.* **2016**, *64*, 8540–8548. [CrossRef] [PubMed]
33. Sobolev, A.P.; Brosio, E.; Gianferri, R.; Segre, A.L. Metabolic profile of lettuce leaves by high-field NMR spectra. *Magn. Reson. Chem.* **2005**, *43*, 625–638. [CrossRef] [PubMed]
34. Huang, Z.-R.; Lin, Y.-K.; Fang, J.-Y. Biological and Pharmacological Activities of Squalene and Related Compounds: Potential Uses in Cosmetic Dermatology. *Molecules* **2009**, *14*, 540–554. [CrossRef] [PubMed]
35. Auffray, B. Protection against singlet oxygen, the main actor of sebum squalene peroxidation during sun exposure, using Commiphora myrrha essential oil. *Int. J. Cosmet. Sci.* **2007**, *29*, 23–29. [CrossRef]
36. Berté, T.E.; Dalmagro, A.P.; Zimath, P.L.; Gonçalves, A.E.; Meyre-Silva, C.; Bürger, C.; Weber, C.J.; dos Santos, D.A.; Cechinel-Filho, V.; de Souza, M.M. Taraxerol as a possible therapeutic agent on memory impairments and Alzheimer's disease: Effects against scopolamine and streptozotocin-induced cognitive dysfunctions. *Steroids* **2018**, *132*, 5–11. [CrossRef]

37. Gallo, M.B.C.; Sarachine, M.J. Biological Activities of Lupeol. *Int. J. Pharm. Biomed. Res.* **2019**, *3*, 46–66.
38. Moujir, L.; Callies, O.; Sousa, P.M.C.; Sharopov, F.; Seca, A.M.L. Applications of Sesquiterpene Lactones: A Review of Some Potential Success Cases. *Appl. Sci.* **2020**, *10*, 3001. [CrossRef]
39. Mandim, F.; Petropoulos, S.A.; Dias, M.I.; Pinela, J.; Kostić, M.; Soković, M.; Santos-Buelga, C.; Ferreira, I.C.F.R.; Barros, L. Phenolic Composition and Biological Properties of *Cynara cardunculus* L. var. altilis Petioles: Influence of the Maturity Stage. *Antioxidants* **2021**, *10*, 1907. [CrossRef]
40. Nerli, E.; Roggero, O.M.; Baj, G.; Tongiorgi, E. In vitro modeling of dendritic atrophy in Rett syndrome: Determinants for phenotypic drug screening in neurodevelopmental disorders. *Sci. Rep.* **2020**, *10*, 2491. [CrossRef]
41. Sharma, P.; Ando, D.M.; Daub, A.; Kaye, J.A.; Finkbeiner, S. High-Throughput Screening in Primary Neurons. *Methods Enzymol.* **2012**, *506*, 331–360. [PubMed]
42. Limpert, A.S.; Mattmann, M.E.; Cosford, N.D.P. Recent Progress in the Discovery of Small Molecules for the Treatment of Amyotrophic Lateral Sclerosis (ALS). *Beilstein J. Org. Chem.* **2013**, *9*, 717–732. [CrossRef] [PubMed]
43. Varkuti, B.H.; Liu, Z.; Kepiro, M.; Pacifico, R.; Gai, Y.; Kameneka, T.; Davis, R.L. High-Throughput Small Molecule Screen Identifies Modulators of Mitochondrial Function in Neurons. *Science* **2020**, *23*, 100931.
44. Lee, H.-M.; Kuijer, M.B.; Ruiz Blanes, N.; Clark, E.P.; Aita, M.; Galiano Arjona, L.; Kokot, A.; Sciaky, N.; Simon, J.M.; Bhatnagar, S.; et al. A Small-Molecule Screen Reveals Novel Modulators of MeCP2 and X-Chromosome Inactivation Maintenance. *J. Neurodev. Disord.* **2020**, *12*, 29. [CrossRef] [PubMed]
45. Kyle, S.M.; Vashi, N.; Justice, M.J. Rett Syndrome: A Neurological Disorder with Metabolic Components. *Open Biol.* **2018**, *8*, 170216. [CrossRef] [PubMed]
46. Passamonti, S.; Vrhovsek, U.; Vanzo, A.; Mattivi, F. Fast Access of Some Grape Pigments to the Brain. *J. Agric. Food Chem.* **2005**, *53*, 7029–7034. [CrossRef]
47. Gasperotti, M.; Passamonti, S.; Tramer, F.; Masuero, D.; Guella, G.; Mattivi, F.; Vrhovsek, U. Fate of Microbial Metabolites of Dietary Polyphenols in Rats: Is the Brain Their Target Destination? *ACS Chem. Neurosci.* **2015**, *6*, 1341–1352. [CrossRef]
48. Mus, A.A.; Goh, L.P.W.; Marbawi, H.; Gansau, J.A. The Biosynthesis and Medicinal Properties of Taraxerol. *Biomedicines* **2022**, *10*, 807. [CrossRef]
49. Buchovecky, C.M.; Turley, S.D.; Brown, H.M.; Kyle, S.M.; McDonald, J.G.; Liu, B.; Pieper, A.A.; Huang, W.; Katz, D.M.; Russell, D.W.; et al. A suppressor screen in Mecp2 mutant mice implicates cholesterol metabolism in Rett syndrome. *Nat. Genet.* **2013**, *45*, 1013–1020. [CrossRef]
50. Tsai, F.-S.; Lin, L.-W.; Wu, C.-R. Lupeol and Its Role in Chronic Diseases. *Adv. Exp. Med. Biol.* **2016**, *929*, 145–175.
51. Wang, Z.; Han, Y.; Tian, S.; Bao, J.; Wang, Y.; Jiao, J. Lupeol Alleviates Cerebral Ischemia–Reperfusion Injury in Correlation with Modulation of PI3K/Akt Pathway. *Neuropsychiatr. Dis. Treat.* **2020**, *16*, 1381–1390. [CrossRef] [PubMed]
52. Ahmad, R.; Khan, A.; Rehman, I.U.; Lee, H.J.; Khan, I.; Kim, M.O. Lupeol Treatment Attenuates Activation of Glial Cells and Oxidative-Stress-Mediated Neuropathology in Mouse Model of Traumatic Brain Injury. *Int. J. Mol. Sci.* **2022**, *23*, 6086. [CrossRef] [PubMed]
53. Yao, X.; Li, G.; Bai, Q.; Xu, H.; Lü, C. Taraxerol Inhibits LPS-Induced Inflammatory Responses through Suppression of TAK1 and Akt Activation. *Int. Immunopharmacol.* **2013**, *15*, 316–324. [CrossRef] [PubMed]
54. Oliveira-Junior, M.S.; Pereira, E.P.; de Amorim, V.C.M.; Reis, L.T.C.; do Nascimento, R.P.; da Silva, V.D.A.; Costa, S.L. Lupeol Inhibits LPS-Induced Neuroinflammation in Cerebellar Cultures and Induces Neuroprotection Associated to the Modulation of Astrocyte Response and Expression of Neurotrophic and Inflammatory Factors. *Int. Immunopharmacol.* **2019**, *70*, 302–312. [CrossRef] [PubMed]
55. Michikawa, M.; Yanagisawa, K. Apolipoprotein E4 induces neuronal cell death under conditions of suppressed de novo cholesterol synthesis. *J. Neurosci. Res.* **1998**, *54*, 58–67. [CrossRef]
56. De Zordi, N.; Cortesi, A.; Kikic, I.; Moneghini, M.; Solinas, D.; Innocenti, G.; Portolan, A.; Baratto, G.; Dall'Acqua, S. The supercritical carbon dioxide extraction of polyphenols from Propolis: A central composite design approach. *J. Supercrit. Fluids* **2014**, *95*, 491–498. [CrossRef]
57. Reynolds, W.F.; McLean, S.; Poplawski, J.; Enriquez, R.G.; Escobar, L.I.; Leon, I. Total assignment of 13C and 1H spectra of three isomeric triterpenol derivatives by 2D NMR: An investigation of the potential utility of 1H chemical shifts in structural investigations of complex natural products. *Tetrahedron* **1986**, *42*, 3419–3428. [CrossRef]
58. Guy, J.; Gan, J.; Selfridge, J.; Cobb, S.; Bird, A. Reversal of neurological defects in a mouse model of Rett syndrome. *Science* **2007**, *315*, 1143–1147. [CrossRef]
59. Duan, W.; Zhang, Y.P.; Hou, Z.; Huang, C.; Zhu, H.; Zhang, C.Q.; Yin, Q. Novel Insights into NeuN: From Neuronal Marker to Splicing Regulator. *Mol. Neurobiol.* **2016**, *53*, 1637–1647. [CrossRef]
60. Clarke, A.J.; Abdala Sheikh, A.P. A perspective on "cure" for Rett syndrome. *Orphanet J. Rare Dis.* **2018**, *13*, 44. [CrossRef] [PubMed]
61. Palomino-Schätzlein, M.; Escrig, R.V.; Boira, H.; Primo, J.; Pineda-Lucena, A.; Cabedo, N. Evaluation of nonpolar metabolites in plant extracts by ^{13}C NMR spectroscopy. *J. Agric. Food Chem.* **2011**, *59*, 11407–11416.

2.6 CONCLUSIONS

The objective of this part of the thesis was the valorization of cardoon leaves extracts (CLEs). The first activity was the characterization of extracts obtained with different extraction methods ($scCO_2$, Naviglio® technology and batch) from plants harvested in various harvest seasons (from spring 2019 to autumn 2020) and in different plantations (Sant'Angelo and Navamont S.p.A. fields).

Using ^1H NMR and GC-MS analysis the composition of $scCO_2$ extracts in comparison to Naviglio® and batch extracts was determined, with particular attention to cynaropicrin content. The extracts from Naviglio® technology are characterized by the presence of fatty acid and a good percentage of cynaropicrin. However, with the Naviglio® technology it was possible to extract only cynaropicrin, as sesquiterpene lactone. Differently, with the batch method it was possible to extract another sesquiterpene lactone: the grosheimin. From all the data, the content of cynaropicrin is higher in the samples from the Terni plantation than the Sant'Angelo plantation. Even if by $scCO_2$ the extraction of cynaropicrin is less efficient, it was possible to extract another sesquiterpene lactone: the 11,13-dihydroxy-8-desoxigrosheimin. By this extraction method waxes were also extracted. In fact, the signals of waxes in GC-MS chromatograms are more evident in $scCO_2$ CLEs than in Naviglio® and batch CLEs. In all the samples it was possible to see, both with NMR and GC-MS analysis, the presence of fatty acids and other triterpenes, such as squalene, or pentacyclic terpenes, such as lupeol.

The obtained CLEs were used for two types of applications. Firstly, CLEs were used to functionalize the films made by cardoon proteins (CPs) and the characterization of the derived films showed a significant improvement of all the properties of the manufactured material. A good compatibility between Cardoon Proteins (CPs) and CLE was observed. Moreover, CLE improved mechanical and barrier properties of the materials and conferred higher antioxidant activity.

Secondly, the bioactive properties of different extracts of cardoon leaves in rescuing neuronal development arrest in an in vitro model of Rett syndrome (RTT) was investigated. While $scCO_2$ cardoon leaves extracts are very hydrophobic fractions, the Naviglio® method is effective in extracting phenolic compounds and less hydrophobic components thanks to the action of polar solvents. Only the scCO2 cardoon leaves extract obtained from plants harvested in spring was able to induce a significant rescue of neuronal atrophy in RTT neurons, while the scCO2 extract from Autumn harvest was active on WT neurons.

The scCO2 hydrophobic extracts are the richest in squalene, 3ß-taraxerol, and lupeol. On the other hand, the Naviglio® extract is rich in cynaropicrin, and exerts a toxic effect on both WT and RTT neurons. Interestingly, when bioactive molecules cynaropicrin, squalene, lupeol, and taraxerol were tested individually, no positive effect was observed whereas a significant neurotoxic effect of cynaropicrin was evident at different concentrations of the pure molecule but also in the case of the extracts. In conclusion, the composition of cardoon extracts should be carefully determined in order to exploit their different pharmacological potential towards neurological diseases.

2.7 REFERENCES

Adekenova, A.S., Sakenova, P.Y., Ivasenko, S.A., Khabarov, I.A., Adekenov, S.M., Berthod, A., 2016. Gram-Scale Purification of Two Sesquiterpene Lactones from Chartolepsis Intermedia Boiss. Chromatographia 79, 37–43. https://doi.org/10.1007/s10337-015-3000-1

Adelusi, T.I., Akinbolaji, G.R., Yin, X., Ayinde, K.S., Olaoba, O.T., 2021. Neurotrophic, anti-neuroinflammatory, and redox balance mechanisms of chalcones. Eur J Pharmacol 891, 173695. https://doi.org/10.1016/j.ejphar.2020.173695

Alexandre, A.M.R.C., Dias, A.M.A., Seabra, I.J., Portugal, A.A.T.G., de Sousa, H.C., Braga, M.E.M., 2012. Biodiesel obtained from supercritical carbon dioxide oil of Cynara cardunculus L. The Journal of Supercritical Fluids 68, 52–63. https://doi.org/10.1016/j.supflu.2012.03.012

Amir, R.E., Van den Veyver, I.B., Wan, M., Tran, C.Q., Francke, U., Zoghbi, H.Y., 1999. Rett syndrome is caused by mutations in X-linked MECP2, encoding methyl-CpG-binding protein 2. Nat Genet 23, 185–188. https://doi.org/10.1038/13810

Auffray, B., 2007. Protection against singlet oxygen, the main actor of sebum squalene peroxidation during sun exposure, using Commiphora myrrha essential oil. International Journal of Cosmetic Science 29, 23–29. https://doi.org/10.1111/j.1467-2494.2007.00360.x

Azmir, J., Zaidul, I.S.M., Rahman, M.M., Sharif, K.M., Mohamed, A., Sahena, F., Jahurul, M.H.A., Ghafoor, K., Norulaini, N.A.N., Omar, A.K.M., 2013. Techniques for extraction of bioactive compounds from plant materials: A review. Journal of Food Engineering, SI: Extraction and Encapsulation 117, 426–436. https://doi.org/10.1016/j.jfoodeng.2013.01.014

Barbosa, C.H., Andrade, M.A., Vilarinho, F., Castanheira, I., Fernando, A.L., Loizzo, M.R., Sanches Silva, A., 2020. A New Insight on Cardoon: Exploring New Uses besides Cheese Making with a View to Zero Waste. Foods 9, 564. https://doi.org/10.3390/foods9050564

Barracosa, P., Barracosa, M., Pires, E., 2019. Cardoon as a Sustainable Crop for Biomass and Bioactive Compounds Production. Chemistry & Biodiversity 16, e1900498. https://doi.org/10.1002/cbdv.201900498

Bauman, M.L., Kemper, T.L., Arin, D.M., 1995. Microscopic observations of the brain in Rett syndrome. Neuropediatrics 26, 105–108. https://doi.org/10.1055/s-2007-979737

Beckman, C.H., 2000. Phenolic-storing cells: keys to programmed cell death and periderm formation in wilt disease resistance and in general defence responses in plants? Physiological and Molecular Plant Pathology 57, 101–110. https://doi.org/10.1006/pmpp.2000.0287

Belichenko, P.V., Oldfors, A., Hagberg, B., Dahlström, A., 1994. Rett syndrome: 3-D confocal microscopy of cortical pyramidal dendrites and afferents. Neuroreport 5, 1509–1513.

Ben Salem, M., Ksouda, K., Dhouibi, R., Charfi, S., Turki, M., Hammami, S., Ayedi, F., Sahnoun, Z., Zeghal, K.M., Affes, H., 2019. LC-MS/MS Analysis and Hepatoprotective Activity of Artichoke (Cynara scolymus L.) Leaves Extract against

High Fat Diet-Induced Obesity in Rats. Biomed Res Int 2019, 4851279. https://doi.org/10.1155/2019/4851279

Benlloch-González, M., Fournier, J.M., Ramos, J., Benlloch, M., 2005. Strategies underlying salt tolerance in halophytes are present in Cynara cardunculus. Plant Science 168, 653–659. https://doi.org/10.1016/j.plantsci.2004.09.035

Berté, T.E., Dalmagro, A.P., Zimath, P.L., Gonçalves, A.E., Meyre-Silva, C., Bürger, C., Weber, C.J., dos Santos, D.A., Cechinel-Filho, V., de Souza, M.M., 2018. Taraxerol as a possible therapeutic agent on memory impairments and Alzheimer's disease: Effects against scopolamine and streptozotocin-induced cognitive dysfunctions. Steroids 132, 5–11. https://doi.org/10.1016/j.steroids.2018.01.002

Clarke, A.J., Abdala Sheikh, A.P., 2018. A perspective on "cure" for Rett syndrome. Orphanet J Rare Dis 13, 44. https://doi.org/10.1186/s13023-018-0786-6

Curt, M.D., Martinez, I., Sanz M., Lourenço A., Gominho J., González, J, Fernández J, 2014. Potential of four selected clones of Cynara cardunculus L. for oil production', Proceedings of the 22nd European Biomass Conference and Exhibition, Hamburg, Germany, 2014, pp. 274–279.

Dai, Q., Yang, Y., Chen, K., Cheng, Z., Ni, Y., Li, J., 2019. Optimization of Supercritical CO2 Operative Parameters to Simultaneously Increase the Extraction Yield of Oil and Pentacyclic Triterpenes from Artichoke Leaves and Stalks by Response Surface Methodology and Ridge Analysis. European Journal of Lipid Science and Technology 121, 1800120. https://doi.org/10.1002/ejlt.201800120

De Zordi, N., Cortesi, A., Kikic, I., Moneghini, M., Baldan, V., Sut, S., Solinas, D., Dall'Acqua, S., 2017. The Supercritical carbon dioxide extraction of ω-3, ω-6 lipids and β-sitosterol from Italian walnuts: a central composite design approach. The Journal of Supercritical Fluids 127, 223–228. https://doi.org/10.1016/j.supflu.2017.02.020

Duran-Frigola, M., Siragusa, L., Ruppin, E., Barril, X., Cruciani, G., Aloy, P., 2017. Detecting similar binding pockets to enable systems polypharmacology. PLoS Comput Biol 13, e1005522. https://doi.org/10.1371/journal.pcbi.1005522

Eljounaidi, K., Comino, C., Moglia, A., Cankar, K., Genre, A., Hehn, A., Bourgaud, F., Beekwilder, J., Lanteri, S., 2015. Accumulation of cynaropicrin in globe artichoke and localization of enzymes involved in its biosynthesis. Plant Science 239, 128–136. https://doi.org/10.1016/j.plantsci.2015.07.020

Encinar, J.M., González, J.F., Sabio, E., Ramiro, M.J., 1999. Preparation and Properties of Biodiesel from Cynara cardunculus L. Oil. Ind. Eng. Chem. Res. 38, 2927–2931. https://doi.org/10.1021/ie990012x

Fernández, J., Curt, M.D., Aguado, P.L., 2006. Industrial applications of Cynara cardunculus L. for energy and other uses. Industrial Crops and Products, 2005 Annual Meeting of the Association for the Advancement of Industrial Crops: The International Conference on Industrial Crops and Rural Development 24, 222–229. https://doi.org/10.1016/j.indcrop.2006.06.010

Fernando, A.L., Costa, J., Barbosa, B., Monti, A., Rettenmaier, N., 2018. Environmental impact assessment of perennial crops cultivation on marginal soils in the Mediterranean Region. Biomass and Bioenergy 111, 174–186. https://doi.org/10.1016/j.biombioe.2017.04.005

Forgo, P., Kövér, K.E., 2004. Gradient enhanced selective experiments in the 1H NMR chemical shift assignment of the skeleton and side-chain resonances of stigmasterol, a phytosterol derivative. Steroids 69, 43–50. https://doi.org/10.1016/j.steroids.2003.09.012

Fratianni, F., Tucci, M., Palma, M.D., Pepe, R., Nazzaro, F., 2007. Polyphenolic composition in different parts of some cultivars of globe artichoke (Cynara cardunculus L. var. scolymus (L.) Fiori). Food Chemistry 104, 1282–1286. https://doi.org/10.1016/j.foodchem.2007.01.044

Fukuda, T., Itoh, M., Ichikawa, T., Washiyama, K., Goto, Y., 2005. Delayed maturation of neuronal architecture and synaptogenesis in cerebral cortex of Mecp2-deficient mice. J Neuropathol Exp Neurol 64, 537–544. https://doi.org/10.1093/jnen/64.6.537

Gallo, M.B.C., Sarachine, M.J., 2009. Biological Activities of Lupeol 21.

Gebhardt, R., 1997. Antioxidative and protective properties of extracts from leaves of the artichoke (Cynara scolymus L.) against hydroperoxide-induced oxidative stress in cultured rat hepatocytes. Toxicol Appl Pharmacol 144, 279–286. https://doi.org/10.1006/taap.1997.8130

Ghasemi, E., Raofie, F., Najafi, N.M., 2011. Application of response surface methodology and central composite design for the optimisation of supercritical fluid extraction of essential oils from Myrtus communis L. leaves. Food Chemistry 126, 1449–1453. https://doi.org/10.1016/j.foodchem.2010.11.135

Gironés-Vilaplana, A., Valentão, P., Andrade, P.B., Ferreres, F., Moreno, D.A., García-Viguera, C., 2012. Phytochemical profile of a blend of black chokeberry and lemon juice with cholinesterase inhibitory effect and antioxidant potential. Food Chem 134, 2090–2096. https://doi.org/10.1016/j.foodchem.2012.04.010

Gominho, J., Curt, M.D., Lourenço, A., Fernández, J., Pereira, H., 2018. Cynara cardunculus L. as a biomass and multi-purpose crop: A review of 30 years of research. Biomass and Bioenergy 109, 257–275. https://doi.org/10.1016/j.biombioe.2018.01.001

Guy, J., Gan, J., Selfridge, J., Cobb, S., Bird, A., 2007. Reversal of neurological defects in a mouse model of Rett syndrome. Science 315, 1143–1147. https://doi.org/10.1126/science.1138389

Ha, T.J., Jang, D.S., Lee, J.R., Lee, K.D., Lee, J., Hwang, S.W., Jung, H.J., Nam, S.H., Park, K.H., Yang, M.S., 2003. Cytotoxic effects of sesquiterpene lactones from the flowers ofHemisteptia lyrata B. Arch Pharm Res 26, 925–928. https://doi.org/10.1007/BF02980201

Haddadi, R., Shahidi, Z., Eyvari-Brooshghalan, S., 2020. Silymarin and neurodegenerative diseases: Therapeutic potential and basic molecular mechanisms. Phytomedicine 79, 153320. https://doi.org/10.1016/j.phymed.2020.153320

Huang, Z.-R., Lin, Y.-K., Fang, J.-Y., 2009. Biological and Pharmacological Activities of Squalene and Related Compounds: Potential Uses in Cosmetic Dermatology. Molecules 14, 540–554. https://doi.org/10.3390/molecules14010540

Ierna, A., Mauromicale, G., 2010. Cynara cardunculus L. genotypes as a crop for energy purposes in a Mediterranean environment. Biomass and Bioenergy 34, 754–760. https://doi.org/10.1016/j.biombioe.2010.01.018

Kaufmann, W.E., MacDonald, S.M., Altamura, C.R., 2000. Dendritic cytoskeletal protein expression in mental retardation: an immunohistochemical study of the neocortex in Rett syndrome. Cereb Cortex 10, 992–1004. https://doi.org/10.1093/cercor/10.10.992

Khadka, B., Lee, J.-Y., Park, D.H., Kim, K.-T., Bae, J.-S., 2020. The Role of Natural Compounds and their Nanocarriers in the Treatment of CNS Inflammation. Biomolecules 10, 1401. https://doi.org/10.3390/biom10101401

Kukić, J., Popović, V., Petrović, S., Mucaji, P., Ćirić, A., Stojković, D., Soković, M., 2008. Antioxidant and antimicrobial activity of Cynara cardunculus extracts. Food Chemistry 107, 861–868. https://doi.org/10.1016/j.foodchem.2007.09.005

Kulkarni, V.A., Firestein, B.L., 2012. The dendritic tree and brain disorders. Molecular and Cellular Neuroscience 50, 10–20. https://doi.org/10.1016/j.mcn.2012.03.005

Lag-Brotons, A., Gómez, I., Navarro-Pedreño, J., Mayoral, A.M., Curt, M.D., 2014. Sewage sludge compost use in bioenergy production – a case study on the effects on Cynara cardunculus L energy crop. Journal of Cleaner Production 79, 32–40. https://doi.org/10.1016/j.jclepro.2014.05.021

Leoncini, S., De Felice, C., Signorini, C., Zollo, G., Cortelazzo, A., Durand, T., Galano, J.-M., Guerranti, R., Rossi, M., Ciccoli, L., Hayek, J., 2015. Cytokine Dysregulation in *MECP2*- and *CDKL5*-Related Rett Syndrome: Relationships with Aberrant Redox Homeostasis, Inflammation, and *ω*-3 PUFAs. Oxidative Medicine and Cellular Longevity 2015, e421624. https://doi.org/10.1155/2015/421624

Mandim, F., Petropoulos, S.A., Dias, M.I., Pinela, J., Kostić, M., Soković, M., Santos-Buelga, C., Ferreira, I.C.F.R., Barros, L., 2021. Phenolic Composition and Biological Properties of Cynara cardunculus L. var. altilis Petioles: Influence of the Maturity Stage. Antioxidants 10, 1907. https://doi.org/10.3390/antiox10121907

Mathe, C., Culioli, G., Archier, P., Vieillescazes, C., 2004. Characterization of archaeological frankincense by gas chromatography–mass spectrometry. Journal of Chromatography A 1023, 277–285. https://doi.org/10.1016/j.chroma.2003.10.016

Mirpoor, S.F., Varriale, S., Porta, R., Naviglio, D., Spennato, M., Gardossi, L., Giosafatto, C.V.L., Pezzella, C., 2022. A biorefinery approach for the conversion of Cynara cardunculus biomass to active films. Food Hydrocolloids 122, 107099. https://doi.org/10.1016/j.foodhyd.2021.107099

Moglia, A., Lanteri, S., Comino, C., Acquadro, A., de Vos, R., Beekwilder, J., 2008. Stress-induced biosynthesis of dicaffeoylquinic acids in globe artichoke. J Agric Food Chem 56, 8641–8649. https://doi.org/10.1021/jf801653w

Moujir, L., Callies, O., Sousa, P.M.C., Sharopov, F., Seca, A.M.L., 2020. Applications of Sesquiterpene Lactones: A Review of Some Potential Success Cases. Applied Sciences 10, 3001. https://doi.org/10.3390/app10093001

Naviglio, D., Scarano, P., Ciaravolo, M., Gallo, M., 2019a. Rapid Solid-Liquid Dynamic Extraction (RSLDE): A Powerful and Greener Alternative to the Latest Solid-Liquid Extraction Techniques. Foods 8, 245. https://doi.org/10.3390/foods8070245

Naviglio, D., Scarano, P., Ciaravolo, M., Gallo, M., 2019b. Rapid Solid-Liquid Dynamic Extraction (RSLDE): A Powerful and Greener Alternative to the Latest Solid-Liquid Extraction Techniques. Foods 8, 245. https://doi.org/10.3390/foods8070245

Nerli, E., Roggero, O.M., Baj, G., Tongiorgi, E., 2020. In vitro modeling of dendritic atrophy in Rett syndrome: determinants for phenotypic drug screening in neurodevelopmental disorders. Sci Rep 10, 2491. https://doi.org/10.1038/s41598-020-59268-w

Pagnotta, M.A., Fernández, J.A., Sonnante, G., Egea-Gilabert, C., 2017. Genetic diversity and accession structure in European Cynara cardunculus collections. PLOS ONE 12, e0178770. https://doi.org/10.1371/journal.pone.0178770

Pandino, G., Lombardo, S., Mauromicale, G., Williamson, G., 2011. Phenolic acids and flavonoids in leaf and floral stem of cultivated and wild Cynara cardunculus L. genotypes. Food Chemistry 126, 417–422. https://doi.org/10.1016/j.foodchem.2010.11.001

Pavić, V., Jakovljević, M., Molnar, M., Jokić, S., 2019. Extraction of Carnosic Acid and Carnosol from Sage (Salvia officinalis L.) Leaves by Supercritical Fluid Extraction and Their Antioxidant and Antibacterial Activity. Plants 8, 16. https://doi.org/10.3390/plants8010016

Portis, E., Barchi, L., Acquadro, A., Macua, J.I., Lanteri, S., 2005. Genetic diversity assessment in cultivated cardoon by AFLP (amplified fragment length polymorphism) and microsatellite markers. Plant Breeding 124, 299–304. https://doi.org/10.1111/j.1439-0523.2005.01098.x

Posadino, A.M., Biosa, G., Zayed, H., Abou-Saleh, H., Cossu, A., Nasrallah, G.K., Giordo, R., Pagnozzi, D., Porcu, M.C., Pretti, L., Pintus, G., 2018. Protective Effect of Cyclically Pressurized Solid–Liquid Extraction Polyphenols from Cagnulari Grape Pomace on Oxidative Endothelial Cell Death. Molecules 23, 2105. https://doi.org/10.3390/molecules23092105

Ramos, P.A.B., Guerra, Â.R., Guerreiro, O., Freire, C.S.R., Silva, A.M.S., Duarte, M.F., Silvestre, A.J.D., 2013. Lipophilic Extracts of Cynara cardunculus L. var. altilis (DC): A Source of Valuable Bioactive Terpenic Compounds. J. Agric. Food Chem. 61, 8420–8429. https://doi.org/10.1021/jf402253a

Ramos, P.A.B., Guerra, Â.R., Guerreiro, O., Santos, S.A.O., Oliveira, H., Freire, C.S.R., Silvestre, A.J.D., Duarte, M.F., 2017. Antiproliferative Effects of Cynara cardunculus L. var. altilis (DC) Lipophilic Extracts. International Journal of Molecular Sciences 18, 63. https://doi.org/10.3390/ijms18010063

Reynolds, W.F., McLean, S., Poplawski, J., Enriquez, R.G., Escobar, L.I., Leon, I., 1986. Total assignment of 13C and 1H spectra of three isomeric triterpenol derivatives by 2D NMR: an investigation of the potential utility of 1H chemical shifts in structural investigations of complex natural products. Tetrahedron 42, 3419–3428. https://doi.org/10.1016/S0040-4020(01)87309-9

Rouphael, Y., Bernardi, J., Cardarelli, M., Bernardo, L., Kane, D., Colla, G., Lucini, L., 2016. Phenolic Compounds and Sesquiterpene Lactones Profile in Leaves of Nineteen Artichoke Cultivars. J. Agric. Food Chem. 64, 8540–8548. https://doi.org/10.1021/acs.jafc.6b03856

Saller, R., Meier, R., Brignoli, R., 2001. The Use of Silymarin in the Treatment of Liver Diseases. Drugs 61, 2035–2063. https://doi.org/10.2165/00003495-200161140-00003

Scavo, A., Pandino, G., Restuccia, C., Parafati, L., Cirvilleri, G., Mauromicale, G., 2019a. Antimicrobial activity of cultivated cardoon (Cynara cardunculus L. var. altilis DC.) leaf extracts against bacterial species of agricultural and food interest. Industrial Crops and Products 129, 206–211. https://doi.org/10.1016/j.indcrop.2018.12.005

Scavo, A., Pandino, G., Restuccia, C., Parafati, L., Cirvilleri, G., Mauromicale, G., 2019b. Antimicrobial activity of cultivated cardoon (Cynara cardunculus L. var. altilis DC.) leaf extracts against bacterial species of agricultural and food interest. Industrial Crops and Products 129, 206–211. https://doi.org/10.1016/j.indcrop.2018.12.005

Shimizu, S., Ishihara, N., Umehara, K., Miyase, T., Ueno, A., 1988. Sesquiterpene glycosides and saponins from Cynara cardunculus L. Chem. Pharm. Bull. 36, 2466–2474. https://doi.org/10.1248/cpb.36.2466

Silva, L.R., Jacinto, T.A., Coutinho, P., 2022a. Bioactive Compounds from Cardoon as Health Promoters in Metabolic Disorders. Foods 11, 336. https://doi.org/10.3390/foods11030336

Silva, L.R., Jacinto, T.A., Coutinho, P., 2022b. Bioactive Compounds from Cardoon as Health Promoters in Metabolic Disorders. Foods 11, 336. https://doi.org/10.3390/foods11030336

Sobolev, A.P., Brosio, E., Gianferri, R., Segre, A.L., 2005. Metabolic profile of lettuce leaves by high-field NMR spectra. Magnetic Resonance in Chemistry 43, 625–638. https://doi.org/10.1002/mrc.1618

Suttiarporn, P., Chumpolsri, W., Mahatheeranont, S., Luangkamin, S., Teepsawang, S., Leardkamolkarn, V., 2015. Structures of Phytosterols and Triterpenoids with Potential Anti-Cancer Activity in Bran of Black Non-Glutinous Rice. Nutrients 7, 1672–1687. https://doi.org/10.3390/nu7031672

Turco, R., Corrado, I., Zannini, D., Gargiulo, L., Di Serio, M., Pezzella, C., Santagata, G., 2022. Upgrading cardoon biomass into Polyhydroxybutyrate based blends: A holistic approach for the synthesis of biopolymers and additives. Bioresource Technology 363, 127954. https://doi.org/10.1016/j.biortech.2022.127954

Ullah, H., Khan, H., 2018. Anti-Parkinson Potential of Silymarin: Mechanistic Insight and Therapeutic Standing. Frontiers in Pharmacology 9.

Weng, S.-M., McLeod, F., Bailey, M.E.S., Cobb, S.R., 2011. Synaptic plasticity deficits in an experimental model of rett syndrome: long-term potentiation saturation and its pharmacological reversal. Neuroscience 180, 314–321. https://doi.org/10.1016/j.neuroscience.2011.01.061

Youdim, M.B.H., Buccafusco, J.J., 2005. Multi-functional drugs for various CNS targets in the treatment of neurodegenerative disorders. Trends Pharmacol Sci 26, 27–35. https://doi.org/10.1016/j.tips.2004.11.007

Zhang, J., Shishatskaya, E.I., Volova, T.G., da Silva, L.F., Chen, G.-Q., 2018. Polyhydroxyalkanoates (PHA) for therapeutic applications. Materials Science and Engineering: C 86, 144–150. https://doi.org/10.1016/j.msec.2017.12.035

CHAPTER 3

ENZYMATIC PROCESSING OF CARDOON SEED OIL

3.1 SUMMARY

Epoxidized fatty acids are precursors of bio-based and biodegradable biolubricants. The third part of this PhD project is focused on the biocatalysed synthesis of these products starting from *Cynara cardunculus* seed oil. The study addressed the problem related to the large percentage of the million tons of lubricants consumed in the world yearly that end up in the environment through leakages and human mistakes (Zainal et al., 2018), thus polluting water, soil, and air (Garcés et al., 2011).

Different epoxidized unsaturated fatty acids were prepared by exploiting enzymatic catalysis and working under mild and sustainable solvent-free conditions. The experimental work started with the characterization of the seed oil followed by the enzymatic hydrolysis of the oil catalysed by the combined action of two lipases endowed with different regioselectivity: lipase B from *Candida antarctica* (CaLB) and lipase from *Thermomyces lanuginosus* (TLL). The reaction was scaled up to 2L of cardoon seed oil and led to a mixture of fatty acids.

The chemo-enzymatic epoxidation was performed in the presence of hydrogen peroxide and lipase CaLB, without any solvent. The process was optimized using pure samples of oleic, linoleic, and linolenic acids. The method allowed the complete epoxidation of the unsaturated fatty acids while avoiding the side reactions typical of the chemical epoxidation procedures. Different formulations of the immobilized lipase were tested in order to identify the optimal experimental conditions.

3.2 INTRODUCTION

About 50% of the lubricants sold and used in the world are dispersed into the environment. These products are mainly based on mineral oils of fossil origin that have poor biodegradability and relevant environmental impact (Almasi et al., 2021). The agroforestry and maritime sectors are today very interested in the use of bio-based lubricants from plant oil, possibly biodegradable, given the pressure that the European Union exerts in terms of environmental sustainability (Directorate-General for Environment). The research of agricultural machinery manufacturers in various countries is therefore focusing on new lubricants and production of hydraulic fluids derived from vegetable oils, which are biodegradable and have low toxicity. The global biolubricants market has already exceeded 2 billion dollars (2016) and significant growth is expected, thanks to the growing environmental awareness of consumers and the spread of stringent regulations on the subject. According to the MRFR (Market Research Future) analysis, the biolubricants market is expected to reach $3.98 billion by the end of 2025 with a robust compound annual growth rate of 7.1%. A significant role for the expansion of the market is played by the development of regulatory frameworks to support biolubricants, as happened in the US (NextChem-Ecosistemi Foundation).

Vegetable oils are not suitable for direct use whereas epoxidized vegetable oils are important building blocks for the preparation of chemical intermediates that are used as biolubricants (Panchal et al., 2017; Syahir et al., 2017). Companies such as Shell and British Petroleum already produce commercial biolubricants based on non-edible plant oils for the development of biodegradable railway track grease (Zainal et al., 2018).

3.2.1 Properties of biolubricants

Any material that reduces friction between two contacting surfaces can work as lubricant (Iqbal, 2014). Any material that derives from a bio-based raw material and has lubricant characteristics can be considered a bio-lubricant (Salimon et al., 2010). To be a good lubricant, a material should have high viscosity, high flash point, good corrosion resistance, low pour point, and high oxidation stability (Zainal et al., 2018).

Compared to petrol-based lubricants, vegetable oils possess excellent lubricant properties: their flash point is generally higher as is their viscosity index and lubricity, they have low evaporative loss and good metal adherence, they show low friction and wear characteristics, besides being biodegradable, renewable, and non-toxic for human health and environment (Ashraful et al., 2014; Panchal et al., 2017; Soni and Agarwal, 2014).

However, they have substandard thermo-oxidative and hydrolytic stability, low temperature characteristics, and, depending on the feedstock, they can be very expensive (Luna et al., 2011; Salimon et al., 2010; Zainal et al., 2018). Their low oxidative and hydrolytic stability leads to product polymerization and degradation, increasing the viscosity and thus negatively affecting product performance. Untreated oils composed of unsaturated fatty acids oxidize rapidly and turn thick due to polymerization processes (Salimon et al., 2010).

Moreover, vegetable oils tend to form macro-crystalline structures at low temperatures, due to uniform stacking of the “bend” triglycerides backbones (Erhan et al., 2006). These disadvantages can be overcome by chemical modifications, mainly on the reactive double bond (Salih et al., 2011) of the alkyl chains and the hydrogen on the β -CH- of the glycerol backbone (Syahir et al., 2017; Zainal et al., 2018).

Concerning viscosity, oils with alkyl chains ≥C18 possess better lubricant characteristics than short alkyl chains oils because the viscosity increases with the increasing of the chain length. Furthermore, viscosity is influenced by the presence of double bonds: one double bond increases the viscosity, while two or more double bonds decrease it (Knothe and Steidley, 2005). Nevertheless, a high number of long alkyl chains leads to poor low temperature characteristics, just as a high number of unsaturated alkyl chains leads to poor oxidation stability (Erhan et al., 2006; Fox and Stachowiak, 2007). Therefore, monounsaturated fatty acids, such as oleic and palmitoleic acids have a good balance between viscosity and oxidative stability (McNutt and He, 2016).

Commonly used oils are sunflower oil, especially high oleic sunflower oil that shows better oxidation stability, rapeseed oil, canola oil, soybean oil, palm oil, jatropha oil, and castor oil (the latter is the only source of C18:1-OH alkyl chains) (Zainal et al., 2018).

3.2.2 Chemical modifications of vegetable oils

Plant oils are prone to different chemical modifications such as transesterification, estolides formation, double bond hydrogenation and epoxidation, subsequent ring opening, and finally acylation of the resulting -OH groups (Pinto et al., 2013), (Salimon et al., 2012).

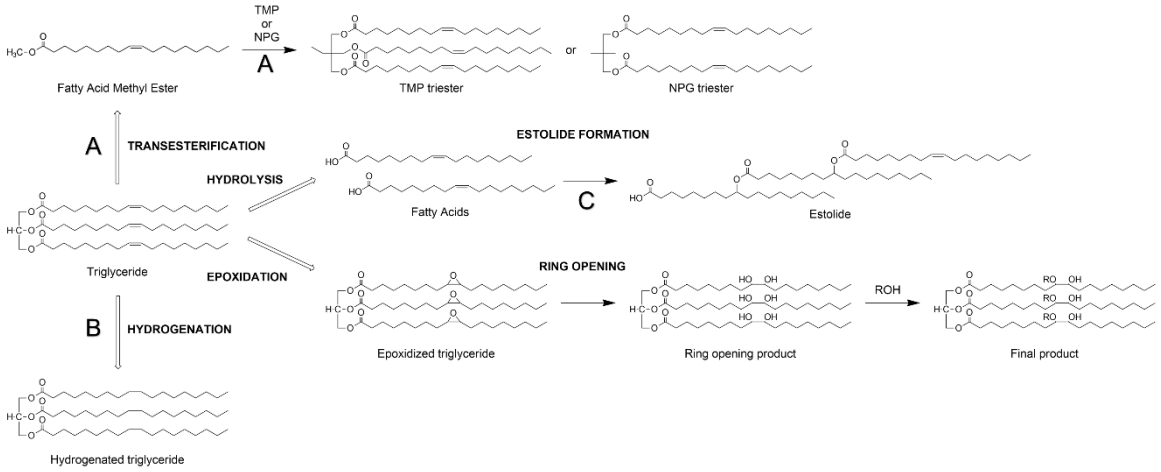

Figure 3.1 *Chemical modifications of triglycerides of vegetable oil.*

During transesterification (figure 3.1 route A) the glycerol backbone is replaced by polyols without β-hydrogens, such as neopentyl glycol (NPG) and trimethylolpropane (TMP). Esterifications include the transformation of fatty acids into esters with long-chain alcohols to obtain biolubricants (Salih et al., 2011). These reactions require mineral acids as catalysts (HCl, H_2SO_4, *p*-toluensulfonic acid) which have the disadvantage of being highly corrosive.

Alternatives are represented by ion-exchange resins or oxides such as Al_2O_3, ZrO_2, TiO_2, Nb_2O_5, Ta_2O_5, WO_3, and zeolites (Nor et al., 2020). The use of solid catalysts for esterification/transesterification processes gives advantages such as higher yields, lower temperature and shorter reaction times (Lye et al., 2020).

The other modifications of plant oils are the hydrogenation of multiple double bonds (figure 3.1, route B). This process is important in the oil and fat oleochemical industries due the possibilities of modifying physical characteristics and increasing oxidation stability (Wagner et al., 2001). Vegetable oils contain multiple unsaturated fatty acids, such as oleic, linoleic, and linolenic acids. In particular, the presence of linoleic and linolenic acids impairs stability even if they are present in very small quantities. By selective hydrogenation, the easily oxidizable compounds are transformed into more stable components and this process allows the use of these products as biolubricants (Ahmed et al., 2015). Industrial hydrogenation process used catalysts like nickel deposited on silica support (Jovanovic et al., 1998), copper (Ravasio et al., 2002), or copper chromite (Rieke et al., 1997). These types of catalysts require above 150°C reaction temperature and high hydrogen pressure.

The double bonds of unsaturated fatty acids can undergo an oligomerization reaction between two or more fatty acid molecules attached to the residual alkyls. Estolides are oligomers that are formed when one fatty acid links to the site of unsaturation of another fatty acid to form oligomeric esters (figure 3.1, route C). The secondary ester linkages formed are more stable toward hydrolysis than triacylglycerols and have better physical properties for use as food-grade biolubricants (Afifah et al., 2019). Oligomerization is performed using catalysts such as layered aluminosilicate or montmorillonite at 210-250°C (Biermann et al., 2011).

Epoxidation is an important method of modifying unsaturation at -C=C- bonds to obtain food-grade biolubricants with optimal pour point, high oxidative stability, higher adsorption to metal surfaces, higher viscosity, and better lubricity with high viscosity index (Abdullah et al., 2016). Epoxidation is performed using peroxy acids, dioxiranes, or peracids as peroxide sources. Solid catalysts are also used, such as acidic ion exchange resins or transition metal-based catalysts (TiO_2/SiO_2, $NbVO/SiO_2$, polyoxometalates, $sulfated/SnO_2$) (Somidi et al., 2014). The epoxidized oils products need to be modified to improve their physicochemical and lubrication properties via esterification reactions or by alkylation, acylation, acyloxylation, amino alkylation, co-oligomerization, hydro-aminomethylation, or hydroformylation.

3.2.3 Chemo-enzymatic epoxidation of vegetable oils

As described above, epoxidation improves the oxidative stability and lubricity of plant oils and their derivatives. Enzymatic epoxidation is a greener alternative to chemical epoxidation and can be used to overcome some disadvantages of the chemical process: low selectivity, formation of acidic by-products, low conversion yield, the use of unstable and explosive phenoxyacids, and the high temperatures of the processes.

In the enzymatic step, the formation of stable peroxy acids takes place in situ by means of the enzymatically catalyzed reaction of H_2O_2 with the carboxylic group of free fatty acids, allowing for a significant suppression of side reactions. Then, the in situ formed peroxy acids spontaneously react with the C=C yielding the epoxide. Lipases (triacylglycerol acyl hydrolases, EC 3.1.1.3) are the enzymes commonly used for catalysing the first step of the reaction (Aouf et al., 2014).

Lipases have a catalytic site with a His-Ser-Asp catalytic triad. The His accepts the Ser hydroxyl proton, which is then activated for the nucleophilic attack on the carbonyl group of the fatty acid substrate. A tetrahedral intermediate is formed, stabilized by interactions of the oxyanion hole, found in all lipases. In the presence of H_2O_2 a peroxyacid is finally released, and the enzyme can restart its catalytic cycle. The C=C bonds of triglycerides and fatty acids are then epoxidized by the peroxyacid through the Prilezhaev epoxidation mechanism for alkenes (figure 3.2) (Zainal et al., 2018).

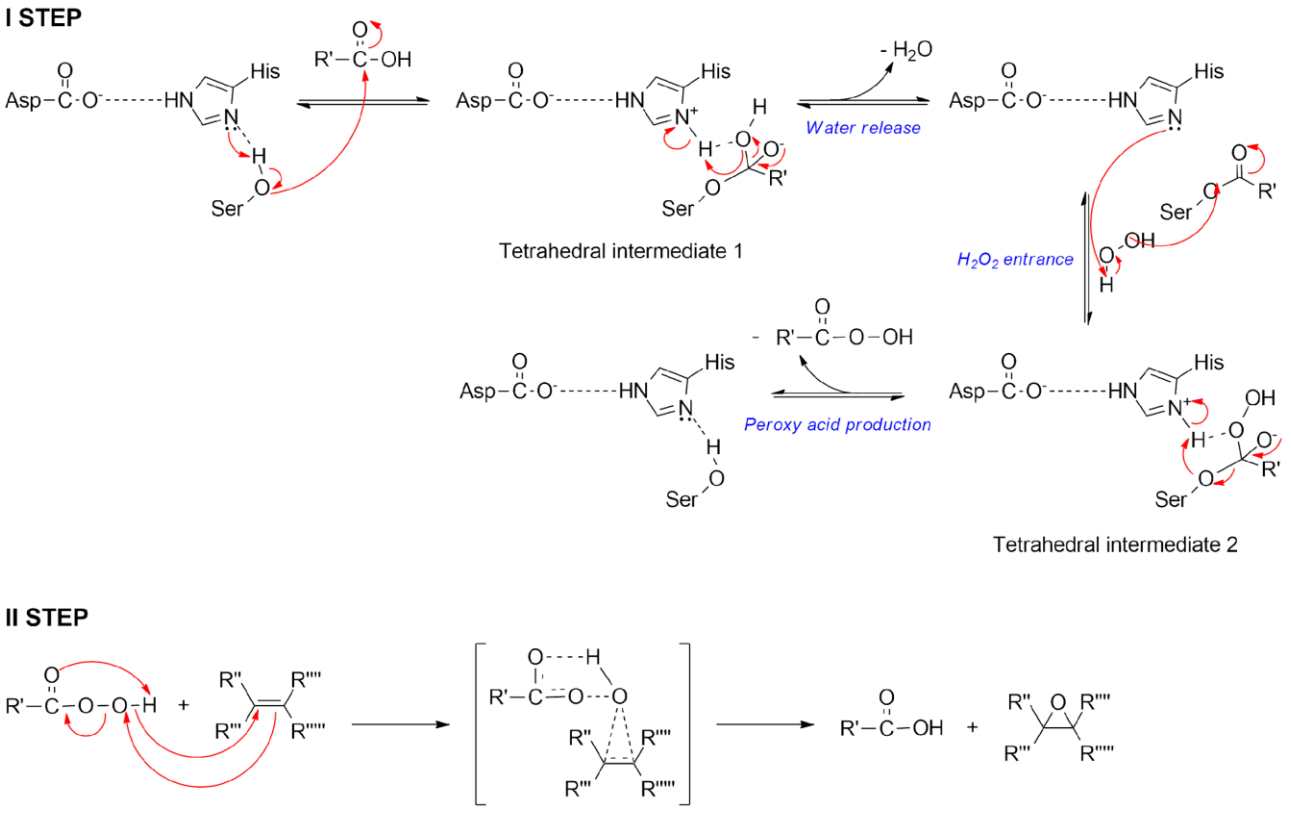

Figure 3.2 *Reaction mechanism of the enzymatic formation of peroxyacids and the subsequent epoxidation of the C=C bonds.*

The scientific literature reports various examples of epoxidation of soybean oil in the presence of hydrogen peroxide and oleic acid in toluene using as biocatalyst a commercially immobilized CaLB, named Novozyme 435. A 90% conversion of double bonds in oxirane rings was reached after 12 hours with at least 4.0% w/w catalyst, up to 25% mol oleic acid, and at least 1:1 molar ratio between double bonds and H_2O_2 (Vlček and Petrović, 2006). The ratio between the double bonds and the hydrogen peroxide molecules is the most critical parameter: in the enzymatic epoxidation of *Lallemantia iberica* seed oil a ratio

up to 1:2 was used, in the presence of 5mol% oleic acid to avoid epoxy mono and diglycerides formation (Aouf et al., 2014; Haitz et al., 2018). The higher the ratio, the faster the reaction, but the presence of the peroxide causes inactivation of the enzyme (Orellana-Coca et al., 2005).

Epoxidized jatropha oil and epoxidized soybean oil showed higher kinematic viscosity at 40°C but lower viscosity index and higher pour point, when compared with the non-epoxidized starting materials (Siniawski et al., 2011). Subsequent opening of the oxirane group, instead, leads to lubricants with ideal characteristics but with higher commercial price (Syahir et al., 2017). In fact, branching introduction increases the oxidation stability and decreases the pour point.

3.2.3.1 Cardoon seed oil

Cardoon (*Cynara cardunculus* L.) seed oil has been attracting an increasing interest in Italy for the bio-plastic industry (Torres et al., 2011). *Cynara cardunculus* fruits are cypselae, usually indicated as cardoon seeds (Gominho et al., 2018) that gives oil with yields in the range of 14.5-32.4% dry matter mass fraction, depending on the extraction method (Raccuia and Melilli, 2007). This oil has a fatty acid profile like sunflower oil, with 11% palmitic, 4% stearic, 25% oleic, and 60% linoleic fatty acids, making it similar to common sunflower oil (Fernández et al., 2006). Therefore, cardoon seed oil can be considered an interesting and sustainable alternative to this edible oil for biorefineries purposes. Study of the composition of cardoon seed oil was performed by the company that provided the cardoons (Dr. Ciancolini at Novamont S.P.A.) and the composition is reported in Table 3.1 below.

Table 3.1 Cardoon seed oil composition % w w^{-1}.

Cardoon seed oil	
Saturated (%)	14,98
Oleic acid (%)	22,72
Tot mufa (%)	22,99
Linoleic acid (%)	61,95
Tot pufa (%)	62,02

Palmitic and stearic acids are saturated, while oleic and linoleic are unsaturated ω9 and ω6 fatty acids, respectively. Previous studies reported the chemical epoxidation of cardoon seed oil using γ-alumina as heterogeneous solid catalyst in the presence of different solvents to obtain plasticizers used in biodegradable films made by poly(lactic acid) and thermoplastic starch (Tesser et al., 2020; Turco et al., 2019).

3.3 OBJECTIVES OF THE CHAPTER: VALORIZATION OF CARDOON SEED OIL THROUGH ENZYMATIC CATALYSIS

This chapter was focused on the valorization of Cardoon seed oil through enzymatic catalysis.

Firstly, cardoon seed oil was hydrolysed enzymatically. The aim was to obtain a complete hydrolysis of cardoon seed oil using mild reaction conditions. For this reason, a combination of native and immobilized lipases was tested. It was demonstrated that using Lipase B from *Candida antarctica* (CaLB) and Lipase from *Thermomyces lanuginosus* (TLL) a complete hydrolysis of cardoon seed oil was achieved. This reaction was scaled up to 2L of cardoon seed oil.

Secondly, a chemo-enzymatic epoxidation of unsaturated fatty acids was performed using immobilized lipases in a solvent-less process.

Epoxidized vegetable oils are important building blocks for the preparation of chemical intermediates for the synthesis of biolubricants and plasticizers. Epoxidation improves the oxidative stability and lubricity of plant oils and their derivatives. Enzymatic epoxidation is a greener alternative to chemical epoxidation and can be used to overcome some disadvantages of the chemical process: low selectivity, formation of acidic by-products, low conversion yield, the use of unstable and explosive phenoxyacids and the high temperatures of the processes.

The epoxidation of pure fatty acids was accomplished, and the conditions optimized.

The ^{1}H NMR and GC-MS characterization demonstrate the complete conversion of the unsaturated fatty acids into the respective epoxidized products. The process was developed in solvent-less conditions at mild temperatures using an immobilized enzyme which enable an easy work-up and isolated yields >98%.

The following step of the research was focused on the processing of the hydrolysed oil, but it is not included in the present thesis because of confidentiality reasons.

3.4 MATERIALS AND METHODS

Materials

Solvents, reagents, and standard solutions of bioactive molecules were purchased from Merck KGaA, Darmstadt (Germany) and used as received if not otherwise specified.

TLL Lipolase 100L #091MI832V was from Sigma-Aldrich, a solution with specific activity of 3176TBU/g.

For the epoxidation study three immobilized enzymes were used. CaLB adsorbed on octadodecyl methacrylic resins (Resindion, Binasco Italy) was from SPRIN Spa (specific activity of 414 TBU/g dry and 884 TBU/g dry, respectively). Novozyme 435 from Novozymes (DK) has a specific activity of 1998 U/g_{dry}, CaLB immobilized on rice husk has a specific activity of 150 U/g_{dry}, according to the tributyrin hydrolysis assay. Cardoon seed oil was kindly provided by Novamont (Novara, Italy).

3.4.1 Characterization of cardoon seed oil: ^{1}H and ^{13}C NMR analysis

20 mg sample were diluted in 700 µL $CDCl_3$. The NMR spectra were acquired at 25 °C by a Varian VNMRS 392 500 NMR spectrometer (11.74 T) operating at 500 MHz for proton and 125 MHz for carbon, using 256 scans for proton and 16000 scans for carbon, interleaved by 7.7 s for proton and 2.05 s for carbon, with 45° pulses, employing a spectral width of 8012.8 Hz for proton and 31250 Hz for carbon over 32 K complex points.

3.4.2 Hydrolysis of 200 mL of cardoon seed oil

200 mL of cardoon seed oil (161.63g) were placed in a 2 L glass beaker with 200 mL of 50 mM PBS buffer at pH 8.0. The ratio oil:buffer was 1:1 (v/v). The biphasic mixture was stirred at 200 rpm on a temperature controlled orbital shaker at 35°C for 10 min. Then 80 g of CaLB (Lipozyme CaLB Novozyme adsorbed on Sepabeads EC-OD/S, 884.40 TBU/g_{dry}) were added to the emulsion to start the reaction. The pH of the reaction was controlled constantly and eventually adjusted with NaOH 0.5 M. After 40 hours, further 40 g of immobilized CaLB were added. After 46 hours 10 mL of native TLL Lipolase 100L (Sigma #091MI832V, 3176 TBU/g wet) were added. The reaction was carried on for 72 hours until complete triglycerides hydrolysis.
Workup: HCl 2N was added to reach pH 1. The mixture was centrifuged for 10 mins at 24°C in a 50 mL plastic tubes. During centrifugation, a thin layer of coagulated native lipase (the enzyme was used protein formed at the interface oil/water and it was removed. The hydrophobic phase was recovered and kept at 4°C for two days to promote the separation of residual water. The solid mixture was then melted at 35°C and washed with 150 mL H_2O. The two phases were separated with the aid of a second centrifugation step. Some residual fatty acids were recovered by washing the immobilized enzyme with 150 mL n-hexane, filtering the solution and then removing the hexane on rotary evaporator.

After the workup 103.58 g of product were obtained and further 14.41 g of fatty acids were recovered from the washing of the immobilized enzyme. In total 117.99 g of product was recovered. The recovered yield was 73%.
TLC analysis (figure 3.3) shows the presence of pure fatty acids in both the product and the oil recovered from the enzyme rinsing.

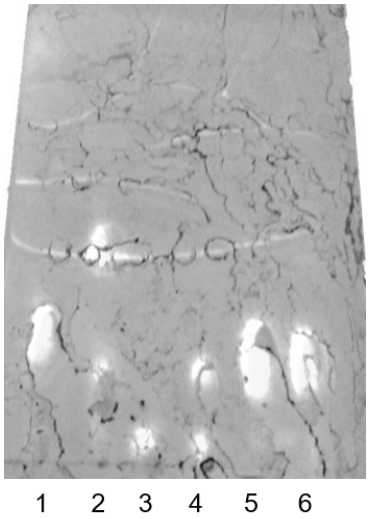

Figure 3.3 *TLC analysis scale-up reaction: 1- Standard Fatty Acid C=C (oleic acid), 2-Cardoon Seed Oil, 3-Buffer after reaction, 4- Washing solution (..), 5- Free Fatty Acids Product, 6- Oil recovered from enzyme wash*

3.4.3 Scale-up of hydrolysis starting from 2 L of cardoon seed oil

2 L of cardoon seed oil were placed in 5 L glass beakers with 2 L PBS buffer 50 mM (sodium-phosphate buffered saline) at pH 8.0. The ratio oil:buffer was 1:1. The liquid was mixed at 130 rpm an incubator at 35°C for 10 min. Then 40mL TLL Lipolase 100L (Sigma #091MI832V, 3176 TBU/g wet) and 600 g CaLB (Lipozyme CaLB Novozyme adsorbed on Sepabeads EC-OD/S, 884.40 TBU/g_{dry}) were added. The pH of the reaction was controlled constantly and eventually adjusted with NaOH 0.5 M. After 75 hours the reaction appeared incomplete from the TLC analysis and 400 g of CaLB and 40 mL of TLL were added to the reaction mixture. The reaction was carried out for 92 hours until complete triglycerides hydrolysis as indicated by the TLC reported in the figure below.
The workup procedure was similar to the one described in section 3.3.2, except the volumes of the water and solvent used in the washing steps, which were modified according to the scale of the reaction. At the end of the workup about 1400 mL of pure free fatty acids were obtained (yield ~ 70%)

3.4.4 TLC analysis

Mobile phase was 98:16 n-hexane: ethyl acetate. 1 µL sample was diluted in 19 µL mobile phase, then 0.5 µL were spotted on 20x20 cm silica gel TLC plate (Supelco). Plates were developed with a solution of potassium permanganate/ potassium hydroxide 1.25/0.5% w/w.

3.4.5 Characterization of hydrolysed cardoon seed oil using ^{1}H NMR

20 mg sample were diluted in 700 µL $CDCl_3$. ^{1}H NMR samples were collected on a Varian VNMRS 500 at 500 MHz.

3.4.6 Chemoenzymatic epoxidation of fatty acids

A certain amount of biocatalyst and fatty acids were mixed in a round flask of 25 mL for 15 minutes at 50°C. After this time, the required amount of H_2O_2 was added to the reaction into small aliquots. Since the oleic acid has a melting point of 16°C and the 9,10-epoxistearic acid (the product) of 60°C, the reactions were performed at 50°C in a water bath. The activities of the biocatalysts are: Novozyme 435 1998 U/g_{dry}, CaLB SOD 884.40 U/g_{dry}, and CaLB immobilized on rice husk 150 U/g_{dry}, according to the tributyrin hydrolysis assay. In the following table are reported the amounts used in each experiment.

The workup of the reaction was the same in all experiments: at the end of the reaction the product was extracted using dichloromethane (3 times x 20 mL DCM). Then, the organic phase was recovered and dried with sodium sulphate and the mixture was kept under stirring for 30 minutes. Sodium sulphate was filtered on a Buchner funnel with filter paper, and the DCM was evaporated with rotavapor, keeping the temperature below 40°C to avoid oxirane rings opening.

3.4.7 Characterization of epoxidized product using ^{1}H NMR and GC-MS analysis

The products of the reactions were characterized by ^{1}H NMR. The samples were prepared dissolving 10 mg of product into 700 µL of $CDCl_3$. Samples were analyzed on a Varian 400MHz.

The derivation of compounds was performed by using Bis(trimethylsilyl)trifluoroacetamide (BSTFA) according with protocols reported in literature (Todea et al., 2015).

The GC-MS samples were prepared by dissolving 1 mg of compound in 1 mL of toluene. GC-MS analysis was carried out in a Shimazu gas chromatograph. The gas chromatograph was equipped with a 30 m x 0.25 mm fused-silica capillary column (SLB5ms) coated with 0.25 µm film of poly(5% phenyl,95% dimethyl siloxane). The temperature was monitored from 100°C to 300°C.

3.5 RESULTS AND DISCUSSIONS

3.5.1 Characterization of cardoon seed oil

A detailed characterization of the cardoon seed oil was performed by NMR spectroscopy. ^{1}H and ^{13}C NMR analysis are widely used to characterize composition of natural oils because different "regions" of triglycerides, diglycerides, monoglycerides and fatty acids resonate at different frequencies. It is possible to distinguish five different characteristics "groups": the glycerol backbone, the carbonyl group, the aliphatic chain, the olefinic group, and the terminal methyl group (figure 3.4).

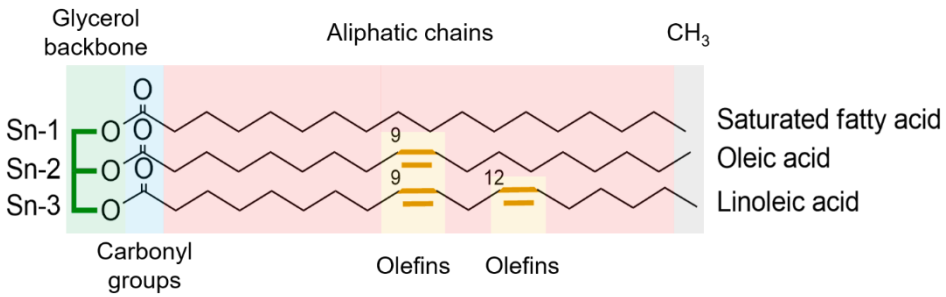

Figure 3.4 *Cardoon oil triglyceride structure (supposed). The glycerol backbone is highlighted in green, the carbonyl groups in blue, the aliphatic chains in pink, the olefins in orange and the terminal methyl group in grey.*

These groups have signals at very specific frequencies, making it possible to distinguish between mono-, di- and triglycerides and types of fatty acids. Table 3.2 shows the classical chemical shifts for ^{1}H NMR and ^{13}C NMR of natural oil lipidic components (Lopes et al., 2016).

Table 3.2 Values (ppm) of the different groups composing natural oil mono-, di-, triglycerides and fatty acids for ^{1}H NMR and ^{13}C NMR analysis, t=triplet, m= multiplet.

Signals	^{1}H NMR chemical shifts (ppm)	^{13}C NMR chemical shifts (ppm)
Glycerol backbone	3.65-5.27 (t)	60-80
Carbonyl group	/	172-174
Aliphatic chain	1.19-1.42 (m)	15-35
Olefins	5.28-5.46 (m)	125-135
Methyl group	0.88-0.97	14

From ^{1}H NMR analysis (figure 3.5) it was possible to deduce that the cardoon seed oil is mainly a triglycerides mixture, with a very low amount of mono- or diglycerides.

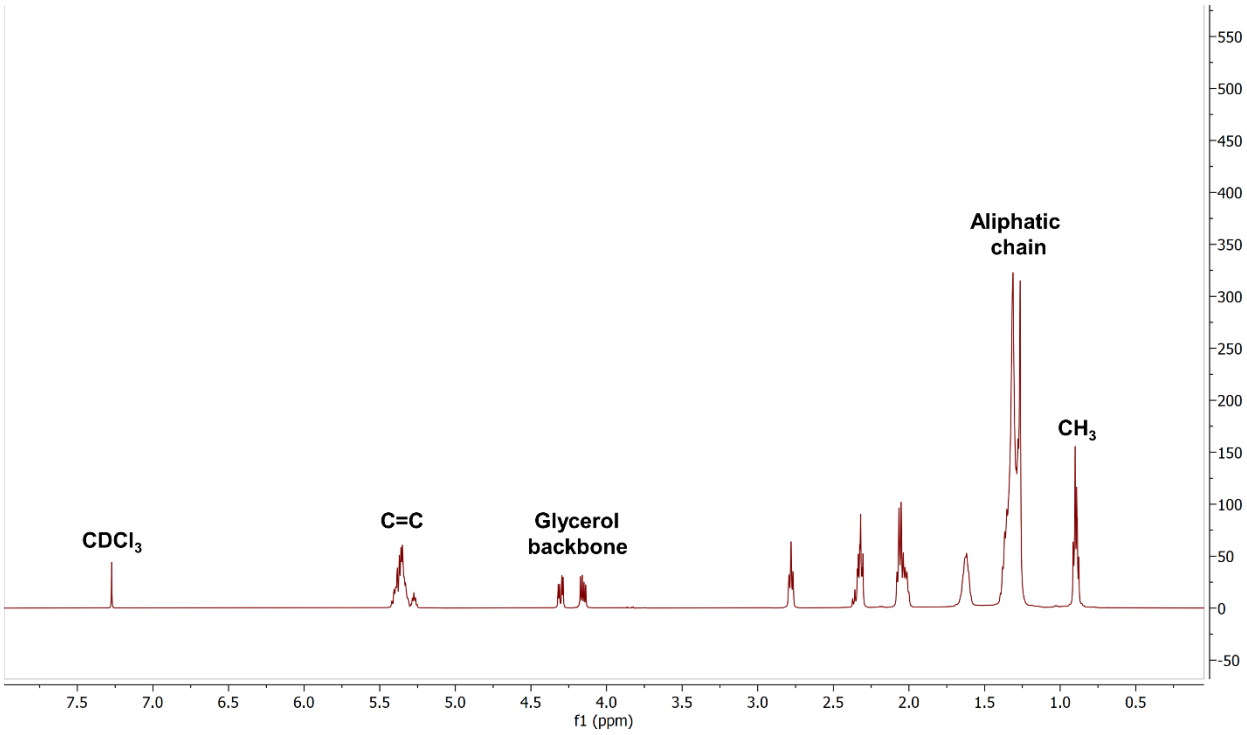

Figure 3.5 *^{1}H NMR analysis of cardoon seed oil. The detailed discussion is reported in the main text.*

Protons of the glycerol backbone resonate at 3.65-5.27 ppm whereas the signals at 4.30 ppm and 4.15 ppm are ascribable to the double doublets attributable to glycerol backbone protons in Sn-1 and Sn-3 position of triglycerides. Triglycerides glycerol backbone protons in Sn-2 position are visible as multiplets at 5.27 ppm. Signals at 3.81 ppm and 3.85 ppm indicate the presence of monoglycerides, even if in a small amount.

The signals of the terminal methyl group provide information on the unsaturation: saturated, ω-7 and ω-9 monounsaturated fatty acids at lower ppm, immediately followed by ω-6 polyunsaturated fatty acids, while ω-3 polyunsaturated fatty acids resonate at higher ppm. Presence of unsaturated fatty acids is confirmed by the signals of double bond protons visible as multiplets at 5.30-5.42 ppm. Polyunsaturated fatty acid (linoleic acid) presence is further confirmed by the signals at 2.75-2.80 ppm, caused by protons on the carbons between two of the double bonds. Monounsaturated fatty acid presence is confirmed by the signals at 2.00-2.10 ppm caused by protons on carbons adjacent to a single double bond. Fatty acids Cα and Cβ are visible at 2.75-2.8 ppm and 1.55-1.65 ppm, respectively. Aliphatic chains are visible in the range 1.25-1.39 ppm.

Figure 3.6 shows the COSY and TOCSY spectra of cardoon seed oil, displaying proton correlations in the molecules composing the mixture. Figure 3.7 reports the DOSY analysis and its Bayesian transformation (Hoeting et al., 2002), from which we can deduce that the mixture is composed mainly by one species or rather by different species with a highly similar structure.

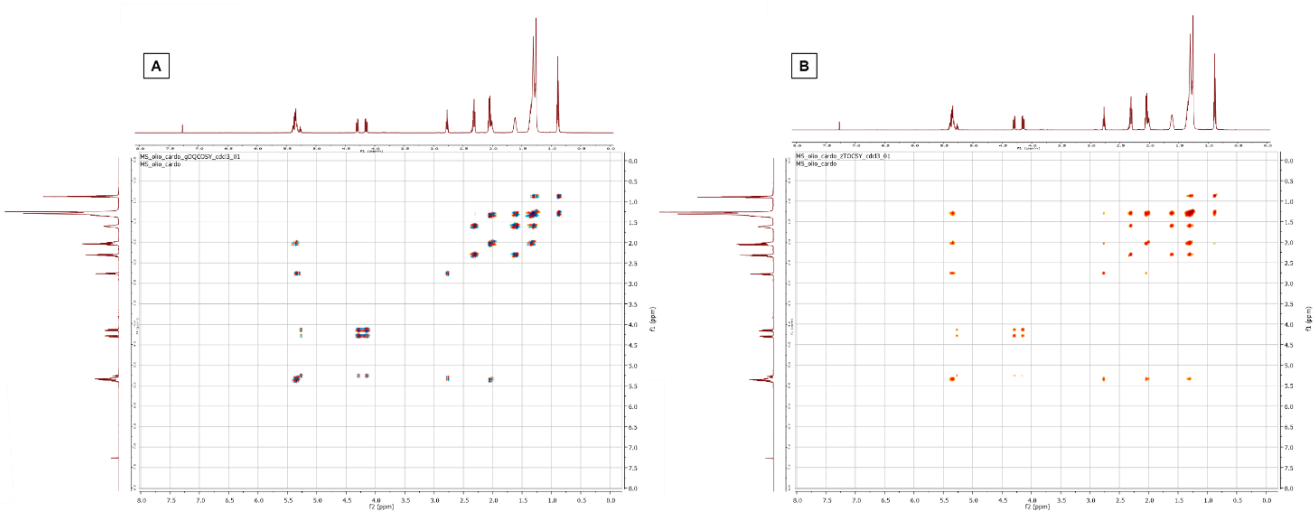

Figure 3.6 *COSY NMR(A) and TOCSY NMR (B) cardoon seed oil analysis that show proton correlations of the components in the mixture.*

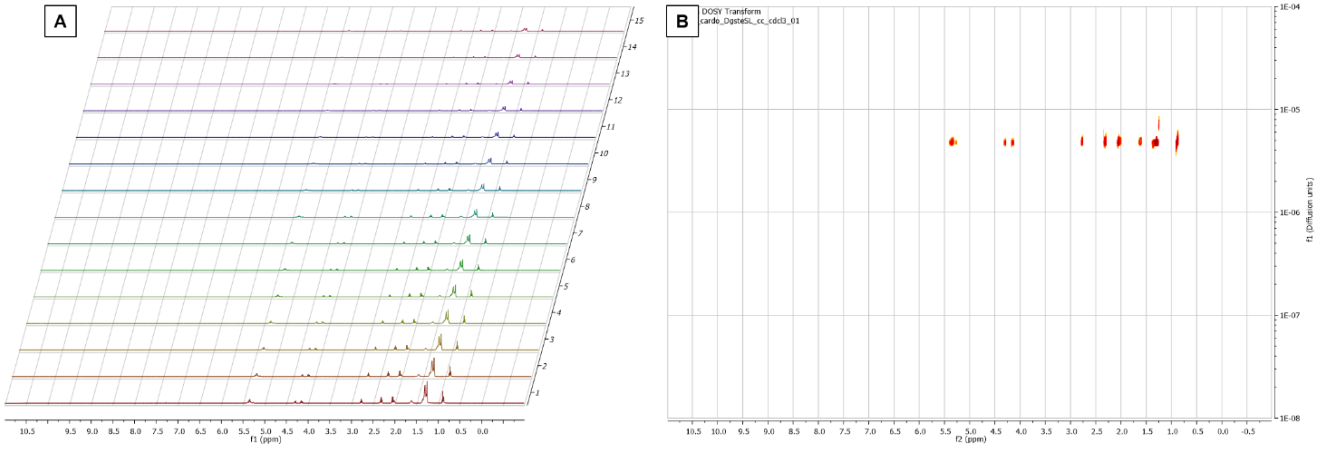

Figure 3.7 *DOSY NMR analysis of cardoon seed oil (A) and Bayesian DOSY transform (B). It is visible that mixture is composed by different species with a highly similar structure.*

The carbon of carbonyl ester group between fatty acids and glycerol backbone in mono-, di- and triglycerides are clearly visible in ^{13}C NMR spectra (figure 3.8) and resonate differently (Khallouki et al., 2008).

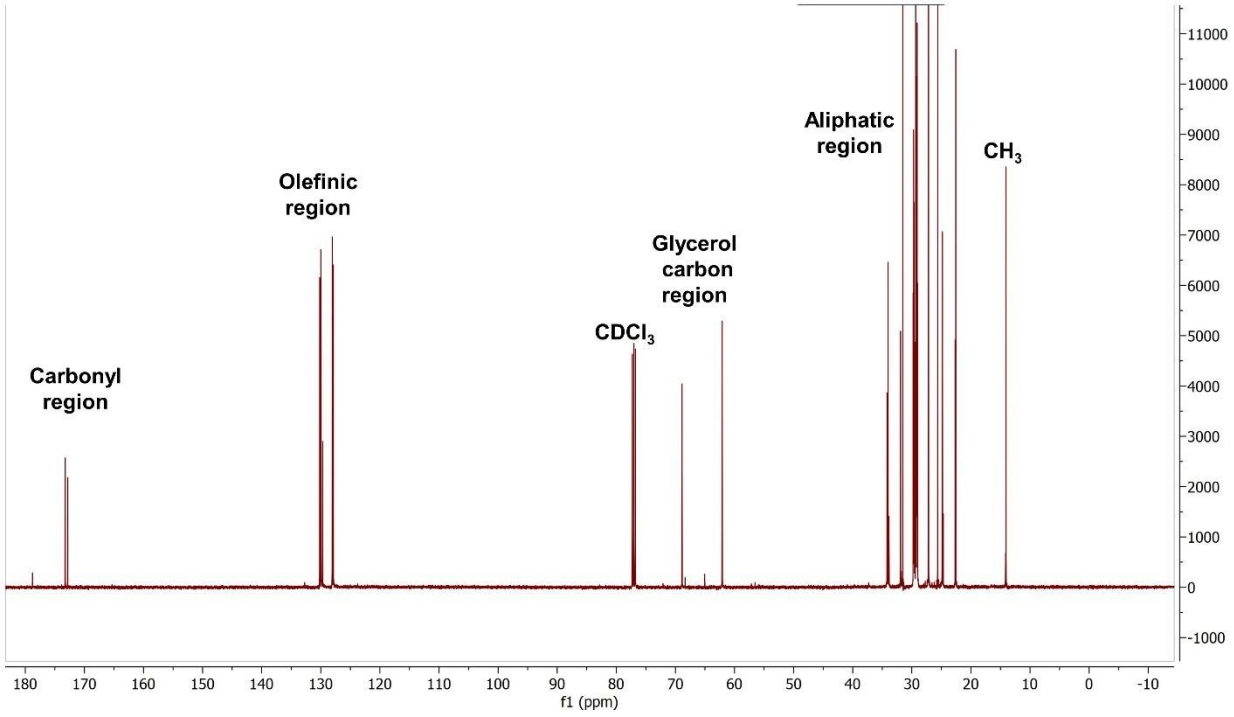

Figure 3.8 *^{13}C NMR analysis of cardoon seed oil.*

The range 22-35 ppm reports the signals of fatty acids aliphatic chains. The terminal methyl group is visible at 14 ppm. Glycerol carbon signals are visible in the range 62-77 ppm, in which the $DCCl_3$ signal falls. The presence of unsaturated fatty acids is confirmed by double bond signals in the olefinic region between 127 ppm and 131 ppm. The most important information about cardoon seed oil components regioselectivity was obtained by the carbonyl region (figure 3.9). In this region it is possible to distinguish between esters bonds found in Sn-1,3, and Sn-2 positions.

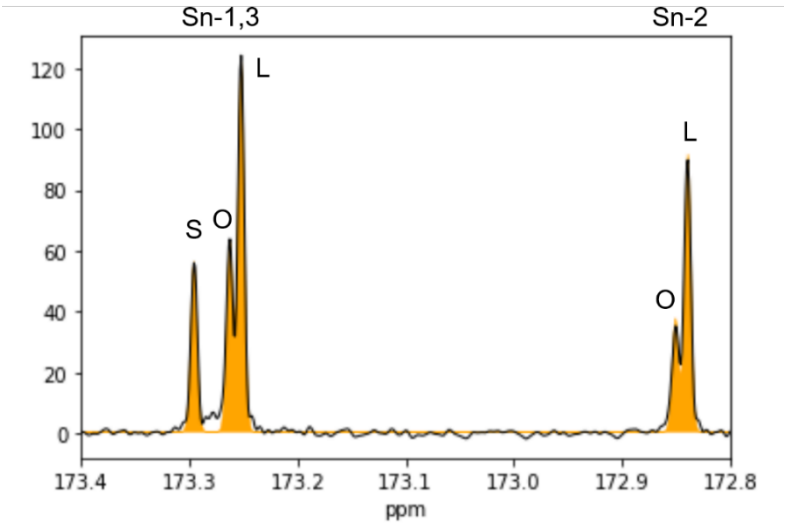

Figure 3.9 Carbonyl region of ^{13}C NMR cardoon seed oil analysis. S= saturated fatty acid, O= oleic acid, L= linoleic acid.

Carbonyls in Sn-1,3 positions resonate at higher ppm than those in Sn-2 position, typically separated by about 0.4 ppm (Khallouki et al., 2008). Saturated fatty acids resonate at higher ppm than monounsaturated, the last immediately followed by polyunsaturated fatty acids. In the cardoon oil ^{13}C NMR spectrum, the carbonyl signals of Sn-1,3 saturated fatty acids are visible at 173.30 ppm. The Sn-1,3 oleic acid signal is visible at 173.26 ppm whereas the Sn-1,3 linoleic acid appears at 173. 25 ppm. Finally, the Sn-2 oleic signals are at 172.85 ppm and the Sn-2 linoleic acid signals at 172.84 ppm. No presence of Sn-2 saturated fatty acids was detected, as expected from the literature (Shahunja et al., 2021).

Figure 3.9 shows the fit, marked in orange, with the sum of five gaussians with the function:

$$f = a \times exp\,(-(x - x0)^2/c^2$$

All signals were considered with the same width. Therefore, the area is proportional to the parameter *a*. Table 3.3 reports all *a* and area % values.

Table 3.3 Chemical shifts (ppm) of carbonyls in ^{13}C analysis of cardoon seed oil, with corresponding a parameters and area % values.

	Shift (ppm)	**a**	**Area %**
Sn-1,3 saturated acid	173.30	55.9	15
Sn-1,3 oleic acid	173.26	62.55	17
Sn-1,3 linoleic acid	173.25	121.56	33
Sn-2 oleic acid	172.85	37.25	10
Sn-2 linoleic acid	172.84	91.14	25

Saturated fatty acids (stearic, palmitic and a very small amount of eicosanoic acid) are present in Sn-1 and Sn-3 positions. However, it is possible to observe in the same positions unsaturated fatty acids (oleic, linoleic, and a very small amount of vaccenic acid). Cardoon seed oil has a high content of linoleic acid, followed by a high content of oleic acid. These are all found in Sn-1, Sn-2, and Sn-3 positions, it thus being impossible to identify a preferred position for linoleic and oleic acids.
From analysis of the olefinic region (figure 3.10A) it is possible to identify signals of double bonds, in the range of 127.8-128.1 ppm for polyunsaturated fatty acids, and 129.6-130.2 ppm for monounsaturated fatty acids. Signals of double bond carbons bonded to aliphatic chains in polyunsaturated fatty acids are visible in the same region of monounsaturated fatty acids double bonds.

Analysis of the glycerol carbons region (figure 3.10B) confirms predominance of triglycerides in the sample. Typically, Sn-2 and Sn-1,3 signals have a shift difference of about 7 ppm; in

our sample they are found at 62 ppm and 69 ppm respectively. Low signals at 65.1 ppm and 68.3 ppm indicate little 1,3-diacylglycerol presence. At 77.08 the $CDCl_3$ signal is visible.

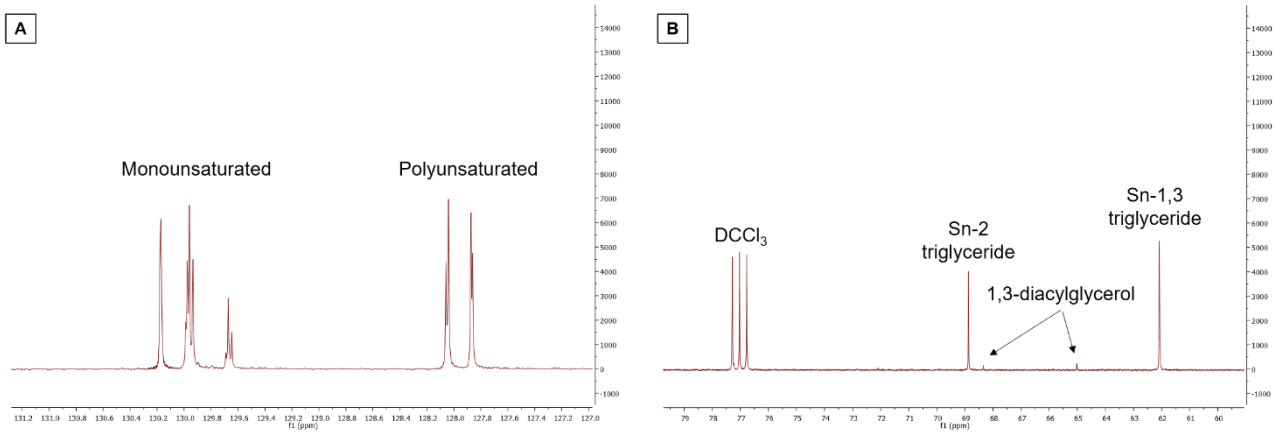

Figure 3.10 Olefinic (A) and glycerol carbon (B) regions of cardoon seed oil ^{13}C NMR analysis.

Figure 3.11 shows HSQC and HMBC spectra of cardoon seed oil, displaying proton-carbon correlations in the molecules composing the sample.

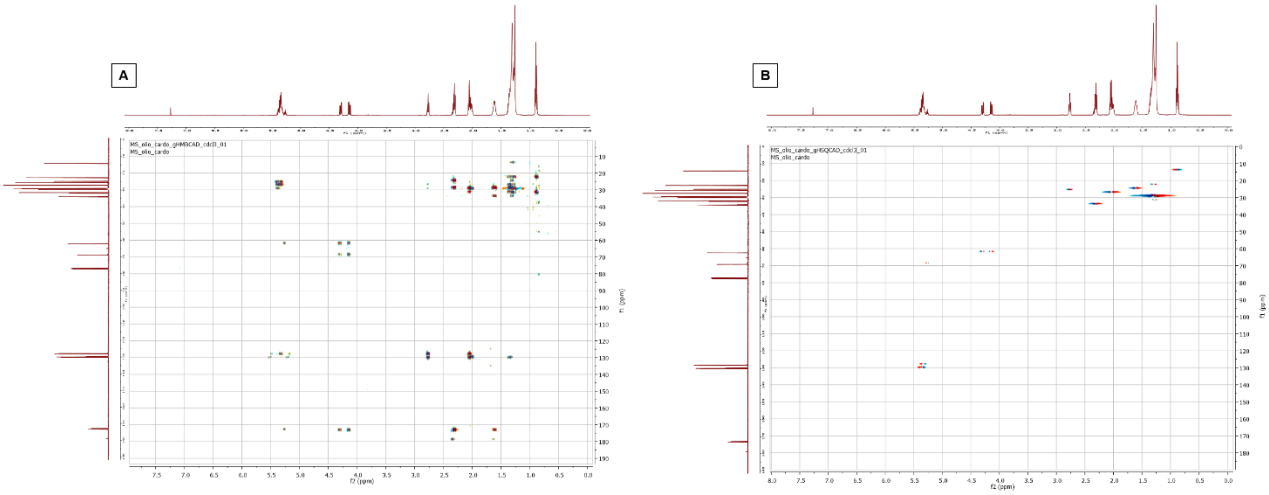

Figure 3.11 *HSQC and HMBC analysis of cardoon seed oil.*

Being the composition comparable to sunflower oil, we supposed also that the fatty acids distribution on the glycerol backbone might be similar. In sunflower oil, saturated fatty acids, such as palmitic or stearic acids, are mainly found in Sn-1,3 positions (16:0 Sn-1>Sn-3>>>Sn-2; 18:0 Sn-3>Sn-1>>>Sn-2), oleic acid is found mainly at the Sn-3 position (Sn-3>Sn-1,Sn-2), and linoleic acid is found in all positions with a preference for the Sn-2 position (Sn-2>Sn-1>Sn-3). It must be underlined that, since oleic and linoleic acids are the main components of sunflower oil and they seem not to have a marked regioselectivity, these two fatty acids are found in practically all positions (Shahunja et al., 2021).

3.5.2 Enzymatic hydrolysis of cardoon seed oil

Cardoon seed oil was hydrolysed using lipases (EC 3.1.1.3, triacylglycerol hydrolases), able to catalyse the hydrolysis leading to glycerol and free fatty acids (figure 3.12). Different formulations of lipases from *Thermomyces lanuginosus* (TLL) and *Candida antarctica* (CaLB) were selected. While CaLB has regioselectivity for the *sn*-1,3 positions, TLL is non regioselective (Cao et al., 1996). Therefore, the combination of these two enzymes allowed complete cardoon oil hydrolysis with no unreacted mono-, di- or triglycerides.

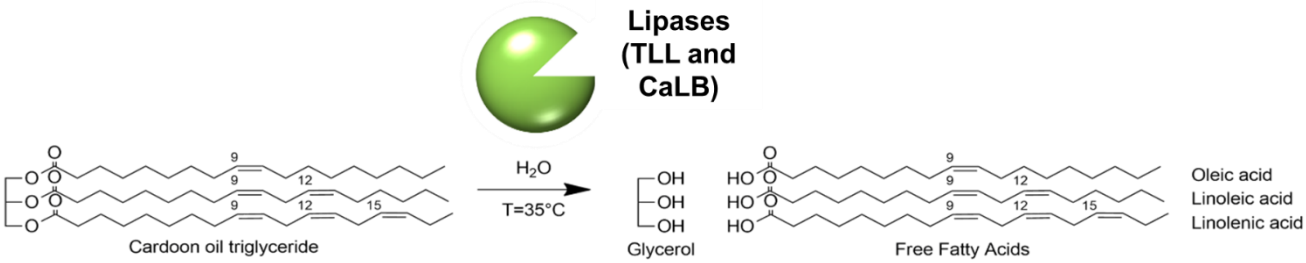

Figure 3.12 *Reaction scheme of lipases triglyceride hydrolysis into Free Fatty Acids and glycerol pH 8.*

The reaction was carried out on the scale of 200mL and 2L of oil. From the reaction on 2L scale 1400 mL of pure free fatty acids were obtained (recovered yield ~ 70%).

Samples were analysed via ^{1}H-NMR to verify the absence of glycerol and ester bonds in the final product. All the products from the two different experiments showed no signals attributable to glycerol, mono- di- or triglycerides and ester bonds, confirming complete hydrolysis. Figure 3.13 shows the spectrum of the 2L scale experiment, highlighting the absence of the glyceride backbone and the presence of the intact double bonds in the unsaturated fatty acids.

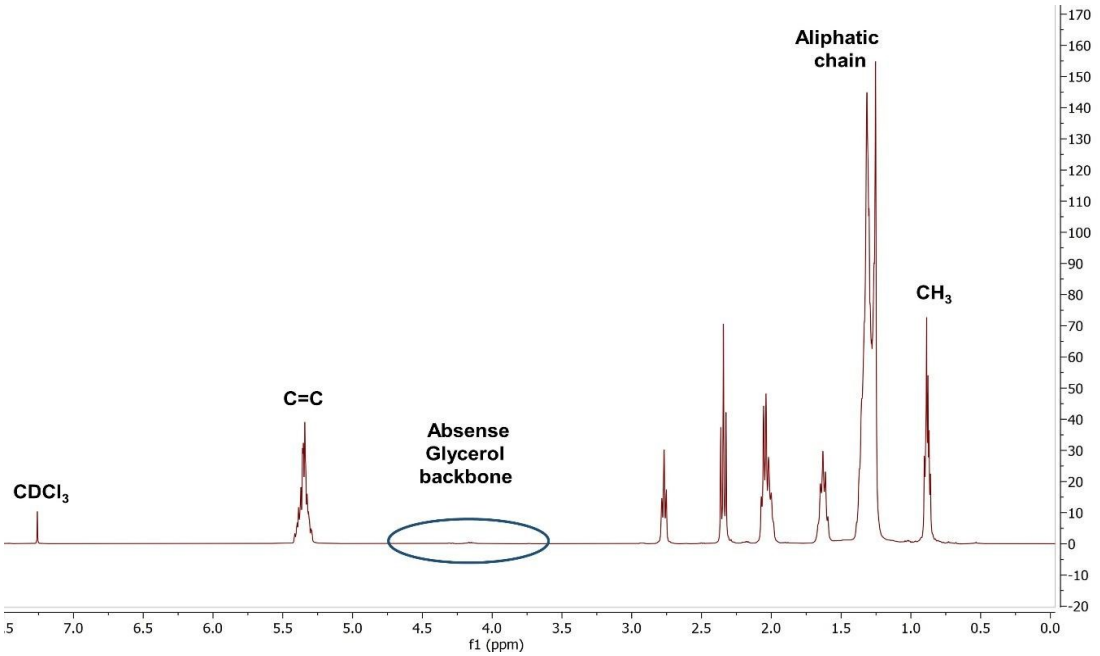

Figure 3.13 *^{1}H-NMR (500 MHz) of final hydrolysed product obtained from the reaction on 2L scale.*

Figure 3.14 shows the superimposition of the products obtained from the reactions on 200 mL and 2L, which were compared to the spectrum of the pure cardoon seed oil, confirming the same free fatty acids composition and glycerol absence in both samples.

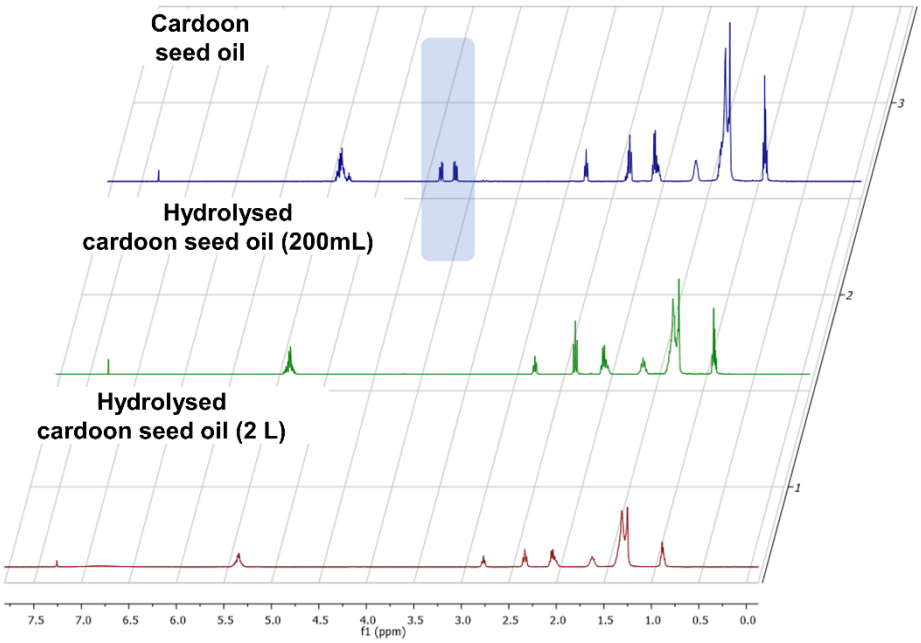

Figure 3.14 *Superimposition and comparison of ^{1}H-NMR spectra from pure cardoon oil (blue) to hydrolysis on 200 mL (green) and on 2L (red)- Triglycerides glycerol backbone signals are highlighted in light blue.*

The ^{1}H-NMR analysis confirms complete cardoon oil hydrolysis. In the region between 3 and 5.20 ppm all the signals related to glycerol backbones are absent. In fact, the glycerol backbone of triglycerides would resonate at 4.45,4.20 ppm for C1 and C3, and 5.15 ppm for C2. Similarly, diglycerides would give signals at 4.45, 4.20 ppm, and 4.64ppm, and 3.90, 3.65 ppm for C1, C2 and C3, respectively, with an additional singlet at 3.65 ppm for the OH, if the hydrolysis had happened in Sn-2 or Sn-3 positions. In the case of hydrolysis at Sn-2 position, the diglycerides signals should be found at 4.36, 4.11 ppm for C1 and C3, and 4.41 ppm for C2, with -OH singlet at 3.58 ppm. Monoglycerides, signals would be 4.36, 4.11 ppm for C1, 3.90 ppm for C2 and 3.81, 3.56 ppm for C3, with two OH singlets at 3.58 ppm and 3.65 ppm, in the case of fatty acids bound to position 1 or 3, or 3.59 ppm for C1 and C3, and 4.13 ppm for C2, with two -OH singlets at 3.65 ppm, in case of fatty acids bound to position 2. Presence of glycerol in the sample would be visible with signals at 3.50 ppm for C1 and C3, and 3.39 ppm for C2, with -OH singlets at 3.65 ppm for position 1 and 3 and 3.58 ppm for position 2.

In the range 5.25-5.44 ppm the signals of double bonds in oleic, linoleic, and linolenic acids are clearly visible, confirming that the protocol did not affect the double bond. The triplet of the carbon atom vicinal to Cα can be seen at 2.30 ppm. The multiplet related to the carbon vicinal to the 9,10 C=C, expected at is not visible, that should be present at 2.18 ppm, is not

visible, while the signals of the carbons in between 9,10 C=C and 12,13 C=C, or 12,13 C=C and 15,16 C=C are present at 2.63 ppm.

The multiplet at 2.0 ppm is related to the carbon atom near the terminal methylene of linolenic acid, whereas the methylene signals of oleic and linoleic acids are visible at 0.88 ppm and 0.90 ppm. The methylene signal of linolenic acid is covered by the signals of the aliphatic chains of oleic, linoleic, and linolenic acids.

The signal around 1.6 ppm was not assigned. In fact, free fatty acids have a multiplet at 1.52 ppm, while fatty acids bound to glycerol have multiplet at 1.64 ppm. Given the absence of other glycerol backbone signals, it is possible that this peak value is caused by a small shift in the ^{1}H NMR spectrum.

3.5.3 Chemoenzymatic epoxidation of unsaturated fatty acids in solvent-less conditions

The chemo-enzymatic epoxidation was initially performed for pure unsaturated fatty acids in order to acquire information necessary to optimize the reaction conditions for the epoxidation of the fatty acid mixture obtained from the hydrolysis of the cardoon seed oil.

Table 3.4 reports experimental conditions and results obtained in the epoxidation of all the fatty acids. The reactions were performed on a 2 g scale of fatty acids at 50°C by changing biocatalysts Novozyme 435, CaLB SOD and CaLB covalently immobilized on rice husk, and their amount (from 225 to 450 U g^{-1}), and the time of reactions (from 2 to 3 hours) in order to obtain the complete conversion of -CH=CH-group of fatty acids into epoxy products. The conversions were calculated by ^{1}H NMR. The products were also characterized by GC-MS. More details are reported below.

Table 3.4 Experimental conditions for the epoxidation of pure oleic, linoleic, and linolenic fatty acids. Reactions were performed on 2g scale at 50°C.

Exp	Substrate	Biocatalyst	Amount of enzyme ($U/g_{substrate}$)	Molar ratio between -CH=CH- group and H_2O_2	Reaction time (h)	Conversion* (%)
1	Oleic acid	Novozyme 435	225	1:2	2	Complete (99)
2	Oleic acid	Novozyme 435	225	1:2	3	Complete (99)
3	Oleic acid	CaLB SOD	225	1:2	2	26
4	Oleic acid	CaLB SOD	225	1:2	3	23
5	Oleic acid	CaLB-RH	225	1:2	2	19
6	Oleic acid	CaLB-RH	225	1:2	3	26

7	Linoleic acid	Novozyme 435	225	1:2	2	96
8	Linoleic acid	Novozyme 435	450	1:2	2	95
9	Linolenic acid	Novozyme 435	450	1:2	3	98

*Determined by ^{1}H NMR

Exp 1-6 H_2O_2 was added in 5 aliquots every 15 minutes.

Exp 7.9 H_2O_2 was added in 10 aliquots every 10 minutes.

Executing the reaction in a short time frame is crucial in order to avoid the spontaneous opening of the epoxy rings and the deactivation of the enzyme exposed to hydrogen peroxide. In that respect, the higher specific activity of Novozymes 435 might be an advantage since the carrier accommodates a much larger amount of protein in a smaller volume and it looks like this factor is beneficial for the preservation of the enzyme activity. Based on the results obtained within oleic acid epoxidation only the Novozymes 435 was employed in the epoxidation of linoleic and linolenic acids.

The epoxidation of the fatty acids was monitored by ^{1}H NMR analysis, following the appearance of a multiplet at 2.90 ppm, generated by the oxiranic protons of the produced epoxy-product, and the disappearance of the multiplet at 5.34 ppm related to the - protons correspondent to the double bond of the fatty acids.

The following equation was used to calculate the conversion into the product:

$$\%\ conversion\ of\ 9{,}10-epoxistearic\ acid = \frac{I_b}{I_a + I_b} \times 100$$

I_a = integration value of the signals of the protons correspondent to the double-bond

I_b = integration value of the signals protons correspondent to the group

3.5.3.1 Epoxidation of oleic acid in solvent-less system

Figure 3.15 shows the ^{1}H NMR spectrum of the 9,10-epoxistearic acid obtained by the chemo-enzymatic epoxidation of oleic acid after 2 hours reaction time, where the complete disappearance of protons correspondent to the double bond and the presence of the multiplet correspondent to the protons of the oxirane group can be observed. The complete conversion of oleic acid in the reaction conditions shown in exp1 table 3.4 was also confirmed by the GC-MS analysis (figure 3.16).

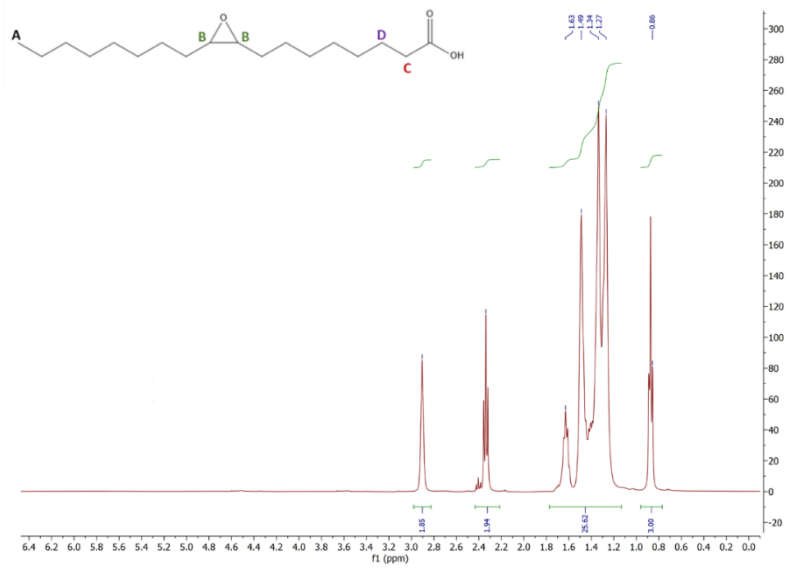

Figure 3.15 *^{1}H NMR spectrum of the product of the epoxidation reaction of oleic acid catalysed by Novozyme 435 in 2h. δ=0.89 ppm, -CH_3 (A); δ=1.36ppm -CH_2- of chain, δ=1.63ppm -CH_2- (D); δ:2,64ppm -CH_2- (C); δ:2.90ppm -CH- (D).*

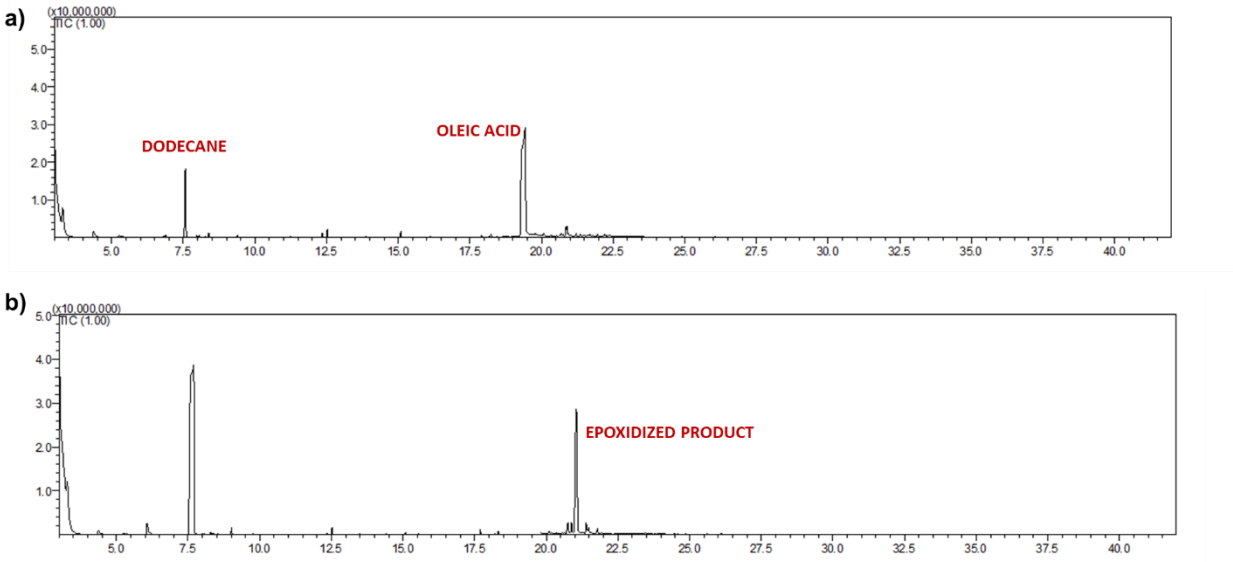

Figure 3.16 *GC-MS chromatograms of a) oleic acid b) reaction mixture after 2 h in which is evident the complete conversion into epoxy product (9,10-epoxistearic acid).*

Figure 3.17 shows ^{1}H NMR spectra of the products resulting from epoxidation of oleic by using CaLB SOD. It's evident that there is the presence of a double bond at 5.4ppm and the signals of oxiranic protons at 2.90 ppm is slightly visible with a conversion of 26% after 2 (figure 3.17a)hours and 23% after 3 hours (figure 3.17b).

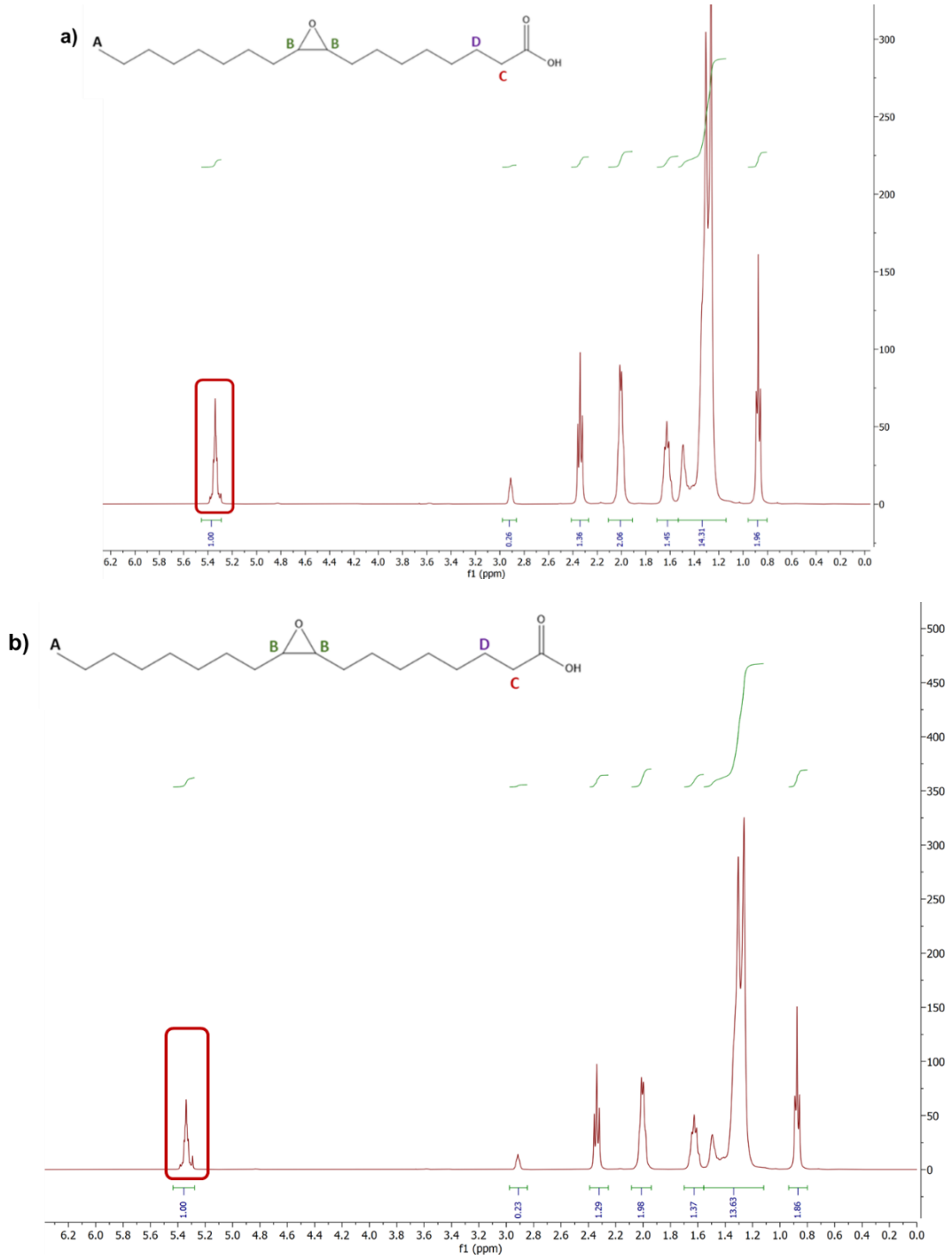

Figure 3.17 *^{1}H NMR spectra of the reaction mixtures of the epoxidation of oleic acid with CaLB SOD a) after 2 h; b) after 3h. The multiplet at 5.34 ppm related to the protons corresponding to the double bond is still visible whereas the signal at 2.90 ppm (oxiranic protons) is slightly visible.*

These results were also corroborated by GC-MS analysis reported in figure 3.18. It is possible to see that in the reaction mixture there is the presence of a signal of oleic acid as well as the signals of the epoxidized product.

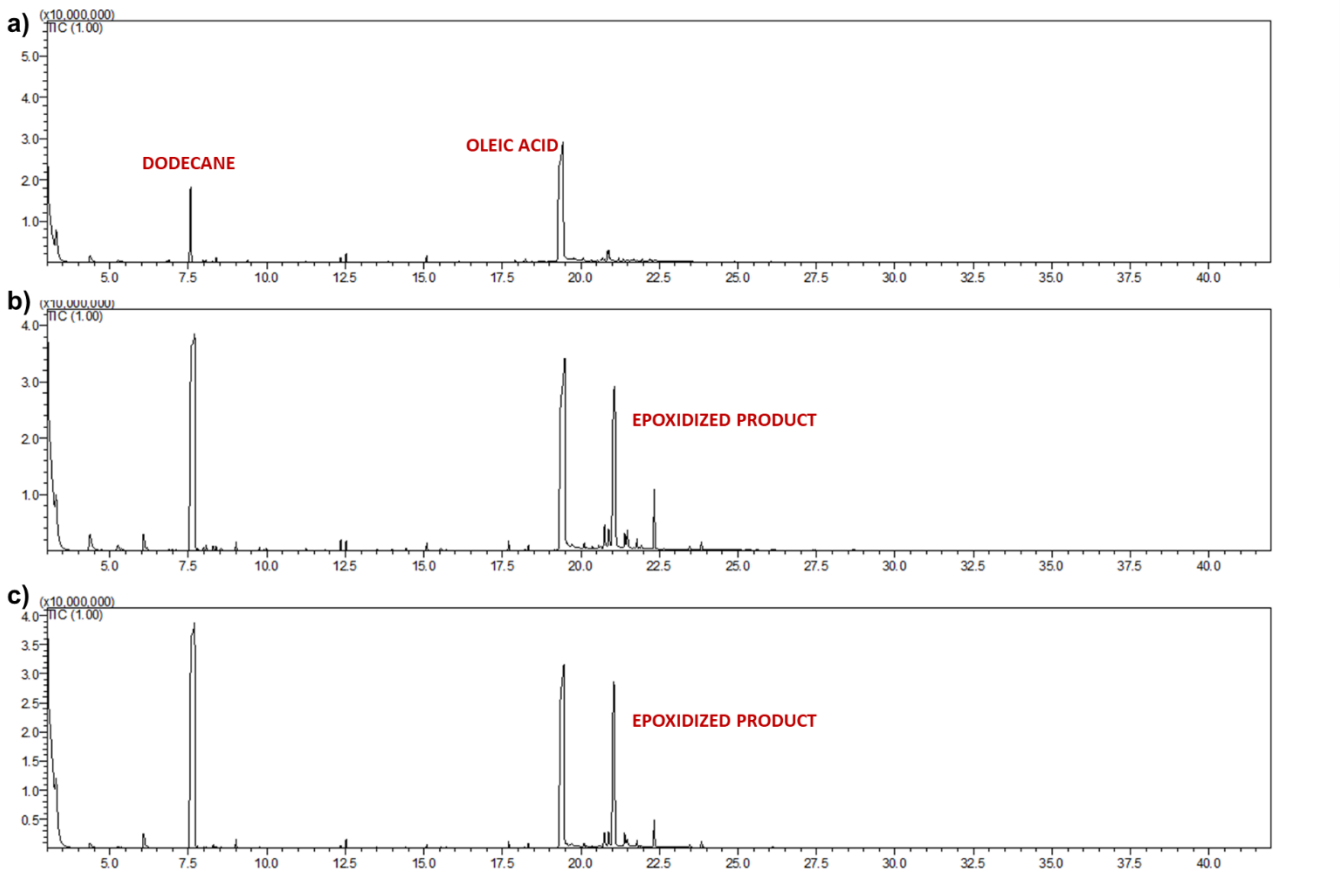

Figure 3.18 *GC-MS chromatograms of a) oleic acid; b) reaction mixture after 2 h; c) reaction mixture after 3 h. The reaction conditions are reported in table 3.4 (exp3-4).*

Figure 3.19 shows the ^{1}H NMR spectra of epoxidation of oleic acid in 2 and 3 hours using, as the biocatalyst, CaLB covalently immobilized on rice husk.

Using this biocatalyst, it is also evident by NMR that there is the presence of a double bond at 5.4ppm and the signals of oxiranic protons at 2.90 ppm is slightly visible with a conversion of 19% after 2 hours (figure 3.19a) and 26% after 3 hours (figure 3.19b). These results were also confirmed by GC-MS analysis in which is possible to see the presence of oleic acid in both reaction mixtures (figure 3.20).

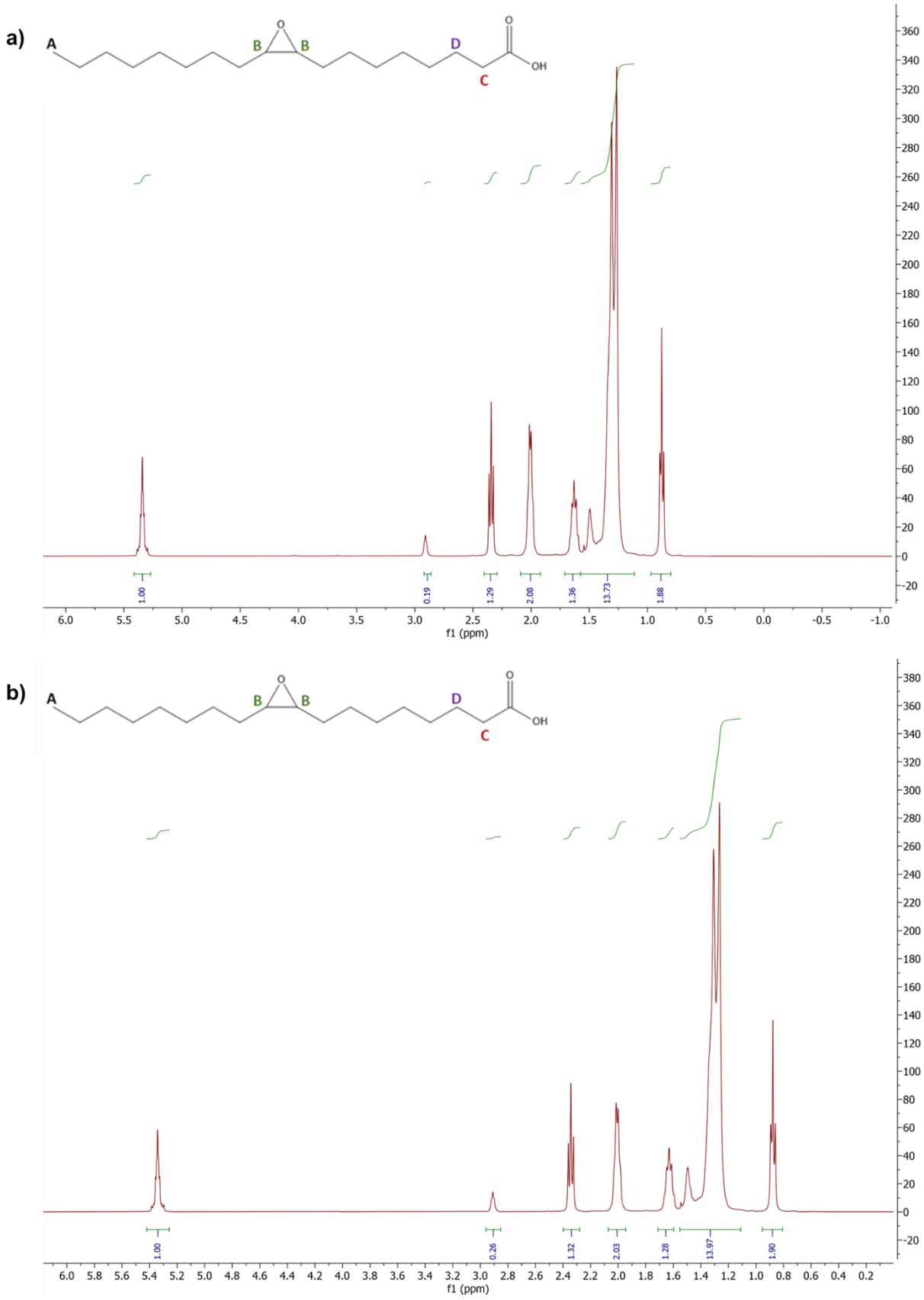

Figure 3.19 *^{1}H NMR spectra of the reaction mixtures of the epoxidation of oleic acid with CaLB immobilized on rice husk: a) after 2 h; b) after 3h. The multiplet at 5.34 ppm related to the protons corresponding to the double bond is still visible whereas the signal at 2.90 ppm (oxiranic protons) is slightly visible.*

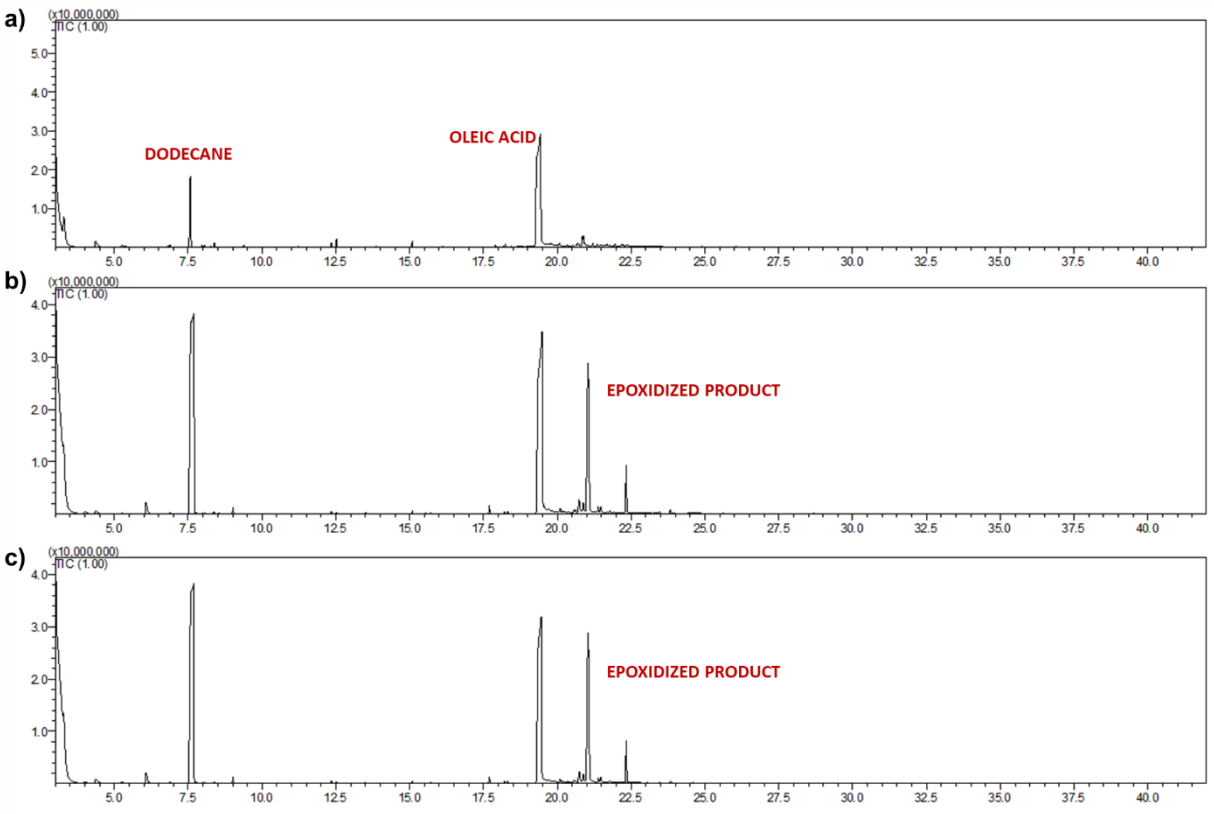

Figure 3.20 GC-MS chromatogram of a) oleci acid, b) reaction mixture after 2 h; c) reaction mixture after 3 h. The reaction conditions are reported in table 3.4 (exp5-6).

It is evident that the two formulations CaLB SOD and CaLB-RH (Table 2.4 entry 3-6) underwent inactivation during the reaction since the conversion value did not increase after 2 hours. The reason might be ascribed to the different porosity or chemical nature of the carriers, which might have different affinity of the H_2O_2. The commercial Novozyme 435 was the most effective biocatalyst, leading to quantitative conversions.

3.5.3.2 Epoxidation of linoleic acid in solvent-less condition

Linoleic acid presents 2 *cis* double bonds in the positions 9 and 12. For the epoxidation of linoleic acid, two experimental protocols were tested: in the first experiment a total amount of 225 $U/g_{substrate}$ of enzyme was added; while in the second one the enzymatic units were doubled to 450 $U//g_{substrate}$. The molar ratio between the double bonds and H_2O_2 was kept at 1:2 as for the oleic acid epoxidation, and the reaction time was fixed at 2 hours.

Figure 3.21 shows the ^{1}H-NMR spectrum of the epoxidation product obtained by using 225 $U/g_{substrate}$ of biocatalyst. It was possible to identify the signals corresponding to the mono epoxidized product (named “b” in the figure) and of the di-epoxidized product (named “c” in the figure). A small amount of unsaturated compound (4%) was present and final conversion at 2 hours was 96%. The isolated yield was 98%$_{w/w}$.

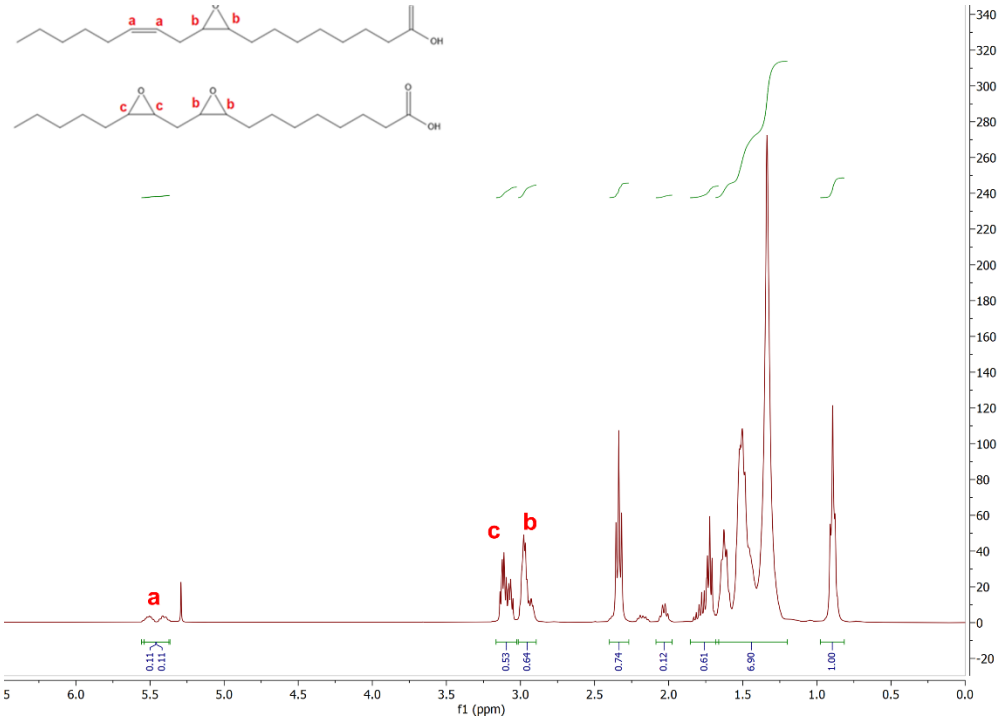

Figure 3.21 *^{1}H NMR spectrum of the reaction mixture of the epoxidation of linoleic acid after 2 h (225 U/g$_{substrate}$).*

Since it was crucial to accelerate the epoxidation reaction and to minimize the competing spontaneous opening of the epoxy ring after formation, a second reaction was performed using 450 U/g$_{substrate}$. In this case, the signal of the protons corresponding to the double bond of the linoleic acid is not visible after 2 hours of reaction, indicating complete conversion. The isolated yield was 95%$_{w/w}$ (figure 3.22). This result was also confirmed by GC-MS analysis (figure 3.23).

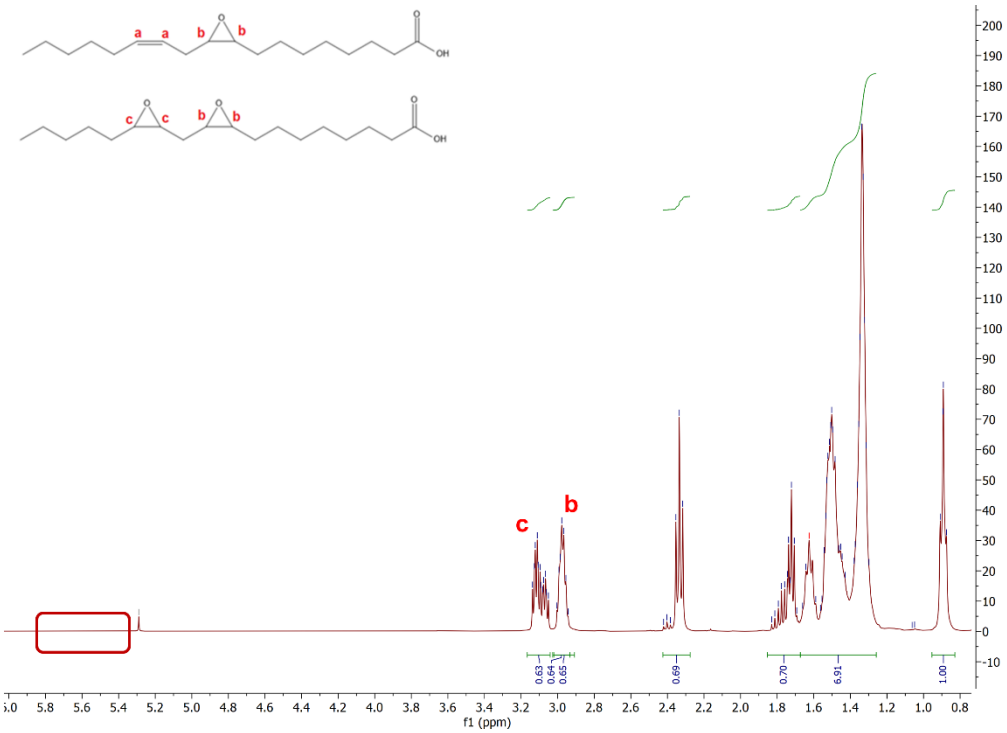

Figure 3.22 *^{1}H NMR spectrum of the product obtained after 2 h of epoxidation of linoleic acid catalysed by 450 U/g$_{substrate}$ of lipase.*

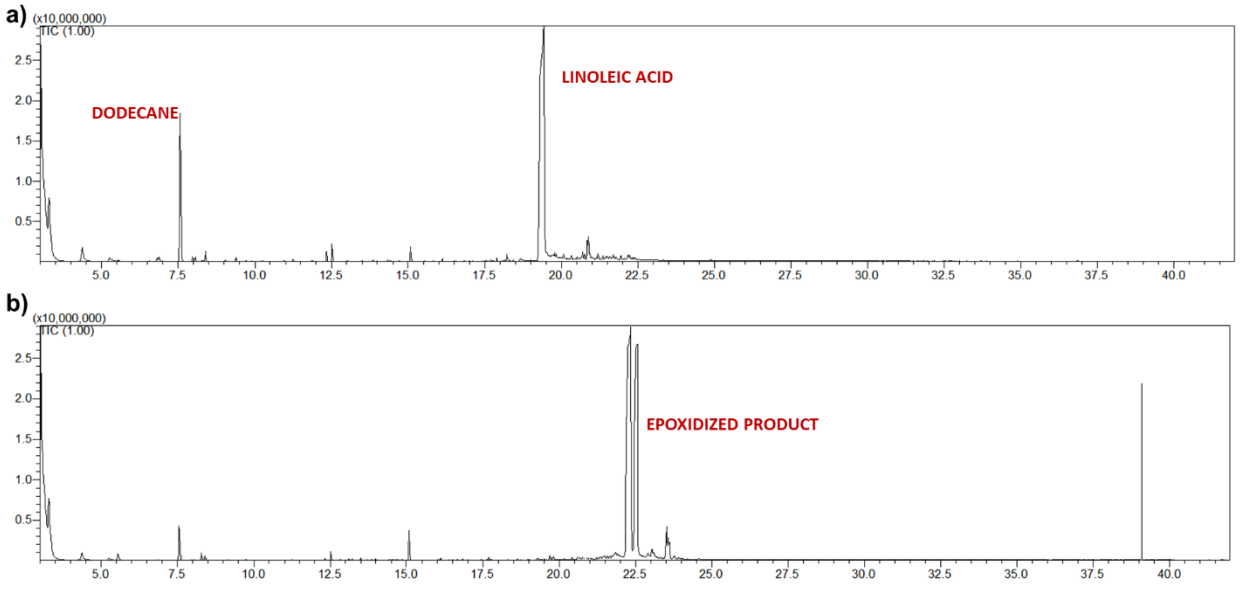

Figure 3.23 *GC-MS chromatogram of a) linoleic acid, b) reaction mixture after 3 h. The reaction conditions are reported in table 3.4 (exp8).*

3.5.3.3 Epoxidation of linolenic acid in solvent-less condition

The experimental protocol for the epoxidation of the linolenic acid was carried out using 450 $U/g_{substrate}$ of Novozyme 435) and a 1:2 molar ratio between the unsaturated groups and H_2O_2. The reaction time was extended to 3 hours due to the presence of three C=C groups.

Figure 3.24 shows the ^1H NMR spectra of the reaction product. As can be seen in figure mm, the signals of the protons corresponding to the double bonds are not present, while it was possible to identify the signals belonging to epoxidized linoleic acids. From these two data, it can be concluded that in the final mixture only the tri-epoxidized product is present. The isolated yield was 98%$_{w/w}$. This result was confirmed also by GC-MS in figure 3.25.

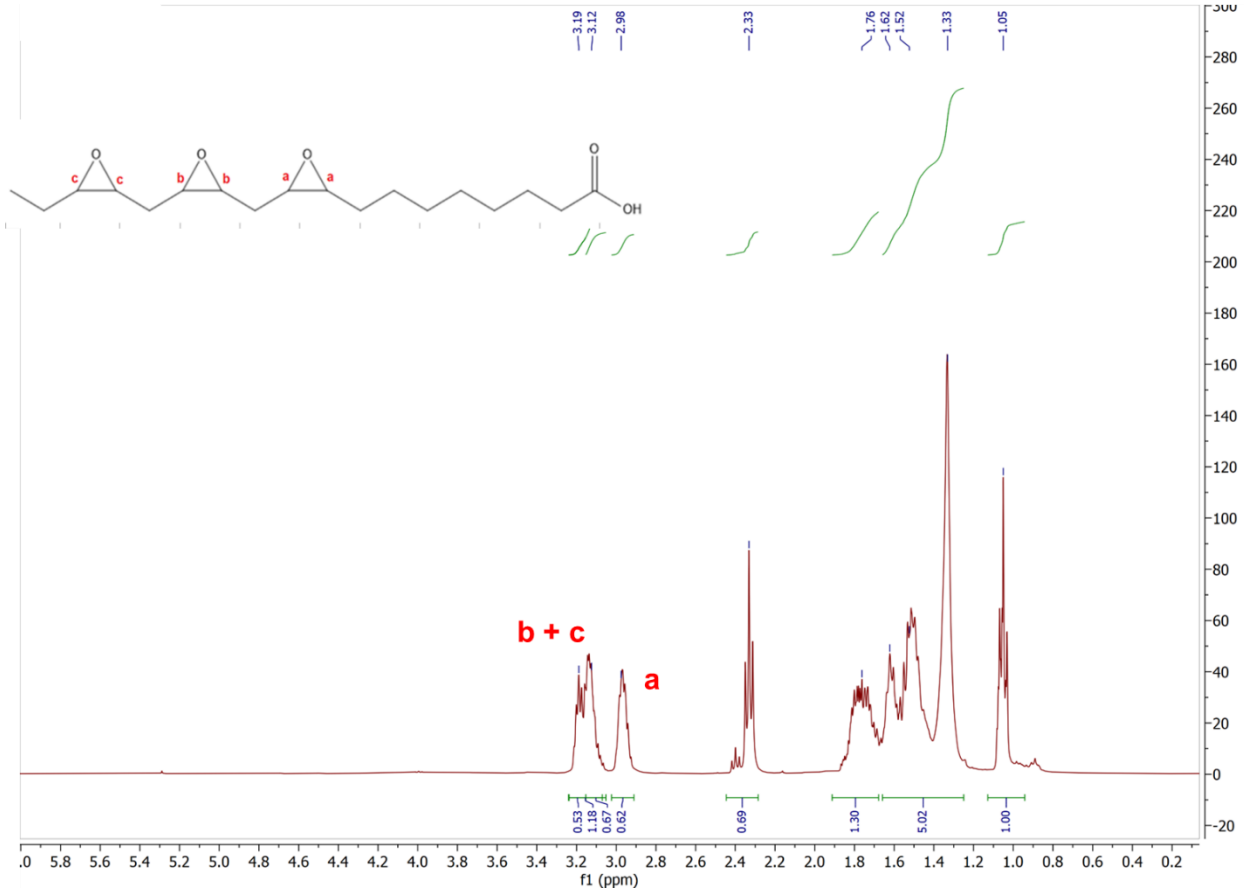

Figure 3.24 *^1H NMR spectrum of the product obtained after 3 h of epoxidation of linolenic acid catalysed by 450 U/g substrate of lipase.*

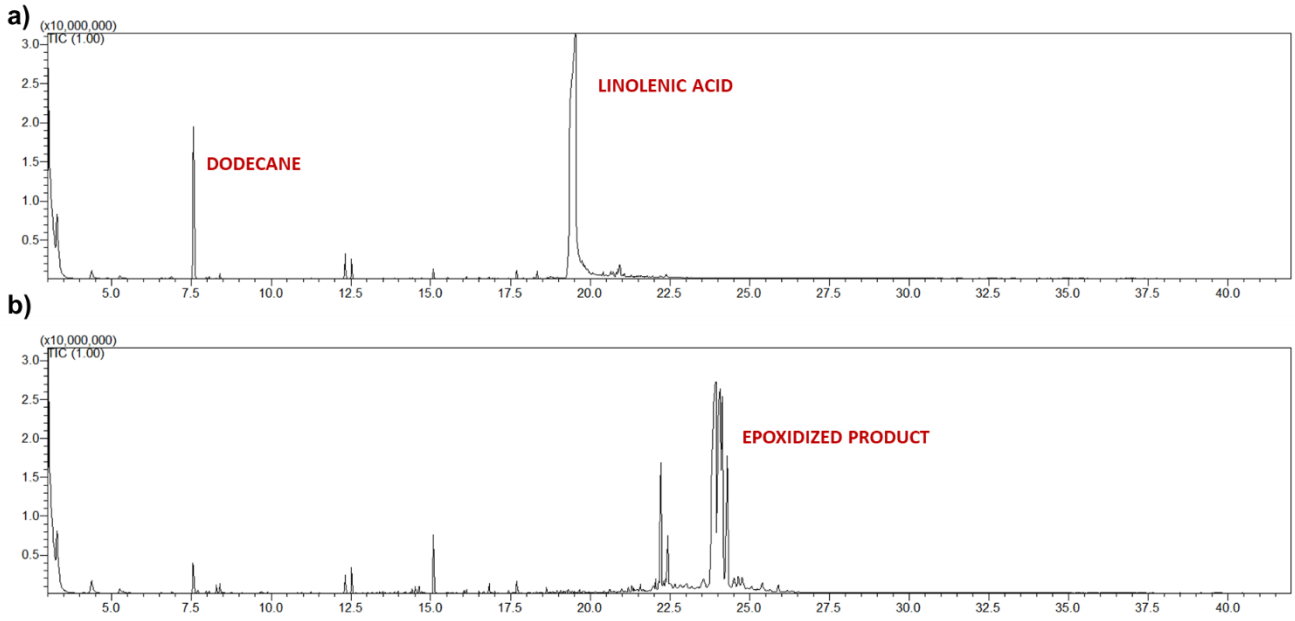

Figure 3.25 *GC-MS chromatogram of a) linoleNic acid, b) reaction mixture. The reaction conditions are reported in table 3.4 (exp9).*

3.6 CONCLUSIONS

The hydrolysis of cardoon seed oil was accomplished using a completely enzymatic process. It was demonstrated that the combination of CaLB and TLL lipases allowed a complete hydrolysis of cardoon seed oil. The used protocol requires buffer and mild temperatures, instead of strong acids or bases at high temperatures. After a simple work-up that avoided the use of organic solvents, a mixture of free fatty acids was obtained, as confirmed by TLC and ^{1}H-NMR analysis.

The epoxidation of pure fatty acids was accomplished, and the conditions optimized, thus preventing the opening of the oxirane rings and inactivation of the enzyme was achieved. The ^{1}H NMR and GC-MS characterization demonstrate the complete conversion of the unsaturated fatty acids into the respective epoxidized products. The process was developed in solventless conditions at mild temperatures using an immobilized enzyme which enables an easy work-up and isolated yields >98%.

3.7 REFERENCES

Abdullah, Saiful Irwan Zubairi, Hasniza Zaman Huri, Nany Hairunisa, Emad Yousif, Roma Choudhury Basu, 2016. Polyesters Based on Linoleic Acid for Biolubricant Basestocks: Low-Temperature, Tribological and Rheological Properties https://journals.plos.org/plosone/article?id=10.1371/journal.pone.0151603

Afifah, A.N., Syahrullail, S., Wan Azlee, N.I., Che Sidik, N.A., Yahya, W.J., Abd Rahim, E., 2019. Biolubricant production from palm stearin through enzymatic transesterification method. Biochemical Engineering Journal 148, 178–184. https://doi.org/10.1016/j.bej.2019.05.009

Ahmed, Yarmo, Salih, Derawi, Yusop, 2015. Synthesis and lubricity properties analysis of branched dicarboxylate esters based lubricant.

Almasi, S., Ghobadian, B., Najafi, G., Soufi, M.D., 2021. A review on bio-lubricant production from non-edible oil-bearing biomass resources in Iran: Recent progress and perspectives. Journal of Cleaner Production 290, 125830. https://doi.org/10.1016/j.jclepro.2021.125830

Aouf, C.A., Durand, E.E., Lecomte, J.J., Figueroa-Espinoza, M.-C.M.-C., Dubreucq, E.E., Fulcrand, H., Villeneuve, P.P., 2014. The use of lipases as biocatalysts for the epoxidation of fatty acids and phenolic compounds. Green Chemistry 16, 1740–1754. https://doi.org/10.1039/c3gc42143k

Ashraful, A.M., Masjuki, H.H., Kalam, M.A., Rizwanul Fattah, I.M., Imtenan, S., Shahir, S.A., Mobarak, H.M., 2014. Production and comparison of fuel properties, engine performance, and emission characteristics of biodiesel from various non-edible vegetable oils: A review. Energy Conversion and Management 80, 202–228. https://doi.org/10.1016/j.enconman.2014.01.037

Biermann, U., Bornscheuer, U., Meier, M.A.R., Metzger, J.O., Schäfer, H.J., 2011. Oils and Fats as Renewable Raw Materials in Chemistry. Angewandte Chemie International Edition 50, 3854–3871. https://doi.org/10.1002/anie.201002767

Cao, L., Fischer, A., Bornscheuer, U.T., Schmid, R.D., 1996. Lipase-Catalyzed Solid Phase Synthesis of Sugar Fatty Acid Esters. Biocatalysis and Biotransformation 14, 269–283. https://doi.org/10.3109/10242429609110280

Directorate-General for Environment, n.d. Public consultation on biobased, biodegradable and compostable plasticst. https://environment.ec.europa.eu/news/public-consultation-biobased-biodegradable-and-compostable-plastics-2022-01-18_en. (accessed 11.24.22).

Erhan, S.Z., Sharma, B.K., Perez, J.M., 2006. Oxidation and low temperature stability of vegetable oil-based lubricants. Industrial Crops and Products, 2005 Annual Meeting of the Association for the Advancement of Industrial Crops: The International Conference on Industrial Crops and Rural Development 24, 292–299. https://doi.org/10.1016/j.indcrop.2006.06.008

Fernández, J., Curt, M.D., Aguado, P.L., 2006. Industrial applications of Cynara cardunculus L. for energy and other uses. Industrial Crops and Products, 2005 Annual Meeting of the Association for the Advancement of Industrial Crops: The International

Conference on Industrial Crops and Rural Development 24, 222–229. https://doi.org/10.1016/j.indcrop.2006.06.010

Fox, N.J., Stachowiak, G.W., 2007. Vegetable oil-based lubricants—A review of oxidation. Tribology International 40, 1035–1046. https://doi.org/10.1016/j.triboint.2006.10.001

Garcés, R., Martínez-Force, E., Salas, J.J., 2011. Vegetable oil basestocks for lubricants. Grasas y Aceites 62, 21–28. https://doi.org/10.3989/gya.045210

Gominho, J., Curt, M.D., Lourenço, A., Fernández, J., Pereira, H., 2018. Cynara cardunculus L. as a biomass and multi-purpose crop: A review of 30 years of research. Biomass and Bioenergy 109, 257–275. https://doi.org/10.1016/j.biombioe.2018.01.001

Haitz, F., Radloff, S., Rupp, S., Fröhling, M., Hirth, T., Zibek, S., 2018. Chemo-Enzymatic Epoxidation of Lallemantia IbericaSeed Oil: Process Development and Economic-Ecological Evaluation. Appl Biochem Biotechnol 185, 13–33. https://doi.org/10.1007/s12010-017-2630-1

Hoeting, J.A., Raftery, A.E., Madigan, D., 2002. Bayesian Variable and Transformation Selection in Linear Regression. Journal of Computational and Graphical Statistics 11, 485–507. https://doi.org/10.1198/106186002501

Iqbal, M., 2014. GATING DESIGN CRITERIA FOR SOUND CASTING 20.

Jovanovic, D., Radovic, R., Mares, L., Stankovic, M., Markovic, B., 1998. Nickel hydrogenation catalyst for tallow hydrogenation and for the selective hydrogenation of sunflower seed oil and soybean oil. Catalysis Today 43, 21–28. https://doi.org/10.1016/S0920-5861(98)00133-3

Khallouki, F., Mannina, L., Viel, S., Owen, R.W., 2008. Thermal stability and long-chain fatty acid positional distribution on glycerol of argan oil. Food Chemistry 110, 57–61. https://doi.org/10.1016/j.foodchem.2008.01.055

Knothe, G., Steidley, K.R., 2005. Kinematic viscosity of biodiesel fuel components and related compounds. Influence of compound structure and comparison to petrodiesel fuel components. Fuel 84, 1059–1065. https://doi.org/10.1016/j.fuel.2005.01.016

Lopes, T.I.B., Ribeiro, M.D.M.M., Ming, C.C., Grimaldi, R., Gonçalves, L.A.G., Marsaioli, A.J., 2016. Comparison of the regiospecific distribution from triacylglycerols after chemical and enzymatic interesterification of high oleic sunflower oil and fully hydrogenated high oleic sunflower oil blend by carbon-13 nuclear magnetic resonance.FoodChemistry212,641–647. https://doi.org/10.1016/j.foodchem.2016.06.024

Luna, F.M.T., Rocha, B.S., Rola, E.M., Albuquerque, M.C.G., Azevedo, D.C.S., Cavalcante, C.L., 2011. Assessment of biodegradability and oxidation stability of mineral, vegetable and synthetic oil samples. Industrial Crops and Products 33, 579–583. https://doi.org/10.1016/j.indcrop.2010.12.012

Lye, Y.-N., Salih, N., Salimon, J., 2020. Optimization of Partial Epoxidation on Jatropha curcas Oil Based Methyl Linoleate Using Urea-hydrogen Peroxide and Methyltrioxorhenium Catalyst. https://doi.org/10.14416/j.asep.2020.12.006

McNutt, J., He, Q. (Sophia), 2016. Development of biolubricants from vegetable oils via chemical modification. Journal of Industrial and Engineering Chemistry 36, 1–12. https://doi.org/10.1016/j.jiec.2016.02.008

NextChem-Ecossitemi Foundation, n.d. Observatory on Biolubricants: position paper. Biolubricants, characteristics, benefits, prospects.

Nor, N.M., Salih, N., Salimon, J., 2020. Optimization of the Ring Opening of Epoxidized Palm Oil using D-Optimal Design. Asian Journal of Chemistry 33, 67–75. https://doi.org/10.14233/ajchem.2021.22938

Orellana-Coca, C., Adlercreutz, D., Andersson, M.M., Mattiasson, B., Hatti-Kaul, R., 2005. Analysis of fatty acid epoxidation by high performance liquid chromatography coupled with evaporative light scattering detection and mass spectrometry. Chemistry and Physics of Lipids 135, 189–199. https://doi.org/10.1016/j.chemphyslip.2005.02.014

Panchal, T.M., Patel, A., Chauhan, D.D., Thomas, M., Patel, J.V., 2017. A methodological review on bio-lubricants from vegetable oil based resources. Renewable and Sustainable Energy Reviews 70, 65–70. https://doi.org/10.1016/j.rser.2016.11.105

Pinto, F., Martins, S., Gonçalves, M., Costa, P., Gulyurtlu, I., Alves, A., Mendes, B., 2013. Hydrogenation of rapeseed oil for production of liquid bio-chemicals. Applied Energy, Special Issue on Advances in sustainable biofuel production and use - XIX International Symposium on Alcohol Fuels - ISAF 102, 272–282. https://doi.org/10.1016/j.apenergy.2012.04.008

Raccuia, S.A., Melilli, M.G., 2007. Biomass and grain oil yields in Cynara cardunculus L. genotypes grown in a Mediterranean environment. Field Crops Research 101, 187–197. https://doi.org/10.1016/j.fcr.2006.11.006

Ravasio, N., Zaccheria, F., Gargano, M., Recchia, S., Fusi, A., Poli, N., Psaro, R., 2002. Environmental friendly lubricants through selective hydrogenation of rapeseed oil over supported copper catalysts. Applied Catalysis A: General 233, 1–6. https://doi.org/10.1016/S0926-860X(02)00128-X

Rieke, R.D., Thakur, D.S., Roberts, B.D., White, G.T., 1997. Fatty methyl ester hydrogenation to fatty alcohol part I: Correlation between catalyst properties and activity/selectivity. Journal of the American Oil Chemists' Society 74, 333–339. https://doi.org/10.1007/s11746-997-0088-y

Salih, N., Salimon, J., Yousif, E., 2011. The physicochemical and tribological properties of oleic acid based triester biolubricants. Industrial Crops and Products 34, 1089–1096. https://doi.org/10.1016/j.indcrop.2011.03.025

Salimon, J., Salih, N., Yousif, E., 2012. Triester derivatives of oleic acid: The effect of chemical structure on low temperature, thermo-oxidation and tribological properties. Industrial Crops and Products 38, 107–114. https://doi.org/10.1016/j.indcrop.2012.01.019

Salimon, Salih, Yousif, 2010. Biolubricants: Raw materials, chemical modifications and environmental benefits - Salimon - 2010 - European Journal of Lipid Science and Technology - Wiley Online Library [WWW Document]. URL https://onlinelibrary.wiley.com/doi/full/10.1002/ejlt.200900205 (accessed 11.11.22).

Shahunja, K.M., Sévin, D.C., Kendall, L., Ahmed, T., Hossain, Md.I., Mahfuz, M., Zhu, X., Singh, K., Singh, S., Crowther, J.M., Gibson, R.A., Darmstadt, G.L., 2021. Effect of topical applications of sunflower seed oil on systemic fatty acid levels in under-two children under rehabilitation for severe acute malnutrition in Bangladesh: a

randomized controlled trial. Nutrition Journal 20, 51. https://doi.org/10.1186/s12937-021-00707-3

Siniawski, M.T., Saniei, N., Stoyanov, P., 2011. Influence of humidity on the tribological performance of unmodified soybean and sunflower oils. Lubrication Science 23, 301–311. https://doi.org/10.1002/ls.157

Somidi, Sharma, Dalai, 2014. Synthesis of Epoxidized Canola Oil Using a Sulfated-SnO2 Catalyst | Semantic Scholar [WWW Document]. URL https://www.semanticscholar.org/paper/Synthesis-of-Epoxidized-Canola-Oil-Using-a-Catalyst-Somidi-Sharma/b8397509890883d5d1aef072eeda27aaca0aefb7 (accessed 11.12.22).

Soni, S., Agarwal, M., 2014. Lubricants from renewable energy sources – a review. Green Chemistry Letters and Reviews 7, 359–382. https://doi.org/10.1080/17518253.2014.959565

Syahir, A.Z., Zulkifli, N.W.M., Masjuki, H.H., Kalam, M.A., Alabdulkarem, A., Gulzar, M., Khuong, L.S., Harith, M.H., 2017. A review on bio-based lubricants and their applications. Journal of Cleaner Production 168, 997–1016. https://doi.org/10.1016/j.jclepro.2017.09.106

Tesser, R., Russo, V., Turco, R., Vitiello, R., Di Serio, M., 2020. Bio-lubricants synthesis from the epoxidized oil promoted by clays: Kinetic modelling. Chemical Engineering Science 214, 115445. https://doi.org/10.1016/j.ces.2019.115445

Todea, A., Otten, L.G., Frissen, A.E., Arends, I.W.C.E., Peter, F., Boeriu, C.G., 2015. Selectivity of lipases for estolides synthesis. Pure and Applied Chemistry 87, 51–58. https://doi.org/10.1515/pac-2014-0716

Torres, Gadalla, Mateo-Sanz, Jiménez Estelle, 2011. Evaluation Tool for the Environmental Design of Chemical Processes | Industrial & Engineering Chemistry Research [WWW Document]. URL https://pubs.acs.org/doi/abs/10.1021/ie201024b (accessed 11.12.22).

Turco, R., Ortega-Toro, R., Tesser, R., Mallardo, S., Collazo-Bigliardi, S., Chiralt Boix, A., Malinconico, M., Rippa, M., Di Serio, M., Santagata, G., 2019. Poly (Lactic Acid)/Thermoplastic Starch Films: Effect of Cardoon Seed Epoxidized Oil on Their Chemicophysical, Mechanical, and Barrier Properties. Coatings 9, 574. https://doi.org/10.3390/coatings9090574

Vlček, T., Petrović, Z.S., 2006. Optimization of the chemoenzymatic epoxidation of soybean oil. J Amer Oil Chem Soc 83, 247–252. https://doi.org/10.1007/s11746-006-1200-4

Wagner, Luther, Mang, 2001. Lubricant base fluids based on renewable raw materials: Their catalytic manufacture and modification - ScienceDirect [WWW Document]. URL https://www.sciencedirect.com/science/article/pii/S0926860X01008912 (accessed 11.11.22).

Zainal, N.A., Zulkifli, N.W.M., Gulzar, M., Masjuki, H.H., 2018. A review on the chemistry, production, and technological potential of bio-based lubricants. Renewable and Sustainable Energy Reviews 82, 80–102. https://doi.org/10.1016/j.rser.2017.09.004

CHAPTER 4

VALORIZATION OF RICE HUSK AS A RENEWABLE CARRIER FOR ENZYME IMMOBILIZATION

4.1 SUMMARY

Rice husk (RH) is an underexploited, low density and highly robust composite material, available in large quantities from rice processing. This biodegradable composite material has been studied in our research group during the last decade, given its potential to replace fossil-based methacrylic epoxy resins that are currently available on the market as immobilization carriers, thus creating a sustainable and economically viable alternative for biocatalysed industrial processed.

In our previous studies, RH was chemically or enzymatically oxidized to introduce functional groups for the covalent linking of diamino spacers, used for the glutaraldehyde mediated bonding of enzymes to be applied in biocatalytic processes. The chemical method (sodium periodate oxidative cleavage of glucose units in cellulose) showed higher efficiency in respect to the enzymatic method (laccase catalyzed oxidation of the primary hydroxyl group of glucose units in cellulose, in the presence of TEMPO radical as mediator).

In comparison with the previous studies developed in our research group, the present research aimed at improving the sustainability and economic viability of the protocols for the covalent immobilization of enzymes on functionalized (oxidized) rice husk. More specifically, the advances were the following: i) development of a method for oxidizing the cellulosic matrix of rice husk with the aid of laccase enzymes, under optimal conditions, that allowed the recycling of the enzyme; ii) the covalent immobilization of enzymes on such oxidized carriers without the introduction of spacers and avoiding the use of the toxic glutaraldehyde; iii) an optimized protocol for the delignification of rice husk that yields a low density and more hygroscopic material for different biotechnological and environmental applications.

The main advantage of the covalent immobilization is represented by the feasibility for consecutive reaction cycles also in aqueous media or a very viscous system since the detachment of the protein is prevented. Notably, there is no covalently immobilized lipase available on the market. Selected immobilized formulations were tested in solventless polycondensation reactions and in the processing of cardoon seed oil (chapter 3).

4.2 INTRODUCTION

4.2.1 Valorization of lignocellulosic biomass

Biomass represents a valid alternative to the use of plastic materials as it allows for an evolution of current chemical industries (which use petroleum as a source of raw materials in bioindustries and biorefineries), with a consequent contribution to the decarbonization of industry and economy (Lola Domnina B. Pestaño and Wilfredo I. José, 2018).

Lignocellulosic biomass represents the largest reserve of organic matter on earth. It constitutes the cell wall of plants and is composed of organic acids, salts, minerals and three biopolymers: cellulose, hemicellulose, and lignin. These three biopolymers are associated with each other, forming a complex heterogeneous matrix whose composition can vary according to the biomass it constitutes and the area in which it is produced. Lignocellulosic materials are currently used for the production of bio-based chemicals, such as substrates for fermentation or as a source of biofuels in biorefineries (Tuck et al., 2012).

However, the concept of valorization of lignocellulosic biomass received increasing attention especially for its potential conversion into products with value-added. The present project aims to respond to this challenge by converting a very inexpensive biomass, rice husk, into a functional material applicable in the biotechnology sector as carrier for enzyme immobilization.

Rice husk (RH) is a lignocellulosic composite material, produced in large quantities in Asian and European countries as a waste from cereal production. It is estimated that for every four tons of rice harvested, one ton of rice husk is produced, with an annual production of 120Mt: of this quantity only 20 Mt is used (Corici et al., 2016).

The rice husk is formed of 20-25% of silicon dioxide (SiO_2) and other metal oxides such as Al_2O_3, Fe_2O_3, CaO, and for the remaining 75-80% is comprised of organic material of the specific composition shown in table 4.1 (Corici et al., 2016).

Table 4.1 Major organic chemical components of rice husk (Corici et al., 2016).

	% w w^{-1}
Cellulose	46.5
Lignin	31.9
Hemicellulose	22.1

The morphology of the rice husk was studied in detail by our research group using scanning electron microscopy (SEM). Figure 4.1 reports SEM images of the entire cuticle of rice husk before and after the milling.

The external surface of rice husk is very rough, with linear ripples of a conical shape that run regularly along the whole surface. The external surface contains a higher concentration of SiO_2 and this confers stiffness and resistance towards external agents (Park et al., 2010). The internal surface, on the other hand, is smoother and consists of a larger quantity of cellulose. In previous studies it was demonstrated that the milling of rice husk (with average

size 200-400μm) retains the typical external and internal morphology, probably due to the toughness conferred by silica. Indeed, the milling of RH is feasible only by knife-mill devices whereas ball mill systems are inefficient (Cespugli et al., 2018).

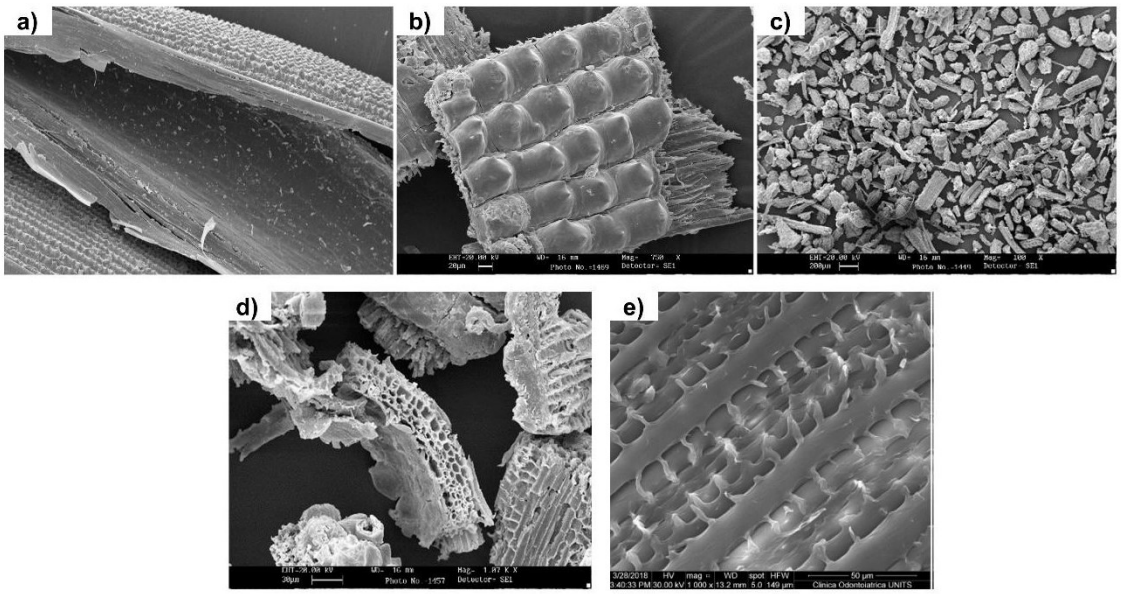

Figure 4.1 *Scanning electron micrographs of rice husk a) view of the external surface; b) external surface with ripples containing lignin and SiO_2; c) rice husk after milling d) fragment of tracheids; e) section of tracheids.*

4.2.2 Functionalization of rice husk surface

The first protocol for the functionalization of rice husk previously developed in our group involved an oxidation process at the level of the cellulosic matrix in order to generate new aldehyde groups to be exploited for the covalent anchoring of the enzymatic protein.

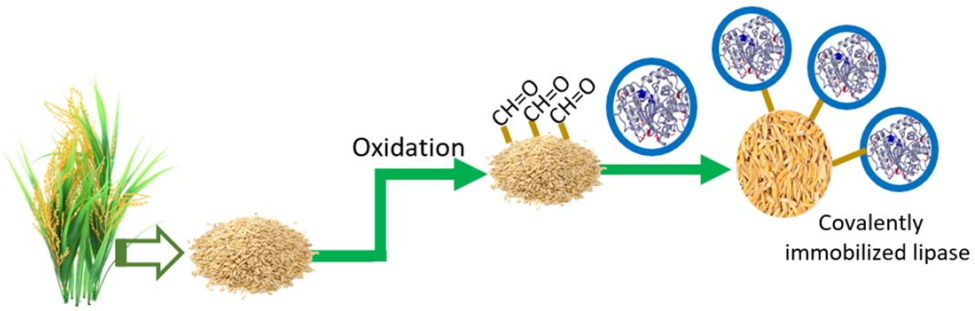

Figure 4.2 *Schematic representation of oxidation of rice husk followed by covalent immobilization of lipases.*

For chemical oxidation, sodium metaperiodate ($NaIO_4$) that causes an oxidative cleavage of the glucose units with the formation of two aldehyde groups (Monsan, 1983, 1981) was used (figure 4.3).

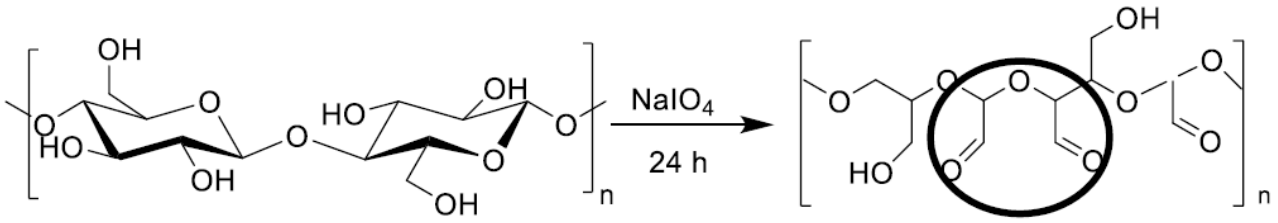

Figure 4.3 *Oxidative cleavage of cellulose using $NaIO_4$.*

The previous investigations (Cespugli et al., 2018; Corici et al., 2016) showed that this method induces an increase of carbonyl groups of more than 380%, whereas carboxylic groups increase by about 66%. The latter are the result of the subsequent oxidation of a fraction of aldehyde groups under oxidative conditions. Oxidative modifications of the lignin cannot be excluded although the microscopic characterization indicates that SiO_2 covers most of the lignin, which appears poorly accessible (Cespugli et al., 2018).

The resulting aldehyde groups were exploited for the insertion of di-amino spacers using hexamethylenediamine (HMDA), via the formation of imine bonds. Finally, glutaraldehyde (GA) was employed as a bi-functional agent to form imine bonds with the spacer and the amine groups of lysine residues present on the surface of the lipase (Corici et al., 2016; Monsan, 1983, 1981).

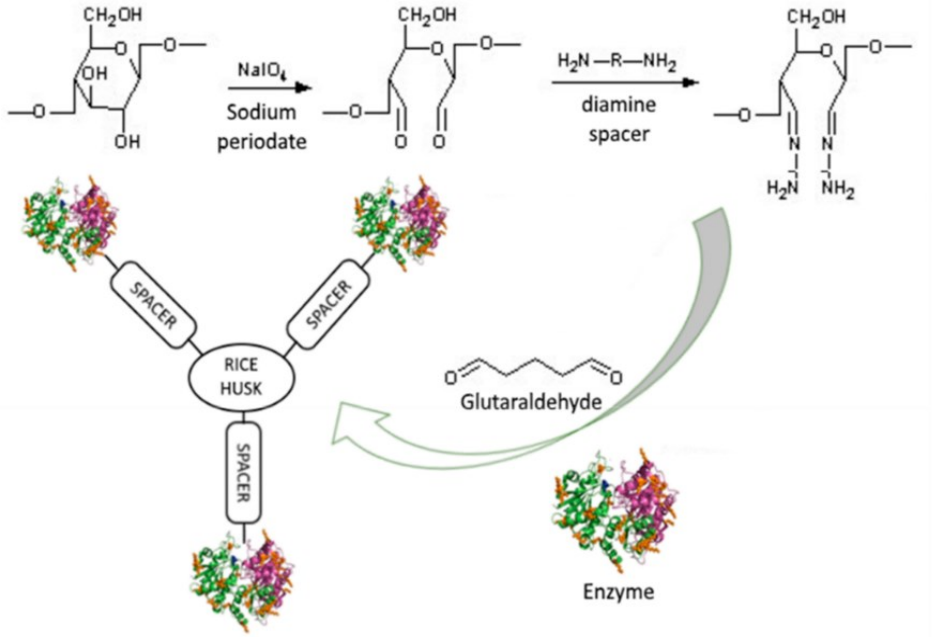

Figure 4.4 *Schematic representation of the oxidation and functionalization of rice husk by using diamine spacer and glutaraldehyde.*

4.2.3 Enzymatic activation of rice husk surface

Recently, Marco Cespugli in his PhD thesis (Cespugli M., 2017) carried out some preliminary tests aiming at improving the sustainability of the immobilization method and the accessibility of rice husk. More specifically, the use of sodium periodate is considered a toxic and hazardous chemical. Effects of oral exposure include alternate hyperactivity and lassitude, weakness, prostration, dyspnoea, and diarrhoea. Mortality was attributed to renal damage (Lent et al., 2017).

The chemical oxidation reaction was replaced by an enzymatic oxidation using laccase in the presence of a chemical mediator. The oxidation of the primary hydroxyl groups of the glucose unit from cellulose was accomplished by means of laccase enzymes in the presence of a “mediator”, namely the TEMPO (2,2,6,6-Tetramethylpiperidin-1-yl)oxyl) radical.

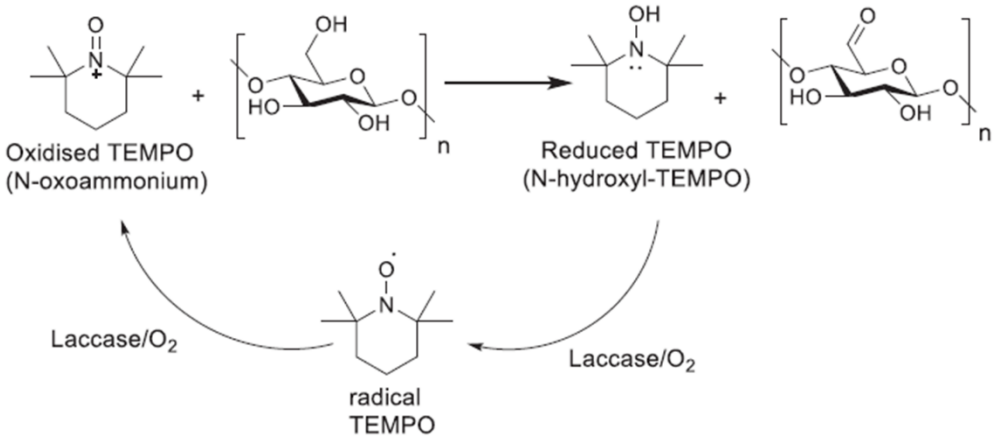

Figure 4.5 *Reaction scheme of enzymatic mediated oxidation of cellulose. The laccase/TEMPO system oxidizes the primary hydroxyl group to an aldehyde.*

Laccases (benzenediol:oxygen oxidoreductase, EC 1.10.3.2) are enzymes of great interest in the biocatalysis field as they use oxygen from air as the last electron acceptor, producing water as a by-product. Laccases belong to a group of polyphenol oxidases, the reduction of oxygen to water is accompanied by the oxidation of a substrate, such as methoxy-substituted monophenols, o,p-diphenols, aminophenols, polyphenols, polyamines, aryl amines, lignin.

Laccases are used as biocatalysts in various industrial applications and most of them require the presence of a mediator. Currently, laccases are used in the paper industry as bleaching agents for fabrics (Osma et al., 2010), in the food industry for the removal of phenolic species from beverages, in the environmental field for the removal of pollutants from water and soils, and finally in the biosensors field (Fabbrini et al., 2001). In organic synthesis, laccases are used for several types of reactions: oxidation reaction of compounds such as aromatic or aliphatic alcohols to the correspondent aldehydes or ketones, radical coupling reactions for the synthesis of polyphenols (Agematu et al., 1993), or dimers of molecules such as penicillin X or bisphenol A (Cameron and Aust, 2001; Uchida et al., 2001). They are also used for the enzymatic regeneration of cofactors used in oxidation reactions (Alvira et al., 2010). Laccases are responsible for the polymerization and depolymerization of lignin,

causing an increased accessibility to cellulose for possible subsequent conversions (Galbe and Zacchi, 2007). Laccases can also mediate the selective modification of the surface of lignocellulosic materials by grafting small organic molecules of phenolic nature onto the lignin component of different materials (Alvira et al., 2010).

Laccases are commonly produced by bacteria, plants, insects, and fungi; they are in particular produced by the *White-rot* species. Their biological function depends on the organism (Thurston Christopher F., 1994), they are responsible for the formation and degradation of lignin, and they are also responsible for wound healing. In fact, in response to an injury, laccases initiate an oxidative polymerization of catechols which generates a "glue" that seals the wound (Claus, 2004). They constitute the largest group of multi-copper blue oxidases since the enzymes contain at least four copper atoms, which confer the typical blue colour.

In general, laccases catalyse the oxidation of numerous aromatic compounds accompanied by the reduction of molecular oxygen to water through the transfer of four electrons.

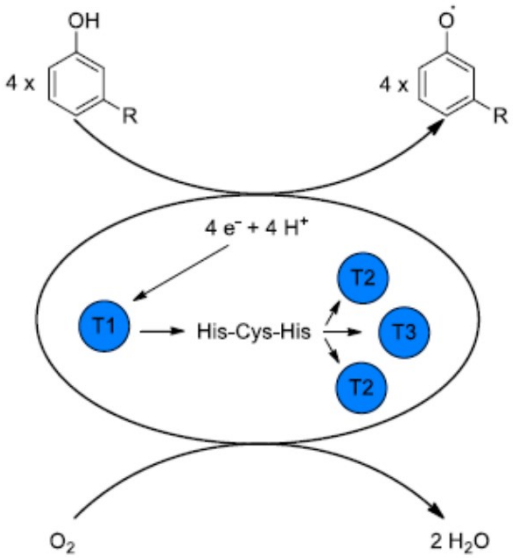

Figure 4.6 *Electronic transfer in laccase oxidation.*

The four copper atoms per functional unit guarantee the catalytic activity of the laccases. Copper atoms are classified in three types based on the coordination of their bonds (figure 4.7).

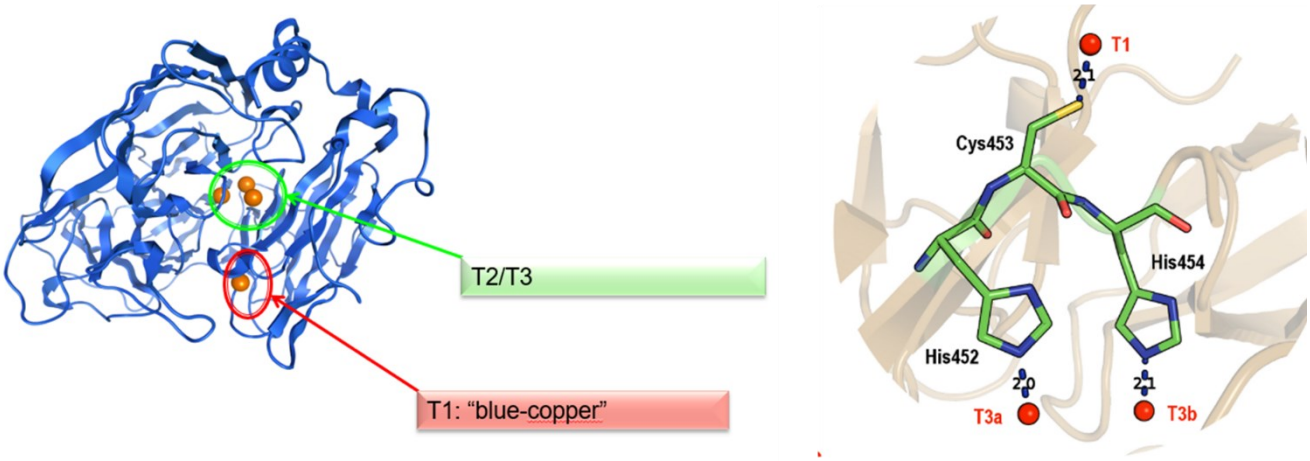

Figure 4.7 *Laccase structure: copper atoms are indicated with orange spheres. On the right: Catalytic site of laccase and coordination bonds.*

Non-phenolic compounds are often not oxidized by laccases because of their low redox potential. Furthermore, big molecules that cannot reach the active site (i.e., lignin) cannot be oxidized (Bourbonnais et al., 1995). To overcome this drawback, a mediator with the function of moving oxidative species outside from the enzyme to the substrate can be used. A mediator is usually a small molecule that acts as an electron shuttle, it is oxidized by the enzyme, moves away from the active site and, in turn, oxidises the substrate (figure 4.8).

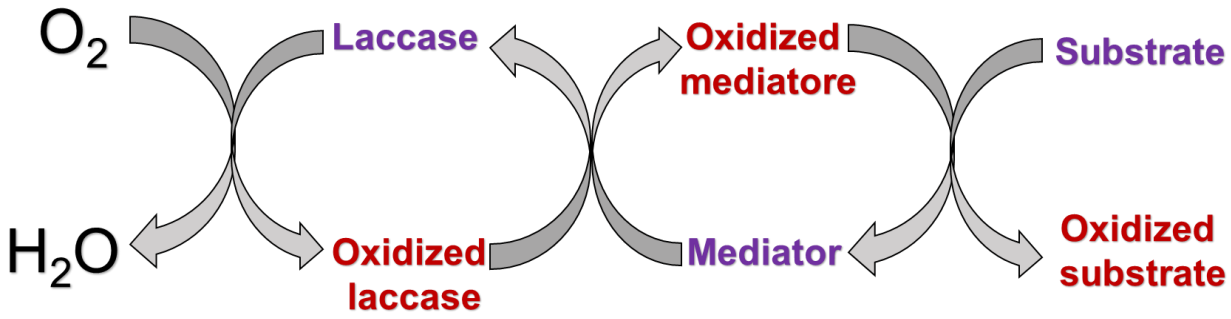

Figure 4.8 *Scheme of the laccase/ mediator system.*

Type one copper (T1) presents a trigonal geometry with a free axial position prone to substrate interaction. Equatorial positions establish coordination bonds with two histidine residues and a cysteine, while the fourth could be variable (Claus, 2004). The redox potential of T1 copper depends on the organism producing the enzyme: in fungal laccases, the redox potential is 700-900 mV, while on plant laccases it is typically lower (330-500 mV), and this difference is due to the different coordination of T1 copper (Andréasson and Reinhammar, 1979). The T1 copper atom is responsible for the blue colour of laccases and of the substrate oxidation (Nakamura, 1958). T2 copper is not detectable in the visible spectrum and is coordinated by two histidine residues. T3 coppers establish a binuclear center with a maximum of absorbance at 330 nm in the oxidized form and are coordinated by six histidine residues next to the T2 copper. This molecular architecture is responsible for the reduction of molecular oxygen by the production of water.

The mono-electronic oxidation of the substrate occurs at the level of the copper center T1 which is the first electron acceptor. The electron through the His-Cys-His is transferred from copper T1 to the trinuclear cluster where the reduction of oxygen to water occurs as previously shown in Figure 4.6.

There are some conditions that a good redox mediator should satisfy: it must be a small molecule able to generate stable radical species, it should not interfere with the catalytic activity of the enzyme while allowing the *in-situ* recyclability and, finally, it should be cost-effective (Potthast et al., 2001). The system consisting of laccase and mediator is called laccase-mediator system (LMS). Many natural and synthetic mediators are reported in the literature (figure 4.9).

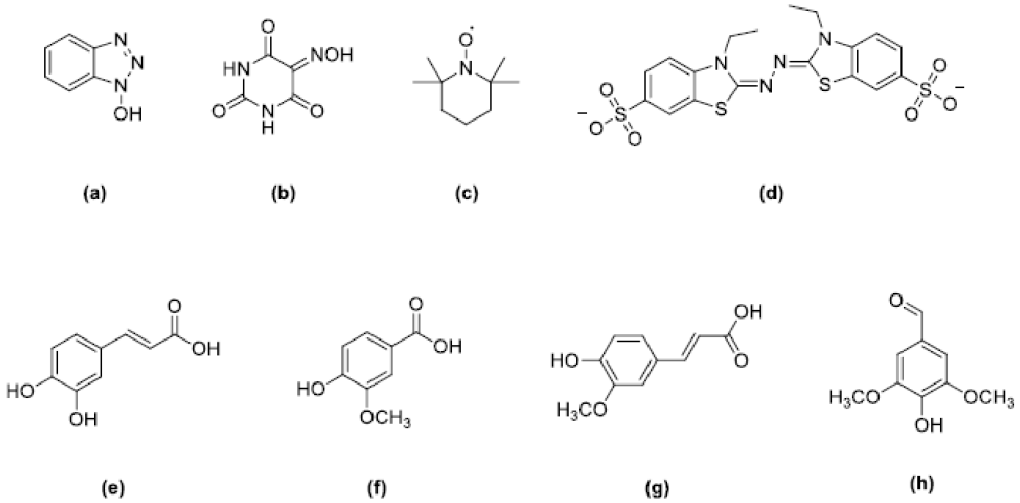

Figure 4.9 *Examples of synthetic and natural mediators of laccases: (a) N-hydroxybenzotriazole (HBT); (b) violuric acid (VLA); (c) 2,2,6,6-tetramethylpiperidine-1-oxyl (TEMPO); (d) 2,2'-azinobis-(3-ethylbenzothiazolin-6-sulfonic acid) (ABTS); (e) caffeic acid; (f) acetovanillone; (g)ferulic acid; (h) syringaldehyde.*

The laccase catalyzed oxidation of the glucose units of the cellulose fraction of RH was first performed by Marco Cespugli in his PhD thesis working in the presence of TEMPO radical as a mediator. TEMPO is oxidized to an oxo-ammonium cation that, in turn, selectively oxidizes the C6 hydroxyl of the glycosidic ring forming an aldehyde via heterolytic cleavage. A fraction of the neo-formed aldehydic group, very sensitive to oxidative conditions, can be further oxidized into carboxylic acid (figure 4.10).

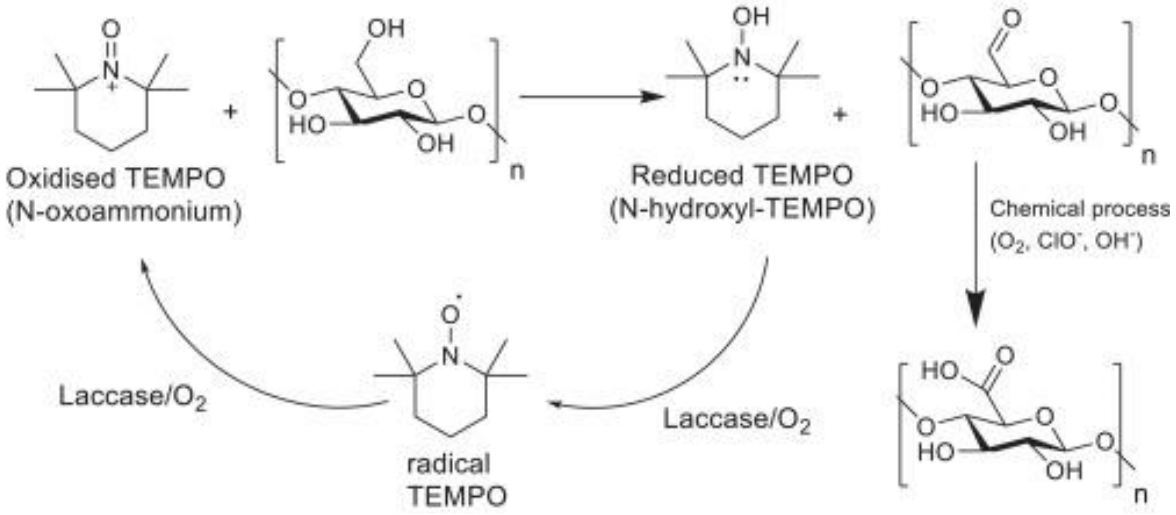

Figure 4.10 *Reaction scheme of cellulose oxidation in the laccase-mediator system (LMS).*

The preliminary tests explicated in the PhD thesis of Marco Cespugli (Cespugli M., 2018), employing laccases for the oxidation of rice husk, indicated that the amount of carbonyl groups for the chemically oxidized rice husk (measured by means of the hydroxylamine hydrochloride assay) are 5 times lower compared with the sodium periodate method. This was achieved by the best performing laccase (laccase from *Trametes sp.*) used at 100U/mL concentration for 48 hours at environmental pressure and 25°C with a 0.1 M pH 5 citrate buffer solution containing 10 mM TEMPO. The reason lies in the fact that sodium periodate leads to the formation of two aldehyde groups in the cellulose structure (figure 4.5).

Moreover, SEM images showed that the aggressive action of sodium periodate determined the erosion of the surface of the rice husk, making the matrix more accessible to reagents. The enzymatically oxidised rice husk was then functionalized with the spacer hexamethylenediamine (HMDA) with the aid of glutaraldehyde as previously described and used for the immobilization (10.000 Units per dry g of carrier) of lipase B from *Candida antarctica.* The hydrolytic activity of the CaLB immobilized on the enzymatically oxidised rice husk resulted a 5.6 fold lower (56 U/g) than that which was achieved by immobilizing the CaLB on the rice husk oxidized by $NaIO_4$ (316 U/g). The result was mainly due to the lower loading achieved with the enzymatically treated matrix (17% of protein *vs* 72%).

In this project we started from this evidence and decided to improve the sustainability of the oxidative process while simplifying the experimental protocol. At the same time, the objective of improving the accessibility of rice husk was addressed by optimizing the protocol for the delignification of this lignocellulosic biomass.

4.2.4 Delignification of rice husk

The previous studies of our group indicated that lignin constitutes at least 30% of the mass of rice husk (Table 4.1). Its role is to create a very hydrophobic external barrier that protects the rice from external agents and also prevents its dehydration. Moreover, hemicellulose represents more than 20% of rice husk mass. Hemicellulose consists of several different sugar units and substitutes side chains that form a low molecular weight linear or branched polymer. This polymer is more soluble than cellulose with a DP (degree of polymerization) of less than 200. Hemicellulose can be hydrolysed by weak acid, it is not crystalline but rather a gel. Covalent hemicellulose-lignin bonds involving ester or ether linkages connect the two biopolymers.

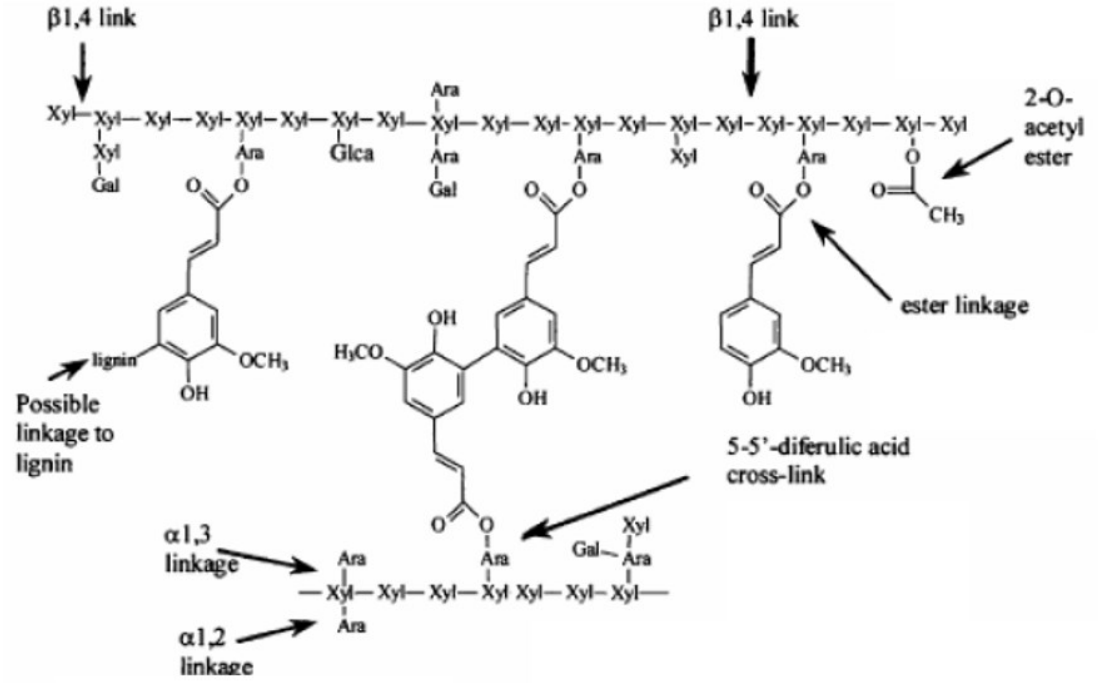

Figure 4.11 *Chemical network that connects hemicellulose with lignin.*

In his PhD thesis Marco Cespugli (Marco Cespugli, 2018) reported some preliminary results obtained by immobilizing a lipase on RH pre-treated with H_2O_2 in a basic environment. The objective was to create a more hydrophilic environment and to increase the accessibility of the enzymes to the cellulose matrix for improving the immobilization yield. The protocols were developed on the basis of bleaching techniques employing ammonia with hydrogen peroxide (Kim and Lee, 2005), or alkaline hydrogen peroxide with sodium hydroxide (Díaz et al., 2014).

Aqueous ammonia solution can cause the hydrolysis of the glucuronic esters responsible for the lignin-hemicellulose matrix integrity whereas the diferulic linkages between cellulose and lignin are promptly broken by oxidative treatments (Zhao et al., 2020).

The hydroperoxide anion produced in the decomposition of H_2O_2 is unable to directly depolymerize lignin, while the hydroxyl radical is a powerful oxidant that causes lignin and

hemicellulose depolymerisation. This radical is formed under alkaline conditions that promote the formation of the hydroperoxide anion via the neutralization of H^+ ions. The produced anion promptly reacts with hydrogen peroxide to form the radical species (Kim and Lee, 2005).

$$H_2O_2 = H^+ + HOO^-$$

$$H_2O_2 + HOO^- = \cdot OH + O_2^- \cdot + H_2O$$

Figure 4.12 *Formation of the hydroxyl radical under basic conditions.*

The optimal pH for the formation of the radical to achieve delignification with an alkaline hydrogen peroxide solution was reported to be 11.5 (Zhao et al., 2014).

According to Wang and co-workers (Wang Z. et al., 2016), the crystalline microfibrils of cellulose of rice husk are resistant to degradation and as was also demonstrated by Marco Cespugli who observed the preservation of the tri-dimensional structure of rice husk after treatments. Rice husks with a granulometry of 0.2-0.4 mm were treated with an 8% hydrogen peroxide solution using sodium hydroxide to adjust the pH at 11.5.

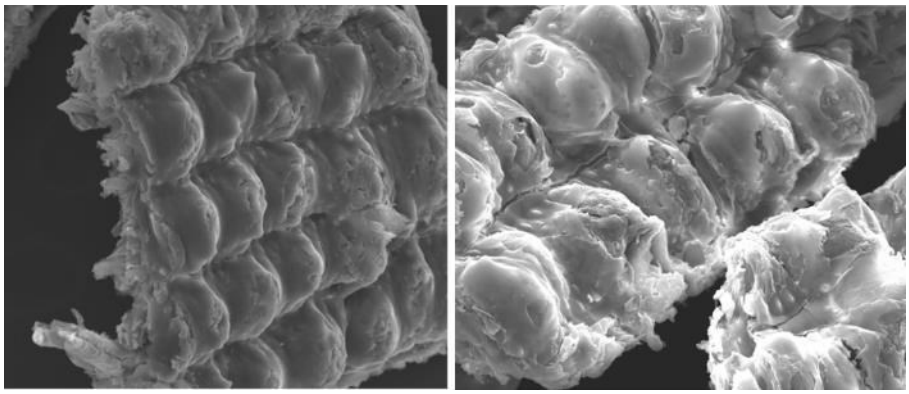

Figure 4.13 *SEM microscopy images of the outer surface of rice husk before (left) and after (right) alkaline hydrogen peroxide pre-treatment.*

SEM microscopy showed that the overall structure of rice husk was preserved, while signs of chemical abrasion were detected on the external surface.

In the present study, the reaction conditions or the delignification of rice husk were optimized, and the resulting material was characterized in detail. Finally, some preliminary immobilization tests were performed.

4.3 OBJECTIVES OF THE CHAPTER: RICE HUSK AS SUSTAINABLE ALTERNATIVE TO THE COMMERCIAL FOSSIL-BASED ORGANIC CARRIERS FOR ENZYME IMMOBILIZATION

To improve the sustainability of the enzymatic process described in chapter 3 a parallel study was carried out by addressing the covalent immobilization of lipases on a renewable carrier: rice husk. The valorization of functionalized rice husk, a lignocellulosic biomass available from rice processing, allows to obtain bio-composite materials suitable for enzyme immobilization.

The sustainability of the functionalization and immobilization procedures was improved compared to previous studies. Protocols for functionalization (oxidation) of rice husk was optimized using a chemo-enzymatic laccase-TEMPO system that allows to reduce the amount of enzyme employed and it also enables its recycling.

More importantly, lipases were directly immobilized covalently on the oxidized rice husk without the use of spacers and the toxic glutaraldehyde as reported in previous studies.

The immobilization results of lipases on rice husk are comparable to those obtained using commercial epoxy methacrylic resins. The use of rice husk as carrier made possible to overcome problems related to the commercial methacrylic resin. Firstly, their high cost and secondly their environmental impact as demonstrated by studies of Life Cycle Assessment (Corici et al., 2016).

It was demonstrated that biocatalysts immobilized on rice husk, because of their stability and robustness, are applicable in various reaction media, including aqueous systems and under mechanical stress. This work intends to be a contribution to develop a new renewable industrial carrier for enzyme immobilization for different industrial applications. Notably, no covalently immobilized lipase is currently commercialized for industrial applications despite the clear advantages deriving from the use of lipases enzymes in aqueous solutions. In this research CaLB immobilized on rice husk, both chemically and enzymatically oxidized, was tested not only in the chemo-enzymatic epoxidation of fatty acids but also in the solvent-free polycondensation of bio-based monomers.

The last part of this work had the objective of improving the accessibility to oxidizing reagents and enzymes, while decreasing the hydrophobicity of this composite material. This objective was achieved through the development of a delignification process that allows to increase the water retention capacity of rice husk decreasing its density while maintaining tri-dimensional structure and robustness.

4.4 MATERIALS AND METHODS

MATERIALS

Lipase B from *Candida antarctica* (EC 3.1.1.3, CAS number 900-162-1, liquid solution, activity: 1372 TBU g^{-1} where TBU = enzymatic Units calculated with tributyrin hydrolysis, protein content = 84 mg mL^{-1}) and Laccase Novozym 51,003 (EC 1.10.3.2., CAS number 80498–15–3) from *Myceliophthora Thermophila* expressed in *Aspergillus sp*. (activity: 64 U ABTS mL^{-1}) were from Novozymes (Denmark).

Lipase from *Thermomyces lanuginosus* (specific activity: 3176 TBU mL^{-1}, liquid solution, protein content = 38 mg mL^{-1}) maltodextrin, Kollidon®25, 2,2,6,6-tetramethylpiperidin-1-yl)oxy (TEMPO), NaOH, $NaIO_4$, Bradford reagent, tributyrin and 2,2′-Azino-bis(3-ethylbenzothiazoline-6- sulfonic acid) diammonium salt (ABTS) were from Sigma-Aldrich.

Lipase from *Rhyzopus oryzae* (powder, activity: 29,496 U g^{-1}) was kindly donated by Amano Corporation (Japan).

Laccase C (EC 1.10.3.2) from *Trametes versicolor* (2176 U ABTS g^{-1}) was from ASA Spezialenzyme GmbH (Germany).

PEG 3000 was from Merck. Arabic gum was from Fluka TM.

Hydroxyethylcellulose was from Esperis S.p.A. (Italy).

The rice husk was kindly donated by Riseria Cusaro, Binasco (Italy).

4.4.1 Chemical oxidation of rice husk

A total of 2 g of rice husk (particle size 200-400μm) previously washed with a mixture of H_2O:ethanol 50:50 (3x3 mL) was placed in a syringe with septum. Then, 50 mL of a 0.20 M $NaIO_4$ solution was added, and the mixture was allowed to react under stirring on the blood rotator for 22 h in the dark and at 25 °C. The solid support became dark brown. At the end of the reaction, the rice husk was filtered and rinsed with deionized water (3x10 mL) until neutrality.

4.4.2 Enzymatic oxidation of rice husk

Protocol at 20°C: 0.2 g of RH was washed with 10 mL phosphate buffer 0.1 M pH 5. To the resulted RH, a 10 mM solution of TEMPO was added, together with the laccase to obtain a final concentration of 8 or 40 U mL^{-1}. Phosphate buffer (0.1 M pH 5) was used to reach a final volume of 25 mL.
Protocol at 70°C: 0.5 g of RH were treated as described above and all reactions were performed at a final concentration of 8 U mL^{-1}. The reaction mixtures were magnetically stirred (350 rpm) and air was insufflated for 2 minutes every 8 hours to increase the exposure of the enzyme to oxygen. At the end of the reaction the mixture was filtered and washed with distilled water (15 mL, 4 times). The recyclability of the laccase solution used at 70°C

was evaluated by removing the oxidized product and then adding fresh RH and TEMPO in the same amount as in the first cycle. The reaction was conducted as described above. Samples were withdrawn and analyzed after 24 and 48h, so that the same laccase solution was employed for a total of 96 h.

4.4.3 Recyclability of laccase from Trametes sp. for the oxidation of rice husk

The first oxidation cycle was carried out at 70°C in sodium citrate buffer 0.1 M pH 5 using a final laccase concentration of 8 U mL^{-1}. The reaction mixtures were magnetically stirred (350 rpm) and air was insufflated for 2 minutes every 8 hours to increase the exposure of the enzyme to oxygen. At the end of the reaction, the recyclability of the laccase was evaluated by removing the oxidized product and then adding fresh rice husk and TEMPO in the same amount as in the first cycle. The reaction was conducted as described above (section 3.3.2). Samples were withdrawn and analyzed after 24 and 48h, so that the same laccase solution was employed for a total of 96 h.

4.4.4 Assays for laccase activity

0.100 mL of 2,2′-Azino-bis(3-ethylbenzothiazoline-6-sulfonic acid) diammonium salt (ABTS) solution (0.02 M), 0.850 mL of citrate buffer and 0.050 mL of enzyme solution 0.125 mg mL-1 were added and the absorbance at 420 nm was monitored for 3 minutes. All the experiments were repeated 5 times. A solution containing 0.100 mL of ABTS, 0.02 M and 0.900 mL of citrate buffer were used as a reference. The laccase activity value (U/mL) was calculated using the following equation:

$$Activity\ {}^{U}/_{mL} = \frac{{}^{\Delta A}/_{min}}{36} \times \frac{V_{tot}}{V_{enz}}$$

4.4.5 Determination of carbonyl groups

The content of carbonyl groups was determined by reaction with hydroxylamine hydrochloride. This reacted with the hydroxylamine formed an oxime and the hydrochloric acid released was then titrated with sodium hydroxide. In 25 min of a 0.25 M solution of hydroxylamine hydrochloride, the pH was brought to 3.20 0.05 with HCl. About 200 mg of rice husk of hydrated oxidized rice was added to the solution and the suspension was allowed to react for 2 h under stirring. After this time, the reaction was titrated with 0.1 M NaOH to bring the pH back to 3.20. At the end of the titration, the mixture was fed, and the rice husk was dried for 6 h in an oven at 120 °C to determine the exact anhydrous weight of the analyzed sample.

To remove any interferences, a white consisting of a non-oxidized rice husk was treated with the same method, which was previously washed 6 times with a mixture ethanol:water

(50:50). Each measurement was performed twice. The content of carbonyl groups was calculated using the following formula:

$$mmol\ aldehyde/g_{carrier}\ \frac{V_{NaOH}\ \times\ C_{NaOH}}{m_{dry\ carrier}}$$

where V_{NaOH} is the volume in mL necessary to adjust the pH of the mixture to 3.20, C_{NaOH} is the concentration of NaOH (0.1 mmol/mL) and m_{dry} carrier is the mass in grams of the anhydrous samples.

4.4.6 Chemical oxidation of RH on 300g scale

300g of rice husk (particle size 200-400µm) previously washed with a mixture of H_2O:ethanol 50:50 (3x1000 mL) was places in a Becker with 22g of $NaIO_4$ and 500mL of deionized water. The mixture was allowed to react under stirring on the blood rotator for 22 h in the dark and at 25°C.At the end of the reaction, the rice husk was filtered and rinsed with deionized water (3x500mL). The rice husk was then dried in oven.

4.4.7 Enzymatic oxidation of RH on 300g scale

300 g of rice husk previously washed were placed in a flask and suspended in 500 mL of 0.1 M citrate buffer at pH 5. Rice husk was left overnight to get completely wet. The next day the mediator TEMPO in a concentration of 10 mM (12.56g) and the enzyme Laccase C are added to this suspension to have a concentration of 20 U/mg (15.13g). After complete dissolution of the TEMPO-mediator and suspension of the enzyme, citrate buffer solution was added to reach the final volume of 1L. The reaction mixture was kept under stirring at T=70°C for 48 hours. During the reaction, a treatment procedure with compressed air is carried out 10 times for 5 minutes. At the end of the reaction, rice husk was filtered and washed with bi-distilled water.

4.4.8 Immobilization of lipases

The lipases were immobilized according to the protocol of Cespugli et al. (2018) modified as follows: 0.2 g of oxidized RH were incubated with 1 mL of solution containing 2000 U (TBU) of each commercial lipase, diluted in phosphate buffer (0.5 M at pH 8). A solution of PEG-3000 (0.5 mL of a 2 mg mL^{-1} solution in phosphate buffer 0.5 M at pH 8) was added as stabilizer.

4.4.9 Lipase hydrolytic activity assay for determining tributyrin Units (TBU)

The activity of enzymatic preparations was assayed by following the tributyrin hydrolysis and by titrating with 0.1 M sodium hydroxide (NaOH), the butyric acid that is released during the

hydrolysis. Potentiometric titrations and pH measurements were performed using a Graphic DL50 Mettler Toledo automatic titrator.

An emulsion composed of 1.5 mL tributyrin, 5.1 mL gum arabic emulsifier (0.6% w v^{-1}) and 23.4 mL water was prepared in order to obtain a final molarity of tributyrin of 0.17 M. Successively, 2 mL of 0.1 M sodium-phosphate buffer (Nap) pH 7.0 was added to 30 mL of tributyrin emulsion and the mixture was incubated in a thermostated vessel at 30°C, equipped with a mechanical stirrer.

After pH stabilization, 100 mg of immobilized biocatalyst or 0.005 mL CaLB native solution was added. The consumption of 0.1 M NaOH was monitored for 14 min. One unit of activity was defined as the amount of immobilized enzyme required to produce 1 mmol of butyric acid per min at 30° C. One unit (U) of lipase activity was defined as the amount of enzyme which liberated 1 mmol of butyric acid per minute under the given assay conditions.

4.4.10 Determination of the leaching of the enzymes after covalent Immobilization

At the end of the test for enzymatic activity, the biocatalyst was removed by filtration and 500 µL of the filtrate was taken, which were subjected to the enzymatic activity assay with tributyrin hydrolysis.

4.4.11 Energy dispersive X-ray spectroscopy (EDS)

Samples were analyzed thanks to the collaboration with Dr Lisa Vaccari and Dr Nicola Ceffarin at ELLETTRA Sincrotrone – Trieste. Non-metallized samples were investigated with Zeiss Supra 40 high resolution Field Emission Gun (FEG) Scanning Electron Microscope (SEM). Images were obtained by collecting secondary electrons with the electron high tension (EHT) equal to 10 keV thanks to an EverhartThornley detector. The microscope was equipped with an Oxford Aztec energy dispersive X-ray spectroscopy (EDS) system and an X-act 10 mm silicon drift detector (SDD) for compositional analysis. The same energy of 10 keV was exploited to collect the silicon signal on the sample.

4.4.12 SEM microscopy

Samples were analysed thanks to the collaboration with Elettra-Synchrotron of Trieste. Samples were metallized with the S150A Sputter Coater instrument (Edwards High Vacuum, Crawley, West Sussex, UK) before being observed with the Leica Stereoscan 430i scanning electron microscope (Leica Cambridge Ltd., Cambridge, UK) integrated with an Si detector (Li) PENTAFET PLUS TM, with an ATW TM window (Oxford Instruments, Oxfordshire, England) for microanalysis.

4.4.13 Stereoscopic microscopy

Samples were analysed thanks to the collaboration with Department of Life Sciences of University of Trieste. The immobilized biocatalysts were characterized by using a stereomicroscope (Leica MZ 16, Leica Microsystems, Wetzlar, Germany), equipped with a Kiralux CS505CU camera (Thorlabs Inc., Newton, NJ, USA).

4.4.14 Delignification of rice husk

5g of rice husk were placed in a Becker with 20 mL H_2O_2 (30%$_{v/v}$) and 0.1 g of NaOH. The mixture is kept under stirring at T=70°C. Foam formation is observed. 40 minutes after reaching the reaction temperature, 15 mL of 30% H_2O_2 and 0.1 g of NaOH are added. After 1 hour and 30 minutes the addition of H_2O_2 (30%$_{v/v}$) and 0.1g of NaOH is repeated.

After the last addition, the foam persists for 1 hour and 45 minutes.

The reaction mixture was kept under stirring for 5 hours. At the end rice husk was filtered and the solid residues are washed with bi-distilled water (3 x 10 mL). Figure 4.14 shows the product of wet (figure 4.14a) and dry (figure 4.14b) delignification

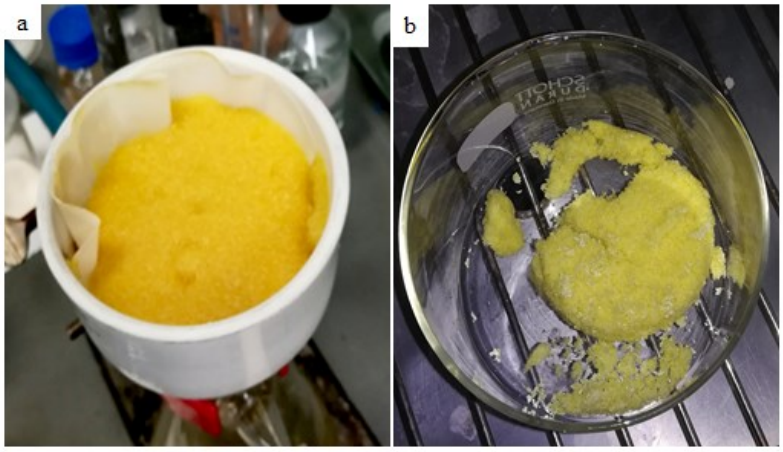

Figure 4.14 *Delignified rice husk a) wet and b) dried.*

The delignified husk samples were analyzed using the IR technique by using FT-IR 4700 JASCO. The spectrum was recorded by pressing the husk sample until obtaining a homogeneous tablet.

4.5 RESULTS AND DISCUSSIONS

4.5.1 Functionalization of rice husk (RH) using a laccase-mediator system (LMS)

The present study intends to overcome two problems related to the previous immobilization protocols that were hampering the scalability of the method. Firstly, the widely documented toxicity of glutaraldehyde (GA), despite which, GA is still used in the food industry according to strictly defined official regulations. The adverse health effects on humans include sensitization of skin and respiratory organs; closed systems are recommended to prevent hazards from GA exposure in industrial plants (Takigawa and Endo, 2006). Secondly, the recyclability of the laccase enzymes used in the oxidative process and the optimization of the protocols for their employment.

Milled RH particles (200-400 μm) were oxidized chemically and enzymatically and the performance of the two different carriers were compared. The chemical oxidation was accomplished using $NaIO_4$. The enzymatic oxidation process was performed taking inspiration from the work of Patel and co-workers that described the oxidation of the C6 hydroxyl of glucose in the cellulose chain catalyzed by laccase in the presence of TEMPO-radical (2,2,6,6-tetramethylpiperidin-1-yl)oxy) (Patel et al., 2011).

Starting from the preliminary work reported in the PhD thesis of Marco Cespugli (Cespugli M., 2018), who tested laccase from *Trametes sp.* and laccase from *Myceliophthora thermophile* in the presence of TEMPO-radical as mediator (figure 4.15a), the oxidation conditions were optimized by using a larger amount of RH (from 0.2 g up to 0.5 g in 10mL buffer) while maintaining the concentration of enzyme as low as 8 U mL^{-1}. At the same time, the temperature was increased from 20°C to 70°C. (figure 4.15b). The efficiency of the two oxidation protocols was compared by quantifying the carbonyl group using the hydroxylamine hydrochloride assay (Cespugli et al., 2018; Giugo et al 2014). The results in Figure 4.15b confirm that it is possible to significantly decrease the amount of enzyme used when the temperature is increased. More importantly the laccase was also recycled. After 48 hours the oxidized RH was removed by filtration and some fresh rice husk was added in the same enzymatic solution. Without the addition of TEMPO, the concentration of carbonyl groups still increased after 24 hours (figure 4.15b) indicating a residual presence of unreacted TEMPO deriving from the first cycle. When TEMPO was added to the recycled enzymatic solution, the carbonyl groups increased by 166% in 24 h and 177% in 48 h. Overall, the data suggests that the TEMPO concentration can be reduced in both cycles and that the oxidation occurs much faster in the second cycle (terminated in 24 h), probably due to an overactivation of the laccase, as a result of some beneficial conformational modifications that improve the electron transfer pathway already observed in previous studies of our group on a different laccase (Ferrario et al., 2015).

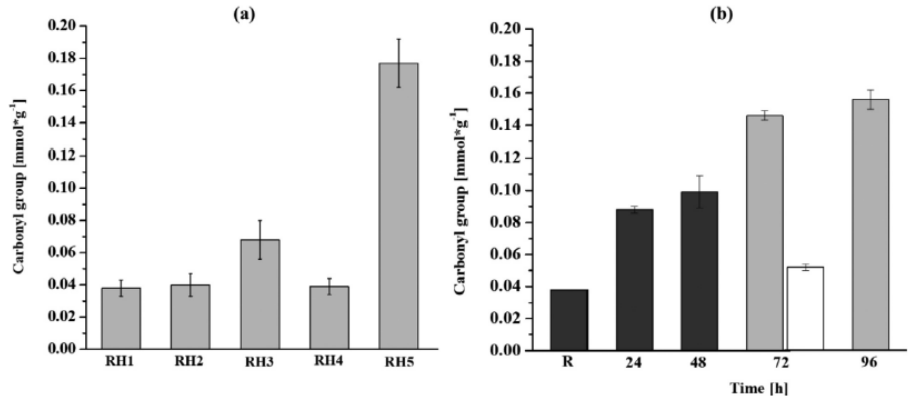

Figure 4.15 *(**a**) Concentration of carbonyl groups in different oxidation treatments at 20 °C. RH1: untreated rise husk; RH2: Novozyme 51,003 20 U mL⁻¹; RH3: Laccase C 8 U mL⁻¹; RH4: Laccase C 40 U mL⁻¹ without TEMPO; RH5: Laccase C 40 U mL⁻¹ with TEMPO. (**b**) Oxidation at 70 °C and Laccase C 8 U mL⁻¹ and recycling of laccase: first 48 h cycle of oxidation (black bars); laccase reused for a second oxidation cycle on fresh RH (grey bars); recycled laccase but without addition of TEMPO.*

It must be underlined that after 96 hours of reaction the laccase from *Trametes sp*. remains active. This suggests that the process can be further optimized in order to maximize the number of oxidative cycles and minimize the economic impact of the process (Spennato et al., 2021). The TEMPO mediator is essential for the effective oxidation of the RH although its concentration might be reduced. However, the next challenge will be to replace the TEMPO mediator with renewable and economic natural mediators (Cañas and Camarero, 2010; Medina et al., 2013).

Finally, the formation of carboxylic groups was evaluated (figure 4.16). Data confirmed that the oxidation of aldehydes to carboxylic groups is not laccase mediated and that there is no significant influence of the enzymatic units employed, or of the type of laccase. Not even the presence of TEMPO affects the formation of carboxylic groups, and the variation of carboxylic groups, both with chemical and laccase treatments, appears limited.

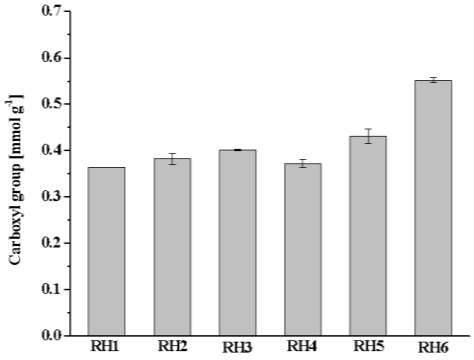

Figure 4.16 *Concentration of carboxyl groups on milled rice husk (RH) upon oxidation in the presence of different laccases and different enzymatic concentrations (Laccase-Mediator System – LMS). RH1: untreated RH; RH2: laccase Novozyme 51003 8 Uml⁻¹ and TEMPO mediator; RH3: Laccase C 8 U ml⁻¹ and TEMPO; RH4: Laccase C 40 U/ml NO TEMPO; RH5: Laccase C 40 U ml⁻¹ with TEMPO; RH6: chemical oxidation by $NaIO_4$.*

The morphology of the RH after chemical oxidation or enzymatic oxidation appeared very different according to SEM characterization. Figure 4.17 shows the corrosive effect of $NaIO_4$ which leads to the oxidative cleavage, opening the access to deeper layers of the material, both inside the tracheid structures (figure 4.17c) and on the outer surface (figure 4.17a). The enzymatic treatment with laccase leads to negligible morphological modification on the external surface, while it leads to a modest increase of the roughness of the internal surface of the tracheids (Spennato et al., 2021).

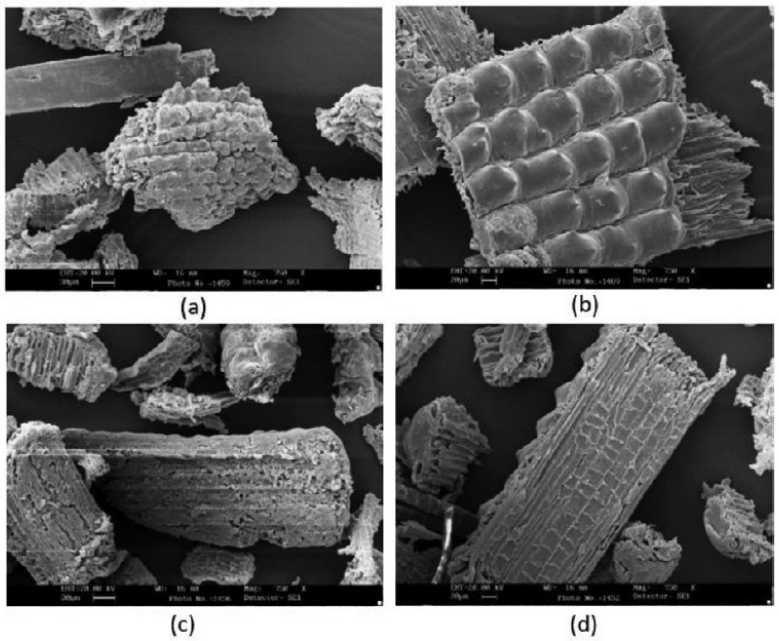

Figure 4.17 *SEM images illustrating the effect of $NaIO_4$ (a, c) vs enzymatic oxidation (b, d) on the morphology of RH. Corrosive effect of the $NaIO_4$ on the surface(a) and on the inner cellulosic matrix of tracheid (d).*

4.5.2 Covalent immobilization of lipases on functionalized rice husk without the use of glutaraldehyde

The aim of this study was to simplify the immobilization protocol, avoiding the use of hexamethylenediamine (HMDA) and of glutaraldehyde (GA). Protocols of immobilization of lipases were developed, exploring the possibility of forming the imine bond directly between the lysine residues and the carbonyl group on C6 obtained with enzymatic oxidation which appears more accessible than the di-aldehyde groups obtained in the chemical oxidation using the toxic $NaIO_4$.

Three different lipases were evaluated: lipase B from *Candida Antarctica* (CaLB), lipase from *Thermomyces lanuginosus* (TLL) and lipase from *Rhizopus oryzae* (ROL) (figure 4.18).

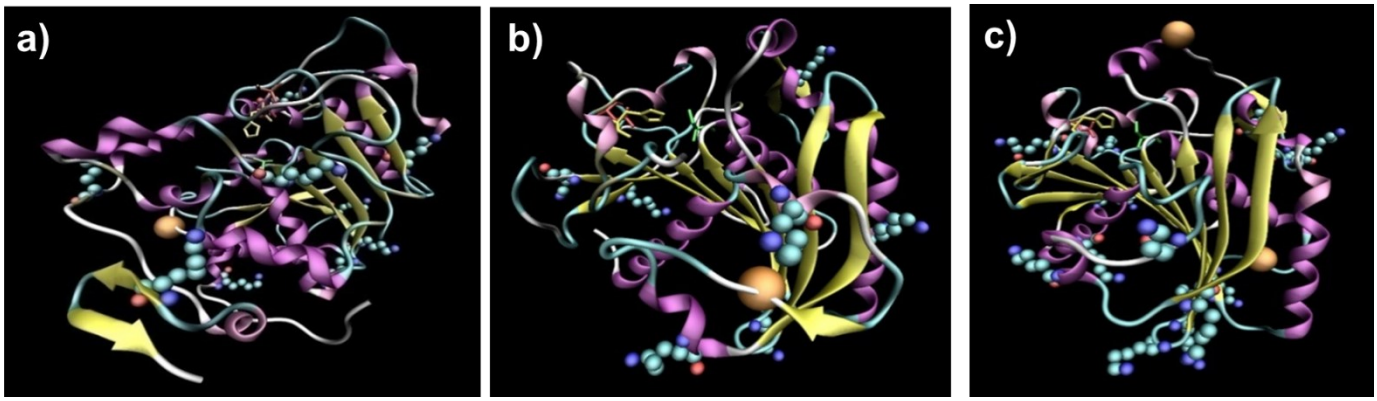

Figure 4.18 *Structure of the lipases used in the study: a) CaLB; b) TLL; c) ROL.*

TLL and ROL undergo interfacial activation (Ferrario et al., 2011) when approaching a hydrophobic phase, whereas CaLB does not undergo significant conformational changes and its active site is permanently accessible (Basso et al., 2007; Ferrario et al., 2011) .

The analysis of the number and the position of lysine residues potentially involved in the covalent binding with the carrier indicates that CaLB and TLL have 9 and 7 lysine respectively, whereas ROL has 15 lysins, one of them located in the proximity of the active site. This feature makes the immobilization of ROL difficult. In fact, the formation of the covalent bond can occlude the active site but also prevent the necessary conformational changes related to interfacial activation. As proof of this, previous data collected in our group showed that the hydrolytic activity is completely lost with the covalent immobilization of ROL in aqueous buffer on methacrylic epoxy resins (Cespugli et al., 2018; Gardossi L. et al., 2012).

Table 4.2 shows the results concerning the immobilization of lipases on rice husk by using a simplified protocol that implies the direct bonding of the enzymes on the aldehyde groups of functionalized rice husk, avoiding spacers and glutaraldehyde (figure 4.19).

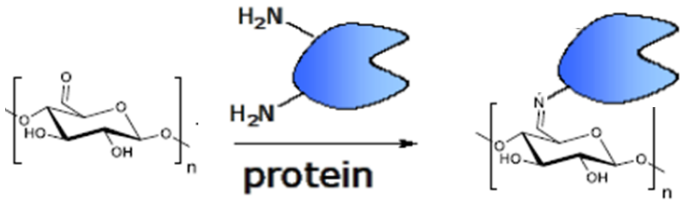

Figure 4.19 *Direct bonding of the lysin residues of enzymes on the aldehyde groups of rice husk oxidized by means of the laccase-mediator method.*

Table 4.2 Results of lipases covalently immobilized on RH. In all cases 10.000 U of lipase per g of RH were employed. The activity is expressed as the average of three measurements. LMS = laccase from *Trametes* sp. + TEMPO mediator. Last three entries were published in ref. (Cespugli et al., 2018) and are reported for comparison.

Lipase	Oxidation Method	Other functionalization	Protein Loaded (%)	Hydrolytic activity (U g^{-1} dry)	Immobilization yield (%)
CaLB	**LMS**	**no**	**65**	**590 ± 2**	**5.9**
TLL	LMS	no	72	974 ± 65	9.74
ROL	LMS	no	53	328 ± 42	3.28
CaLB	$NaIO_4$	no	33	290 ± 45	2.90
TLL	$NaIO_4$	no	56	643 ± 67	6.43
ROL	$NaIO_4$	no	32	171 ± 14	1.71
CaLB	LMS	GA	55	155 ± 5	1.55
CaLB	$NaIO_4$	GA	65	< 50	< 0.5
CaLB	**LMS**	**HSDA+GA§**	**17**	**56 ± 25**	**0.56**
CaLB	$NaIO_4$	HSDA+GA§	72	316	3.16
CaLB	n.a.	Epoxy (on methacrylic resin)§	95	709	7.09

§ previously published

The data from table 4.2 indicates that the simplified protocol significantly increases the specific activity of CaLB immobilized on enzymatically oxidized RH (results in bold). This might be explained by the reactivity of glutaraldehyde as a crosslinker that involves different functional groups on the enzyme thus inducing an array of covalent modifications that affect enzyme activity. Compared with CaLB immobilized on commercial epoxy methacrylic resins, the immobilization yield is 5.9 with respect to 7.09, mainly due to the lower loading capacity of the RH. It must be underlined that the immobilization yield of lipases, when covalently linked, is generally very low due to their hydrophobic surface that hampers a correct orientation of the enzyme upon bonding. Additionally, for TLL and ROL the conformational mobility, which is necessary for displaying the catalytic activity, represents a challenge (Cespugli et al., 2018; Gardossi L. et al., 2012).

Very few studies report the actual immobilization yield accompanied by the evaluation of the protein leaching from the support as a proof of the robust anchorage of the enzyme on the carrier (Cantone et al., 2013; Ferrario et al., 2011).

4.5.3 Stability and recyclability of covalently immobilized lipases in aqueous media

The stability of the immobilized lipases on oxidized rice husk was evaluated in term of hydrolytic cycles of tributyrin, under vigorous mechanical stirring in aqueous media, demonstrating that CaLB and TLL on laccase oxidised rice husk have an excellent stability after 10 hydrolytic cycles, with about 80% and 70% of recovered activity, respectively. Details are available in figure 5 of manuscript “Turning biomass into functional composite materials: Rice husk for fully renewable immobilized biocatalysts” reported below (Spennato et al., 2021).

On the other hand, ROL retains only 15% of activity and this is ascribed to the leaching of ROL from RH as it is possible to see in figure 4.20; this also shows the absence of leaching for CaLB and TLL.

Notably, when the pH of the aqueous solution was modified to 4.5, the leaching of the enzymes was evident also for the TLL and CaLB formulation, confirming that the bonding of the enzyme to the RH matrix occur *via* the reversible formation of imino bonds, undergoing hydrolysis at acidic pH.

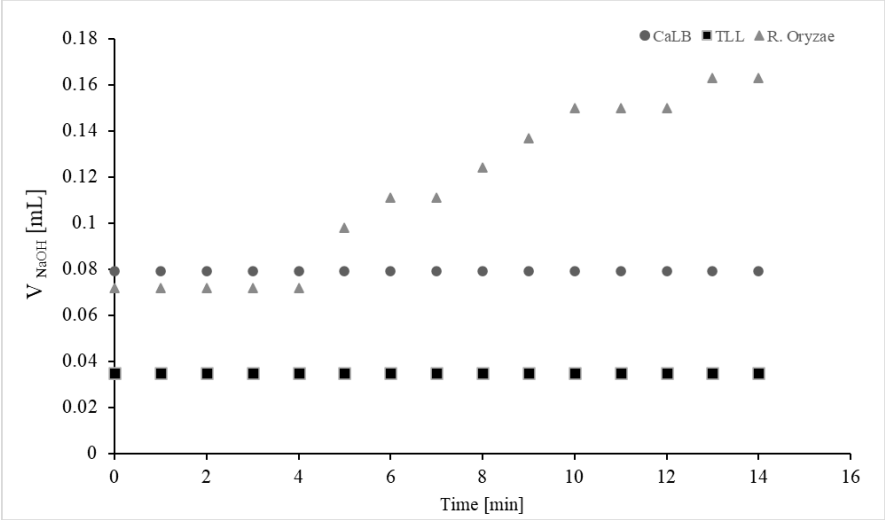

Figure 4.20 *Study of the leaching of the three lipases (CaLB, TLL and ROL) from the functionalized RH carrier after immobilization. The presence of the native enzyme in the aqueous solution was evaluated by measuring the residual activity present in the aqueous solution after filtration of the immobilized biocatalysts employed for the hydrolysis of tributyrin. The procedure was repeated for ten cycles.*

The leaching of ROL, despite the 15 lysine residues available for immobilization, is probably ascribable to a combination of structural and superficial characteristics that prevent an effective adsorption of the enzyme on the carrier and the nucleophilic attack of the amino groups of the lysine residues (Basso et al., 2007). Notably, ROL displays also the lowest protein loading as reported in table 4.2. Indeed, aqueous media induces unfavourable conformation modifications in some lipases as is demonstrated in molecular dynamics simulations (Ferrario et al., 2011) and to the best of our knowledge the only effective protocol

for the covalent immobilization of ROL was developed in organic media (Gardossi L. et al., 2012).

The results of this study were published in manuscript C reported below, which also describes a procedure for the physical immobilization of lipase TLL on rice husk. The latter study was carried out outside the context of the present PhD thesis work by other scientists.

4.5.4 **Manuscript C** *"Turning biomass into functional composite materials: Rice husk for fully renewable immobilized biocatalysts"*

EFB Bioeconomy Journal 1 (2021) 100008

Contents lists available at ScienceDirect

EFB Bioeconomy Journal

journal homepage: www.elsevier.com/locate/bioeco

Turning biomass into functional composite materials: Rice husk for fully renewable immobilized biocatalysts

Mariachiara Spennato [a], Anamaria Todea [a], Livia Corici [a,#], Fioretta Asaro [a], Nicola Cefarin [b], Gilda Savonitto [c], Caterina Deganutti [a], Lucia Gardossi [a,*]

[a] Department of Chemical and Pharmaceutical Sciences, University of Trieste, Via L. Giorgieri 1, Trieste 34127, Italy
[b] Elettra-Sincrotrone Trieste SCpA, SS 14, km 163.5, Basovizza, Trieste TS 34149, Italy
[c] Department of Life Sciences, University of Trieste, Via L. Giorgieri 10, Trieste 34127, Italy

ARTICLE INFO

Keywords:
Biocatalysis for bioeconomy
Covalent immobilization of lipases
Rice husk
Renewable immobilization carriers
Laccase oxidation of cellulose

ABSTRACT

Rice husk is an underexploited, low density and highly robust composite material, massively available from rice processing. Here we report two new procedures for the formulation of immobilized lipases applicable in fats and oils transformations. The enzymes were covalently anchored on aldehyde groups introduced on rice husk by laccase-catalysed oxidation of the cellulose component. The method avoids the use of toxic glutaraldehyde while allows for the application and recycling of the biocatalysts in aqueous media. The second method used a fluidized bed granulator for the coating of the particles of rice husk (200–400 μm) in the presence of water-soluble binders. The formulations are mechanically stable and suitable for applications in different hydrophobic media. Both methods allow for the recovery and reuse of the rice husk at the end of the life cycle of the biocatalysts.

1. Introduction

When considering the largest scale applications of enzymes in industry, they include glucose isomerase for production of high fructose syrup (10^7 ton/y), β-galactosidases for lactose hydrolysis in milk (10^5 ton/y), and lipase for transesterification of food oil (10^5 ton/y). All these processes are embedded in bioeconomy value chains and utilize immobilized enzymes (DiCosimo et al., 2013). An immobilized insoluble enzymatic formulation not only enables their reusability, thus lowering production costs, but also reduces waste stream generation (Girelli et al., 2020). In the last years, we have tackled the challenge of making biocatalysis more sustainable and suitable for the large-scale processes of bioeconomy by developing immobilized biocatalysts that exploit residual biomass from agricultural products. Achieving both the environmental and economic sustainability of immobilized enzymes is quite challenging, since the "ready to use" carriers, such as fossil-based methacrylic resins, are quite expensive and also responsible of greenhouse gas emission (Kim et al., 2009). Finally, the stability of organic fossil-based carriers was reported unsatisfactory under chemical and mechanical stress (Hilterhaus et al., 2008; Pellis et al., 2015; Korupp et al., 2010).

Considering that for bulk products the allowable cost contribution of immobilized enzymes should be around 0.05 € $kg_{product}^{-1}$ (Tufvesson et al., 2011), rice husks (RH) attracted our attention as a potential renewable carrier for enzyme immobilization. This lignocellulosic material is the second most abundant biomass globally, produced in around 120 Mt per year, of which only 20 Mt are used (Tuck et al., 2012). RH is an extremely robust composite material made of SiO_2, lignin, hemicellulose and cellulose, (Corici et al., 2016) which provides a versatile chemical platform for introducing functionalities (Raynaud 2014). It also meets circularity criteria because it can be re-utilized at the end of its proposed industrial application (Contreras et al., 2012). Finally, as natural material, it has the subsidiary advantage that it is subjected to less stringent legislative constraints even after chemical modification (Raynaud 2014). The tubular structure of tracheids confers to RH a very low density (< 0.4 g mL^{-1}), while SiO_2 is responsible for its remarkable mechanical robustness.

Our previous studies reported the chemical oxidative cleavage ($NaIO_4$) of the cellulose present in RH for the introduction of carbonyl functionalities, which were exploited for the binding of enzymes in the presence of glutaraldehyde as crosslinking agent (Corici et al., 2016; Cespugli et al., 2018; Pellis et al., 2017).

Applications of lipases in an aqueous environment require the covalent anchoring of the enzyme on the carriers for preventing the detachment of the protein and its partition in the medium (Biermann et al. 2000, Schmid and Verger 1998). Despite the wide number of studies present in the literature (Hanefeld et al., 2009), very few examples of co-

* Corresponding author.
E-mail address: gardossi@units.it (L. Gardossi).
Present Addresses: "Coriolan Drăgulescu" Institute of Chemistry, Mihai Viteazul 24, 300223 Timișoara, Romania

https://doi.org/10.1016/j.bioeco.2021.100008
Received 23 March 2021; Received in revised form 26 May 2021; Accepted 26 May 2021

valent binding on solid supports with satisfactory and clearly stated immobilization yields have been reported so far because of their structural and conformational features (Hilterhaus et al., 2008; Cantone et al., 2013). We have previously reported (Cespugli et al., 2018) that CaLB can be immobilized covalently on chemically oxidized RH after the introduction of a hexamethylenediamine spacer (HMDA) and employing glutaraldehyde as bi-functional agent able to form imine bonds with the spacer and the amine groups of lysine residues present on the surface of the lipase. The toxicity of GA is widely documented although it is still used in food industry according to strictly defined official regulations. The adverse health effects on humans include sensitization of skin and respiratory organs and closed-systems are recommended to prevent hazards from GA exposure in industrial plants (Takigawa and Endo 2006; Toxicological Profile, 2015; EFSA, 2011)

The present study illustrates two sustainable and scalable methods that demonstrate how it is possible to exploit RH as immobilization carrier while overcoming the use of toxic reagents, such as $NaIO_4$ and glutaraldehyde. The first approach exploits laccase enzymes for the oxidation of the cellulose component of RH and the introduction of aldehyde groups usable for the direct covalent anchoring of proteins. The method was validated with lipase B from *Candida antarctica* (CaLB) and lipase from *Thermomyces lanuginosus* (TLL), applied in the hydrolysis of triglycerides in aqueous media. The second immobilization method employs a fluidized bed granulator for the coating of RH with TLL in the presence of water-soluble binders and allows for the inexpensive immobilization of lipases to be used in low-water media.

2. Materials and methods

2.1. Chemicals

Lipase B from *Candida antarctica* (EC 3.1.1.3, CAS number 9001–62–1, liquid solution, activity: 1372 TBU g^{-1} (TBU = enzymatic Units calculated with tributyrin hydrolysis), protein content = 84 mg mL^{-1}) and Laccase Novozym 51,003 (EC 1.10.3.2., CAS number 80,498–15–3) from *Myceliophthora thermophila* expressed in *Aspergillus sp.* (activity: 64 U_{ABTS} mL^{-1}) were from Novozymes (Denmark). Lipase from *Thermomyces lanuginosus* (specific activity: 3176 TBU g^{-1}, liquid solution, protein content = 38 mg mL^{-1}) maltodextrin, Kollidon®25, 2,2,6,6-tetramethylpiperidin-1-yl)oxy (TEMPO), NaOH, $NaIO_4$, Bradford reagent, tributyrin and 2,2′-Azino-bis(3-ethylbenzothiazoline-6-sulfonic acid) diammonium salt (ABTS) were from Sigma-Aldrich. Lipase from *Ryzopus oryzae* (powder, activity: 29,496 U g^{-1}) was kindly donated by Amano Corporation (Japan). Laccase C (EC 1.10.3.2) from *Trametes versicolor* (2176 U_{ABTS} g^{-1}) was from ASA Spezialenzyme GmbH (Germany). PEG 3000 was from Merck. Arabic gum was from Fluka™. Hydroxyethylcellulose was from Esperis S.p.A. (Italy). The RH was kindly donated by Riseria Cusaro, Binasco (Italy), milled and sieved as previously reported (Cespugli et al., 2018). All enzymatic specific activities and protein content reported above were determined independently.

2.2. Chemical oxidation of rice husk

The chemical oxidation of RH was performed as previously described by Cespugli et al. (2018)

2.3. Assays for enzymes activity

Activity of laccases was evaluated using the ABTS method reported by Piscitelli et al. (2005) (see supplementary materials method S1).

The activity of lipases (hydrolysis of tributyrin) was assayed as previously described by Cespugli et al. (2018), Martins et al. (2013b).

2.4. Enzymatic oxidation of RH

Protocol at 20 °C: a 10 mM solution of TEMPO was added to 0.2 g of RH previously washed with 10 mL sodium citrate buffer 0.1 M pH 5. The laccase and the phosphate buffer were added to obtain a final concentration of 8 or 40 U mL^{-1} in 25 mL total. The protocol at 70 °C employed sodium citrate buffer 0.1 M pH 5 using a final laccase concentration of 8 U mL^{-1}. The reaction mixtures were magnetically stirred (350 rpm) and air was insufflated for 2 min every 8 h to increase the exposure of the enzyme to oxygen. At the end of the reaction, the mixture was filtered and washed with distilled water (15 mL, 4 times). The recyclability of the laccase was demonstrated as reported in ESI (Electronic Supplementary Information, method S2).

2.5. Immobilization of lipases on oxidized RH

The lipases were immobilized according to the protocol of Cespugli et al. (2018) modified as follows: on 0.2 g of oxidized RH by adding 1 mL of solution containing 2000 U (TBU) of each commercial lipase, diluted in phosphate buffer (0.5 M at pH 8) and adding PEG-3000 (0.5 mL of a 2 mg mL^{-1} solution in phosphate buffer 0.5 M at pH 8) as stabilizer.

2.6. Determination of carbonyl and carboxylic groups content

The content of carbonyl and carboxylic groups were determined as previously described by Cespugli et al. (2018). The details are included in the ESI material as method S3 and S4

2.7. Physical immobilization of lipase TLL on RH

The immobilization of TLL on 100 g of RH in the presence of polyvinylpyrrolidone (Kollidon®25), maltodextrin and hydroxyethyl cellulose was carried out in a fluid bed granulator Mini-Glatt fluidized bed (Glatt GMbH, Binzen, Germany) equipped with a conical vessel (volume of 0.75 L), three metallic filters and a timing filter blowing. The immobilization was performed by adapting a procedure previously described by Trastullo et al. (2015) and details are available in ESI as method S5.

2.8. Energy dispersive X-ray spectroscopy (EDS)

Non-metallized samples were investigated with Zeiss Supra 40 high-resolution Field Emission Gun (FEG) Scanning Electron Microscope (SEM). Images were obtained by collecting secondary electrons with the electron high tension (EHT) equal to 10 keV thanks to an Everhart-Thornley detector. The microscope was equipped with an Oxford Aztec energy dispersive X-ray spectroscopy (EDS) system and an X-act 10 mm silicon drift detector (SDD) for compositional analysis. The same energy of 10 keV was exploited to collect the silicon signal on the sample (Figure S1).

2.9. SEM microscopy

Samples were metallized with the S150A Sputter Coater instrument (Edwards High Vacuum, Crawley, West Sussex, UK) before being observed with the Leica Stereoscan 430i scanning electron microscope (Leica Cambridge Ltd., Cambridge, UK) integrated with an Si detector (Li) PENTAFET PLUS TM, with an ATW TM window (Oxford Instruments, Oxfordshire, England) for microanalysis.

2.10. Stereoscopic microscopy

The immobilized biocatalysts were characterized by using a stereomicroscope (Leica MZ 16, Leica Microsystems, Wetzlar, Germany), equipped with a Kiralux CS505CU camera (Thorlabs Inc., Newton, NJ, USA).

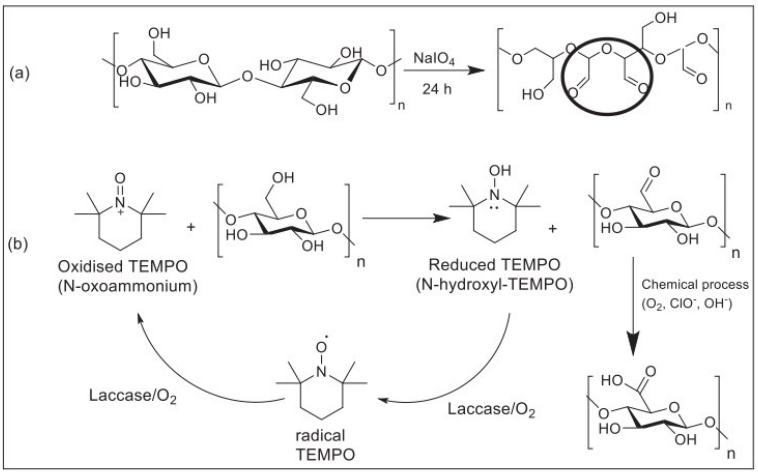

Fig. 1. Schematic comparison of the chemical and enzymatic mediated oxidation of cellulose. The $NaIO_4$ causes the oxidative cleavage of the glucose with the formation of two aldehyde groups. The laccase/TEMPO system oxidizes the primary hydroxyl group to an aldehyde, which undergoes spontaneous oxidation to carboxyl group.

2.11. Synthesis of butyl butyrate catalyzed by immobilized TLL in hexane and toluene

The immobilized TLL (160 mg) were incubated for 1 h at 48 °C in hexane or toluene (6.676 mL). The reaction was initiated by the addition of 1-butanol (0,618 mL) and butyric acid (0,206 mL) at 3:1 molar ratio. The reactions were carried out at 48 °C, in an orbital shaker (250 rpm) for 24 h and monitored by HPLC as reported in ESI (method S6). Control reactions without enzyme were performed under identical conditions. All the experiments were made in duplicate and the mean values were considered.

2.12. Synthesis of butyl butyrate catalyzed by physically immobilized TLL in isooctane

1-butanol (0.25 mL) and butyric acid (0.25 mL) (1:1 molar ratio) were added to 9.5 ml of isooctane and 130 mg immobilized TLL. The reaction was incubated at 45 °C in an orbital shaker (250 rpm) for 21 h and monitored as reported in ESI (method S7). All the experiments were made in duplicate and the mean values were considered.

3. Results and discussion

3.1. Enzymatic functionalization of RH

The covalent binding of proteins on any carrier requires the introduction of functional groups able to form suitable bonds with the side chains of amino acids present on the protein surface. We have previously reported the functionalization of RH through an oxidative cleavage of the cellulosic component by means of $NaIO_4$ (Corici et al., 2016; Cespugli et al., 2018). To improve the sustainability and scalability of the oxidative process, a protocol was developed in which the toxic $NaIO_4$ was replaced by laccase enzymes, copper-oxidases present in various organisms like bacteria, plants, insects and fungi (Claus 2004). Big molecules and non-phenolic compounds are oxidized with difficulty by laccases due to the reduced accessibility of the active site and also because of their low redox potential (Bourbonnais et al. 1995). This drawback can be overcome with the use of a *laccase-mediator system* (LMS), namely by adding a small molecule able to generate stable radical species (Cañas and Camarero 2010). In our work we have taken inspiration from the work of Patel and co-workers that describes the oxidation of the C_6 hydroxyl of glucose in the cellulose chain catalyzed by laccase in the presence of TEMPO-radical (Patel et al., 2011) (Fig. 1b)

In the present study, milled RH particles (0.2–0.4 mm) were oxidized by laccase from *Trametes* sp. and laccase from *Myceliophthora thermophile* and the content of carbonyl groups was assessed using the hydroxylamine hydrochloride assay (Cespugli et al., 2018; Guigo et al., 2014). Data in Fig. 2a indicate that laccase from *Trametes* sp. was more effective in oxidizing the RH and that the TEMPO mediator was necessary. The amount of the resulting carbonyl groups depends on the laccase units, with the highest concentration achieved in the presence of 40 U mL^{-1} of laccase from *Trametes* sp.

To decrease the amount of laccase in the oxidation process, a larger amount of RH was used in the reaction mixture while maintaining the same concentration of enzyme (Fig. 2b). The temperature was also increased to 70 °C and the recyclability of the laccase for further oxidative cycles was demonstrated. After 48 h of enzymatic treatment, the oxidized RH was removed by filtration and some fresh rice-husk was added in the enzymatic solution. Fig. 2b shows that without the addition of TEMPO the concentration of carbonyl groups still increased after 24 h, indicating a residual presence of unreacted TEMPO deriving from the first cycle. When TEMPO was added to the recycled enzyme, the carbonyl groups increased by 166% in 24 h and 177% in 48 h. Overall, the data suggest that the TEMPO concentration can be reduced in both cycles and that the oxidation occurs much faster in the second cycle (terminated in 24 h), thus demonstrating the recyclability of the laccase. The observed higher activity in the second cycle could be ascribed to activation phenomena occurring upon exposure to high temperature or denaturing factors, as reported in our study on laccase from *Stecchernum ochraceum* 1833. By means of molecular dynamics simulations we disclosed minor superficial conformational modifications of the laccase that improve its activity without causing severe unfolding nor the disruption of the electron transfer pathway (ETP) (Ferrario et al., 2015).

Current data on the preservation of the activity of the laccase from *Trametes* sp. during 96 h of reaction at 70 °C suggest that the enzymatic oxidative functionalization of RH can be further optimized in order to maximize the number of cycles and minimize of economic impact of the treatment. The TEMPO mediator seems to play a major role and although its concentration can be reduced, its environmental and economic impact deserves for further attention. Future studies will be focused on the replacement of TEMPO with renewable and inexpensive mediator molecules, which have been proved effective in previous studies (Cañas and Camarero 2010; Medina et al., 2013)

In all cases, the content of carbonyl groups measured after the enzymatic LMS method (Fig. 2a) resulted to be considerably lower than the 1 mmol g^{-1} obtained with 0.2 M $NaIO_4$. This difference can be partially ascribed to the formation of two carbonyl groups per each glucose

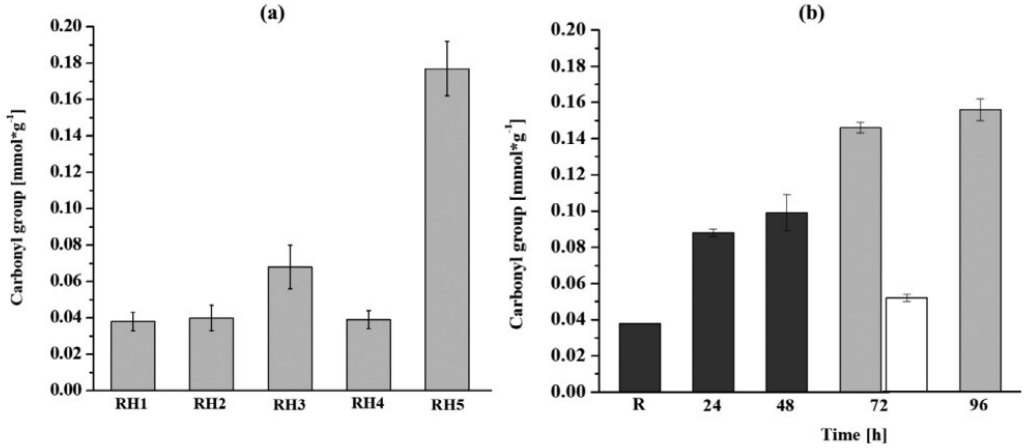

Fig. 2. (a) Concentration of carbonyl groups upon different oxidation treatments at 20 °C. RH1: untreated rise husk; RH2: Novozyme 51,003 20 U mL^{-1}; RH3: Laccase C 8 U mL^{-1}; RH4: Laccase C 40 U mL^{-1} without TEMPO; RH5: Laccase C 40 U mL^{-1} with TEMPO. (b) Oxidation at 70 °C and recycling of laccase: first 48 h cycle of oxidation (black bars); laccase reused for a second oxidation cycle on fresh RH (gray bars); recycled laccase but without addition of TEMPO.

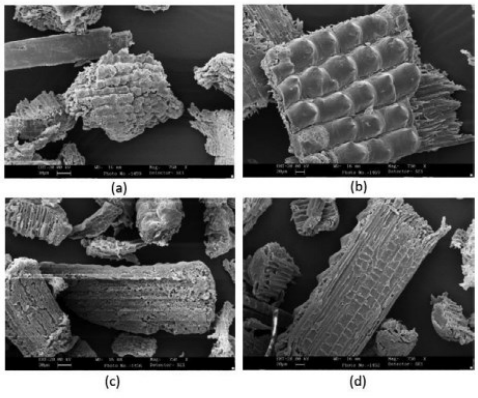

Fig. 3. SEM images illustrating the effect of $NaIO_4$ (a, c) vs enzymatic oxidation (b, d) on the morphology of RH. Corrosive effect of the $NaIO_4$ on the surface(a) and on the inner cellulosic matrix of tracheid (d).

unit, whereas in the case of LMS oxidation one single carbonyl group per glucose unit is formed. Moreover, SEM microscopy highlighted the corrosive effect of $NaIO_4$, which leads to marked covalent modification of the polysaccharide because of the oxidative cleavage, opening the access to deeper layers of the material (Fig. 3), both inside the tracheid structures (Fig. 3c) and on the outer surface (Fig. 3a).

Fig. 3 indicates the poor selectivity of the $NaIO_4$ towards the various components of the lignocellulosic matrix of the RH. On the contrary, the enzymatic treatment with laccase causes negligible morphological modification on the external surface, while leads to a modest increase of the roughness of the internal surface of the tracheids.

Morphological studies making use of energy dispersive X-ray spectroscopy (EDS) were of aid in understanding the robustness of the outer surface of the husk and, more precisely, the localization of SiO_2 (Park et al., 2003; Coletta et al., 2013). Using the EDS (Fig. 4 right) the Kα1 signal of the silicon (ESI Figure S1) was collected (green dots) to appreciate the presence SiO_2 on the surface of the RH and to confirm its role in protecting the rice grain from mechanical and chemical agents.

The formation of carboxylic groups during both the chemical and enzymatic oxidation processes were also evaluated (ESI Figure S2) and they confirmed that the oxidation of aldehydes to carboxylic groups is not laccase mediated.

3.2. Glutaraldehyde free covalent immobilization of lipases on RH

In the present study, we aimed at simplifying the immobilization protocol, by reducing the synthetic steps while avoiding the use of glutaraldehyde (GA). We have explored the possibility to form the imine bond directly between lysine residues and the carbonyl group on C_6 formed *via* laccase oxidation, which appears more accessible than the di-aldehyde groups obtained using $NaIO_4$. Two more lipases were tested in the study: lipase from *Thermomyces lanuginosus* (TLL) and lipase from *Rhizopus oryzae* (ROL), which are widely employed in the food sector for the transesterification of oils and fats (Higashiyama and Sumida 2004). Therefore, avoiding the use of glutaraldehyde in their formulations would be desirable (Zeiger et al., 2005).

The tri-dimensional models of the lipases are reported in ESI (Figure S 3). TLL and ROL undergo interfacial activation (Ferrario et al. 2011) when approaching a hydrophobic phase, whereas CaLB does not undergo significant conformational changes and its active site is permanently accessible (Ferrario et al. 2011, Basso et al., 2007). The analysis of the number and the position of lysine residues potentially involved in the covalent binding with the carrier indicates that CaLB and TLL have 9 and 7 lysines respectively, whereas ROL has 15 lysines, one of them located in the proximity of the active site. That feature makes the immobilization of ROL quite challenging, since the formation of the covalent bond can occlude the active site but also prevent the necessary conformational changes connected to the interfacial activation. Indeed, previous data collected in our group showed that the hydrolytic activity is completely lost upon covalent immobilization of ROL in aqueous buffer on methacrylic epoxy resins (Gardossi et al., 2012).

Data reported in Table 1 demonstrate that TLL and CaLB can be anchored directly on the enzymatically oxidized RH, while avoiding the use of glutaraldehyde and spacers. Higher loading was obtained in the case of RH oxidized enzymatically, indicating a regio-preference in the formation of imine bonds with the more accessible aldehyde groups on C_6.

The use of glutaraldehyde causes a significant reduction of the specific activity of CaLB formulations, probably ascribable to the forma-

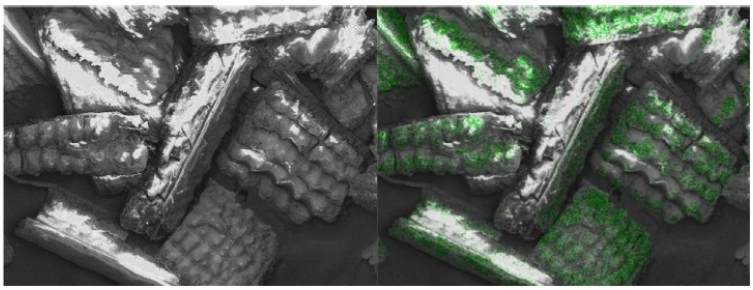

Fig. 4. Left: SEM image of fragments of milled RH, showing the linear ripples with conical shape on the external surface. Right: 2D map the distribution of SiO_2.

Table 1
Formulations of lipases covalently immobilized on RH. In all cases 10.000 U of lipase per g of RH were employed. The activity is expressed as the average of three measurements. LMS=laccase from *Trametes* sp. + Tempo mediator. Last three entries were published in ref. (Cespugli et al., 2018) and are reported for comparison.

Lipase	Oxidation method	Other functionalization	Protein loaded (%)	hydrolytic activity (Ug^{-1}_{dry})	immobilization yield (%)
CALB	LMS	no	65	590±2	5.9
TLL	LMS	no	72	974± 65	9.74
ROL	LMS	no	53	328± 42	3.28
CALB	$NaIO_4$	no	33	290±45	2.90
TLL	$NaIO_4$	no	56	643 ± 67	6.43
ROL	$NaIO_4$	no	32	171 ± 14	1.71
CALB	LMS	GA	55	155±5	1.55
CALB	$NaIO_4$	GA	65	<50	<0,5
CaLB	LMS	HMDA+GA[§]	17	56 ± 25	0.56
CaLB	$NaIO_4$	HMDA+GA[§]	72	316	3.16
CaLB	n.a.	Epoxy (on methacrylic resin)[§]	95	709	7.09

[§] previously published.

tion of unspecific covalent bonds and crosslinks. When compared to our previously published data of immobilization of CaLB on RH chemically oxidized and functionalized with diamino spacers with GA, the specific activity with the simplified protocol is almost doubled. The immobilization yield is comparable to that observed for CaLB immobilized on epoxy methacrylic carrier (Cespugli et al., 2018)

The immobilization yields are in line with previous experimental data obtained in the covalent immobilization of different lipases on epoxy methacrylic resins using aqueous buffer as immobilization medium, which have been always below 10% (Pellis et al., 2016; Gardossi et al., 2012). The difficulties encountered in the covalent immobilization of lipases have been discussed previously and they are ascribable both to their conformational and superficial structural features (Cantone et al., 2012; Ferrario et al., 2011). Conversely, very few studies report the actual immobilization yield accompanied by the evaluation of the protein leaching from the support, as a proof of the robust anchorage of the enzyme on the carrier. At the best of our knowledge, no covalently immobilized lipase is commercialized for industrial applications, although the hydrolytic applications of these enzymes request this type of formulation for enabling an efficient recycling of the biocatalyst and the reduction of the costs. As a matter of fact, an analysis of Tufvesson and co-workers (Tufvesson et al., 2011) indicated that in the case of biocatalysts immobilized by adsorption 63% of the material cost is ascribable to the carrier and only 37% to the enzyme. Taking into account that the cost of carriers for covalent immobilization is about 2–6 times higher, it is evident that the economic viability of these biocatalysts is mainly linked to the price of the carrier and the preservation of the enzyme activity across multiple reaction cycles (i.e. productivity). Therefore, there are several potential advantages deriving from the covalent immobilization of lipases on oxidized rice husk. Firstly the cost of the carrier is reduced; secondly the enzyme can be separated by the hydrolysis product and recycled, thus further decreasing the economic impact of the biocatalyst; finally, the re-use of the non-fossil and biodegradable carrier at the end of the biocatalyst life cycle would integrate environmental and economic sustainability.

3.3. Stability and recyclability of covalently immobilized lipases in aqueous media

The stability of the immobilized lipases was evaluated in the hydrolysis of tributyrin, under vigorous mechanical stirring. The results in Fig. 5 indicate an excellent stability of CaLB on rice husk and TLL on rice husk after 10 reaction cycles, with about 80% and 70% of recovered activity, whereas ROL retains only 15% of activity, which was ascribed to the leaching of ROL from RH, as experimentally observed (ESI, Figure S4). Notably, all biocatalysts reported in Table 1 were tested for protein leaching and only ROL formulations showed the detachment of the protein from the carrier.

Despite the presence of 15 lysine residues, ROL forms covalent bonds with difficulty, as also evident from the lower percentage of protein loaded (Table 1). This behavior cannot be ascribed to a unique factor, but rather to the combination of structural and superficial features (e.g. glycosylation) that prevent an effective adsorption of the enzyme on the carrier and the nucleophilic attack of the amino groups of the lysines (Basso et al., 2007). The observed loss of activity is most probably connected to conformational modifications occurring during the immobilization in aqueous systems, (Ferrario et al., 2011) as previously illustrated by some molecular dynamics simulations. The exposure to aqueous media induces unfavorable conformational modifications in some lipases, by causing the occlusion of the active site but also a rearrangement of the catalytic residues responsible for the catalytic mechanism (Ferrario et al., 2011). This observation would explain why the covalent immobilization of ROL is much more efficient when carrier out in a hydrophobic media (Gardossi et al., 2012).

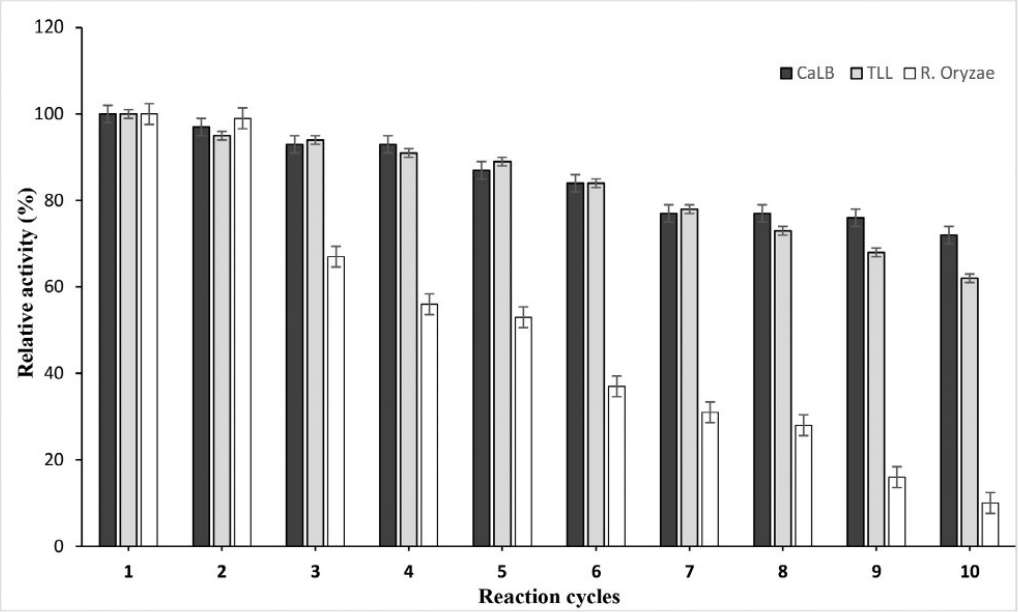

Fig. 5. Operational stability of CaLB on rice husk (black bar) TLL on rice husk (gray bar) and ROL on rice husk (white bar) in multiple hydrolytic cycles expressed as the percentage of retained activity after each cycle. Measurements were carried out in duplicate and reported as the average value.

3.4. Physical immobilization of TLL in a fluidized bed

The second part of the study was aimed by developing scalable procedures for the immobilization of lipases to be applied in low-water hydrophobic media, while ensuring environmental and economic sustainability. Generally, the application of immobilized enzymes in hydrophobic media does not require the covalent binding of the protein to the carrier, since the enzyme has a lower affinity for the hydrophobic phase (Pellis et al., 2015).

Lipase TLL was selected for the study and it was immobilized on milled RH (200–400 μm) in a fluidized bed in the presence of an aqueous solution of different binders approved for pharmaceuticals and food applications: Kollidon 25 (polyvinylpyrrolidone=PVP) (Reddy and Sharma, 2020), hydroxyethyl cellulose (HEC) (Di Giuseppe 2018) and maltodextrin (MLDX) (Velásquez-Cock et al., 2018). A uniform layer of enzyme coated the RH and the immobilized biocatalysts appear as distinct particles, without any example of agglomerates (Fig. 6).

3.5. Synthesis of butyl butyrate catalyzed by TLL physically immobilized on rice husk particles

The efficiency of the TLL formulations obtained through physical immobilization was evaluated in the synthesis of butyl butyrate starting from butyric acid and 1-butanol (Martins et al., 2013a). This short chain fruity ester, present in pineapple flavor (Martins et al., 2013), is used in perfumes and fragrances, waxes, washing, cleaning, cosmetics and personal care products (Xin et al., 2016). Three organic solvents were tested: toluene (log P 2.5), hexane (log P 3.5) and isooctane (log P 4.6). Figs. 7 illustrates the time-course of the reactions in hexane and toluene, indicating striking differences of performance of the biocatalysts. In hexane,PVP-TLL leads to complete conversion in less than 5 h, whereas the profiles of the other two reactions suggest some lag-time before the starting of the reactions, possibly ascribable to some mass transfer limitation. Conversions > 93% were achieved in all cases and it was noticed that the absence of agglomerates confers high mechanical stability to the formulations, preventing disaggregation and production of fines upon stirring.

All reactions carried out in toluene were considerably slower: PVP-TLL was the best performing formulation with > 80% conversion after 8 h of reaction, while MLDX-TLL stopped working after 10% of conversion.

Control reactions were performed in the absence of the biocatalyst, using lipase free particles of RH treated in the fluidized bed only with the binders. Moreover, blank experiments demonstrated the absence of any aspecific adsorption of the substrate on the biocatalyst when incubated in toluene (ESI Figure S5).

When the synthesis was conducted in isooctane (Batistella et al., 2012), the substrates were employed in equimolar amounts, resulting in a lower concentration of 1-butanol as compared to the previous synthesis. In this way we wanted to verify the possibility to achieve quantitative conversion even without using an excess of the polar alcohol, which is known to affect negatively the stability of enzymes.

Interestingly, HEC-TLL and MLDX-TLL performed significantly better as compared to what was previously observed in toluene and with similar conversions and reaction rate, whereas the reaction catalyzed by PVP-TLL stopped after 35% of conversion due to the formation of aggregates. However, figure 9b shows how the addition of 0.1% v/v of water improved the behavior of PVP-TLL, by preventing the aggregation. These data suggest that the performance of PVP-TLL improves in the presence of hydrophilic components in the reaction mixture, and explain the higher observed efficiency of this formulation in the presence of a higher concentration of the hydrophilic 1-butanol (Fig. 8). Therefore, the operational conditions must be optimized according to the LogP of the medium, the nature of the substrates and also the water content (Basso et al., 2001) Previous studies demonstrated that TLL can work efficiently in a wide range of water activity values, going from 0.33 to 0.97 (Persson et al., 2002; Adlercreutz 2013). Therefore, the hydration appears to exert only a minor effect on the intrin-

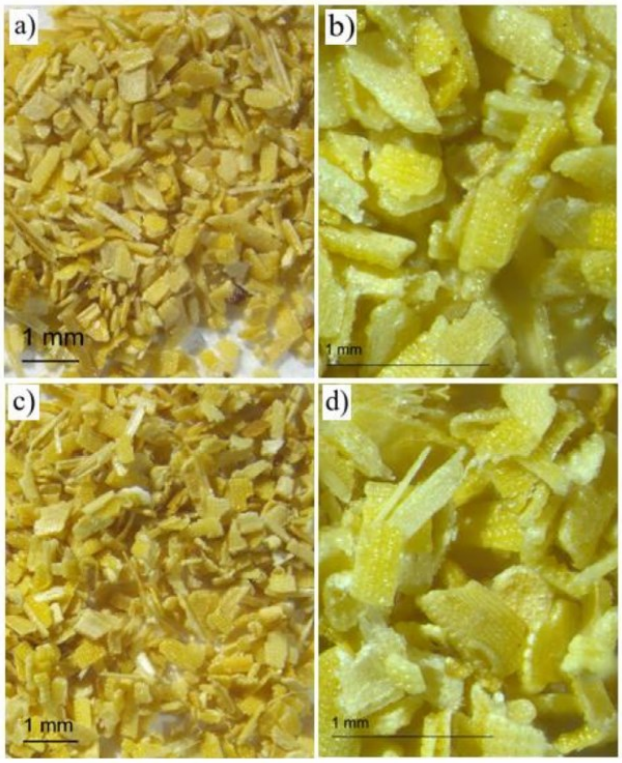

Fig. 6. TLL physically immobilized on rice husk particles and prepared using a fluidized bed reactor. Images obtained by means of stereoscopic microscopy at different magnification values: PVP (a)–10x (b)–60x and HEC (a)–10x (b)–60x.

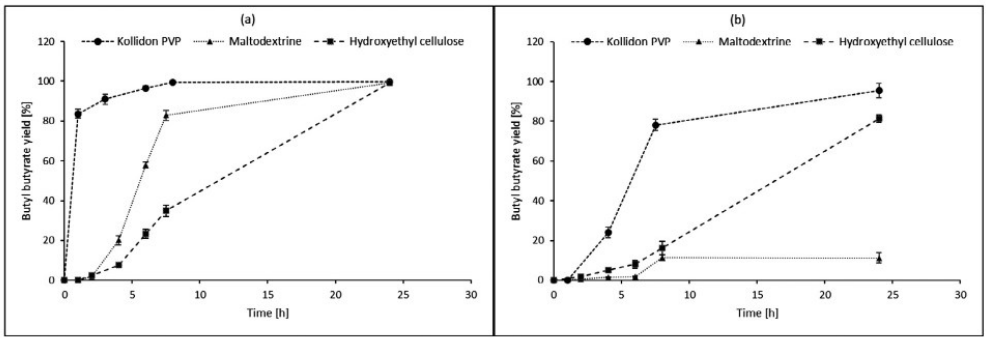

Fig. 7. Reaction profiles of the synthesis of butyl butyrate synthesis catalyzed by TLL physically immobilized on rice husk particles in hexane (a) and toluene (b).

sic activity of the lipase, whereas the partition phenomena appear to predominate.

3.6. Stability of physically immobilized TLL and reusability of rice husk

PVP-TLL and HEC-TLL were tested under hydrolysis conditions and vigorous stirring in order to evaluate the mechanical stability of the formulations but also to monitor the detachment of the enzyme from the RH. The determined hydrolytic activities (TBU) were 4459 Ug^{-1} for HEC-TLL and 6609 U g^{-1} for PVP-TLL. Compared to the previously immobilized TLL onto silica granules, the hydrolytic activities obtained in this study were at least 2 times higher (Ferrer et al., 2002). Microscope images (ESI Figure S6) demonstrate that the integrity of the RH is fully preserved after 10 cycles of reaction under vigorous mechanical stirring. It must be noted, that after 4 years of storage at 4 °C PVP-TLL and HEC-TLL preserved 96% and 82% of hydrolytic activity respectively. No microbial contamination was observed, indicating the long-term stability of the two formulations.

Notably, the most widely employed commercial formulation of TLL is Lipozyme TL IM (Sven et al., 1996), which consists in agglomerates having a size of about 600 μm, made by the enzyme adsorbed on silica particles (< 100 μm) with the aid of a binder. They are mechanically stable for both batch and fixed bed column operation but only in low water media. RH confers to the biocatalyst the additional advantage of

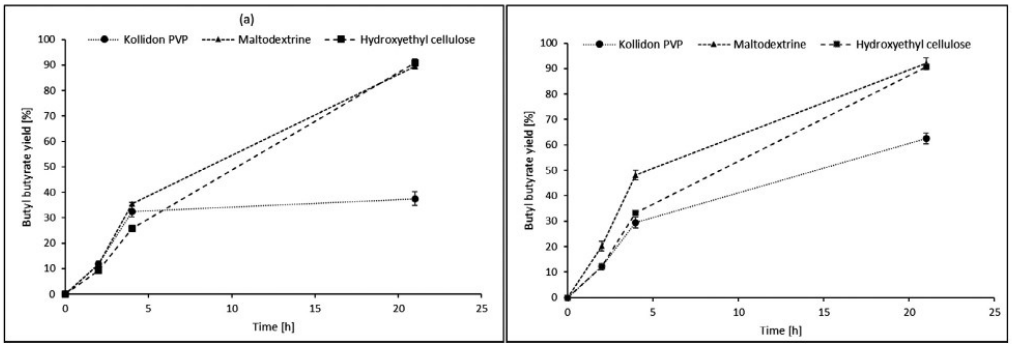

Fig. 8. Synthesis of butyl butyrate catalyzed by the three different formulations of immobilized TLL in isooctane (a) and isooctane with addition of 0.1% (v/v) of H_2O (b).

being made by a single robust fragment of composite material, which does not undergo disaggregation or the formation of fines under physical stress.

Concerning the reusability of RH, data confirm that the enzyme detaches from RH (>90%) after one cycle in aqueous solution (Figure S6) but the carrier remains intact (Figure S7). Therefore, at the end of the biocatalyst life cycle, the RH can be reutilized either as immobilization carrier or for secondary uses (Contreras et al., 2012).

In order to perform a very preliminary analysis of the economic sustainability of new value chains for the valorization of rice, we considered the Italian context. Rice mills sell only a fraction of rice husk for a maximum price of 90€ ton^{-1} (CCIAA, 2021). That rice husk is used by florists, farmers for animal litter and poultry farms. Some of the rice husk is employed by mills also for the internal production of energy and steam required for parboiled rice production. However, the ash content of burnt rice husk is very high (about 20% by weight) compared to other biomass such as poplar (1.0%) and dealing with the large amount of remaining ash is extremely difficult. Therefore, rice husks can be sustainably used as a fuel for energy recovery only when their ash is used as a resource. When burnt at 700 °C, rice husk yields ash contains 97% silica in amorphous form, which has many applications such as in constructional works, in the production of porcelain or as amendant in paddy fields. (Sekifuji and Tateda 2019).

Notably, the costs of commercial organic carriers, are around 50 € kg^{-1} for adsorption immobilization, which means that they have no chemical functionalities on their surface, but they simply interact with the protein by weak non-covalent interactions (Tufvesson et al., 2011). Carriers price reaches 100–300 € kg^{-1} when they are functionalized for covalent immobilization, and these figures make evident that there is potential for new uses of rice husk and that rice mills would find more advantageous to sell larger amounts of rice husk to industries able to transform it in added value products, which, at the end of their life cycle, could be transformed in energy or eventually return to the soil. The latter use would be particularly feasible for biocatalysts applied in the food sector, where nontoxic substrates are processed.

Conclusions

Data here reported demonstrate that RH is a versatile natural composite material that can be used both for the covalent and physical immobilization of lipases. The covalent immobilization was performed by anchoring the protein directly on the functionalized carrier, without the need of spacers or glutaraldehyde, leading to stable formulations of TLL and CaLB, retaining > 70% of activity after 10 cycles of hydrolysis. These biocatalysts, because of their stability and robustness, are applicable in various reaction media and under mechanical stress. The functionalization of RH was achieved by means of laccases in the presence of TEMPO mediator and the laccase was reused for different oxidative cycles. The next optimization steps will be focused on the replacement of TEMPO with renewable mediator molecules.

The inexpensive and easily scalable immobilization of lipase TLL was achieved using a fluid-bed granulator and water-soluble binders. Because of the low toxicity of the materials and the possibility of reusing the RH at the end of the biocatalyst life cycle, this method appears appropriate for industrial applications in low-aqueous media requesting low-toxic, inexpensive and sustainable solutions.

Overall, the methods here presented intend to provide a contribution to the development of a new wave of renewable industrial carriers for enzyme immobilization, able to replace petrol-based materials and to overcome their natural capital cost (Raynaud J., 2014).

Authors contribution

Conceptualization: Lucia Gardossi, Mariachiara Spennato
Methodology: Mariachiara Spennato, Livia Corici
Validation: Mariachiara Spennato, Anamaria Todea, Fioretta Asaro
Investigation: Mariachiara Spennato, Nicola Cefarin, Gilda Savonitto, Caterina Deganutti
Writing - Original Draft Preparation: Mariachiara Spennato, Anamaria Todea, Lucia Gardossi, Livia Corici, Caterina Deganutti
Writing - Review & Editing: Mariachiara Spennato, Anamaria Todea, Lucia Gardossi, Fioretta Asaro
Supervision Lucia Gardossi
Funding acquisition Lucia Gardossi

Declaration of Competing Interest

The authors declare that they have no known competing financial interests or personal relationships that could have appeared to influence the work reported in this paper.

Acknowledgment

The authors are grateful to Italian Ministero dell'Istruzione dell'Università e della Ricerca for the financial support provided through the CARDIGAN project (CARDoon valorisation by InteGrAted biorefiNery, Progetti di Ricerca di Interesse Nazionale -Bando 2017). Livia Corici is grateful to the European Commission for a fellowship (grant agreement No. 289253 - REFINE project). We are grateful to Marco Cespugli, Simone Lotteria and Francesca Vita for the assistance in the characterization of the materials.

Supplementary materials

Supplementary material associated with this article can be found, in the online version, at doi:10.1016/j.bioeco.2021.100008.

References

Adlercreutz, P., 2013. Immobilisation and application of lipases in organic media. Chem. Soc. Rev 42, 6406–6436.

Basso, A., De Martin, L., Ebert, C., Gardossi, L., Linda, P., Zlatev, V., 2001. Activity of covalently immobilised PGA in water miscible solvents at controlled a_{w}. *J. Mol. Catal. B: Enzym* 11, 851–855.

Basso, A., Braiuca, P., Cantone, S., Ebert, C., Linda, P., Spizzo, P., Caimi, P., Hanefeld, U., Degrassi, G., Gardossi, L., 2007. *In silico* analysis of enzyme surface and glycosylation effect as a tool for efficient covalent immobilization of CalB and PGA on Sepabeads®. Adv. Synth. Catal 349, 877–886.

Batistella, L., Ustra, M.K., Richetti, A., Pergher, S.B., Treichel, H., Oliveira, J.V., Lerin, L., de Oliveira, D., 2012. Assessment of two immobilized lipases activity and stability to low temperatures in organic solvents under ultrasound-assisted irradiation. Bioprocess. Biosyst. Eng. 35 (3), 351–358.

Cañas, A.I., Camarero, S., 2010. Laccases and their natural mediators: biotechnological tools for sustainable eco-friendly processes. Biotechnol. Adv 28, 694–705.

Cantone, S., Spizzo, P., Fattor, D., Ferrario, V., Ebert, C., Gardossi, L., 2012. Lipases for bio-based chemistry: efficient immobilised biocatalysts for competitive biocatalysed processes. Chim. Oggi 30 (3), 10–14.

Cantone, S., Ferrario, V., Corici, L., Ebert, C., Fattor, D., Spizzo, P., Gardossi, L., 2013. Efficient immobilisation of industrial biocatalysts: criteria and constraints for the selection of organic polymeric carriers and immobilisation methods. Chem. Soc. Rev 42, 6262–6276.

Cespugli, M., Lotteria, S., Navarini, L., Lonzarich, V., Del Terra, L., Vita, F., Zweyer, M., Baldini, G., Ferrario, V., Ebert, C., Gardossi, L., 2018. Rice husk as an inexpensive renewable immobilization carrier for biocatalysts employed in the food, cosmetic and polymer sectors. Catalysts 8, 471.

CCIAA 2021, https://www.paviaprezzi.it/ingrosso/pavia/index?screen=medie

Claus, H., 2004. Laccases: structure, reactions, distribution. Micron 35, 93–96.

Coletta, V.C., Rezende, A.C., da Conceição, R., Polikarpov, I., Guimarães, F.E.G., 2013. Mapping the lignin distribution in pretreated sugarcane bagasse by confocal and fluorescence lifetime imaging microscopy. Biotechnol. Biofuels 6, 43.

Contreras, L.M., Schelle, H., Sebrango, C.R., Pereda, I., 2012. Methane potential and biodegradability of rice straw, rice husk and rice residues from the drying. Water Sci. Technol. 65, 1142–1149.

Corici, L., Ferrario, V., Pellis, A., Ebert, C., Lotteria, S., Cantone, S., Voinovich, D., Gardossi, L., 2016. Large scale applications of immobilized enzymes call for sustainable and inexpensive solutions: rice husks as renewable alternatives to fossil-based organic resins. RSC Adv. 6, 63256–63270.

Di Giuseppe E., Analogue materials in experimental tectonics. 2018, 10.1016/B978-0-12-409548-9.10909-1.

DiCosimo, R., McAuliffe, J., Pouloseb, A.J., Bohlmann, G., 2013. Industrial use of immobilized enzymes. Che. Soc. Rev. 42 (15), 6437–6474.

EFSA, 2011, https://www.efsa.europa.eu/sites/default/files/consultation/110712a.pdf

Ferrario, V., Ebert, C., Knapic, L., Fattor, D., Basso, A., Spizzo, P., Gardossi, L., 2011. Conformational changes of lipases in aqueous media: a comparative computational study and experimental implications. Adv. Synth. Catal. 353, 2466–2480.

Ferrario, V., Chernykh, A., Fiorindo, F., Kolomytseva, M., Sinigoi, L., Myasoedova, N., Fattor, D., Ebert, C., Golovleva, L., Gardossi, L., 2015. Investigating the role of conformational effects on laccase stability and hyperactivation under stress conditions. ChemBioChem 6, 2365–2372. doi:10.1002/cbic.201500339.

Ferrer, M., Plou, F.J., Fuentes, G., Cruces, M.A., Andersen, L., Kirk, O., Christensen, M., Ballesteros, A., 2002. Effect of the immobilization method of lipase from *Thermomyces lanuginosus* on sucrose acylation. Biocatal Biotransform 20 (1), 63–71.

Gardossi L., Sinigoi L., Spizzo D., Fattor D. Method for covalent immobilization of enzymes on functionalized solid polymeric supports. 2012, WO2012085206 (A1); EP2655611 (A1).

Girelli, A.M., Astolfi, M.L., Scuto, F.R., 2020. Agro-industrial wastes as potential carriers for enzyme immobilization: a review. Chemosphere 244, 125368.

Guigo, N., Mazeau, K., Putaux, J.L., Heux, L., 2014. Surface modification of cellulose microfibrils by periodate oxidation and subsequent reductive amination with benzylamine: a topochemical study. Cellulose 21, 4119–4133.

Hanefeld, U., Gardossi, L., Magner, E., 2009. Understanding Enzyme Immobilisation. Chem. Soc. Rev. 38, 453–468.

Higashiyama K., Sumida M., Process for production of transesterified oils/fats or triglycerides, 2004, WO04/024930.

Hilterhaus, L., Minow, B., Mller, J., Berheide, M., Quitmann, H., Katzer, M., Thum, O., Antranikian, G., Zeng, A.P., Liese, A., 2008. Practical application of different enzymes immobilized on sepabeads. Bioprocess Biosyst. Eng. 31, 163–171.

Kim, S., Jiménez-González, C., Dale, B.E., 2009. Enzymes for pharmaceutical applications-a cradle-to-gate life cycle assessment. Int J. Life Cycle Assess 14, 392–400.

Korupp, C., Weberskirch, R., Müller, J.J., Liese, A., Hilterhaus, L., 2010. Scaleup of lipase–catalyzed polyester synthesis. Org. Process Res. Dev. 14, 1118–1124.

Martins, A.B., Friedrich, J.L.R., Cavalheiro, J.C., Garcia-Galan, C., Barbosa, O., Ayub, M.A.Z., Fernandez-Lafuente, R., Rodrigues, R.C., 2013a. Improved production of butyl butyrate with lipase from *Thermomyces lanuginosus* immobilized on styrene–divinylbenzene beads. Bioresour. Technol. 134, 417–422.

Martins, A.B., Friedrich, J.L., Rodrigues, R.C., Garcia-Galan, C., Fernandez-Lafuente, R., Ayub, M.A., 2013b. Optimized butyl butyrate synthesis catalysed by *Thermomyces lanuginosus* lipase. Biotechnol Prog 29 (6), 1416–1421.

Medina, F., Aguila, S., Baratto, M.C., Martorana, A., Basosi, R., Alderete, J.B., Vazquez–Duhalt, R., 2013. Prediction model based on decision tree analysis for laccase mediators. Enzyme Microb. Technol. 52 (1), 68–76.

Park, B., Wi, G.S., Lee, H.K., Singh, P.A., Yoon, T., Kim, S.Y., 2003. Characterization of anatomical features and silica distribution in rice husk using microscopic and micro–analytical techniques. Biomass Bioenergy 25, 319–327.

Patel, I., Ludwig, R., Haltrich, R., Rosenau, T., Potthast, A., 2011. Studies of the chemoenzymatic modification of cellulosic pulps by the laccase-TEMPO system. Holzforschung 65, 475–481.

Pellis, A., Corici, L., Sinigoi, L., D'Amelio, N., Fattor, D., Ferrario, V., Ebert, C., Gardossi, L., 2015. Towards feasible and scalable solvent-free enzymatic polycondensations: integrating robust biocatalysts with thin film reactions. Green Chem. 17, 1756–1766.

Pellis, A., Ferrario, V., Zartl, B., Brandauer, M., Gamerith, C., Herrero Acero, E., Ebert, C., Gardossi, L., Guebitz, G.M., 2016. Enlarging the tools for efficient enzymatic polycondensation: structural and catalytic features of cutinase 1 from *Thermobifida cellulosilytica*. Catal. Sci. Technol. 6, 3430–3442.

Pellis, A., Ferrario, V., Cespugli, M., Corici, L., Guarneri, A., Zartl, B., Herrero Acero, E., Ebert, C., Guebitz, Ebert C., Guebitz, G.M., Gardossi, L, 2017. Fully renewable polyesters *via* polycondensation catalyzed by *Thermobifida cellulosilytica* cutinase 1: an integrated approach. Green Chem. 19, 490–502.

Persson, M., Wehtje, E., Adlercreutz, P., 2002. Factors governing the activity of lyophilised and immobilised lipase preparations in organic solvents. ChemBioChem 3 (6), 566–571 3.

Raynaud, J., 2014. Valuing plastics: the business case for measuring, managing and disclosing plastic use in the consumer goods industry. United Nations Environ. Program. (UNEP). https://www.oceanrecov.org/pdp/valuing-plastic-report.html.

Reddy, R.D.P., Sharma, V., 2020. Additive manufacturing in drug delivery applications: a review. Int. J. Pharma. 589, 119820.

Schmid, R.D., Verger, R., 1998. Lipases: interfacial enzymes with attractive applications. Angew. Chem. Int. Ed 37, 1608–1633.

Sekifuji, R., Tateda, M., 2019. Study of the feasibility of a rice husk recycling scheme in Japan to produce silica fertilizer for rice plants. Sustain. Environ. Res. 29 (11), 1–9.

Sven P., Morkeberg L.A., Per A., Method of enzyme immobilization on a particulate silica carrier for synthesis inorganic media. 1996.US19960676367.

Takigawa, T., Endo, Y., 2006. Effects of Glutaraldehyde exposure on human health. J. Occup. Health 48, 75–87.

Toxicological Profile, 2015, https://www.atsdr.cdc.gov/sites/peer_review/tox_profile_glutaraldehyde.html.

Trastullo, R., Dolci, L.S., Passerini, N., Albertini, B., 2015. Development of flexible and dispersible oral formulations containing praziquantel for potential schistosomiasis treatment of pre-school age children. Int. J. Pharm. 495 (1), 536–550.

Tuck, C.O., Perez, E., Horvath, I.T., Sheldon, R.A., Poliakoff, M., 2012. Valorization of biomass: deriving more value from waste. Science 337, 695–699.

Tufvesson, P., Lima-Ramos, J., Nordblad, M., Woodley, M.J., 2011. Guidelines and cost analysis for catalyst production in biocatalytic processes. Org. Process. Res. Dev. 15, 266–274.

Velásquez-Cock, J., Gañán, P., Gómez H., C., Posada, P., Castro, C., Dufresne, A., Zuluaga, R., 2018. Improved redispersibility of cellulose nanofibrils in water using maltodextrin as a green, easily removable and non-toxic additive. Food Hydrocoll. 79, 30–39.

Xin, F., Basu, A., Yang, K.-L., He, J., 2016. Strategies for production of butanol and butyl-butyrate through lipase-catalyzed esterification. Bioresour. Technol. 202, 214–219.

Zeiger, E., Gollapudi, B., Spencer, P., 2005. Genetic toxicity and carcinogenicity studies of glutaraldehyde-a review. Mutat. Res. 589 (2), 136–151.

4.5.5 Scaling up of the immobilization process

The immobilization of CaLB on RH was carried out on a 300 g scale, using both the chemical and the enzymatic oxidation methods. The chemical oxidated RH yielded a batch of covalently immobilized CaLB with a specific activity of 65 U/g (tributyrin test) whereas the RH oxidized by the laccase-TEMPO method led to a specific activity of 149 U/g. The two formulations were tested by Dr Anamaria Todea in the solvent free polycondensation of glycerol azelaic and dimethylitaconate, giving the results reported in table 4.3.

Table 4.3 Results obtained in the solvent-free polycondensation catalyzed by CaLB covalently immobilized on RH oxidized by chemical and enzymatic methods.

Type of functionalization of the support	Hydrolitic activity of the biocatalyst (U/g_{dry})*	Amount of immobilized CaLB per g monomers $_{enzyme}$)	Mn	Mw	PDI
Chemical oxidation	65	0.96	756	824	1.09
Enzymatic oxidation	149	0.42	762	820	1.08

*Unit for g of biocatalyst

The experiments were carried out using the same amount of enzyme per g of monomer. Overall, the results indicate that the scaling up of the oxidation protocol must be optimized and the enzymatic method appears more suitable for being upscaled.

Within the context of the present polycondensation study, a review manuscript has been written, which is reported herein (Manuscript D, section 4.5.5.1).

4.5.5.1 **Manuscript D** "Azelaic Acid: A Bio-Based Building Block for Biodegradable Polymers"

polymers

MDPI

Review

Azelaic Acid: A Bio-Based Building Block for Biodegradable Polymers

Anamaria Todea [1], Caterina Deganutti [1], Mariachiara Spennato [1], Fioretta Asaro [1], Guglielmo Zingone [1], Tiziana Milizia [2] and Lucia Gardossi [1,*]

[1] Department of Chemical and Pharmaceutical Sciences, University of Trieste, Via L. Giorgieri 1, 34127 Trieste, Italy; atodea@units.it (A.T.); cdeganutti@units.it (C.D.); mariachiara.spennato@phd.units.it (M.S.); fasaro@units.it (F.A.); zingone@units.it (G.Z.)
[2] Novamont S.p.A., Via G. Fauser 8, 28100 Novara, Italy; tiziana.milizia@novamont.com
* Correspondence: gardossi@units.it

Abstract: Azelaic acid is a dicarboxylic acid containing nine C atoms, industrially obtained from oleic acid. Besides its important properties and pharmacological applications, as an individual compound, azelaic acid has proved to be a valuable bio-based monomer for the synthesis of biodegradable and sustainable polymers, plasticizers and lubricants. This review discusses the studies and the state of the art in the field of the production of azelaic acid from oleic acid, the chemical and enzymatic synthesis of bio-based oligo and polyester and their properties, including biodegradability and biocompostability.

Keywords: azelaic acid; bio-based monomers; bio-based polymers; biodegradability; biocompostability

Citation: Todea, A.; Deganutti, C.; Spennato, M.; Asaro, F.; Zingone, G.; Milizia, T.; Gardossi, L. Azelaic Acid: A Bio-Based Building Block for Biodegradable Polymers. *Polymers* **2021**, *13*, 4091. https://doi.org/10.3390/polym13234091

Academic Editors: Cristiano Varrone and Alessandro Pellis

Received: 12 October 2021
Accepted: 19 November 2021
Published: 24 November 2021

1. Introduction

The production of fine chemicals, new materials and products from renewable feedstocks represents a continuous challenge. Several procedures have been reported in the literature or patented in the last decade for the main biomass components: carbohydrates (75%), lignins (20%), fats and oils (5%) [1]. Regarding oleochemical developments, the oxidative cleavage of unsaturated fatty acids to produce dicarboxylic acids, hydroxy acids, and amino acids has received great attention in the last decade [2]. Two main oleochemical products obtained by the cleavage of unsaturated fatty acids are sebacic acid and azelaic acid.

Azelaic acid (AzA) is a naturally occurring saturated nine carbon atom dicarboxylic acid found in whole grains, wheat, rye and barley [2], first detected in rancid fats. It can be formed endogenously from substrates such as longer-chain dicarboxylic acids and processes like the metabolism of oleic acid, and ψ-oxidation of monocarboxylic acids. The azelaic acid market is predicted to reach USD 160 million by 2023 and the applications include pharmacological ingredients, polymers, plastics, lubricants and materials for electronics [3]. The aim of the present review is to highlight the potential of azelaic acid as powerful building block for the synthesis of bio-based and biodegradable polymers, with a special emphasis on the green synthetic routes, embracing both chemical and enzymatic methods.

2. Azelaic Acid: A Bio-Based Monomer with Pharmacological Properties

The pharmacological applications of azelaic acid have been studied since the 1980s [4] and azelaic acid has been approved by both the FDA (US Food and Drug Administration) and by the EMA (European Medicines Agency) for different external uses. Formulations of AzA (15–20% *w*/*w*) are used in the treatment of inflammatory acne vulgaris with medium to moderate severity [5].

Moreover, it is widely used in the treatment of skin pigmentation [6,7] and melasma [8]. Concerning the mechanism of action, azelaic acid exerts an inhibitory effect against tyrosinase, a key enzyme for the synthesis of melanin and in this sense, it is active, above all, at the level of hyperactive melanocytes, while sparing normal ones. Kinetic studies have revealed that the inhibitory action is linked to the presence of the two carboxylic groups at the end of the carbon chain [9]. In particular, the mechanism sees an acid-base interaction between the two functional groups of azelaic acid and the residues of histidines present in the catalytic site, linked to copper [9,10].

However, AzA may also exert its activity against tyrosinase indirectly by inhibiting the interaction with thioredoxin reductase associated with the plasma membrane [11]. The dithiol form of thioredoxin is a powerful cellular reducing agent involved in defense reactions against oxidative stress mainly due to photochemical reactions between ultraviolet rays (UV) and oxygen present at the molecular level. Thioredoxin reductase catalyzes the disulfide reduction of oxidized thioredoxin by NADPH, leading to the formation of two thiol groups that bind the active site of the tyrosinase enzyme [12]. When azelaic acid inhibits the reduction of extracellular chemical species, electrons flow in the direction of oxidized thioredoxin to increase the intracellular concentration of reduced thioredoxin that acts as a potent inhibitor of tyrosinase thus preventing melanin biosynthesis. It has been seen that the catalysis of the melanogenesis enzyme is reduced by 58% in the presence of reduced thioredoxin, compared to the activity performed when all the thioredoxin is in an oxidized form.

Furthermore, the thioredoxin reductase/thioredoxin system is shown to be a principal electron donor for the ribonucleotide reductases which regulate DNA synthesis [13]. Consequently, the inhibitory action on the enzyme could be exploited as a therapeutic benefit even in diseases related to tumor proliferation and to colonization by pathogens. In fact, it has been found that thioredoxin reductase and thioredoxin are overexpressed in many aggressive tumors, where they participate in carcinogenesis, tumor progression and drug resistance. In this case, thioredoxin is involved not only in the activation of ribonuocleotide reductase, but also in promoting many other biochemical pathways, very often not desired [14]. It follows that the inhibition of thioredoxin reductase would lead to the advantage of blocking all the activities mediated by the thioredoxin [15].

The inhibition of DNA synthesis gives azelaic acid bacteriostatic properties, useful in treating diseases with the presence of bacteria as elements of etiopathogenesis. In particular, it has been shown that the active ingredient has clinical efficacy in acne therapy and that the inhibition of thioredoxin reductase, located in the bacterial cytosol, is one of the mechanisms of action of AzA [11]. Formulations of azelaic acid (20% *w*/*w*), applied twice a day, cause a reduction in intrafollicular microbial populations, with a 2500-fold reduction of the *S. epidermidis* microorganism after 2 months, together with a 97.7% decrease in the concentration of *P. acnes* [5]. In addition, the inhibition of mitochondrial enzymes by azelaic acid, determines the blocking of cellular respiration, with consequent cytostatic effects, or cytotoxic if at higher concentrations, the inhibition being dose dependent [16]. Nevertheless, the total safety of administering the drug in humans has been highlighted several times, since in vitro and in vivo it does not bring toxic effects to cells not affected by pathologies. As a result, dicarboxylic acid can be exploited when it is necessary to intervene against abnormal cells. This is the case of cancer cells, which are more sensitive to antimitochondrial agents and internalize azelaic acid within them in quantities three times higher than normal cells [17]. Therefore, preferential cytotoxic and antiproliferative effects are obtained on tumor cells, through the blocking action of cellular respiration and the interruption of DNA synthesis, by inhibiting the enzymes mentioned so far.

In the presence of the acne pathology, the keratinocytes hyperproliferate and differentiate in an anomalous way, and in addition to this the desquamation process is also altered. Consequently, there is an accumulation of dead cells that induces the formation of primary lesions, defined as microcomedones. The set of various factors can subsequently cause microscopic lesions to evolve into inflammatory or noninflammatory comedones, typical of

acne [18]. Various studies have shown that azelaic acid modulates epidermal differentiation in vivo and that it has a marked antiproliferative cytostatic effect on keratinocyte cultures in vitro. This activity is primarily the consequence of the indirect inhibitory action on ribonucleotide reductase and of the competitive inhibitory action on the fundamental enzymes of the mitochondrial respiratory chain. However, the differentiation of keratinocytes is mainly influenced by the reduction of protein synthesis of keratin precursors. In clinical practice, the reduction in the number of keratinocytes in the skin surface is linked to a lower formation of comedones, followed by a marked improvement in acne-affected skin. Therefore, after long-term exposure to the active ingredient, protein distribution returns to normal, with advantageous results in therapy [19].

The AzA anti-inflammatory response [20–22] and activity [23,24] were demonstrated as well. It has been shown that the molecule is efficient in inhibiting in vitro the oxidation of aromatic compounds and the lipoperoxidation of arachidonic acid (C 20: 4, n 6), which are processes induced by the presence of hydroxyl radicals (HO·). These studies have shown that azelaic acid acts as a "free radical scavenger", in other words, it mitigates the toxic effect of reactive oxygen species (ROS), which are powerful chemical mediators of the inflammatory response [25]. It has also been shown that azelaic acid can prevent the production of ROS, such as superoxide anion (O^{2-}) and hydroxyl radical (HO^{-}), generated by human neutrophils, without interfering with chemotaxis and phagocytosis. A significant decrease in oxidative tissue damage at the inflammation site is thus obtained, both for the direct mechanism on free radicals and for the inhibitory action on the production of new radicals, mediated by neutrophils.

Arresting the development of ROS represents in itself a possible strategy in the control of diseases such rosacea, another very common pathology that affects the skin, and in particular the facial area. Although the pathogenesis of rosacea has not yet been fully understood, free radical damage has been found to worsen the clinical condition [26]. Nevertheless, it is the keratinocytes that play a decisive role in promoting the inflammatory cascade, which favors the onset of skin diseases. In fact, keratinocytes lead to the production of immune signals and the secretion of cytokines, in response to various promoter factors, including UV rays [22].

3. Azelaic Acid Synthetic Routes

An ozonolysis method for industrial production of bifunctional monomers, such as azelaic acid, has been applied by some oleochemical companies, like Emery, Croda Sipo and more recently P2 science. This process presents some disadvantages such as high energy and technologic demand to produce ozone and some potential risks associated with ozone utilization [27]. The ozonolysis route involves firstly a primary ozonide of oleic acid and ozone via 1,3 cycloaddition. Secondly, the resulting 1,2,4-trioxolane is oxidized to carboxylic acids under oxidative reaction conditions [28].

The application of hydrogen peroxide as an oxidant has been industrialized in Porto Torres by Matrica ("Novamont S.p.A.-Chimica Vivente per la Qualità della Vita", 2019) by building up a plant capable of producing azelaic and pelargonic acid by different sources using 25,000–30,000 tons/year of vegetable oils [27]. The patented processes of Novamont S.p.A. related to the valorization of vegetable oils directly into different carboxylic acids include three main steps: (i) the triglycerides olefinic double bong oxidation by using an aqueous solution of hydrogen peroxide to obtain an intermediate compound containing vicinal diols, (ii) a second oxidation step of the two hydroxyl groups of the vicinal diol to carboxylic groups using a compound containing oxygen and a catalyst capable of catalyzing the oxidation and (iii) a hydrolysis reaction of acidic triglycerides after separation of the monocarboxylic acids. By this method, azelaic acid or brassylic acid can be obtained with yields of up to 80% [29,30].

Different strategies for the improvement of AzA production have been reported in the literature and they were focused on one step ozonolysis, on the optimization of the oxidation reaction from the second step or on the enzymatic and chemo-enzymatic

synthesis. Figure 1 illustrates the main routes reported for the synthesis of azelaic acid starting from oleic acid.

An improvement of the second oxidation step of oleic acid was achieved in the 1960s by implementing the in situ formation of performic acid from H_2O_2 and HCOOH in combination with ozonolysis to yield AzA up to 95% [31]. Lower yields (71%) were obtained when oxidation was performed using H_2O_2, phosphotungstic acid, or tungstic acid as the catalyst precursor and quaternary ammonium salts as phase transfer catalysts [32]. Other oxides containing Mo-, V-, Mn-, Co-, Fe-, and Pb- or salts and tungstic acid were reported with yields of AzA ranging from 70 to 87%. The decomposition of the secondary ozonide product was investigated by using microwaves without a catalyst and the AzA yield was 70–80% [28].

An alternative to heavy metal oxidants was claimed by a Japanese patent in 2009, which reports the cleavage of methyl oleate in H_2O_2/H_2O under subcritical conditions at 180–370 °C and 1–25 MPa. However, the reported yield was 31%, with concomitant drawbacks due to high-energy consumption and corrosion problems [28,33].

Two sustainable methods for the production of AzA as alternatives to the ozonolysis of oleic acid was reported by Benessere et al. The first method proceeds in two steps, coupling the oxidation of oleic acid (OA) to 9,10-dihydroxystearic acid (DSA) with oxidative cleavage by sodium hypochlorite. The second method involves a chemocatalytic system consisting of H_2O_2/H_2WO_4 for direct oxidative cleavage of the double bond of OA at 373 K [34].

A green route for the synthesis of azelaic and pelargonic acid starting from 9,10-dihydroxystearic acid (DSA) was reported by Kulik et al. by applying different supported gold catalysts in an aqueous solution. The reaction mechanism and the stability of the gold based catalyst were discussed in detail [35].

Recently, a green one-pot synthesis of azelaic acid and other valuable derivatives of oleic acid was proposed by Laurenza et. al. [36]. Rare earth metal (REM) triflates and commercial molybdenum dioxo dichloride ($MoCl_2O_2$) in the presence hydrogen peroxide allowed a selective oxidation of methyl oleate to azelaic acid or to methyl oleate epoxide.

A chemo-enzymatic route (Figure 1, route B) was described by Brenna et al. [2], which represents an alternative to ozonolysis for the transformation of oleic acid into AzA and PA in three steps. Initially, the peroleic acid is formed by epoxidation of the unsaturated acid (oleic acid) using a lipase in the presence of 35% H_2O_2. The resulting oxirane was subjected to in situ acid-catalyzed opening to form the diol. The obtained 9,10-dihydroxystearic acid was then chemically oxidized using atmospheric oxygen as a stoichiometric oxidant in the presence of catalytic quantities of $Fe(NO_3)_3 \cdot 9H_2O$, (2,2,6,6-tetramethylpiperidin-1-yl)oxyl (TEMPO) and NaCl, yielding the 9,10-dioxostearic acid. In the last step, the AzA and PA were achieved after the cleavage by 35% H_2O_2 under mild conditions in the absence of any other catalyst. The reported isolated yield for AzA was 44% and the purification did not require chromatographic methods.

Similarly, a Chinese patent reports an environmentally friendly technology for preparing AzA by an enzymatic catalysis oxidation system. The oleic acid undergoes the epoxidation catalyzed by nonspecified lipases in the presence of H_2O_2 and a noble metal, followed by the cleavage of the resulted diol to obtain AzA and PA. The reported AzA yield was 60–70% [37].

AzA can be synthesized also through fermentative oxidation with a 67% yield, as reported in a patent of Anderson et.al. The fermentation of oleic acid or triglycerides with Candida tropicalis yields 1,19-nonadec-9-enoic acid that is transformed by ozonolysis in the presence of Na-X zeolite catalyst. The advantage of this method, although the fermentative oxidation time takes up to 180 h, is that the formation of PA is avoided. The method was reported as useful for the oxidation of PA to AzA [38].

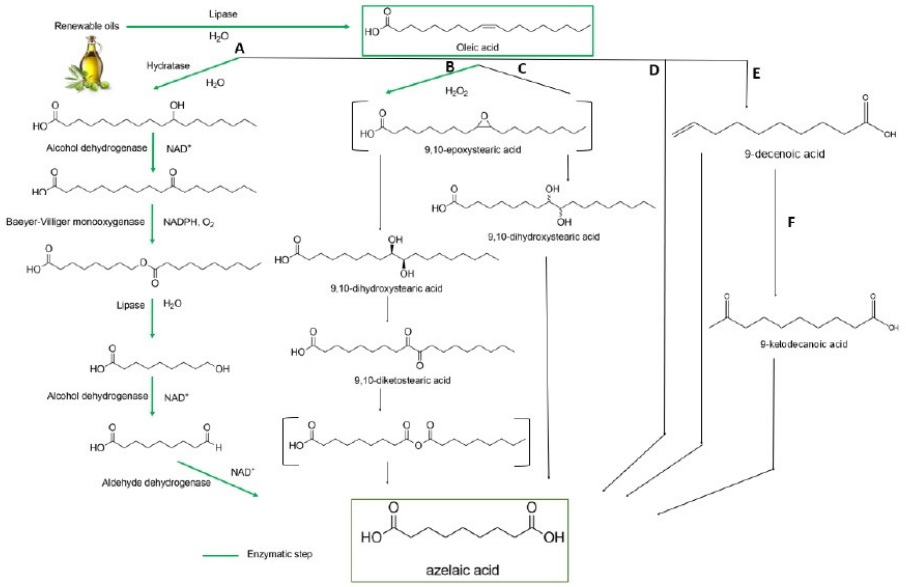

Figure 1. The main routes reported for synthesis of azelaic acid starting from oleic acid: **A**—enzymatic route [39], **B**—chemo-enzymatic route [2], **C**—two step route with epoxide [34], **D**—direct cleavage, **E**—two step pathway with metathesis of oleic acid, **F**—three step route [28].

Only a few biocatalytic methods for AzA synthesis are reported in the literature (Figure 1A). Song et al. developed a multistep enzymatic procedure for the synthesis of AzA from oleic acid, 10-hydroxystearic acid [40] and vegetable oils [39]. The biocatalytic route consisted of the use of recombinant *Escherichia coli* cells expressing the genes encoding an oleate hydratase from *Stenotrophomonas maltophilia*, an alcohol dehydrogenase (ADH) from *Micrococcus luteus*, and a Bayer–Villiger monooxygenase (BVMO) from *Pseudomonas putida* KT2440 for the transformation of oleic acid into 9-(nonanoyloxy)nonanoic acid. In the further step, the hydrolysis of this compound was mediated by a cell extract of *E. coli* expressing the esterase gene from *P. fluorescens* to pelargonic acid and 9-hydroxynonanoic acid followed by the oxidation catalyzed by an ADH from *P. putida* GPo1. The reported substrates for AzA synthesis were olive oil, soybean oil, fatty acid methyl esters from microalgae and yeast derived oils. Although the described biocatalytic route is interesting, the concentration of the final product in the reaction medium did not exceed 5–10 millimolar.

Finally, a German patent described in 1974 the oxidation of the terminal -CH_3 group of PA by *Debaryomyces pfaffii*, but the AzA yield was only 6% [41].

4. Azelaic Acid in the Synthesis of Bio-Based Polymers

In the last few decades several studies were focused on combining renewable and biodegradable polyester synthesis mainly driven by environmental reasons. In this context, different building blocks obtained from renewable resources have been proved as suitable raw materials for the synthesis of polymers [42].

In 2018, from the total amount of 2.11 million tons of bio-based plastics, about 57% (1.2 million tons) were nonbiodegradable [43]. Currently, modified starch-based bioplastic and several polyesters, including poly(lactic acid) (PLA), aliphatic-aromatic copolyesters, polyhydroxyalkanoates (PHAs), and poly(butylene succinate) (PBS) are the main biodegradable polymers available on the market [44].

The use of dicarboxylic acids as raw materials was studied by several groups, especially for the synthesis of polyesters due to the commercial potential of these products.

Poly-(ethylene succinate) (PES) and poly(butylene succinate) (PBS) are promising materials for many conventional plastic replacements because of their biodegradability, acceptable mechanical strength, and comparable softening temperature to low-density polyethylene and polystyrene [45].

The enzymatic synthesis of polyesters starting from dicarboxylic acids (C4-C16) and different diols became a green alternative to harsh reaction conditions and, starting from the 1980s, lipases were successfully used as catalysts by different groups [46].

4.1. Azelaic Acid Based Copolyesters

Different polyesters of azelaic acid were reported up to date in the literature. The successfully used diols and dicarboxylic acid as co-monomers for the AzA polyesters are summarized in Table 1, divided onto bio-based and non-bio-based co-monomers. It can be observed that the enzymatic synthesis up to date was performed using three bio-based monomers: glycerol, pentaerythritol and PEG. Among the non-bio-based monomers, 1,6-HDO was used via the enzymatic route. All the other polyesters were synthesized via chemical catalysis. Details relating to the applications, properties and synthesis conditions are included in the following subchapters.

Table 1. Co-monomers used for synthesis of AzA based esters/polyesters.

	Co-Monomer(s)	Synthesis Route	Reference
Bio-based monomers	1,4-butadiol + glutaric acid	Chemical	[47]
	glycerol	Chemical and enzymatic	[48–53]
	Glycerol + FA	Enzymatic	[54]
	succinic acid + glycerol	Chemical	[55]
	pentaerythritol	Enzymatic	[54]
Non-bio-based	ethandiol	Chemical	[56]
	1,8ODO + glutaric acid	Chemical	[47]
	diglycerol	Chemical	[57]
	lauric alcohol	Enzymatic	[58,59]
	1,6-HDO + ECM * 1,6-HDO +/− PEG	Enzymatic	[60]

* ECM—end caper molecule: Sorbic alcohol/12-hydroxystearic acid/trimethylolpropane oxetane/2-hydroxyethyl methacrylate; FA—fatty acid.

4.1.1. Chemical Synthesis and Properties of Azelaic Acid Oligo and Polyesters

The synthesis of the polyesters mentioned in Section 4.1 was performed in different reaction conditions and linear or hyperbranched products were obtained. For linear polymer/copolymers different diols and dicarboxylic acid were tested. The hyperbranched polyesters involved the use of glycerol as polyol together with free acid or the dimethyl ester of azelaic acid. The M_n determined value was in the range 1852–5410 g/mol and the highest value was reported for dibutyltin (IV) oxide as catalyst [48]. The synthesis of polyglycerol-azelaic acid polyesters (Figure 2) starting from polyglycerol-3/diglycerin and different vegetable oils in the presence of *p*-toluene sulfonic acid at different molar ratios and temperatures in the range 175–180 °C was patented by Giuliani et. al. The reaction products were analyzed by SEC and were tested for several cosmetic applications [57].

Glycerol-diacids oligoesters including polyglycerol azelate were synthesized by the same group using different catalysts such as titanium(IV) butoxide, [52,53] and [dibutyltin(IV) oxide] [51]. The reactions were performed at 150 °C in 22 h in a solvent-less system or in the presence of organic solvents (DMSO/DMF or toluene). MALDI-TOF MS, 1D and 2D NMR techniques were used for product characterization. The most efficient catalyst was $Ti(OBu)_4$.

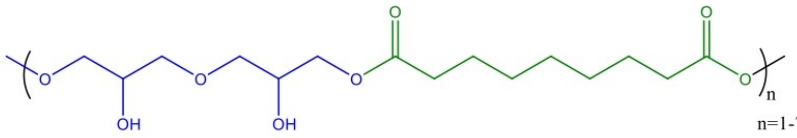

Figure 2. Chemical structure of the polyglycerol-azelaic acid polyesters obtained using diglycerol and different vegetable oils as raw materials.

The poly(glycerol azelate) polyester was synthesized also at 125 °C in aluminum pans [49] or at 140 °C under nitrogen atmosphere [50]. The degradation of the products was also tested and the results indicated that the biodegradation upon burial in soil was slower than the hydrolysis after incubation in PBS buffer [50].

The synthesis, thermal characterization and enzymatic degradation of poly(ethylene azelate) was also reported. The polymers were synthesized by two-step melt polycondensation using $Ti(OBu)_4$ as catalyst at 190 °C. GPC, DSC, WAXD and other techniques were used for characterization. The biodegradation of poly(ethylene azelate) was studied in PBS solution (chemical hydrolysis) and using a mixture of lipases from *R.delemar* and *P. cepacia*, indicating a faster degradation as compared to poly-ε-caprolactone [56].

Cho et al. obtained glycerol esters starting from six different dicarboxylic esters, including dimethyl azelate. Among the tested substrates, the highest conversion was obtained when dimethyl azelate was used, yielding 2,3-dihydroxy-propyl methyl azelate and 1,3-dimethoxyazelyloxy propan-2-ol [61]. Potassium hydroxide was used as catalyst and the mixture was heated at 80 °C. The obtained mono- and diesters were isolated and characterized by FT-IR, NMR, LC-MS techniques and their molecular weights were 277 g/mol and 461 g/mol.

The AzA-based polyesters synthesized by the chemical route were characterized by medium molecular weight determination and for some of them the thermal properties were evaluated.

Among the reported data, the highest molecular weights were obtained for the terpolymers containing AzA, glycerol and a diol/diacid (Table 2). The melting point values in all cases were under 100 °C. For the terpolymers containing glutaric acid and diols as co-monomers, the melting point values were lower.

Table 2. Thermal and mechanical properties of AzA-based polymers.

Co-monomer	M_n [g/mol]	M_w [g/mol]	T_g [°C]	T_m [°C]	Young Modulus [MPa]	Reference
Glutaric acid + 1,4BDO/ Glutaric acid + 1,8ODO	45,100–60,300 45,900–61,200	81,800–121,200 86,700–120,400	−7.2...+22.2 +25.1...+43.3	+20.0...+45.5 +47.1...+62.7	52.–287 60.5–362.6	[47]
Glycerol + succinic acid	515–3656	13,883–24,626	−24...−7	84.7...91.5	n.d.	[55]
Glycerol	2316	3010.8	n.d	n.d	n.d.	[52]
Glycerol	3245	5970	n.d	n.d	n.d.	[53]
Glycerol	11,690	28,056	n.d	n.d	n.d.	[51]
Glycerol	n.d.	n.d.	n.d.	~100	n.d.	[49]
Glycerol	1852–2873	3111–6981	n.d.	n.d.	0.98–11.1	[50]
Ethandiol	21,000	47,040	−60	62	n.d.	[56]

n.d.—not determined.

A series of copolymers containing AzA and glycerol have been reported by different groups (Table 2). The medium molecular weight values of most products were less than 10,000 g/mol except the reports of Wyatt et al. from 2012 when highest M_w value did

not exceed 30,000 g/mol. No other thermal or mechanical properties of these polymers were reported.

All these results indicate that up to date the studies were focused on the catalyst development whereas minimal attention was devoted to structural analysis of the product.

4.1.2. Technical, Cosmetic and Pharmaceutical Applications of Chemically Synthesized Polyesters Containing Azelaic Acid Moieties

Polymers containing AzA units were chemically synthesized by different groups and it was demonstrated that the insertion of AzA contributes to the flexibility, elasticity and hydrophobicity of the formed products [35]. Flexible polyester resins containing AzA are suitable for impact-resistant floor coverings. Furthermore, azelaic acid-based plasticizers are used to enhance low temperature flexibility in resilient polyvinyl chloride products [35] and more details will be discussed in the following section.

The patent of Giuliani et al, describes the incorporation of polyglycerol-azelaic acid polyesters into cosmetic compositions as active components at a concentration in the range of 0.01 to 20% (*w*/*w*). Formulations such as restructuring lotion, sebum-normalizing shampoo, tricological serum, conditioning cream, body milk, leave-on cleanser were prepared. The protective effect against thermal stress on the hair was demonstrated by treating locks with a shampoo and also with a leave-on formulation containing polyglyceryl-3-azelaiate with subsequent exposure to three consecutive heat cycles.

Inflammation studies indicate that polyglyceryl-3-azelate has a significant inhibitory effect on TNF-α gene expression. Moreover, the polyglyceryl-3-azelate demonstrated an anti-inflammatory effect (reduction of TNF-α) greater than azelaic acid [57].

Azelaic acid diglycinate is presented in a patent as a bioconvertible compound since it is capable of releasing, after hydrolysis by lipase in the sebaceous follicle, at least one active agent against acne with antibacterial and/or anti-inflammatory activity [62].

4.2. Terpolymers Containing Azelaic Acid

For tuning the azelaic acid polyester properties, terpolymer synthesis was performed using different chain length diols or glycerol and aliphatic/aromatic diacids or correspondent diesters (Figure 3).

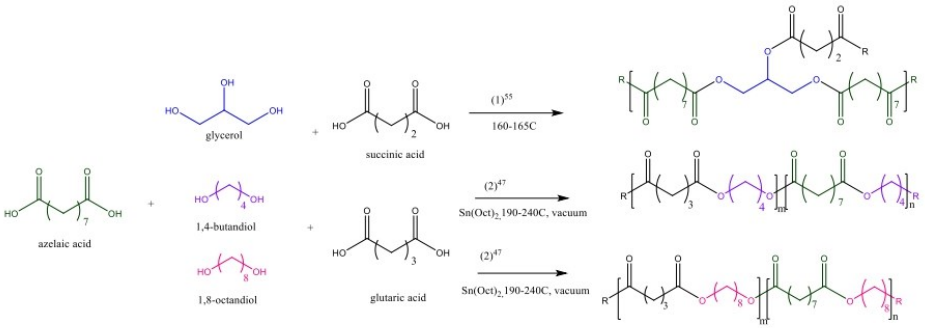

Figure 3. Polyesterification reaction of Aza, glycerol, succinic acid (1) [55]; synthesis of poly(butylene glutarate-co-butylene azelate) and poly(octylene glutarate-co-octylene azelate) copolyesters in two steps (2) [47].

Baharu et al. synthesized new elastic polymers via polyesterification of glycerol with AzA and succinic acids. The polyesterifications were performed catalyst free at 160–165 °C for 2 h, followed by incubation in Petri dishes as films at 125 °C for 48 h. The chemical structure was proved by FT-IR, NMR analysis and the medium molecular weight was determined by SEC. The Đ values were in the range of 6.73–26.9 [55].

Poly(butylene glutarate-co-butylene azelate) (PBGA) and poly(octylene glutarate-*co*-octylene azelate) (POGA) copolyesters were synthesized by a two-step melt esterification at 190 °C and polycondensation process at 240 °C under vacuum using $Sn(Oct)_2$. Different

monomer compositions were tested and the products were characterized by GPC, NMR, TG, DSC, WAXD and tensile test. As expected, the isodimorphic structural behavior was affected by the chain length of the co-monomer diols [47].

Biodegradable aliphatic-aromatic polyesters including polybutylene terephthalate-butylenazelate were synthesized starting from dimethyl terephthalate, azelaic acid and a butandiol in a two-step process including a melt esterification at 200 °C and a polycondensation at 240 °C under vacuum [63].

4.3. Enzymatic Synthesis of Azelaic Acid Based Esters and Polyesters

Enzymes are efficient and sustainable alternatives to metal catalysts used in polycondensation (e.g., tin, titanium and antimony) since they are efficient at mild reaction temperatures ranging between 40 and 90 °C, whereas conventional chemo-catalytic polycondensations are carried out at T > 150 °C [64]. They also work in solvent-free systems and catalyze highly selective synthesis, enabling the production of functionalized polyesters with controlled architectures [65]. More importantly, enzymatically synthetized polyesters are inherently biodegradable since the same enzymes can catalyze both their synthesis and hydrolysis. Enzymatic polycondensation generally leads to products characterized by moderate molecular weight. According to Comerford et al., this drawback can be overcome by a two-step procedure where the biocatalyst is removed after a preliminary step, which is followed by a thermally driven elongation step [66]. Notably, polyesters with highly regular structures and molecular weights below 2500 g/mol have applications in cosmetic formulations in film forming [67] and are used for coating and adhesive applications.

Hydrolytic enzymes and lipases were employed for the synthesis of esters and polyesters of AzA, also with the aim of improving its compatibility, with respect to other ingredients of cosmetic and dermatologic formulation. It is known that AzA suffers from low-solubility, high melting point and large dosage requirement, which limit wide application in cosmetics and pharmaceutical products [58]. Moreover, some side effects are associated with the acid character of the molecule, demonstrated by high dosage pharmaceutical preparations.

The enzymatic synthesis of esters and polyesters based on AzA are reported in few patents and research papers (Figure 4). In some patents related to the enzymatic synthesis of esters/polyesters starting from dicarboxylic acid and diols, AzA is mentioned as a possible reagent but no details related to the AzA synthesized and characterized products are given [68,69]. Khairudin et al. synthesized dilauryl azelate ester by using Novozyme 453 as catalyst. The synthesis was optimized in two reports, one by using an artificial neural network ANN-based design of experiment [58] and by central composite rotatable design [59]. The optimization of the process parameters included the enzyme amount, reaction time, reaction temperature, and molar ratio of substrates. Both methods proved their efficiency and high R^2 (coefficient of determination) values were obtained.

Curia et al. synthesized AzA polyesters using 1,6-hexanediol and sorbic alcohol/12-hydroxystearic acid/trimethylolpropane oxetane/2-hydroxyethyl methacrylate as end capping molecule. The reactions were performed in $scCO_2$ using Novozyme 435 as catalyst. The conversions were higher than 96% and the medium molecular weight were in the range of 1500–2400 [70].

In a later study, the same group synthesized specific end-functionalized amphiphilic copolymers based on azelaic acid, 1,6-hexanediol and PEG in $scCO_2$. The M_n values determined based on GPC analysis were in the range 1700–3200 g/mol [60].

When dimethyl azelate was used as monomer together with glycerol in the presence of lipase Novozyme 435, a medium molecular weight of 2200 was obtained (400 mbar) in 48 h. When the pressure during the reaction decreased (150 mbar), a significant increase of the molecular weights (higher 20,000 g/mol) was observed [71]. Several lipases were mentioned in the summary of the invention, but the examples were performed only by using the commercial lipase Novozyme 435.

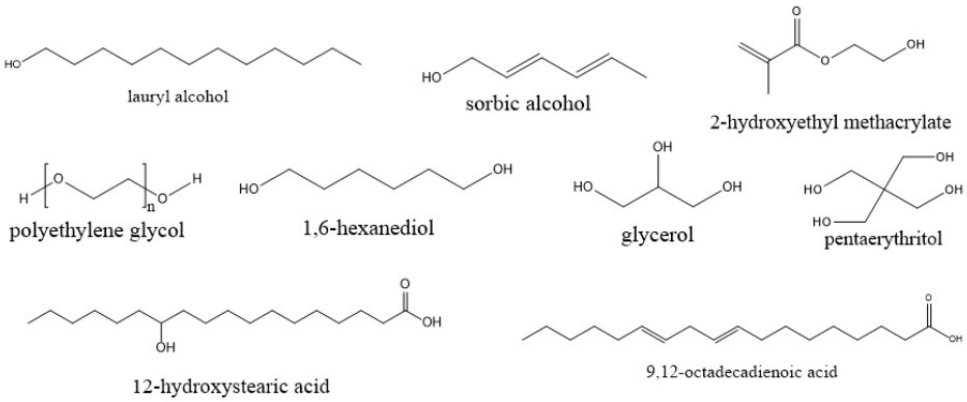

Figure 4. Typical examples of co-monomers used in enzyme-catalyzed polymerization of azelaic acid.

Highly branched high-molecular weight AzA polyesters were synthesized by a one-pot enzymatic system and reported by Nguyen et al. The first approach was focused on polyester synthesis starting from glycerol, azelaic acid, and tall oil fatty acid (TOFA) using Novozyme 435. The molecular weights after 25 h polymerization time, were in the range 20,900 to 39,700 g/mol with polydispersity indexes (Đ) between 3.2 and 5 (SEC analysis). The second azelaic acid derivatives was synthesized through a chemo-enzymatic reaction system. First, the pentaerythritol and azelaic acid were mixed and the reaction was performed at 180 °C and in the second stage the temperature was decreased and glycerol, azelaic acid, TOFA and Novozyme 435 were added. The SEC determined molecular weights were in the range of 16,800–57,800 g/mol and the Đ in the range 2.8–4.5 [54].

The enzymatically synthetized esters and polyesters of AzA were studied especially for their thermal properties (TG, DSC), their ability to form films, aggregates and for the cytotoxicity and antibacterial activity. The antibacterial activity of dilaurylazelate was evaluated against the pathogen bacteria *Staphylococcus epidermidis* S273 and the cytotoxicity was tested on 3T3 normal fibroblast cells. The results revealed that, compared to AzA, the ester is nontoxic, safe for pharmaceutical applications and presents promising antibacterial properties [59].

The thermal telechelics synthesized by Curia et al, starting from AzA, 1,6HDO and four different end-capping molecules, indicate that the T_m and the enthalpy of melting (ΔH_m) of the products are highly dependent on the end-capping molecule. It was clearly demonstrated that the bulkier structure of the end-cappers alters the crystalline structure [70].

Interesting properties were reported for copolymers based on azelaic acid, 1,6-hexanediol and PEG. Besides the thermal properties, the authors demonstrated that these polymers are capable of forming self-assembled aggregates in an aqueous environment. The thermal characterization of polymers revealed that a longer PHAz backbone presents larger crystallites (higher T_m and enthalpy of melting (ΔH_m)). The aggregation in water was confirmed by comparison of NMR and the coumarin-6 loading tests proved the lipophilic molecules' ability for dispersion and stabilization in an aqueous environment [60]. The products also showed significant surface tension reduction, indicating that the azelaic acid-based copolymers might find applications as surfactants in detergents and body-care formulations [60].

The AzA derivatives synthesized by Nguyen et al. were used for solid film preparation and characterized by DSC and water contact angle (WCA) measurements. The results showed that the acid/diacid composition had an effect for the hydrophilic/hydrophobic balance of the films. The AzA content was directly correlated to the increase of WCA up to 141 [54].

4.4. Polyamides Containing Azelaic Acid

Polyamides obtained by reacting AzA with different amines (Figure 5) are already commercial materials The most used is a polyamide synthetized from AzA and 1,6-diaminohexane, named nylon 6,9 (T_g 52 °C, M_w repeated unit 268 g/mol) [72].

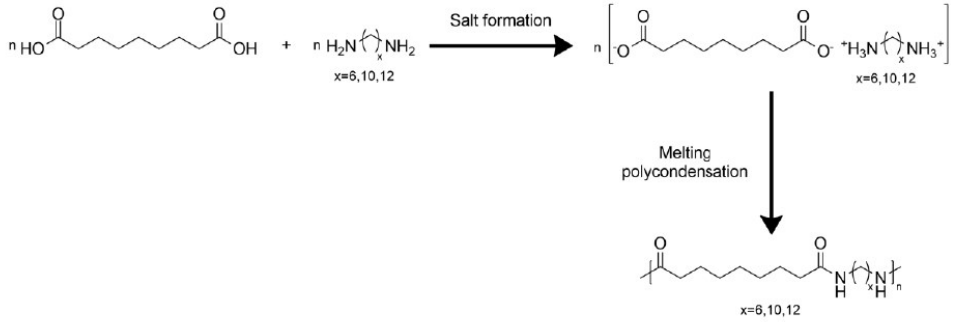

Figure 5. Synthesis and chemical structure of polyamide 6,9, polyamide 10,9 and polyamide 12,9.

Aliphatic polyamides, or nylons, are semicrystalline polymers with properties that change according to the ratio between amides and methylene groups. These materials are not biodegradable and possess great mechanical properties given by strong intermolecular hydrogen binding interactions [73]. Long-chain nylons, where the polar groups are separated by more than six carbon atoms, have both polyethylene properties and polyamide properties. They show low water absorption, good behavior at low temperatures, low density, and low hydrolysis sensitivity, the same as polyethylenic materials, and high melting temperature, good aesthetic properties and good processability, the same as polyamide materials [74].

Copolyamides of 1,4-butanediamine and a mixture of AzA and glutaric acid were synthetized with the aim of analyzing the structure of odd carbon number polyamides. The odd carbon number in their chain imposes a torsion of the amides groups to establish correct H-bonds, creating a γ structure. These polyamides presented a M_w in the range 40,000–51,000 g/mol, a predominant melting peak in the range 220–244 °C, T_d (thermal decomposition temperature) in the range 422–455 °C and a T_g in the range 50–71 °C. The higher M_w was achieved when AzA was 50% molar percentage in the acid mixture, while the lower T_g was obtained for the homopolymer with 100% AzA. Results suggested that a similar predominant hydrogen bonding structure was present in all the analyzed polyamides [73].

Tao et al. synthetized via step-melting polycondensation three different "environmentally friendly" aliphatic polyamides from AzA and 1,6-diaminohexane, 1,10-decanediamine or 1,12-diaminododecane, respectively [75]. AzA and 1,10-decanediammine are industrially obtained from plant oil and castor oil, respectively, while 1,6-diaminohexane can be obtained starting from biorenewable glucose and cellulose. They found that the diamine with a lower number of carbon atoms in its chain led to higher polymerization degrees, higher melting temperature and higher thermostability of the final material but higher T_g, if compared to the ones with C10 and C12. With 1,6-diaminohexane, the final material had M_n 51,300 g/mol, T_m 214 °C, polymerization degree 190, T_d 435 °C and T_g 56 °C. With 1,10-decanediamine, the final material had M_n 38,900 g/mol, T_m 203 °C, polymerization degree 120, T_d 430 °C and T_g 52 °C. With 1,12-diaminododecane, the final material had number-average molecular weight 38,500 g/mol, T_m 195 °C, polymerization degree 100, T_d 425 °C and T_g 50 °C. A shorter chain in the diamino compound leads to the formation of more regular and symmetrical chains that are more easily polymerized and have a higher overall density of amide groups that increases the T_m. Conversely, short chains give to the

final material low flexibility and softness, and a decrease in T_g with the increase in CH_2 group of the diamine cross-linker.

Interestingly, glycine addition to the nylon formulation confers biodegradability to the final product. When more than at least 2% *w*/*w* glycine is mixed with one polyamide-producing monomer, such as hexamethylene diamine with AzA, it is possible to obtain biodegradable nylon that can be used in devices such as gardeners' tools, solving the environment plastic dispersion related to their use [76].

AzA polyamides with hot melt adhesive properties for PVC, steel, aluminum, wood, and textile materials are synthetized from different monomer mixture compositions. One composition example is AzA 41% equiv. polymeric fatty acids, 1,18-oxtodecane dicarboxylic acid and amines (ethylenediamine and piperazine) [77]. Another example is represented by dicarboxylic acid, including AzA, polymeric fatty acids, cyclic diamines or/and non-cyclic aliphatic diamines with an odd carbon number in their chain, and additionally organic diamines [78]. Copolymers with 0.5–25% *w*/*w* polyamine, with at least 11 N atoms, and equimolar quantities of dicarboxylic acids, including AzA, and eventually lactams or ω-aminodicarboxylic acids as ulterior polymer-forming monomers, show hot-melt adhesive properties [79]. The addition of AzA in the polyamide formulation of water-soluble textile adhesives, sizing agents or coatings renders them insoluble, and is therefore not recommended [80].

An electric conductive material with ferroelectricity was obtained through polycondensation of a diamine, composed of at least 50% mol of 2-methyl-1,5-pentanediamine, and a dicarboxylic acid mixture, composed of at least 50% mol of AzA. This polyamide is used as a sensor and noise-adsorbing material [81]. Moreover, a mixture of hexamethylene diamine with adipic acid, hexamethylene diamine with AzA and/or sebacic acid, and hexamethylene diamine with isophthalic acid and/or terephthalic acid was used to create transparent oxygen-barrier layers for food applications [82]. AzA is also found in a flame-retardant formulation composed of a thermoplastic polyamide resin, a thermoplastic polyester resin, a reinforcing or bulking filler and a fire retardant. AzA can be used as a component in both polyamide and polyester resins [83].

Finally, Modiri-Delshad et al. produced aromatic polyamide/amino acid Fe_3O nanocomposites with increased thermal stability. Aromatic polyamides are classified as high-performance polymers for their high T_g, good resistance to chemicals, temperature, and oxidation and they were obtained through the polycondensation of AzA, with 4,4′-diphenilsulfone (Figure 6), yielding products characterized by M_n 19,000 g/mol, M_w 42,000 g/mol and a main decomposition step at 420–470 °C [84].

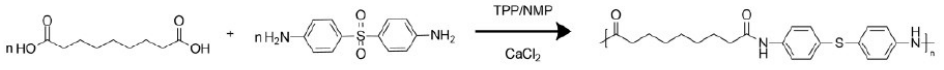

Figure 6. Polyamide synthesis from AzA and 4,4′-diamino diphenyl sulfone. TPP—triphenyl phosphite, NMP—N-methyl-2-pyrrolidone.

5. Azelaic Acid as Component of Plasticizers and Lubricants

The first requisite for a plasticizer is to decrease the glass transition temperature (T_g) of the final polymeric product, thereby enhancing its flexibility and workability [85]. In addition, both plasticizers and lubricants should have low volatility and low tendency for migration between surfaces to avoid changes over time in the finished product qualities and avoid environmental contamination [86].

Azelaic acid is widely used as plasticizer or lubricant in commercial products [87]. In the form of ester or polyester, it can be added to polymeric mixtures to vary the characteristics of the final product.

As a monoester, AzA esterified with aliphatic or aromatic alcohols, confers enhanced cold-temperature resistance to a vulcanizate of an olefinic copolymer. Dibenzyl azelate and diamyl azelate were added at 5–60% weight of the total composition as plasticizers in rubber-like polymers [88].

Different diesters of AZA were synthetized from natural precursors obtained through ozonolysis of crambe seed oil, which led to a mixture of brassylic and azelaic acid. These diacids, when reacted with alcohols of variable chain length at low temperature (4–10 °C) in the presence of a catalyst such as *p*-toluenesulfonic acid, yielded a mixture of diesters that were used at 32% in weight as plasticizers for PVC. Interestingly, the presence of AzA increases the PVC compatibility, the light stability, and the low-temperature flexibility, but also increases the tendencies to migrate outside the final product and the volatility [89].

Polyester plasticizers containing AzA gained importance during the 1970s as PVC plasticizers for their low volatility and low migration tendencies, and various patents dating back to that period will be referred to in the following. However, compared to simpler molecules, they had to be added in higher concentration to the final product, negatively affecting its mechanical properties, in particular at low temperature [90].

Hydroxypolyesters of AzA and 1,4-butanediol or 1,6-hexanediol with or without sebacic acid, were synthetized at high T (Table 3). Among the different molecules obtained, hydroxypoly-1,6-hexanediol azelate and hydroxypoly-1,4-butanediol azelate have a molecular weight about 40,000 g/mol and 25,000 g/mol respectively. These copolymers are used as PVC plasticizers. They are used in packaging and wrapping fields because of their low volatility and low tendency to creep, together with high cold impact resistance and good solvent extraction stability [91].

Polyester plasticizers based on dicarboxylic acids C4-C12, including AZA, glycols C2-C8 and 2,2-dibromomethyl-1,3-propane diol, show flame-retardant properties. These polyesters are added to synthetic resins, mainly foams, that have a high tendency to inflame in air [92].

To control the M_w of the product, AzA plasticizers are obtained with glycols and a terminator agent, such as hydroxyl and monocarboxy-substituted alkanes or mixtures of monobasic acids and monofunctional alcohols. The molecular weight of these polymers can be easily controlled by varying the glycols and the terminator chain lengths [93]. Other polyesters at low molecular weight were obtained reacting benzenedicarboxylic acids, dicarboxylic acids C5-C12 and neopentyl glycol-ethylene glycol mixture with a terminator agent, such as a monofunctional alcohol C6-C13 or a monocarboxylic acid C6-13. The dicarboxylic acids that showed the best results were AZA and adipic acids. The low Mw in the range 500–2000 g/mol confers to these polyesters a low tendency to migration and marring. These plasticizers have a high affinity for PVC resins, but low affinity for polystyrene and acrylonitrile butadiene styrene (ABS) resins, avoiding plasticizer migration between different plastic surfaces [94]. Differently, plasticizers compatible with different plastics such as PVC, rubber, PVC-like and rubber-like plastics were obtained starting from diacids, including AzA, with a mixture composed of 85–90% highly hindered diol and 10–15% short chain diol in the presence of catalysts [95].

New AzA-based plasticizers were created from PET recycling. AzA-based oligoesters were synthetized from the reaction of AzA with polyols at high T. These were then reacted with waste PET in the presence of a catalyst and 2-ethylenexanol as terminator. The plasticizer obtained can be used for PVC resins, substituting low M_w phthalates, which are dangerous for both the environment and human health [96].

Table 3. Structure, function and synthesis route of AzA-based lubricants and plasticizers.

Starting Material	Structure	Function	Synthesis Route	REF
AZA + 2-methyl-2-ethyl-1,3-propanediol	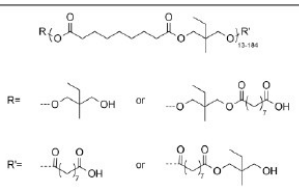	Lubricating oil	chem	[97]

Table 3. *Cont.*

Starting Material	Structure	Function	Synthesis Route	REF
AZA + nonanoic acid + trimethylolpropane (TMP)	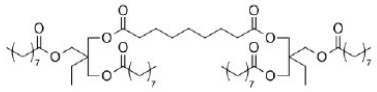	Lubricant	chem	[98]
AZA + propylene glycol mono-n-butyl ether	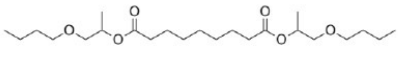 Di(butoxypropyl)azelate	Lubricant diester	chem	[99]
diethyl azelate + 2-ethylhexanol	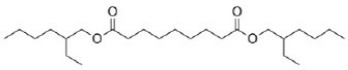 Bis(2-ethylhexyl) azelate (DOZ)	Lubricant	BIO	[100]
AZA + propylene glycol + lauric acid	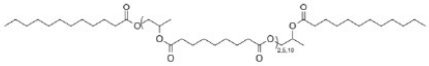	Plasticizer (PVC)	chem	[93]
AZA + 1,2-propylene glycol + lauric acid (terminator) + 2-ethylhexanol (terminator)	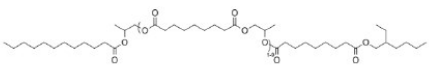	Plasticizer	chem	[80]
AZA + 1,4-butanediol	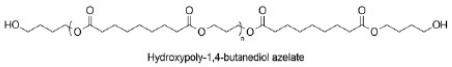 Hydroxypoly-1,4-butanediol azelate	Plasticizer (PVC)	chem	[91]
AZA + alcohol C4-10 (n-butyl, isobutyl, n-pentyl, isopentyl, 2-methylpenthyl ecc)	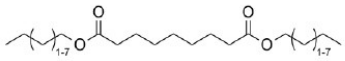	Plasticizer (PVC) diester	chem	[89]
AZA + benzyl alcohol	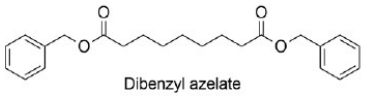 Dibenzyl azelate	Plasticizer (rubber-like polymers)	chem	[88]
AZA + 1-pentanol	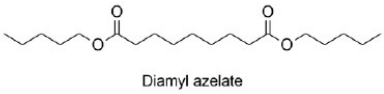 Diamyl azelate	Plasticizer (rubber-like polymers)	chem	[88]

Similar to plasticizers, the requisites for lubricants are: a high viscosity index that means minimum viscosity change with temperature, a high flash point, good resistance to corrosion, high stability to oxidation, low temperature fluidity and low pour point, to reduce friction and facilitate movement between surfaces [101].

Bis(2-ethylhexyl) azelate, or DOZ, is a common commercial lubricant obtained from diethyl azelate and 2-ethylhexanol. DOZ has a M_w of 412.6 g/mol, a viscosity index of 138 and a pour point of −62.22 °C (PubChem). Recently, this diester was synthetized through the transesterification of diethyl azelate and 2-ethylhexanol in the presence of immobilized lipase B from *Candida antarctica* [100].

Di(butoxypropyl)azelate is synthetized from AzA and propylene glycol mono-n-butyl ether. Diesters and triesters of dicarboxylic acids with a carbon chain length of 9 or less, including AzA, and a branched monovalent glycol ether C3-C25 are good lubricant oils with excellent lubricity and low T characteristics. Notably, these lubricants have both low viscosity and low volatility because of their low Mw but high polarity that impedes their migration outside the final product [99].

Esterification of AzA with di-ethylene glycol and 2-ethylhexane in the presence of n-benzene disulfonic acid as catalyst, allows the production of two lubricants with a

pour point of −53.89 °C and a flash point > 240.56 °C. It is possible to create lubricants "tailor made" from a dibasic acid C6-20, a glycol, and a mono-functional compound as terminator, in this case a mono-hydroxy alcohol or a mono-carboxylic alcohol. Varying the composition, polyesters with different lubricating properties, low pour point and flat viscosity–temperature properties were obtained [102].

One of the characteristics required for a lubricant is to have good oxidation stability. The presence of hydrogen in the β-position in the lubricant molecule is, therefore, a problem. To overcome this problem, hindered glycols with no hydrogen in the β-position were reacted with dicarboxylic acids, including AZA, in the presence of a catalyst. The obtained polyesters were oil-soluble and with a M_w in the range 10,000–1,000,000 g/mol. They are used as viscosity index improvers or thickening agents in lubricants, conferring to the final product a high viscosity index, enhanced shear stability and, most of all, good oxidative stability [103]. For the same reason, lubricants with a low pour point, made by reacting AzA with pelargonic acid and trimethylol propane (TMP) at 180–210 °C, were devised. The dicarboxylic and monocarboxylic acids can be obtained through ozonolysis of fatty acids from animal and vegetal sources, while TMP is a polyol with no hydrogen in the β-position [98]. Super-polyesters are created from AzA and 2-methyl-2-ethyl-1,3-propanediol. These polyesters have a M_w between 4000–50,000 g/mol and have good solubility in synthetic ester lubricating oils, working as thickening agents increasing viscosity, viscosity index and thermal decomposition resistance to the final lubricant [97].

6. Studies on the Biodegradation of Azelaic Acid Polymers

Azelaic acid, being a bio-based monomer, offers the opportunity to produce a more sustainable polymer as long as they meet some criteria associated with the efficient use of resources and more precisely: (i) the use of resources being cultivated on (at least) an annual basis; (ii) full valorization of biomass according to a cascade use; (iii) reduction of the carbon footprint and greenhouse emissions; (iv) saving and substituting fossil resources "step by step". Consequently, the employment of AzA in plastic production may mitigate the "upstream" environmental impact of plastics, which refers to the impact generated from the extraction of raw materials to the manufacturing of plastic feedstock. However, the use of a bio-based monomer does not imply the automatic reduction of the "downstream" environmental impact of plastics, namely the impact generated once the consumer has discarded the product [104].

Indeed, polymers and plastics derived from biomass can be either biodegradable or non-biodegradable whereas there are different fossil-based plastics, such as polycaprolactone, that are biodegradable according to the relevant standards. On the other hand, there are several bio-based plastics on the market that are highly resistant to biodegradation due to their chemical structure (e.g., polyethylene from biomass).

According to the United Nations Environment Programme (UNEP), 8 Mt of plastic are poured into the oceans each year, an equivalent to a full truckload every minute [105]. Collecting and recycling plastics represents an answer to the problem [106] but not all polymeric and plastic products can be collected and recycled, some examples include cosmetic ingredients, lubricants, food service plastics, mulching films for agriculture, and fishing nets.

In the past, several methods such as thermal, pyrolytic, photochemical and photodegradation were used to solve the polyester environmental problem related to the end-of-life of packaging. However, the harsh degradation conditions, by-product formation and harmful gases are the major disadvantages that should be minimized, possibly through the biodegradation and recycling of organic carbon within biological pathways [107].

Ideally, the ecodesign of polymers and plastics should respond to the specific usage and disposal requirements of each different plastic product. Since biodegradation does not depend on the resource basis of a material, the misuse of bio-based plastics might lead to downstream environmental impact [30], which must be prevented through adequate and clear labelling. Because biodegradation occurs at different rates in soil and in water, there

is the necessity for standards which define clearly how plastic waste must be managed in different environments. The European standard EN 13432 "Requirements for packaging recoverable through composting and biodegradation" [108] entails "at least 90% disintegration after twelve weeks, 90% biodegradation (CO_2 evolvement) in six months, and includes tests on ecotoxicity and heavy metal content". This is the standard for biodegradable packaging designed for treatment in industrial composting facilities and anaerobic digestion. Another standard, the ASTM D 6691 [109] offers a test method to assess biodegradation in water.

The mechanism of polyester biodegradation involves two major steps. First, a superficial degradation occurs due to the formation of a microbial biofilm generated after the hydrolysis of some ester bonds and small particles are generated. Then the enzymes secreted by microorganisms catalyze the depolymerization of the polymer chain into oligomers or monomers [110]. There are several factors that affect the enzymatic degradation of a polyester, such as its chemical structure, but also by their physical properties: crystallinity, melting point (T_m), glass transition temperature (T_g), etc. [111].

The following paragraphs report the up-to-date degradation methods applied to azelaic acid-based polyesters and polyesteramides. Among the degradation methods previously mentioned for the compounds containing azelaic acid, the studies were focused basically on enzymatic degradation, chemical degradation and biodegradation in sludge or compost.

The enzymatic degradation of four different aliphatic polyester films containing 1,4-butanediol and dimethyl succinate, dimethyl glutarate, dimethyl suberate and dimethyl azelate units was evaluated by Shirahama et al. The experiments were performed at 37 °C and the enzymatic degradation of the polyester films were examined in buffer solutions using three different enzymes: cholesterol esterase from *Pseudomonas* sp., *R. delemar* lipase, and lipase B from *Pseudomonas fragi*. The experiments were performed at the optimal pH for each enzyme and the efficiency of the degradation was evaluated by mass loss measurement, molecular weight, and thermal properties. Among the tested enzymes the cholesterol esterase was the most efficient on the azelaic acid-1,4-butanediol polyesters. In the presence of the lipases, about 80% of the mass was lost in 200 h when lipase B from *Ps. fragi* was used, while the presence of the lipase from *R. delemar* was less effective (10% in 200 h) [112].

The chemical and enzymatic hydrolysis of poly(ethylene azelate) (PEAz) prepared by the two-stage melt polycondensation method was evaluated in comparison with polycaprolactone. The chemical hydrolysis rates, however, were very slow. The enzymatic hydrolysis was performed using a mixture of *R.delemar* and *P.cepacia* lipases at 30 °C in phosphate buffer pH 7. The degradation was monitored by weight loss measurement and even though compared to the PCL, the weight loss for PEAz was about four times higher, but since the molecular weight (PCL 60,000 g/mol, PEAz 21,000 g/mol), the melting point and the crystallinity of the samples were different, the authors indicated a comparable degradation rate with PCL. Morphological analysis by SEM confirmed the extension of the erosion surface in time and were correlated with the weight loss values [56].

In a later study, the same group synthesized and compared the enzymatic degradability of the poly(butylene azelate) (PBAz) polyesters with poly(ethylene azelate) (PEAz) and poly(propylene azelate) (PPAz). The samples were formulated as films and the enzymatic degradation studies were performed in similar conditions: 30 °C, phosphate buffer solution (pH 7.2) and a mixture of *Rhizopus delemar* lipase and *Pseudomonas cepacia* lipase (9:1 *w*/*w* lipases ration). The degree of biodegradation was estimated from the mass loss and were compared to the PCL enzymatic hydrolysis. The highest mass loss was observed for poly(propylene azelate) when after 35 days 40 mg/cm^2 of the mass was lost while for the poly-ethylene and -butylene azelates the mass loss was significantly slower (less than 5 mg/cm^2). The degradation behavior of the poly(propylene azelate) was attributed mainly to the lower crystallinity, 27% for PPAz, compared to 50–55% for PEAz and PBAz and 60% for PCL. Moreover, in the same study, a comparison of the mass loss values during

degradation of the succinate, azelate, sebacate, polyesters and PCL was included. The results revealed that the enzymatic degradation rate of the azelaic acid polyesters was about four times lower compared to the succinic acid-based polyesters but twice as high, compared to the sebacic acid based polyesters. The results indicate that the enzymatic degradation in the presence of lipases is strongly affected by the samples' crystallinity [113].

The enzymatic degradation of azelaic acid and 1,4-butanediol copolymers formulated as films was evaluated by using *Rhizopus oryzae* lipase at 25 and 37 °C up to 50 days, by weight loss monitoring and morphologically by SEM technique. The synthesis of the polyesters was performed by two-stage melt polycondensation at 150 °C and 180 °C. A comparison of the enzymatic degradability of polyesters containing azelaic and succinic acid moieties, as well as random copolymers containing 1,4-butanediol and the two dicarboxylic units, was performed and considerable differences were observed. The results indicated that copolymers have significant amorphous domains and facilitate enzymatic attack [114].

The degradation of a series of polyesteramides prepared from 1,4:3,6-dianhydro-D-glucitol α-amino acids and aliphatic dicarboxylic acids of the methylene chain length ranging from 2 to 10, including azelaic acid, was evaluated by three degradation methods: soil burial degradation, degradation in an activated sludge and enzymatic degradation.

The soil burial degradation test was carried out at pH 6.8, temperature 27 °C, humidity 70–80% in the soil prepared at Nagoya University farm. The weight recovered after 60 days of incubation of the polyesteramide film containing azelaic acid was 45%. Compared to the polyesteramides containing a shorter methylene chain length, the recovered weight was higher.

The degradation in an activated sludge was performed at 27 °C and monitored by BOD and size exclusion chromatography measurements. The BOD biodegradability values obtained for the all the poly(ester amide)s series were in the range 0–40% while for the azelaic acid polyesteramides, the value was 5%.

For the enzymatic degradation studies, seven different enzymes were considered: porcine pancreas lipase, porcine liver esterase, *Rhizopus delemar* lipase, *Rhizopus arrhizus* lipase, *Pseudomonas* sp. cholesterol esterase, *Pseudomonas* sp. lipase and *Streptomyces rochei* carboxylase. The experiments were performed at 37 °C for 24 h and the degradation was monitored by water-soluble total organic carbon (TOC) measurement. In addition to polyesteramides for this study, the corresponding polyesters were also considered as substrates. For the azelaic acid-based substrates, the results obtained in the presence of the porcine pancreas lipase and papain are presented and discussed. The results revealed that the enzymatic degradability of the polyesteramide compared to the polyester was about three times lower and, compared to the other polyesteramides from the series, the degradability was dependent on the methylene chain length of the dicarboxylic acid component [115].

The hydrolytic degradation of poly(glycerol-azelaic acid) synthesized via melt polycondensation at 140 °C in the absence of catalyst and solvent and of the correspondent hydroxyapatite nanocomposites was studied by Chenani et. al. Overall, the weight loss of the samples was gradually decreasing, which can be attributed to the interactions of water molecules with ester bonds in the PGAZ macromolecule. However, incorporating nanoparticles led to enhanced weight loss and hydrolytic degradation rate. The number of ester bonds has grown in the presence of higher amounts of nanoparticles and the water affinity and tendency improved. The hydrolytic degradation was evaluated in neutral conditions (pH 7) and in alkaline conditions (pH 11). In neutral conditions, the weight loss of the samples over 30 days was monitored and the gradually decrease of the samples in time was attributed to the interactions of water molecules with ester bonds but the incorporation of the nanoparticles led to strengthening the weight loss and hydrolytic degradation rate. At pH 11, a more accelerated decrease of the mass was observed, which was attributed to possible hydrolysis in the presence of the hydroxylic ions, but for the nanocomposites the hydrolysis rate was slowed and the weight fraction mass was about 30% higher compared to the sample without the nanoparticles [116].

The biodegradation of poly(sorbital azelate-*co*-sorbital citrate) polyester films was evaluated by Kesavan et al. at pH 7 in a phosphate cradle arrangement for up to 90h and 38.8% of the mass was lost. The results were compared with the data obtained for poly(mannitol glutarate-co-mannitol citrate) in similar conditions and even though the weight loss was slightly higher (42.8), a difference of 4% cannot be considered significant [117].

7. Conclusions and Future Perspectives

Bio-based polymers and plastics are objects of interest for their potential contribution to the resolution of the environmental impact caused by fossil-based plastics, because they promote the transition towards renewable raw materials. The environmental benefit is magnified when the bio-based polymers are also biodegradable and biocompostable, since they allow for the re-introduction of the organic carbon into the biogenic cycles, for instance, in the form of compost for the soil. Nowadays, the research in the field of the synthesis of bio-based polymers is mature for the delivery of new polymeric products and solutions, which are competitive in terms of performance beyond being sustainable.

The aim of the present literature study was to provide a new perspective on the potential of azelaic acid as bio-based monomer for the synthesis of an array of products applicable in different fields, from packaging, cosmetic and pharmaceutical use. Apart from its pharmacological properties, azelaic acid, due to its double carboxylic groups, was successfully used for different oligo and polymer synthesis with applications as a plasticizer or as lubricants. Moreover, in recent years, the biodegradation of azelaic acid derivatives has been evaluated and promising results have been obtained. This renewal of interest towards azelaic acid materials was emphasized since the possibility of obtaining bio-based products was demonstrated. Moreover, the importance and potential of azelaic acid for industrial applications was demonstrated by its industrial synthesis on a large scale.

Fully green synthesis routes of the azelaic acid derivatives (polyesters, polyamides) by selection of suitable catalysts, reaction media or solvent-less conditions, already allow the production of products for the cosmetic and pharma industries. Consequently, several interesting new materials containing azelaic acid will be obtained through polymerization using bi- or tri-component systems and will represent a renewable alternative to existing materials. In conclusion, the wealth of knowledge gathered in the last decades paves the way to the development of advanced technological solutions able to combine and valorize the chemical and pharmacological properties of this monomer, while benefiting from the sustainability and biodegradability of the new polymeric products.

Author Contributions: Conceptualization, A.T. and L.G. data curation, A.T., T.M., writing—original draft preparation: A.T., C.D., M.S., F.A., G.Z., T.M., L.G.; writing—review and editing: A.T., L.G., M.S., F.A., T.M.; visualization, A.T., M.S.; supervision, A.T., L.G., T.M.; project administration A.T., L.G., T.M.; funding acquisition, A.T., L.G., T.M.; All authors have read and agreed to the published version of the manuscript.

Funding: This work has been partially financed by Regione Piemonte, project PRIME, POR FESR 2014/2020. This project has received funding from the European Union's Horizon 2020 research and innovation program under the Marie Skłodowska-Curie grant agreement No 101029444.

Institutional Review Board Statement: Not applicable.

Informed Consent Statement: Not applicable.

Conflicts of Interest: The authors declare no conflict of interest.

References

1. Sheldon, R.A. Green and sustainable manufacture of chemicals from biomass: State of the art. *Green Chem.* **2014**, *16*, 950–963. [CrossRef]
2. Brenna, E.; Colombo, D.; Di Lecce, G.; Gatti, F.G.; Ghezzi, M.C.; Tentori, F.; Tessaro, D.; Viola, M. Conversion of oleic acid into azelaic and pelargonic acid by a chemo-enzymatic route. *Molecules* **2020**, *25*, 1882. [CrossRef] [PubMed]
3. Azelaic Acid Market Size 2020: Top Countries Data with Global Demand Analysis and Opportunity Outlook 2024—MarketWatch. Available online: https://www.marketwatch.com/press-release/azelaic-acid-market-size-2020-top-countries-data-with-global-demand-analysis-and-opportunity-outlook-2024-2020-10-29 (accessed on 15 December 2020).
4. Nazzaro-Porro, M. Azelaic acid. *J. Am. Acad. Dermatol.* **1987**, *9*, 157–160. [CrossRef]
5. Gollnick, H. A new therapeutic agent: Azelaic acid in acne treatment. *J. Dermatol. Treat.* **1990**, *1*, S23–S28. [CrossRef]
6. Pérez-Bernal, A.; Muñoz-Pérez, M.A.; Camacho, F. Management of facial hyperpigmentation. *Am. J. Clin. Dermatol.* **2000**, *1*, 261–268. [CrossRef]
7. Vashi, N.A.; Kundu, R.V. Facial hyperpigmentation: Causes and treatment. *Br. J. Dermatol.* **2013**, *169*, 41–56. [CrossRef]
8. Rendon, M.; Berneburg, M.; Arellano, I.; Picardo, M. Treatment of melasma. *J. Am. Acad. Dermatol.* **2006**, *54*, 272–281. [CrossRef]
9. Hearing, V.J.; Tsukamoto, K. Enzymatic control of pigmentation in mammals. *FASEB J.* **1991**, *5*, 2902–2909. [CrossRef]
10. Marmol, V.; Beermann, F. Tyrosinase and related proteins in mammalian pigmentation. *FEBS Lett.* **1996**, *381*, 165–168. [CrossRef]
11. Schallreuter, K.U.; Wood, J.W. A possible mechanism of action for azelaic acid in the human epidermis. *Arch. Dermatol. Res.* **1990**, *282*, 168–171. [CrossRef]
12. Wood, J.M.; Schallreuter, K.U. Reduced thioredoxin inhibits melanin biosynthesis: Evidence for the formation of a stable bis-cysteinate complex with tyrosinase. *Inorg. Chim. Acta* **1988**, *151*, 7. [CrossRef]
13. Holmgren, A. Thioredoxin. *Annu. Rev. Biochem.* **1985**, *54*, 237–271. [CrossRef] [PubMed]
14. Holmgren, A.; Lu, J. Thioredoxin and thioredoxin reductase: Current research with special reference to human disease. *Biochem. Biophys. Res. Commun.* **2010**, *396*, 120–124. [CrossRef] [PubMed]
15. Urig, S.; Becker, K. On the potential of thioredoxin reductase inhibitors for cancer therapy. *Semin. Cancer Biol.* **2006**, *16*, 452–465. [CrossRef]
16. Passi, S.; Picardo, M.; Nazzaro-Porro, M.; Breathnach, A.; Confaloni, A.M.; Serlupi-Crescenzi, G. Antimitochondrial effect of saturated medium chain length (C8-C13) dicarboxylic acids. *Biochem. Pharmacol.* **1984**, *33*, 103–108. [CrossRef]
17. Picardo, M.; Passi, S.; Sirianni, M.C.; Fiorilli, M.; Russo, G.D.; Cortesi, E.; Barile, G.; Dermatologico, I.; Gallicano, S. Activity of azelaic acid on cultures of lymphoma and leukemia-derived cell lines, normal resting and stimulated lymphocytes and 3T3 fibroblasts. *Biochem. Pharmacol.* **1985**, *34*, 1653–1658. [CrossRef]
18. Gollnick, H.; Cunliffe, W.J.; Berson, D.; Dreno, B.; Finlay, A.; Leyden, J.J.; Shalita, A.R.; Thiboutot, D. Management of acne: A report from a global alliance to improve outcomes in acne. *J. Am. Acad. Dermatol* **2003**, *52*, 43–51.
19. Sieber, M.A.; Hegel, J.K.E. Azelaic acid: Properties and mode of action. *Skin Pharmacol. Physiol.* **2013**, *27*, 9–17. [CrossRef]
20. Draelos, Z.D.; Elewski, B.; Staedtler, G.; Havlickova, B. Azelaic acid foam 15% in the treatment of papulopustular rosacea: A randomized, double-blind, vehicle-Controlled study. *Cutis* **2013**, *92*, 306–317.
21. Gollnick, H.; Layton, A. Azelaic acid 15% gel in the treatment of rosacea. *Expert Opin. Pharmacother.* **2008**, *9*, 2699–2706. [CrossRef]
22. Mastrofrancesco, A.; Ottaviani, M.; Aspite, N.; Cardinali, G.; Izzo, E.; Graupe, K.; Zouboulis, C.C.; Camera, E.; Picardo, M. Azelaic acid modulates the inflammatory response in normal human keratinocytes through PPARγ activation. *Exp. Dermatol.* **2010**, *19*, 813–820. [CrossRef]
23. Coda, A.B.; Hata, T.; Miller, J.; Audish, D.; Kotol, P.; Two, A.; Shafiq, F.; Yamasaki, K.; Harper, J.C.; Del Rosso, J.Q.; et al. Cathelicidin, kallikrein 5, and serine protease activity is inhibited during treatment of rosacea with azelaic acid 15% gel. *J. Am. Acad. Dermatol.* **2013**, *69*, 570–577. [CrossRef] [PubMed]
24. Kosmadaki, M.; Katsambas, A. Topical treatments for acne. *Clin. Dermatol.* **2017**, *35*, 173–178. [CrossRef] [PubMed]
25. Passi, S.; Picardo, M.; Zompetta, C.; de Luca, C.; Breathnach, A.S.; Nazzaro-porro, M. The oxyradical-scavenging activity of azelaic acid in biological systems. *Free Radic. Res.* **1991**, *15*, 17–28. [CrossRef] [PubMed]
26. Jones, D.A. Rosacea, reactive oxygen species, and azelaic acid. *J. Clin. Aesthet. Dermatol.* **2009**, *2*, 26–30.
27. De Leon Izeppi, G.A.; Dubois, J.L.; Balle, A.; Soutelo-Maria, A. Economic risk assessment using Monte Carlo simulation for the production of azelaic acid and pelargonic acid from vegetable oils. *Ind. Crops Prod.* **2020**, *150*, 112411. [CrossRef]
28. Köckritz, A.; Martin, A. Synthesis of azelaic acid from vegetable oil-based feedstocks. *Eur. J. Lipid Sci. Technol.* **2011**, *113*, 83–91. [CrossRef]
29. Bieser, A.; Borsotti, G.; Digioia, F.; Ferrari, A.; Pirocco, A. Continuous Process for the Production of Derivatives of Saturated Carboxylic Acids. Patent WO2011080297, 7 July 2011.
30. Bastioli, C.; Borsotti, G.; Merlin, A.; Milizia, T. Process for the Catalytic Cleavage of Vegetable Oils. U.S. Patent 2012/0226060 A1, 6 September 2012.
31. Ackman, R.G.; Retson, M.E.; Gallay, L.R.; Vandenheuvel, F.A. Ozonolysis of unsaturated fatty acids. *Can. J. Chem.* **1961**, *39*, 25–28. [CrossRef]
32. Shi, C.-W.; Chen, Y.-P. Preparation of Azelaic Acid by Oxidation with Hydrogen Peroxide and Ozone. 2006. Available online: https://www.researchgate.net/publication/294680528_Preparation_of_azelaic_acid_by_oxidation_with_hydrogen_peroxide_and_ozone (accessed on 10 June 2021).

33. Sato, M.; Sasaki, Y.; Komatsu, M. Production Method of Carboxylic Acid Compound. Patent JP2009155320A, 14 November 2008.
34. Benessere, V.; Cucciolito, M.E.; De Santis, A.; Di Serio, M.; Esposito, R.; Ruffo, F.; Turco, R. Sustainable Process for Production of Azelaic Acid Through Oxidative Cleavage of Oleic Acid. *J. Am. Oil Chem. Soc.* **2015**, *92*, 1701–1707. [CrossRef]
35. Kulik, A.; Martin, A.; Pohl, M.M.; Fischer, C.; Köckritz, A. Insights into gold-catalyzed synthesis of azelaic acid. *Green Chem.* **2014**, *16*, 1799–1806. [CrossRef]
36. Laurenza, A.G.; Casiello, M.; Anzivino, M.; Caputo, D.; Catucci, L.; Dell'Anna, M.M.; Fusco, C.; Rizzi, V.; Pantone, V.; D'Accolti, L.; et al. Green Procedure for One-Pot Synthesis of Azelaic Acid Derivatives Using Metal Catalysis. *Recent Innov. Chem. Eng.* **2018**, *11*, 185–191. [CrossRef]
37. Method for Preparing Azelaic Acid by Enzyme Catalysis of Hydrogen Dioxide Oxygenated Oleic Acid. Chinese Patent 101200735, 18 June 2008.
38. Kevin, A.; Douglas, W.; Fayter, F.; McVay, H. Process for Making Polycarboxylic Acids. Patent US005962285, 5 October 1999.
39. Seo, E.J.; Yeon, Y.J.; Seo, J.H.; Lee, J.H.; Boñgol, J.P.; Oh, Y.; Park, J.M.; Lim, S.M.; Lee, C.G.; Park, J.B. Enzyme/whole-cell biotransformation of plant oils, yeast derived oils, and microalgae fatty acid methyl esters into n-nonanoic acid, 9-hydroxynonanoic acid, and 1,9-nonanedioic acid. *Bioresour. Technol.* **2018**, *251*, 288–294. [CrossRef] [PubMed]
40. Song, J.W.; Lee, J.H.; Bornscheuer, U.T.; Park, J.B. Microbial synthesis of medium-chain α,ω-dicarboxylic acids and ω-aminocarboxylic acids from renewable long-chain fatty acids. *Adv. Synth. Catal.* **2014**, *356*, 1782–1788. [CrossRef]
41. Akira, T.; Seiichi, U. Saitama, Preparation of Oxygen-Containing Organic Compounds Containing a Carboxyl Group Including Peroxycarboxylic Acids. Patent DE2853847C2, 14 December 1977.
42. Robert, T.; Friebel, S. Itaconic acid-a versatile building block for renewable polyesters with enhanced functionality. *Green Chem.* **2016**, *18*, 2922–2934. [CrossRef]
43. Hatti-Kaul, R.; Nilsson, L.J.; Zhang, B.; Rehnberg, N.; Lundmark, S. Designing Biobased Recyclable Polymers for Plastics. *Trends Biotechnol.* **2020**, *38*, 50–67. [CrossRef]
44. Bastioli, C. *Handbook of Biodegradable Polymers*; De Gruyter: Berlin, Germany, 2020; ISBN 9781501511981.
45. Takasu, A.; Iio, Y.; Oishi, Y.; Narukawa, Y.; Hirabayashi, T. Environmentally benign polyester synthesis by room temperature direct polycondensation of dicarboxylic acid and diol. *Macromolecules* **2005**, *38*, 1048–1050. [CrossRef]
46. Bassanini, I.; Hult, K.; Riva, S. Dicarboxylic esters: Useful tools for the biocatalyzed synthesis of hybrid compounds and polymers. *Beilstein J. Org. Chem.* **2015**, *11*, 1583–1595. [CrossRef] [PubMed]
47. Yu, Y.; Wei, Z.; Liu, Y.; Hua, Z.; Leng, X.; Li, Y. Effect of chain length of comonomeric diols on competition and miscibility of isodimorphism: A comparative study of poly(butylene glutarate-co-butylene azelate) and poly(octylene glutarate-co-octylene azelate). *Eur. Polym. J.* **2018**, *105*, 274–285. [CrossRef]
48. Zamboulis, A.; Nakiou, E.A.; Christodoulou, E.; Bikiaris, D.N.; Kontonasaki, E.; Liverani, L.; Boccaccini, A.R. Polyglycerol hyperbranched polyesters: Synthesis, properties and pharmaceutical and biomedical applications. *Int. J. Mol. Sci.* **2019**, *20*, 6210. [CrossRef]
49. Kadhum, A.A.H.; Baharu, M.N.; Mahmood, M.H. Elastic polyesters from glycerol and azelaic acid. *Adv. Mater. Res.* **2011**, *233*, 2571–2575. [CrossRef]
50. Chongcharoenchaikul, T.; Thamyongkit, P.; Poompradub, S. Synthesis, characterization and properties of a bio-based poly(glycerol azelate) polyester. *Mater. Chem. Phys.* **2016**, *177*, 485–495. [CrossRef]
51. Wyatt, V.T. Lewis acid-catalyzed synthesis of hyperbranched polymers based on glycerol and diacids in toluene. *J. Am. Oil Chem. Soc.* **2012**, *89*, 313–319. [CrossRef]
52. Wyatt, V.T.; Nuñez, A.; Foglia, T.A.; Marmer, W.N. Synthesis of hyperbranched poly(glycerol-diacid) oligomers. *J. Am. Oil Chem. Soc.* **2006**, *83*, 1033–1039. [CrossRef]
53. Wyatt, V.T.; Strahan, G.D.; Nuñez, A. The lewis acid-catalyzed synthesis of hyperbranched oligo(glycerol-diacid)s in aprotic polar media. *J. Am. Oil Chem. Soc.* **2010**, *87*, 1359–1369. [CrossRef]
54. Nguyen, H.D.; Löf, D.; Hvilsted, S.; Daugaard, A.E. Highly branched bio-based unsaturated polyesters by enzymatic polymerization. *Polymers* **2016**, *8*, 363. [CrossRef] [PubMed]
55. Baharu, M.N.; Kadhum, A.A.H.; Al-Amiery, A.A.; Mohamad, A.B. Synthesis and characterization of polyesters derived from glycerol, azelaic acid, and succinic acid. *Green Chem. Lett. Rev.* **2015**, *8*, 31–38. [CrossRef]
56. Papageorgiou, G.Z.; Bikiaris, D.N.; Achilias, D.S.; Karagiannidis, N. Synthesis, crystallization, and enzymatic degradation of the biodegradable polyester poly(ethylene azelate). *Macromol. Chem. Phys.* **2010**, *211*, 2585–2595. [CrossRef]
57. Giuliani, G.; Benedusi, A.; Mascolo, A.; Marzani, B.; Bregaglio, G. Polyglycerol-Azelaic Acid Polyesters for Cosmetic Applications. Patent WO 2014/020158 Al, 6 February 2014.
58. Khairudin, N.; Basri, M.; Fard Masoumi, H.R.; Sarah Samiun, W.; Samson, S. Lipase-catalyzed synthesis of dilauryl azelate ester: Process optimization by artificial neural networks and reusability study. *RSC Adv.* **2015**, *5*, 94909–94918. [CrossRef]
59. Khairudin, N.; Basri, M.; Masoumi, H.R.F.; Samson, S.; Ashari, S.E. Enhancing the bioconversion of azelaic acid to its derivatives by response surface methodology. *Molecules* **2018**, *23*, 397. [CrossRef]
60. Curia, S.; Howdle, S.M. Towards sustainable polymeric nano-carriers and surfactants: Facile low temperature enzymatic synthesis of bio-based amphiphilic copolymers in $scCO_2$. *Polym. Chem.* **2016**, *7*, 2130–2142. [CrossRef]
61. Cho, G.H.P.; Yeong, S.K.; Ooi, T.L.; Chuah, C.H. Glycerol esters from the reaction of glycerol with dicarboxylic acid esters. *J. Surfactants Deterg.* **2006**, *9*, 147–152. [CrossRef]

62. Baldo, F.; Nguyen, Q.L.; Pham, D.-M. Combination of a light ray and a lipase-bioconvertible compound for improving skin and/or hair appearance. U.S. Patent 2011/0130704 A1, 2 June 2011.
63. Bastioli, C.; Milizia, T.; Floridi, G.; Scaffidi Lallaro, A.; Cella, G.; Tosin, M. Biodegradable Aliphatic -Aromatic Polyesters. WO 2006/097353 A1, 21 September 2006.
64. Pellis, A.; Gardossi, L. *Integrating Computational and Experimental Methods for Efficient Biocatalytic Synthesis of Polyesters*, 1st ed.; Elsevier Inc.: Amsterdam, The Netherlands, 2019; Volume 627, ISBN 9780128170953.
65. Guarneri, A.; Cutifani, V.; Cespugli, M.; Pellis, A.; Vassallo, R.; Asaro, F.; Ebert, C.; Gardossi, L. Functionalization of Enzymatically Synthesized Rigid Poly(itaconate)s via Post-Polymerization Aza-Michael Addition of Primary Amines. *Adv. Synth. Catal.* **2019**, *361*, 2559–2573.
66. Comerford, J.W.; Byrne, F.P.; Weinberger, S.; Farmer, T.J.; Guebitz, G.M.; Gardossi, L.; Pellis, A. Thermal upgrade of enzymatically synthesized aliphatic and aromatic oligoesters. *Materials* **2020**, *13*, 368. [CrossRef] [PubMed]
67. Ansorge-Schumacher, M.B.; Thum, O. Immobilised lipases in the cosmetics industry. *Chem. Soc. Rev.* **2013**, *42*, 6475–6490. [CrossRef] [PubMed]
68. Gross, R.A.; Kumar, A.; Kalra, B. Enzyme-Catalyzed Polycondensations. US 6972315 B2, 6 December 2005.
69. Dierker, M.; Weichold, C.; Althaus, S.; Zander, L.; Prinz, D. Cosmetic Compositions Containing Esters Based on 2-Propylheptanol. US 864652B2, 4 February 2014.
70. Curia, S.; Barclay, A.F.; Torron, S.; Johansson, M.; Howdle, S.M. Green process for green materials: Viable low-temperature lipase-catalysed synthesis of renewable telechelics in supercritical CO_2. *Philos. Trans. R. Soc. A Math. Phys. Eng. Sci.* **2015**, *373*, 1–16. [CrossRef]
71. Vonderhagen, A.; Gates, J.A.; Hill, K.; Lagarden, M.; Tesmann, H. Enzymatic Synthesis of Polyesters. US005962624A, 5 October 1999.
72. Nylon 6,9—Poly(Hexamethylene Azelamide). Available online: http://polymerdatabase.com/polymers/nylon6-9.html (accessed on 15 July 2021).
73. Olmo, C.; Casas, M.T.; Martínez, J.C.; Franco, L.; Puiggalí, J. Crystalline structures and structural transitions of copolyamides derived from 1,4-diaminobutane and different ratios of glutaric and azelaic acids. *Polymers* **2019**, *11*, 572. [CrossRef]
74. Cotarca, L.; Delogu, P.; Nardelli, A.; Maggioni, P.; Bianchini, R.; Sguassero, S.; Alini, S.; Dario, R.; Clauti, G.; Pitta, G.; et al. Efficient and scaleable methods for ω-functionalized nonanoic acids: Development of a novel process for azelaic and 9-aminononanoic acids (nylon-6,9 and nylon-9 precursors). *Org. Process Res. Dev.* **2001**, *5*, 69–76. [CrossRef]
75. Tao, L.; Liu, K.; Li, T.; Xiao, R. Preparation and properties of biobased polyamides based on 1,9-azelaic acid and different chain length diamines. *Polym. Bull.* **2020**, *77*, 1135–1156. [CrossRef]
76. Davies, J.; Biederman, G.J.; Coco, C. Biodegradable Nylon and Method for the Manufacture Thereof. Patent EP 2842406A1, 4 March 2015.
77. Wroczynski, R.J. Polyamide from Polymerc Fatty Acid and Long Chain Dicarboxylc Acid. Patent US4882414, 21 November 1989.
78. Harman, N.W. Long Open Assembly Time Vinyl-Bonding Polyamide from Dimer Acid. Patent US4853460, 1 August 1989.
79. Oenbrink, G.; Haeger, H.; Richter, R. Polyamide Graft Copolymers. Patent US 6538073B1, 25 March 2003.
80. Fagerburg, D.R.; Davis, B.; Kibler, C.J. Water-Soluble Polyamdes from Alkyleneoxy bis(propyl-amine). Patent US3882090, 6 May 1975.
81. Ogawa, S.; Yoshinaka, S.; Hayashi, T. Polyamide and Resin Composition. Patent US 2004/0068090 A1, 8 April 2004.
82. Presenz, U.; Hewel, M. Transparent Polyamide and Multiply Barrer Films Containing Same. Patent US005686192A, 11 November 1997.
83. Ahmad, S.; Kamal, M.Z.; Sankaranarayanan, R.; Rao, N.M. Thermostable Bacillus subtilis Lipases: In Vitro Evolution and Structural Insight. *J. Mol. Biol.* **2008**, *381*, 324–340. [CrossRef]
84. Modiri-Delshad, T.; Khoobi, M.; Shabanian, M.; Khonakdar, H.A.; Shafiee, A. Synthesis, Thermal and Combustion Properties of New Polyamide/Amidoacid@Fe_3O_4 Nanocomposite. *Adv. Polym. Technol.* **2018**, *37*, 559–565. [CrossRef]
85. Bocqué, M.; Voirin, C.; Lapinte, V.; Caillol, S.; Robin, J.J. Petro-based and bio-based plasticizers: Chemical structures to plasticizing properties. *J. Polym. Sci. Part A Polym. Chem.* **2016**, *54*, 11–33. [CrossRef]
86. Matthews, D.M. Fat-Based synthetic lubricants. *J. Am. Oil Chem. Soc.* **1979**, *56*, 841–844. [CrossRef]
87. Soutelo-Maria, A.; Dubois, J.L.; Couturier, J.L.; Cravotto, G. Oxidative cleavage of fatty acid derivatives for monomer synthesis. *Catalysts* **2018**, *8*, 464. [CrossRef]
88. Smith, W.C. Esters of Azelaic Acid as Plasticizers for Rubberlike Polymers. Patent US 2469748, 10 May 1949.
89. Nieschlag, H.J.; Tallent, W.H.; Wolff, I.A.; Palm, W.E.; Witnauer, L.P. Diester plasticizers from mixed crambe dibasic acids. *Ind. Eng. Chem. Prod. Res. Dev.* **1967**, *6*, 201–204. [CrossRef]
90. Lamont, J.; Aylesworth, R.D.; Beimesch, B.J. Mixed-Terminated Polyester Plasticzers. Patent US 4122057, 24 October 1978.
91. Blaschke, F. Polyester Plasticizer for Polymers of Vinyl Chloride and Process for Preparing the Same. Patent US3331803, 18 July 1967.
92. Daniels, D.A.; Park, K.; Prince, A.E. Flame Retardant Polyester Plasticizers Containing 2,2-dibromoethylene-1,3-propanediol. Patent US 3700957, 24 October 1972.
93. Chang, S.; Ridgway, R.W. Oligomeric Polyesters from Long-Chan Dicarboxylic Acids as Plasticezers for Vinyl. US-4029627-A, 14 June 1977.

94. Mertz, W.J.; Braun, R.J. Polyvinyl Chloride Compositions Plasticized with Copolyesters. Patent US4876304, 24 October 1989.
95. Eapen, T. Polymeric Plasticizers and a Process for Preparing the Same. Patent US-5281647-A, 25 January 1994.
96. Langer, E.; Wasśkiewicz, S.; Lenartowicz-Klik, M.; Bortel, K. Application of waste poly(ethylene terephthalate) in the synthesis of new oligomeric plasticizers. *Polym. Degrad. Stab.* **2015**, *119*, 105–112. [CrossRef]
97. Knowles, E.C.; Sweeney, W.M. Super-Polyester Lubricant Composition. Patent US3162602, 22 December 1964.
98. Samsodin, N.; Shahruddin, S. Preparation of Biopolyol Esters for Lubricant Application. Patent US 9885006 B2, 6 February 1988.
99. Kuratomi, T.; Nagano, K. Lubricant base oil. *Int. J. Pharm.* **2009**, *56*, 1986–2001.
100. Gómez, M.; Murcia, M.D.; Serrano-Arnaldos, M.; Gómez, E.; Gómez, J.L.; Hidalgo, A.M.; Máximo, M.F. Developing the rate equations for two enzymatic Ping-Pong reactions in series: Application to the bio-synthesis of Bis(2-ethylhexyl) azelate. *Biochem. Eng. J.* **2020**, *161*, 107691. [CrossRef]
101. Zainal, N.A.; Zulkifli, N.W.M.; Gulzar, M.; Masjuki, H.H. A review on the chemistry, production, and technological potential of bio-based lubricants. *Renew. Sustain. Energy Rev.* **2018**, *82*, 80–102. [CrossRef]
102. Sanderson, R.T. Polyester, Synthetic Lubricants. Patent US 2628974, 17 February 1953.
103. Kitahara, S.; Shikatani, Y.; Igarashi, J. Oil-Soluble Polyester, Additive for Lubricating Oil, and Lubricating Oil Composition. Patent EP 0727455A2, 21 August 1996.
104. Raynaud, J. Valuing Plastics: The Business Case for Measuring, Managing and Disclosing Plastic Use in the Consumer Goods Industry. Available online: https://wedocs.unep.org/bitstream/handle/20.500.11822/25302/Valuing_Plastic_ES.pdf?sequence=1&isAllowed=y%0Awww.gpa.unep.org%0Awww.unep.org/pdf/ValuingPlastic/ (accessed on 10 July 2021).
105. Jambeck, J.; Geyer, R.; Wilcox, C.; Siegler, T.R.; Perryman, M.; Andrady, A.; Narayan, R.; Law, K.L. Plastic waste inputs from land into the ocean. *Science* **2015**, *347*, 768–771. [CrossRef]
106. The New Plastics Economy Rethinking the Future of Plastics. Available online: http://www3.weforum.org/docs/WEF_The_New_Plastics_Economy.pdf (accessed on 10 February 2021).
107. Gricajeva, A.; Nadda, A.K.; Gudiukaite, R. Insights into polyester plastic biodegradation by carboxyl ester hydrolases. *J. Chem. Technol. Biotechnol.* **2021**. [CrossRef]
108. EN 13432—European Standards. Available online: https://www.en-standard.eu/search/?q=EN+13432 (accessed on 28 April 2020).
109. ASTM D. 6691—European Standards. Available online: https://www.en-standard.eu/search/?q=ASTM+D+6691 (accessed on 28 April 2020).
110. Ding, Y.; Huang, D.; Ai, T.; Zhang, C.; Chen, Y.; Luo, C.; Zhou, Y.; Yao, B.; Dong, L.; Du, X.; et al. Bio-Based Poly(butylene furandicarboxylate-co-glycolate) Copolyesters: Synthesis, Properties, and Hydrolysis in Different Aquatic Environments for Water Degradation Application. *ACS Sustain. Chem. Eng.* **2021**, *9*, 1254–1263. [CrossRef]
111. Urbanek, A.K.; Mirończuk, A.M.; García-Martín, A.; Saborido, A.; de la Mata, I.; Arroyo, M. Biochemical properties and biotechnological applications of microbial enzymes involved in the degradation of polyester-type plastics. *Biochim. Biophys. Acta-Proteins Proteomics* **2020**, *1868*, 140315. [CrossRef] [PubMed]
112. Shirahama, H.; Kawaguchi, Y.; Aludin, M.S.; Yasuda, H. Synthesis and enzymatic degradation of high molecular weight aliphatic polyesters. *J. Appl. Polym. Sci.* **2001**, *80*, 340–347. [CrossRef]
113. Papageorgiou, G.Z.; Bikiaris, D.N.; Achilias, D.S.; Papastergiadis, E.; Docoslis, A. Crystallization and biodegradation of poly(butylene azelate): Comparison with poly(ethylene azelate) and poly(propylene azelate). *Thermochim. Acta* **2011**, *515*, 13–23. [CrossRef]
114. Díaz, A.; Franco, L.; Estrany, F.; Del Valle, L.J.; Puiggalí, J. Poly(butylene azelate-co-butylene succinate) copolymers: Crystalline morphologies and degradation. *Polym. Degrad. Stab.* **2014**, *99*, 80–91. [CrossRef]
115. Okada, M.; Tsunoda, K.; Tachikawa, K.; Aoi, K. Biodegradable polymers based on renewable resources. IV. Enzymatic degradation of polyesters composed of 1,4:3.6-dianhydro-D-glucitol and aliphatic dicarboxylic acid moieties. *J. Appl. Polym. Sci.* **2000**, *77*, 338–346. [CrossRef]
116. Hosseini Chenani, F.; Rezaei, V.F.; Fakhri, V.; Wurm, F.R.; Uzun, L.; Goodarzi, V. Green synthesis and characterization of poly(glycerol-azelaic acid) and its nanocomposites for applications in regenerative medicine. *J. Appl. Polym. Sci.* **2021**, *138*, 1–14. [CrossRef]
117. Kesavan, A.; Rajakumar, T.; Karunanidhi, M.; Ravi, A. Degradation and thermal behavior of copolyesters synthesized by direct liquefy polycondensation. *Mater. Today Proc.* **2021**. [CrossRef]

4.5.6 Delignification of rice husk

The studies carried out so far on immobilization of enzymes on rice husk (RH) indicate that the major limitation of the method is represented by the low loading of protein. The PhD thesis of Marco Cespugli (Cespugli M., 2017) explicated some preliminary attempts to improve the accessibility of RH by removing the hydrophobic lignin on the surface. By treating the RH with alkaline H_2O_2 it is possible to remove lignin and increase the water retention capacity of the composite material, while maintaining its tri-dimensional structure. However, no significant improvement was observed in terms of carbonyl group concentration after laccase-TEMPO oxidation. Conversely, a low protein loading and poor hydrolytic activity of covalently immobilized CaLB was reported. The present study started from these results and firstly optimized the protocol for the delignification and carried out a detailed characterization of the delignified rice husk.

The delignification was carried out with hydrogen peroxide and NaOH under more concentrated conditions. The efficiency of the delignification protocol was assessed through ATR-IR characterization. ATR-IR (Attenuated Total Reflectance) is a sampling technique used in conjunction with infrared spectroscopy which enables the direct analysis of solid or liquid samples without further preparation. The ATR uses the properties of the evanescent wave in total reflection. In this technique, the sample was placed in close contact with an optical element (internal reflection element or ATR crystal) consisting of a crystal with a high refractive index. The IR ray emitted from the source, before reaching the sample, first passes through this element: when the angle of incidence is greater than the critical angle, the phenomenon known as total reflection occurs. This reflection forms the evanescent wave that extends into the sample. The number of reflections can be changed by varying the angle of incidence. The beam is then captured by the detector when the crystal is released. The spectra were recorded by pressing the sample of rice husk until a homogeneous pellet was obtained.

In order to analyse the signals of the ATR-IR spectra of the rice husk, 3 references samples were recorded (figure 4.21): untreated rice husk (black), cellulose tissue (pink), the blue trace is relevant to the IR spectrum of column SiO_2 (Merck) from KBr pellet.

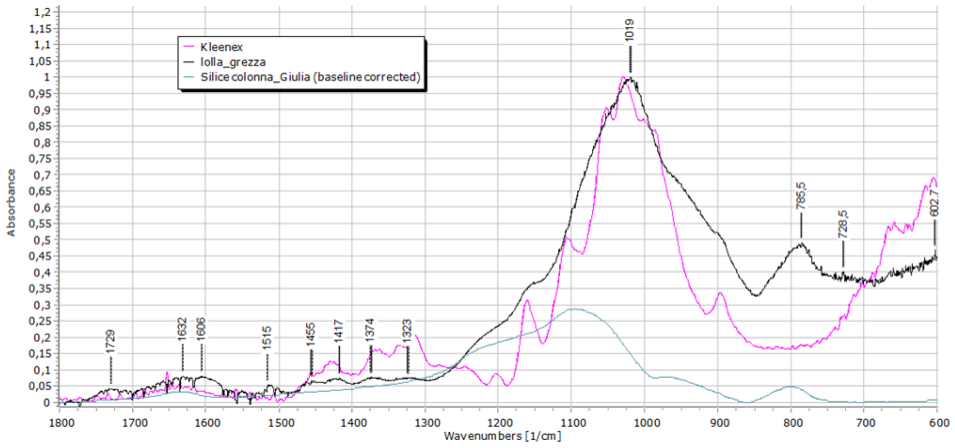

Figure 4.21 *Spectra of 3 references samples: untreated rice husk (black), cellulose tissue (pink) and column SiO2 (Merck) from KBr pellet (blue).*

The fingerprint region for characterization is between 1800-600 cm^{-1}. The most diagnostic signals of the untreated rice husk are detailed in table 4.4.

Table 4.4 Diagnostic signal for characterization of rice husk

cm^{-1}	**Functional Group**
1729	Stretching C=O
1632	Adsorbed water
1608	Stretching C=C aromatic ring of lignin
1417	Stretching CH lignin
1323	Stretching C-O lignin
1220	SiO_2, C-C- lignin, stretching C-O e C=O
1202	cellulose
1160	Esters group of cellulose and lignin
1109	Cellulose
894	cellulose
785	SiO_2

Hemicellulose signals are largely overlapped with cellulose absorptions.

Figure 4.22 shows ATR-IR spectra of delignified rice husk obtained from experimental protocol developed during PhD's thesis.

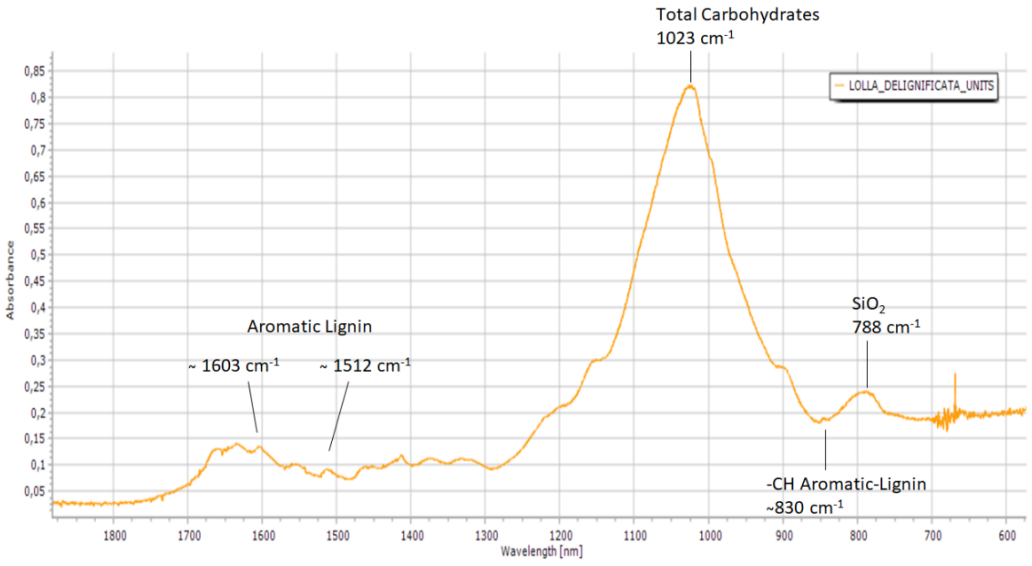

***Figure 4.22** ATR-IR spectra of the delignified RH.*

Fingerprint region is between 1800-600 cm^{-1}. The efficiency of delignification can be qualitatively determined by observing the height of the following peaks: 830 cm^{-1} referring to aromatic -CH of lignin and 1512 e 1603 cm^{-1} that identify stretching C=C of lignin aromatic ring.

Figure 4.23 shows a comparison between ATR-IR spectra of untreated rice husk and delignified rice husk (RH_UNITS).

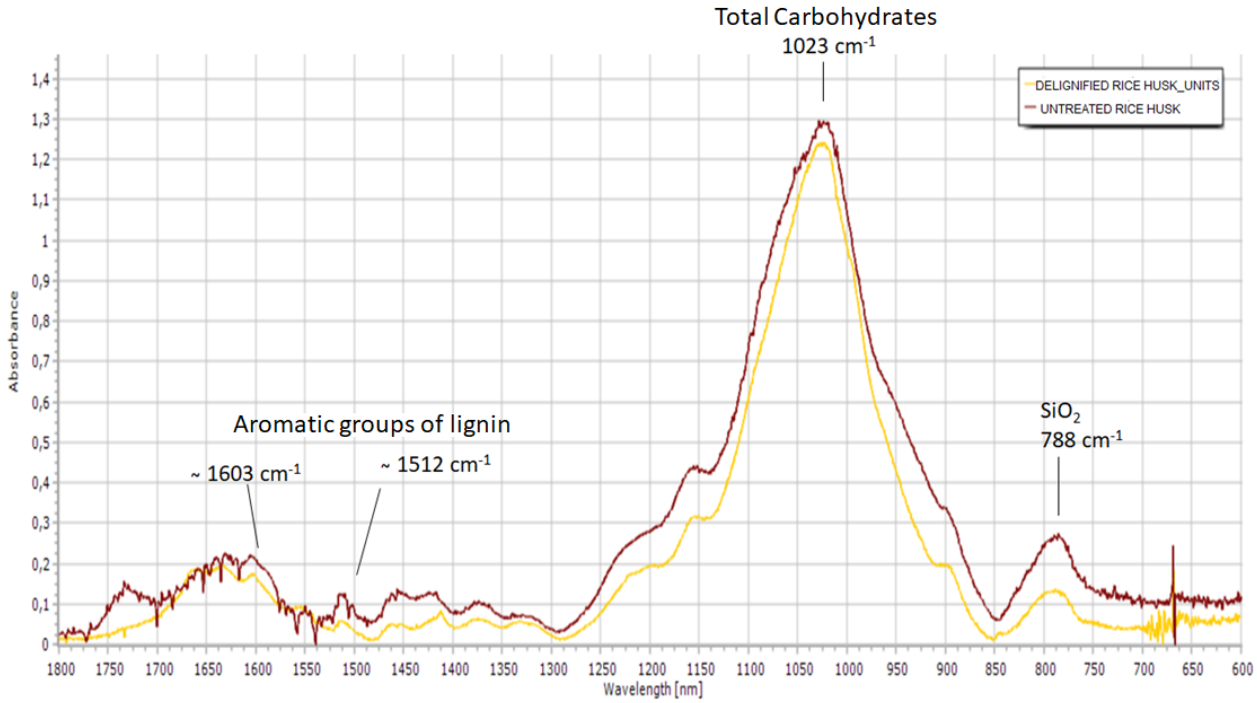

Figure 4.23 *Spectra of untreated rice husk (red) and delignified rice husk (yellow).*

From figure 4.23 it is possible to observe a reduction of lignin content in delignified rice husk (yellow spectrum). The peak at 830 cm^{-1} identifies the signals of aromatic -CH of lignin, peaks at 1512 and 1603 cm^{-1} refer to stretching C=C of lignin aromatic ring, and the peak of SiO_2 is visible at 788 cm^{-1}.

Due to the presence of silica, it is not possible to quantitatively examine the spectra according to the Galletti method (Galletti et al.,2010), which provides information on the composition of herbaceous biomass. This method consists of the integration of 3 regions of the spectrum:

- 1480-1440 cm^{-1} inversely proportional to cellulose content
- 1530-1397 cm^{-1} lignin content
- 1142-1093 cm^{-1} region used for normalization

For rice husk this method is strongly influenced by the presence of considerable signals of SiO_2 that increase the integration in the normalization region. This causes an underestimation of lignin content and at the same time overestimation of cellulose.

Therefore, to proceed with the quantification of lignin in the various samples, a simpler method was used: only a few characteristic signals were considered, which are shown in table 4.5 where HC indicates hemicellulose, L lignin and SiO_2 silica. Specifically, table 4.5 shows the absorbance values for the characteristic peaks considered.

Table 4.5 Absorbance values for selected and normalized peaks.

	A1 **Acetyl HC**	**A2** **ring L**	**A3** **ring L**	**A4** **C-O L**	**A5** **C-O**	**A6** **SiO_2**
cm^{-1}	1730	1600	1510	1220	1200	790
Absorbance	0.0450	-0.0025	0.0253	0.1959	0.2084	0.2354

The ATR-IR spectra in Figure 4.23 and the table 4.5 show that rice husk obtained after the delignification treatment appears to have very low quantities of lignin. Figure 4.24 shows the variation of the ratio between hemicellulose, lignin, and SiO_2 after the treatment, confirming the selective removal of lignin and hemicellulose with respect to SiO_2.

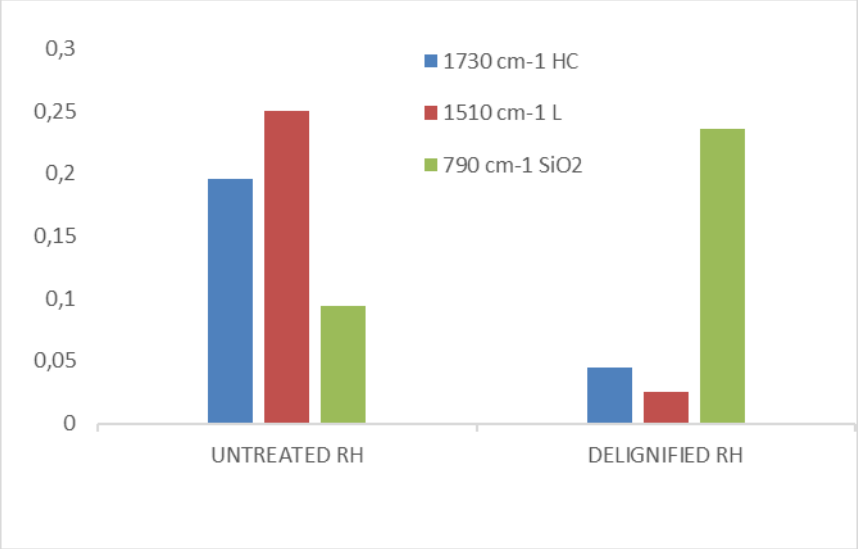

Figure 4.24 *Variation of absorbance values of selected peaks.*

A further morphological characterization was performed with the energy dispersive X-ray spectroscopy (EDS) thanks to the collaboration with Dr Lisa Vaccari and Dr Nicola Cefarin of ELETTRA Sincrotrone, Trieste. The method allowed for the collection of the silicon Kα1 signal (figure 4.25 on the left) and the localization of SiO_2 (figure 4.25 on the right). This allowed us to understand the robustness of the external surface of the peel (Park et al., 2003; Coletta et al. al., 2013). The presence of SiO_2 on the surface of the RH confirms its role in protecting the rice grain from mechanical and chemical agents.

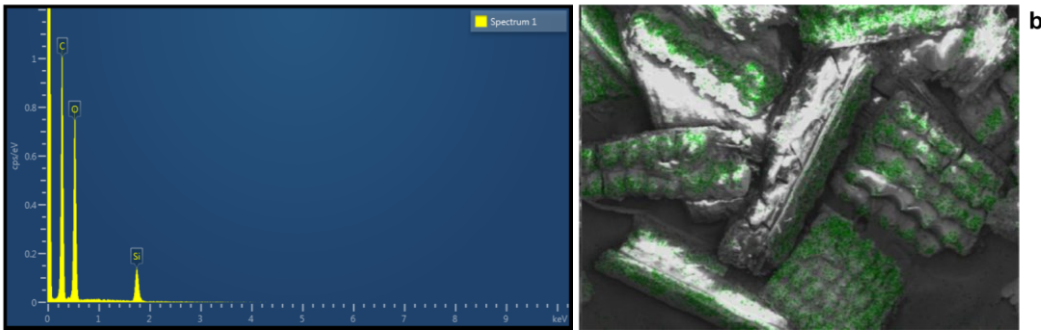

Figure 4.25 *SEM image of fragments of milled RH, showing the linear ripples with conical shape on the external surface rich in SiO_2 (green); Spectrum of energy dispersive X-ray spectroscopy (EDS) analysis acquired with a beam energy of 5 keV.*

The EDS analysis confirms that the RH preserves its tridimensional structure after the delignification process. More importantly, most of the SiO_2 is retained on the surface of the composite material, thus preserving the mechanical robustness of RH.

4.5.7 Immobilization of CaLB on delignified rice husk

The covalent immobilization of lipases was finally carried out also on the delignified RH. With respect to the previous protocols, a larger amount of enzyme was employed (72000 U per g of carrier *vs* 10000 U) in an attempt to improve the immobilization yield.

Table 4.6 reports the results, which were also compared to previous data.

Table 4.6 Results of lipase immobilization on 0.200 g scale of dry support (untreated RH, delignified RH both chemically and enzymatically oxidized by LMS system and on epoxy resin.

Type of support	Enzyme	Protein loaded ($U/g_{dry\ carrier}$)	Protein immobilized (%)	Hydrolytic activity of the immobilized biocatalyst (U/g_{dry})
Untreated RH chemically oxidized	CaLB	72000	12	146
Delignified RH chemically oxidized			10	174
Untreated RH enzymatically oxidized	CaLB	72000	20	173
Delignified RH enzymatically oxidized			11	220
Epoxy methacrylic resin			52	1502
Untreated RH chemically oxidized	CaLB	10000	33	290*
Untreated rice husk enzymatically oxidized			65	590*

*See data in table 4.2 above and manuscript C (Spennato et al.,2021)

Results indicate that an increase of the protein loading is not achievable by offering a larger amount of protein to the support. Rather, there is a waste of enzyme in the immobilization process with a maximum of 20% of protein effectively loaded. The best performance was obtained with enzymatically oxidized delignified RH (220 U/g) which is, however, lower than the result previously obtained with the raw RH oxidized enzymatically (590 U/g

4.6 CONCLUSIONS

This part of the thesis work reports the valorization of rice husk, a natural composite material, as a carrier for the sustainable immobilization of lipases. Compared to previous studies the sustainability of the functionalization and immobilization protocols were improved. The laccase-TEMPO functionalization (oxidation) of rice husk was performed with an optimized protocol that allows not only for the reduction of the amount of enzyme employed but also enables its recycling. The oxidation method has the advantage of operating at pH values close to neutrality, avoiding side reactions such as ß-eliminations in cellulose that cause the depolarization of the polysaccharidic chain. More importantly, lipases were directly immobilized covalently on the oxidized rice husk without the use of spacers and the toxic glutaraldehyde. Future studies will aim to optimize the recycling of the laccase and to replace the TEMPO mediator with bio-based renewable mediators. Here, data had demonstrated a good stability and recyclability of lipases TLL and CaLB covalently immobilized on rice husk retaining > 70% of activity after 10 cycles of hydrolysis. The results are comparable to those obtained using commercial epoxy methacrylic resins, which have the disadvantage of being fossil-based, non-biodegradable, and expensive. These immobilized biocatalysts, due to their stability and robustness, are applicable in various reaction media, including aqueous systems, and under mechanical stress. Overall, all these methods are intended to be a contribution to the development of a new renewable industrial carrier for enzyme immobilization for different industrial applications, this being able to replace petrol-based materials and to overcome their natural capital cost. Notably, no covalently immobilized lipase is currently commercialized for industrial applications despite the clear advantages deriving from the use of lipase enzymes in aqueous solutions. Indeed, the use of lipases immobilized by adsorption on organic resins undergo detachment in the presence of water. Notably, the cost analysis of the most commonly used lipase adsorbed on polymeric resins (Novozymes 435) indicates that 63% of the cost is due to the support and only 37% to the enzyme. The last part of this research was focused on the delignification of rice husk with the objective of improving its accessibility to oxidizing reagents and enzymes, while decreasing the hydrophobicity of this composite material. The results obtained so far indicate that the rice husk increases water retention capacity, decreases its density, while maintaining its tri-dimensional structure and robustness. However, no significant improvement in terms of protein loading and biocatalyst performance has been observed in the enzymes immobilized on the delignified rice husk.

4.7 REFERENCES

Agematu, H., Tsuchida, T., Kominato, K., Shibamoto, N., Yoshioka, T., Nishida, H., Okamoto, R., Shin, T., Murao, S., 1993. Enzymatic dimerization of penicillin X. J. Antibiot. (Tokyo) 46, 141–148. https://doi.org/10.7164/antibiotics.46.141

Alvira, P., Tomás-Pejó, E., Ballesteros, M., Negro, M.J., 2010. Pretreatment technologies for an efficient bioethanol production process based on enzymatic hydrolysis: A review. Bioresour. Technol. 101, 4851–4861. https://doi.org/10.1016/j.biortech.2009.11.093

Andréasson, L.-E., Reinhammar, B., 1979. The mechanism of electron transfer in laccase-catalysed reactions. Biochim. Biophys. Acta BBA - Enzymol. 568, 145–156. https://doi.org/10.1016/0005-2744(79)90282-1

Basso, A., Braiuca, P., Cantone, S., Ebert, C., Linda, P., Spizzo, P., Caimi, P., Hanefeld, U., Degrassi, G., Gardossi, L., 2007. In Silico Analysis of Enzyme Surface and Glycosylation Effect as a Tool for Efficient Covalent Immobilisation of CalB and PGA on Sepabeads®. Adv. Synth. Catal. 349, 877–886. https://doi.org/10.1002/adsc.200600337

Bourbonnais, R., Paice, M.G., Reid, I.D., Lanthier, P., Yaguchi, M., 1995. Lignin oxidation by laccase isozymes from Trametes versicolor and role of the mediator 2,2'-azinobis(3-ethylbenzthiazoline-6-sulfonate) in kraft lignin depolymerization. Appl. Environ. Microbiol. 61, 1876–1880.

Cameron, M.D., Aust, S.D., 2001. Cellobiose dehydrogenase–an extracellular fungal flavocytochrome. Enzyme Microb. Technol. 28, 129–138. https://doi.org/10.1016/S0141-0229(00)00307-0

Cañas, A.I., Camarero, S., 2010. Laccases and their natural mediators: biotechnological tools for sustainable eco-friendly processes. Biotechnol. Adv. 28, 694–705. https://doi.org/10.1016/j.biotechadv.2010.05.002

Cantone, S., Ferrario, V., Corici, L., Ebert, C., Fattor, D., Spizzo, P., Gardossi, L., 2013. Efficient immobilisation of industrial biocatalysts: criteria and constraints for the selection of organic polymeric carriers and immobilisation methods. Chem. Soc. Rev. 42, 6262–6276. https://doi.org/10.1039/C3CS35464D

Cespugli M., 2017. Integration of bioinformatics analysis and experimental biocatalysis for a comprehensive approach to the synthesis of renewable polyesters. Università degli studi di Trieste.

Cespugli, M., Lotteria, S., Navarini, L., Lonzarich, V., Del Terra, L., Vita, F., Zweyer, M., Baldini, G., Ferrario, V., Ebert, C., Gardossi, L., 2018. Rice Husk as an Inexpensive Renewable Immobilization Carrier for Biocatalysts Employed in the Food, Cosmetic and Polymer Sectors. Catalysts 8, 471. https://doi.org/10.3390/catal8100471

Claus, H., 2004. Laccases: structure, reactions, distribution. Micron, XIIIth International Conference on Invertebrate Dioxygen Binding Proteins 35, 93–96. https://doi.org/10.1016/j.micron.2003.10.029

Corici, L., Ferrario, V., Pellis, A., Ebert, C., Lotteria, S., Cantone, S., Voinovich, D., Gardossi, L., 2016. Large scale applications of immobilized enzymes call for sustainable and

inexpensive solutions: rice husks as renewable alternatives to fossil-based organic resins. RSC Adv. 6, 63256–63270. https://doi.org/10.1039/C6RA12065B

Díaz, A.B., Blandino, A., Belleli, C., Caro, I., 2014. An Effective Process for Pretreating Rice Husk To Enhance Enzyme Hydrolysis. Ind. Eng. Chem. Res. 53, 10870–10875. https://doi.org/10.1021/ie501354r

Fabbrini, M., Galli, C., Gentili, P., Macchitella, D., 2001. An oxidation of alcohols by oxygen with the enzyme laccase and mediation by TEMPO. Tetrahedron Lett. 42, 7551–7553. https://doi.org/10.1016/S0040-4039(01)01463-0

Ferrario, V., Chernykh, A., Fiorindo, F., Kolomytseva, M., Sinigoi, L., Myasoedova, N., Fattor, D., Ebert, C., Golovleva, L., Gardossi, L., 2015. Investigating the Role of Conformational Effects on Laccase Stability and Hyperactivation under Stress Conditions. ChemBioChem 16, 2365–2372. https://doi.org/10.1002/cbic.201500339

Ferrario, V., Ebert, C., Knapic, L., Fattor, D., Basso, A., Spizzo, P., Gardossi, L., 2011. Conformational Changes of Lipases in Aqueous Media: A Comparative Computational Study and Experimental Implications. Adv. Synth. Catal. 353, 2466–2480. https://doi.org/10.1002/adsc.201100397

Galbe, M., Zacchi, G., 2007. Pretreatment of lignocellulosic materials for efficient bioethanol production. Adv. Biochem. Eng. Biotechnol. 108, 41–65. https://doi.org/10.1007/10_2007_070

Gardossi L., Sinigoi L., Spizzo D., Fattor D., 2012. Method for covalent immobilization of enzymes on functionalized solid polymeric supports. 2012, WO2012085206 (A1); EP2655611 (A1).

Kim, T.H., Lee, Y.Y., 2005. Pretreatment of corn stover by soaking in aqueous ammonia. Appl. Biochem. Biotechnol. 124, 1119–1131. https://doi.org/10.1385/ABAB:124:1-3:1119

Lent, E.M., Crouse, L.C.B., Eck, W.S., 2017. Acute and subacute oral toxicity of periodate salts in rats. Regul. Toxicol. Pharmacol. RTP 83, 23–37. https://doi.org/10.1016/j.yrtph.2016.11.014

Lola Domnina B. Pestaño and Wilfredo I. José, 2018. Development of Torrefaction Technology for Solid Fuel Using Renewable Biomass.

Medina, F., Aguila, S., Baratto, M.C., Martorana, A., Basosi, R., Alderete, J.B., Vazquez-Duhalt, R., 2013. Prediction model based on decision tree analysis for laccase mediators. Enzyme Microb. Technol. 52, 68–76. https://doi.org/10.1016/j.enzmictec.2012.10.009

Monsan, 1983, 1981. Enzymes immobilized on a solid support containing cellulose and lignin.

Nakamura, T., 1958. Purification and physico-chemical properties of laccase. Biochim. Biophys. Acta 30, 44–52. https://doi.org/10.1016/0006-3002(58)90239-7

Osma, J.F., Toca-Herrera, J.L., Rodríguez-Couto, S., 2010. Uses of Laccases in the Food Industry. Enzyme Res. 2010, e918761. https://doi.org/10.4061/2010/918761

Park, E.J., Lee, J.H., Yu, G.-Y., He, G., Ali, S.R., Holzer, R.G., Osterreicher, C.H., Takahashi, H., Karin, M., 2010. Dietary and genetic obesity promote liver inflammation and tumorigenesis by enhancing IL-6 and TNF expression. Cell 140, 197–208. https://doi.org/10.1016/j.cell.2009.12.052

Patel, I., Ludwig, R., Haltrich, D., Rosenau, T., Potthast, A., 2011. Studies of the chemoenzymatic modification of cellulosic pulps by the laccase-TEMPO system: 11th EWLP, Hamburg, Germany, August 16–19, 2010 65, 475–481. https://doi.org/10.1515/hf.2011.035

Potthast vA., Rosenau T., Fischer K., 2001. Oxidation of Benzyl Alcohols by the Laccase-Mediator System (LMS) a Comprehensive Kinetic Description [WWW Document]. URL https://www.degruyter.com/document/doi/10.1515/HF.2001.008/html (accessed 11.25.22).

Spennato, M., Todea, A., Corici, L., Asaro, F., Cefarin, N., Savonitto, G., Deganutti, C., Gardossi, L., 2021. Turning biomass into functional composite materials: rice husk for fully renewable immobilized biocatalysts. EFB Bioeconomy J. 100008. https://doi.org/10.1016/j.bioeco.2021.100008

Takigawa, T., Endo, Y., 2006. Effects of glutaraldehyde exposure on human health. J. Occup. Health 48, 75–87. https://doi.org/10.1539/joh.48.75

Thurston Christopher F., 1994. The structure and function of fungal laccases | Microbiology Society,https://www.microbiologyresearch.org/content/journal/micro/10.1099/13500872-140-1-19 (accessed 11.7.22).

Tuck, C.O., Pérez, E., Horváth, I.T., Sheldon, R.A., Poliakoff, M., 2012. Valorization of biomass: deriving more value from waste. Science 337, 695–699. https://doi.org/10.1126/science.1218930

Uchida, H., Fukuda, T., Miyamoto, H., Kawabata, T., Suzuki, M., Uwajima, T., 2001. Polymerization of bisphenol A by purified laccase from Trametes villosa. Biochem. Biophys. Res. Commun. 287, 355–358. https://doi.org/10.1006/bbrc.2001.5593

Wang Z., Jiaying L., Barford J.P., Hellgradt K., McKay G., 2016. A comparison of chemical treatment methods for the preparation of rice husk cellulosic fibers.

Zhao, C., Shao, Q., Chundawat, S.P.S., 2020. Recent advances on ammonia-based pretreatments of lignocellulosic biomass. Bioresour. Technol. 298, 122446. https://doi.org/10.1016/j.biortech.2019.122446

Zhao, C., Shao, Q., Li, B., Ding, W., 2014. Comparison of Hydrogen Peroxide and Ammonia Pretreatment of Corn Stover: Solid Recovery, Composition Changes, and Enzymatic Hydrolysis. Energy Fuels 28, 6392–6397. https://doi.org/10.1021/ef5013837

ANNEX 1

List of publications:

- M. Spennato, A. Todea, L. Corici, F. Asaro, N. Cefarin, G. Savonitto, C. Deganutti, L. Gardossi, "*Turning biomass into functional composite materials: rice husk for fully renewable immobilized biocatalysts*", Bioeconomy Journal 2021, 1, 100008; https://doi.org/10.1016/j.bioeco.2021.100008

- S. F. Mirpoor, S. Varriale, R. Porta, D. Naviglio, M. Spennato, L. Gardossi, C. V. L. Giosafatto, C. Pezzella, "*A biorefinery approach for the conversion of Cynara cardunculus biomass to active films*", Food Hydrocolloids 2021, Food Hydrocolloids, 122, 107099; https://doi.org/10.1016/j.foodhyd.2021.107099

- A. Todea, C. Deganutti, M. Spennato, F. Asaro, G. Zingone, T. Milizia, L. Gardossi, "*Azelaic Acid: A Bio-Based Building Block for Biodegradable Polymers*", Polymers 2021, 13(23), 4091; https://doi.org/10.3390/polym1323409

- M. Spennato, O. M., Roggero, S. Varriale, F. Asaro, A. Cortesi, J. Kašpar, E. Tongiorgi, C. Pezzella, L. Gardossi. "*Neuroprotective properties of cardoon leaves extracts against neurodevelopmental deficits in an in vitro model of Rett syndrome depend on the extraction method and harvest time*", Molecules 2022, 27(24), 8772; https://doi.org/10.3390/molecules27248772

Oral communications:

- M. Spennato, A. Todea, F. Asaro, J. Kaspar, A. Cortesi, L. Gardossi, "*Functionalized rice husk as renewable immobilization carrier for biocatalysis"* XVIII PHD DAY OF CONSORZIO INTERUNIVERSITARIO REATTIVITÀ CHIMICA E CATALISI

List of poster contributions at conferences:ù

- C. Deganutti, M. Spennato, A. Todea, F. Asaro, L. Gardossi, "*Lipases and cardoon: a green way to obtain bioplasticizers*" Green chemistry Postgraduate summer school, July 2020, Venice

- M. Spennato, C. Deganutti, A. Todea, F. Asaro, L. Gardossi, "*Solvent-free cascade synthesis of bio-based plasticizers catalysed by Lipases*" Bncm2021, May 2021 (online conference)

- M. Spennato, C. Deganutti, A. Todea, F. Asaro, L. Gardossi, "*Lipases for the biocatalysed synthesis of bio-based plasticizers*" EFB2021, 10-14 May 2021 (online conference)

- M. Spennato, C. Deganutti, A. Todea, F. Asaro, L. Gardossi, "*Biocatalysed process for the synthesis of bio-based plasticizers*" Biotrans2021, July 2021 (online conference)

- M. Spennato, A. Todea, G. Savonitto, F.Asaro, J. Kaspar, L. Gardossi, "*Laccase mediated functionalization of composite lignocellulosic Biomass for enzyme immobilization*" 6th international conference of IMTB (implementation of Microreactor Technology in biotechnology, June 2022, Portorose (Slovenia)

- A. Todea, F. Asaro, M. Spennato, F. Zappaterra, L. Gardossi "*Making the enzymatic synthesis of bio-based polyesters feasible: from Bioinformatics to pilot plant*" International applied biotechnology conference: biotech, June 2022 Paris (France)

National and international awards for research activities

"WORLD BIOPRODUCT DAY" SOCIAL CAMPAIGN Award, dissemination video awarded as "BEST PROPOSAL" for the "#INNOVATIVE #YOUTH" category.

Award promoted by the European Bioeconomy Network (EuBioNet), in collaboration with the World Bioeconomy Forum and the European Projects Transition2bio and Biovoices.

ACKNOWLEDGEMENTS

First and foremost, I would like to thank Prof. Lucia Gardossi, supervisor of this thesis for helping me to grow both professionally and humanly during these years, for being a guide who inspired me daily with her passion and enthusiasm.

I acknowledge Prof. Asaro for her support and her help for all the spectroscopic characterization, Prof. Kaspar for the GC-MS characterization, Prof. Cortesi for his help in the supercritical CO_2 extraction method. A special thanks to the memory of Dario Solinas who taught me how to use supercritical extractor.

I would like to thank to the neurobiology research group of the University of Trieste led by Prof. Tongiorni for the neuronal tests and in particular to Dott.ssa Ottavia Roggero.

I am grateful to all partners of CARDIGAN project for the collaboration and the profitable network.

I would like to thank to all the research group headed by Prof. Lucia Gardossi where this thesis work was carried out. In particular, to Dr Anamaria Todea for her continuous support and for having become a dear friend on which you can always count on, to Dr Federico Zappaterra for preparing the coffee when it was most needed, and to Dott.ssa Demi Vattovaz who shared these years with me with joy and friendship.

I would like to thank all my family, especially to my parents for allowing me to live my dreams and realize my projects with their help and support, for being close to me in the most difficult moments, teaching me how to overcome obstacles with grit and courage